

Enhanced Hanford Low- Activity Waste Glass Property Data Development: Phase 3

June 2020

CE Lonergan

JL George

D Cutforth

T Jin

P Cholsaipant

SE Sannoh

CH Skidmore

BA Stanfill

SK Cooley

GF Piepel

R Russell

JD Vienna

DISCLAIMER

This report was prepared as an account of work sponsored by an agency of the United States Government. Neither the United States Government nor any agency thereof, nor Battelle Memorial Institute, nor any of their employees, makes **any warranty, express or implied, or assumes any legal liability or responsibility for the accuracy, completeness, or usefulness of any information, apparatus, product, or process disclosed, or represents that its use would not infringe privately owned rights.** Reference herein to any specific commercial product, process, or service by trade name, trademark, manufacturer, or otherwise does not necessarily constitute or imply its endorsement, recommendation, or favoring by the United States Government or any agency thereof, or Battelle Memorial Institute. The views and opinions of authors expressed herein do not necessarily state or reflect those of the United States Government or any agency thereof.

PACIFIC NORTHWEST NATIONAL LABORATORY
operated by
BATTELLE
for the
UNITED STATES DEPARTMENT OF ENERGY
under Contract DE-AC05-76RL01830

Printed in the United States of America

Available to DOE and DOE contractors from the
Office of Scientific and Technical Information,
P.O. Box 62, Oak Ridge, TN 37831-0062;
ph: (865) 576-8401
fax: (865) 576-5728
email: reports@adonis.osti.gov

Available to the public from the National Technical Information Service
5301 Shawnee Rd., Alexandria, VA 22312
ph: (800) 553-NTIS (6847)
email: orders@ntis.gov <<https://www.ntis.gov/about>>
Online ordering: <http://www.ntis.gov>

Enhanced Hanford Low-Activity Waste Glass Property Data Development: Phase 3

June 2020

CE Lonergan
JL George
D Cutforth
T Jin
P Cholsaipant
SE Sannoh
CH Skidmore
BA Stanfill
SK Cooley

GF Piepel
R Russell
JD Vienna

Prepared for
the U.S. Department of Energy
under Contract DE-AC05-76RL01830

Pacific Northwest National Laboratory
Richland, Washington 99354

Executive Summary

This work was performed for the U.S. Department of Energy (DOE) Office of River Protection (ORP) to provide expert evaluation and experimental work in support of the River Protection Project vitrification technology development¹. The long-term objective of this work is to expand the property-composition database for Hanford site low-activity waste (LAW) glasses and property-composition models to cover the balance of the mission for the Hanford Waste Treatment and Immobilization Plant (WTP). When this effort is complete, enhanced LAW glass property-composition models will be developed.

Twenty LAW glass compositions were designed using a space-filling statistical approach that used compositional constraints and previous compositions as input for development. The glasses were batched using oxides and carbonates and melted at temperatures from 1150°C up to 1250°C. Two glasses were modified due to gross inhomogeneities after preparation. After preparation, the as-melted glass compositions were analyzed and the resulting measured compositions showed relatively good agreement with target values, showing no batching errors or substantive losses due to volatilization. However, for some glasses, SO₃ was not fully incorporated into the glass structure. For these glasses, the final glass compositions were obtained by substituting measured SO₃ values for target SO₃ values and renormalizing the remaining glass components to have a total mass fraction of 1.0.

The glasses were subjected to heat treatments at varying temperatures [following a LAW container centerline cooling (CCC) profile] as well as an isothermal hold at 950°C for 24 hours (± 2 hours) for crystal fraction determination. Three glasses contained detectable crystals after the 950°C isothermal hold, with crystallinity values ranging from 0 to 13.4 wt%, as determined by X-ray diffraction (XRD). After CCC, 4 of the 20 glasses contained detectable crystals, with crystal concentrations varying from 0 to 46.45 wt% (by XRD). The quenched and CCC glasses were then subjected to various tests.

Density, sulfate solubility, electrical conductivity, and viscosity were measured on the quenched glasses while the Vapor Hydration Test (VHT) and Product Consistency Test (PCT) responses were determined for both the quenched and CCC samples.

The average of the 20 measured density values was 2.68 g/cm³, with a minimum of 2.61 g/cm³ and a maximum of 2.72 g/cm³. The viscosity was measured at four temperatures (950°C, 1050°C, 1150°C, and 1250°C). The viscosity values at 1150°C (η_{1150}) presented in this work were determined using the Vogel-Fulcher-Tammann (VFT) equation. The η_{1150} values as determined by the VFT equation ranged from 10.47 to 59.26 poise. Electrical conductivity was also measured at varying temperatures and fit with the VFT equation, the resulting EC values at 1150°C ranged from 52 to 71 S/m.

For the PCT response, 5 of the quenched glasses and 9 of the CCC glasses had normalized releases for boron (NR [B]) that were greater than 2 g/m² and 5 of the quenched glasses and 8 of the CCC glasses had normalized releases for sodium (NR[Na]) that were greater than 2 g/m², the Hanford Waste Treatment and Immobilization Plant (WTP) contract limit.¹ The VHT response was not able to be measured (because of the extent of sample alteration) for a total of 6 of the 20 quenched glasses and 11 of the 20 CCC glasses. Those alteration rates are indicated with a “greater than” value. The VHT results exceeded the WTP contract limit of 50 g/m²/d (DOE 2000) for 11 of the quenched glasses and 12 of the CCC glasses. There was a wide distribution of VHT corrosion rates, with values varying from 0.58 to >270 g/m²/d for quenched glasses and from 3.4 to >329 g/m²/d for CCC glasses.

¹ DOE. 2000. *Design, Construction, and Commissioning of the Hanford Tank Waste Treatment and Immobilization Plant*. Contract DE-AC27-01RV14136, as amended, U.S. Department of Energy, Office of River Protection, Richland, WA.

The SO₃ concentrations measured in the baseline glasses varied from 0.138 to 1.203 wt%. After sulfur-saturation, the SO₃ concentrations increased significantly. These were considered to be the experimentally determined SO₃ solubility values of the Phase 3 glasses. In most glasses, the SO₃ solubility (i.e., the saturated SO₃ concentrations) was between 1.143 and 2.416 wt%. Finally, it is desirable for developing property-composition models that some Phase 3 glasses had PCT and VHT results above contract limits.

Acknowledgments

The authors gratefully acknowledge the financial support provided by the U.S. Department of Energy Office of River Protection Waste Treatment Plant Project managed by Tom Fletcher, with technical oversight by Albert Kruger.

The authors thank Kevin Fox and Thomas Edwards of Savannah River National Laboratory for their help in the analysis and testing of the glasses. We also thank Dong-Sang Kim (PNNL) for his technical review, Matt Wilburn (PNNL) for his editorial review, and Hans Brandal and Veronica Perez (PNNL) for programmatic support during the conduct of this work.

Acronyms and Abbreviations

BP	Borkowski and Piepel (2009)
CCC	container centerline cooling
DIW	deionized water
DOE	U.S. Department of Energy
DWPF	Defense Waste Processing Facility
EA	Environmental Assessment
EC	electrical conductivity
EGCR	experimental glass composition region
HDI	How Do I
IC	ion chromatography
ICP-AES	inductively coupled plasma atomic emission spectroscopy
KH	potassium hydroxide fusion
LAW	low-activity waste
LM	lithium metaborate fusion
LRM	Low-Activity Reference Material
MCC	multi-component constraint
NR	normalized release
NQAP	Nuclear Quality Assurance Program
ORP	Office of River Protection
PCT	Product Consistency Test
PNNL	Pacific Northwest National Laboratory
PS	sodium peroxide fusion
PSAL	Process Science Analytical Laboratory
QA	quality assurance
R&D	research and development
RPD	relative percent difference
SCC	single-component constraint
SD	standard deviation
SFD	space-filling design
SRNL	Savannah River National Laboratory
SSM	sulfate saturated melt
VFT	Vogel-Fulcher-Tammann
VHT	Vapor Hydration Test
WTP	Waste Treatment and Immobilization Plant
XRD	X-ray diffraction

Contents

Executive Summary	ii
Acknowledgments.....	iv
Acronyms and Abbreviations	v
1.0 Introduction.....	1
1.1 PNNL LAW Glass Formulation Contributions	1
1.2 Quality Assurance.....	2
2.0 Experimental Methods.....	3
2.1 Composition Design and Glass Fabrication.....	3
2.1.1 Statistical Design of Glass Compositions.....	4
2.1.2 Glass Batching and Melting	7
2.2 Compositional Modifications.....	8
2.2.1 LAWPh3-05	8
2.2.2 LAWPh3-19	10
2.3 Chemical Composition Analysis.....	11
2.4 Density Measurements.....	12
2.5 Viscosity Measurements	13
2.6 Electrical Conductivity Measurements	13
2.7 Crystal Fraction Determination at 950°C (isothermal heat treatment)	14
2.8 Crystal Fraction in Container Centerline Cooling Samples.....	14
2.9 Product Consistency Testing Analysis.....	15
2.10 Vapor Hydration Testing Analysis	16
2.11 Sulfate Solubility Determination	17
3.0 Results and Discussion	19
3.1 Chemical Analysis of Glass Composition (performed by SRNL).....	19
3.2 Density	20
3.3 Viscosity (η).....	21
3.4 Electrical Conductivity (σ)	22
3.5 Crystal Fraction of Heat-Treated Glasses	23
3.6 PCT Response.....	25
3.7 VHT Response.....	29
3.8 Sulfur Solubility.....	30
4.0 Summary	33
5.0 References.....	34
Appendix A – Images of As-Quenched Glasses	A.1
Appendix B – Images of Samples Post-Vapor Hydration Test.....	B.1
Appendix C – Analyzed Compositions for As-Quenched Glasses	C.1
Appendix D – Viscosity Data	D.1

Appendix E – Electrical Conductivity Data.....E.1
Appendix F – Images of Crystal-Containing Heat-Treated Glasses (after isothermal holds at
950°C and CCC) F.1
Appendix G – XRD Data for All LAW Phase 3 Glasses..... G.1
Appendix H – Sulfate Solubility Compositional Analysis H.1

Figures

Figure 2.1. Cross-section image of LAWPh3-05 after third melt (top), and image of LAWPh3-05_mod6 after the second melt (bottom).	9
Figure 2.2. Images of LAWPh3-19 after the 3rd melt (top) and LAWPh3-19_mod1 after the second melt (bottom).	11
Figure 2.3. Plot of temperature schedule during CCC heat treatment of Hanford LAW glasses.	15
Figure 2.4. General setup for conducting VHTs as shown in ASTM C1663.	16
Figure 3.1. $\ln[\text{NR}]$ for B compared to Na for quenched (bottom) and CCC (top) glasses (solid line = 1:1; dashed line = the WTP contract limit).	28
Figure 3.2. Comparison of $\ln[\text{NR} (\text{g/L})]$ of B and Na for quenched versus CCC-treated samples of Phase 3 enhanced LAW glasses.	29
Figure 3.3. Target sulfur concentration and analyzed sulfur concentration in the baseline and the sulfur-saturated glasses.	32

Tables

Table 2.1. Single-component constraints used to develop the Phase 3 LAW glass matrix.	3
Table 2.2. Multi-component constraints used to develop the LAW Phase 3 glass matrix.....	4
Table 2.3. Space-filling design glass compositions in mass fractions (not including Cl, P ₂ O ₅ , and F) of the original matrix glasses and the two modified glasses (LAWPh3-05_mod6 and LAWPh3-19_mod1).....	6
Table 2.4. Concentrations in mass fractions of the “Others” components for all glasses, including the mods.....	7
Table 2.5. Melt temperatures and times for all glasses prepared in this study.....	8
Table 2.6. Compositions, in mass fraction, of the original glass LAWPh3-05 and the corresponding modifications that were melted during this work.....	10
Table 2.7. Compositions, in mass fraction, of the original LAWPh3-19 and the corresponding modification that was melted during this work.....	10
Table 2.8. Preparation and measurement methods used in reporting the measured concentrations of each of the elements of the study glasses (Fox et al. 2020).....	12
Table 2.9. Container centerline cooling profile for LAW glass. ¹	14
Table 2.10. Measurement methods used in reporting the concentrations of each of the analytes of the wash solutions (Fox et al. 2020).	18
Table 3.1. Densities of Phase 3 enhanced LAW glasses. Each glass was measured on three different samples (except LAWPh3-06, LAWPh3-18, and LAWPh3-20, each of which was measured on six different samples).....	20
Table 3.2. The measured viscosities at 1150°C, the VFT model coefficients from fitting measured data, and the VFT model calculated viscosity values at 1150°C.	21
Table 3.3. Electrical conductivity measurements, and the corresponding temperatures, for select glasses in LAW Phase 3.....	22
Table 3.4. Arrhenius model coefficients and calculated electrical conductivity values for select glasses in LAW Phase 3 with measured EC data.....	23
Table 3.5. Crystal amount and type for the LAW Phase 3 glasses after heat treatments. This table only lists the glasses with crystal phases detected after heat treatments; for the glasses not listed, they were amorphous after both isothermal and CCC treatments.....	25
Table 3.6. Normalized release values (in g/m ²) for all LAW Phase 3 glasses for the following analytes: Na, B, and Si.	27
Table 3.7. Measured alteration rate (g/m ² /d) and alteration thickness (µm) from the VHT for quenched and CCC glasses.	30
Table 3.8. Target and measured baseline values of SO ₃ and SO ₃ solubility values for samples of Phase 3 LAW glasses.....	31

1.0 Introduction

The U.S. Department of Energy (DOE) Office of River Protection (ORP) requested that Pacific Northwest National Laboratory (PNNL) provide expert evaluation and experimental work in support of the River Protection Project vitrification technology development (DOE 2020). This work was performed under the PNNL project titled “ORP Glass Support Work.” One task of this project—Enhanced Hanford Waste Glass Models—is the subject of this report. The long-term objective of this work is to expand the property-composition database for Hanford site low-activity waste (LAW) glasses and property-composition models to cover the balance of the mission for the Hanford Waste Treatment and Immobilization Plant (WTP). When this effort is complete, enhanced LAW glass property-composition models will be developed.

The WTP project has previously developed LAW glass property-composition models to formulate glass compositions and qualify LAW glasses for disposal (Piepel et al. 2007). These models were based on data from crucible-scale tests with simulants, crucible-scale tests with actual waste, and scaled-melter tests with simulants collected under conditions similar to those that will be experienced in full-scale operations. Subsequent work (including the work described in this report) was conducted to expand the available glass compositional space to contain glasses with higher waste loadings. This is done by extending the limits of the experimental glass composition region (EGCR) used for testing.

Experimental data were collected on glass compositions covering the EGCR support developing property-composition models that can (1) discriminate between glass compositions that satisfy and fail the requirements, and (2) adequately predict glass properties of compositions that satisfy all requirements. The term *qualified glass composition region* refers to the subset of the EGCR where all processing and product-quality constraints are satisfied with sufficient confidence after accounting for applicable uncertainties. Expansion of the data to be used in the models for operations allows for reduced risk, higher waste loadings, and optimally performing glass forms.

1.1 PNNL LAW Glass Formulation Contributions

The glasses in this study were prepared and characterized in multi-phase iterations, each with its own compositional constraints and glass composition design approach. The first two phases involved layered-statistical designs with 36 (Phase 1, Russell et al. 2017) and 41 (Phase 2, Russell et al. 2020) glasses, where the compositional regions of interest were defined based on single-component constraints (SCCS) and multi-component constraints (MCCs). The layered design approach was used to achieve an optimal compositional coverage while minimizing extreme compositions that could not be processed. In Phase 3, a statistical space-filling design (SFD) approach was used to develop a matrix of 20 glasses that covered the same EGCR as Phase 2. The Phase 2 (and 3) EGCR focuses on LAW glasses with higher concentrations of Na₂O (the main component in LAW). The SFD approach resulted in a more complete distribution of LAW glass compositions over the Phase 2 and 3 EGCR.

Once prepared, the LAW Phase 3 glasses were subjected to the following characterization techniques and analyses upon quenching and/or after heat treatment: chemical analysis for composition, Product Consistency Test (PCT), Vapor Hydration Test (VHT), viscosity, electrical conductivity, X-ray diffraction (XRD), scanning electron microscopy, sulfur solubility, and density. Heat treatments included isothermal holds as well as container centerline cooling (CCC) temperature profiles.

This report presents the glass compositions and glass property data from the enhanced Hanford LAW glass property data development effort for the LAW Phase 3 glasses. We summarize the experimental methods used at PNNL to fabricate, heat treat, and test the 20 glasses designed in this effort, including two glasses that were modified due to inhomogeneity issues.

1.2 Quality Assurance

This work was performed in accordance with the Pacific Northwest National Laboratory (PNNL) Nuclear Quality Assurance Program (NQAP). The NQAP complies with the United States Department of Energy Order 414.1D, *Quality Assurance*, and 10 CFR 830 Subpart A, *Quality Assurance Requirements*. The NQAP uses NQA-1-2012, Quality Assurance Requirements for Nuclear Facility Application as its consensus standard and NQA-1-2012, Subpart 4.2.1, as the basis for its graded approach to quality.

The NQAP works in conjunction with PNNL's laboratory-level Quality Management Program, which is based upon the requirements as defined in the United States Department of Energy (DOE) Order 414.1D, *Quality Assurance*, and 10 CFR 830, Nuclear Safety Management, Subpart A, *Quality Assurance Requirements*.

The work of this report was performed to the QA level of applied research.

2.0 Experimental Methods

This section describes how the glass compositions were established and the data were obtained. The descriptions include the methods for glass composition design and fabrication (Section 2.1), needed composition modifications (Section 2.2), chemical composition analysis (Section 2.3), density determination (Section 2.4), viscosity measurement (Section 2.5), electrical conductivity measurement (Section 2.6), crystal fraction determination from isothermal heat treatments (Section 2.7), secondary phase identification from CCC heat treatments (Section 2.8), PCT response (Section 2.9), VHT response (Section 2.10), and sulfate solubility measurement (Section 2.11).

2.1 Composition Design and Glass Fabrication

JMP® version 14.0.0¹ was used to design the matrix of 20 glasses covering the same EGCR studied in Phase 2 (Russell et al. 2020). Table 2.1 and Table 2.2 show the SCCs and MCCs, respectively, that specify the EGCR for Phases 2 and 3.

Table 2.1. Single-component constraints used to develop the Phase 3 LAW glass matrix.

SCC Variable	Minimum (mass fraction)	Maximum (mass fraction)
Al ₂ O ₃	0.0600	0.1250
B ₂ O ₃	0.0600	0.1375
CaO	0.0200	0.1100
Cr ₂ O ₃	0.0030	0.0060
Fe ₂ O ₃	0.0000	0.0150
K ₂ O	0.0000	0.0575
Li ₂ O	0.0000	0.0000
MgO	0.0000	0.0135
Na ₂ O	0.2100	0.2600
SO ₃	0.0010	0.0200
SiO ₂	0.3490	0.4700
SnO ₂	0.0000	0.0350
V ₂ O ₅	0.0000	0.0400
ZnO	0.0200	0.0360
ZrO ₂	0.0295	0.0650
Others (Cl+F+P ₂ O ₅)	0.0036	0.0269

¹ Copyright © 2018 SAS Institute Inc.

Table 2.2. Multi-component constraints used to develop the LAW Phase 3 glass matrix.

MCC	Minimum	Maximum
NAlk (mass fraction)	0	0.26 ^(c)
SO ₃ (wt%)	0	Composition dependent solubility limit ^(a)
Viscosity (η_{1150} , P)	10	100 ^(b)
ZrO ₂ + SnO ₂ (mass fraction)	-	0.10
ZrO ₂ + SnO ₂ + Al ₂ O ₃ (mass fraction)	-	0.17
NAlk – ZrO ₂ – SnO ₂ – CaO (mass fraction)	-	0.15 ^(c)

(a) Based on the model presented by Vienna et al. (2014), which normalized out the SO₃ component. That model was re-expressed to include the SO₃ component, which resulted in a model that was nonlinear in some components.

(b) η_{1150} = viscosity at 1150°C, expressed as a linear mixture model, as discussed by Piepel et al. (2015, 2016).

(c) $NAlk = Na_2O + 0.66K_2O + 2Li_2O$.

2.1.1 Statistical Design of Glass Compositions

For this phase of the LAW work (Phase 3), a space-filling design (SFD) of 20 glass compositions was desired which covered the EGCR specified by the SCCs and MCCs in Table 2.1 and Table 2.2. Prior to Phase 3, there were existing LAW glass compositions in the same EGCR, as described by Russell et al. (2017, 2020). At the time the statistical design was developed, there was no established path for creating an SFD subject to non-linear constraints (the SO₃ solubility constraint) that augment existing glasses. The software package JMPTM did have the capability to generate SFDs, but it did not, by default, have the capability to create an SFD to optimally augment some set of existing glasses. It also did not have the capability to apply non-linear constraints when specifying the design space of interest, so the following procedure was implemented:

1. Generate 50,000 points that fill the LAW Phase 3 composition region satisfying the SCCs and MCCs.
2. Select from those points to create 40 possible SFDs.
3. Compare those SFDs with design metrics and plots.
4. Choose the best design based on step 3 and prepare the final design for use.

Each of these steps is described below.

- **Step 1:** The software package R (version 3.4.3) was used to generate a set of 50,000 glass compositions to represent the composition space of interest for the LAW Phase 3 design matrix. The design space of interest is defined by SCCs on each of 15 main glass components. These SCCs are the lower and upper limits on the respective components in terms of mass fraction of the overall glass composition (in Table 2.1). One of these 15 main components is an “Others” component that is composed of fixed proportions of 3 minor components: 17.34 wt% for Cl, 26.33 wt% for F, and 56.33 wt% P₂O₅. There are also six MCCs, which help define the design space of interest. These six MCCs involve predicted viscosity at 1150°C of the glass melt based on glass composition, a constraint on the predicted sulfate solubility, and several other linear combinations of two to five main components. The viscosity constraint is a linear constraint, while the sulfate solubility constraint is a non-linear constraint.

Prior to applying the R code used to generate the set of 50,000 representative compositions, the coefficient for the “Others” component in the viscosity and sulfate solubility models had to be updated based on the list of main components and minor components involved in the intended LAW

Phase 3 design space. Calculations for this coefficient update were also conducted using the software package R. The 50,000 compositions were generated randomly. They do not constitute any uniform grid that covers the design space of interest. However, 1- and 2-dimensional plots of the 50,000 compositions as well as summary statistics that describe ranges of the main components suggest that the 50,000 compositions do provide a good overall coverage of the intended design space.

- **Step 2:** Because no standard software existed to generate augmented SFDs, the standard JMP™ SFD code was modified to create augmented designs. Because this was a new procedure, additional standard SFDs were created to determine if the new, augmented SFD code created designs that were consistent with the intent of the created computer code. Therefore, two types of SFDs consisting of 20 glass compositions each were generated from 50,000 candidate points: (1) standard SFDs according to the standard space filling maxPro metric (Joseph et al. 2015) and (2) augmented SFDs according to the maxPro metric where the glasses to be augmented were the 42 LAW Phase 2 glasses (Russell et al. 2020). Because there were 50,000 points to choose from, it was not feasible to conduct an exhaustive search of all possible standard and augmented test matrices of the desired size of 20 glasses. Therefore, the statistical software JMP™ was used to generate 20 candidate SFDs of each kind, resulting in a total of 40 SFDs. Each of the 40 SFDs that was generated by JMP™, and the corresponding random seeds, was saved for reproducibility.
- **Step 3:** Because the method for creating SFDs to augment existing points was new, additional tests to assess its accuracy were conducted. The statistical software R was used to compute metrics for each of the 40 designs to determine how well they covered the composition region of interest and complement the LAW Phase 1 and 2 glasses (Russell et al. 2017, 2020). The metrics we used are described by Borkowski and Piepel (2009), hereafter referred to as “BP.” Using design visualizations (scatterplot matrices and modified dot points) and the BP metrics, the five SFDs that best filled the established composition region but were furthest (on average) from the existing LAW Phase 2 (Russell et al. 2020) compositions were identified. To differentiate among those five top designs, the BP metrics were compared with respect to the LAW Phase 1 glasses in Russell et al. (2017) to identify the design that is most novel with respect to all studied LAW glasses in Phases 1 and 2.
- **Step 4:** These results were compared, and the final design was chosen because it filled the composition region well while not overlapping the LAW Phase 1 and 2 glasses. Finally, the chosen SFD was prepared for use by using the software package R. First, the order of the 20 glass compositions was randomized so that the glasses could be tested in numerical order as listed, without fear of bias due to experimental order. Next, the “Others” component was divided into its three components: Cl, F, and P₂O₅. Finally, the compositions (in mass fractions) were rounded to five digits that summed to 1.00000, the level of precision required for accurate batching. The final matrix of 20 glass compositions is shown in Table 2.3 with the “Others” shown in Table 2.4.

Table 2.3. Space-filling design glass compositions in mass fractions (not including Cl, P₂O₅, and F) of the original matrix glasses and the two modified glasses (LAWPh3-05_mod6 and LAWPh3-19_mod1).

Glass ID	Al ₂ O ₃	B ₂ O ₃	Cr ₂ O ₃	Fe ₂ O ₃	Na ₂ O	SiO ₂	ZrO ₂	CaO	SnO ₂	SO ₃	ZnO	K ₂ O	MgO	V ₂ O ₅	Others	Total ^(b)
LAWPh3-01	0.06576	0.13506	0.00574	0.00537	0.24131	0.35582	0.05981	0.04456	0.03076	0.00528	0.02070	0.00676	0.01235	0.00281	0.00791	1.00000
LAWPh3-02	0.06869	0.13158	0.00520	0.00045	0.22707	0.34922	0.04765	0.04673	0.01553	0.00447	0.03091	0.02886	0.01084	0.02854	0.00426	1.00000
LAWPh3-03	0.06502	0.06620	0.00344	0.01403	0.21585	0.39958	0.05358	0.04093	0.01578	0.00538	0.03033	0.05005	0.01176	0.00254	0.02553	1.00000
LAWPh3-04	0.06363	0.12757	0.00494	0.00367	0.22210	0.35803	0.03392	0.09524	0.00349	0.01274	0.02243	0.00895	0.00415	0.02756	0.01158	1.00000
LAWPh3-05 ^(a)	0.06186	0.06195	0.00557	0.01051	0.22524	0.39153	0.06059	0.02442	0.03024	0.00895	0.02126	0.02903	0.01126	0.03267	0.02492	1.00000
LAWPh3-05_mod6	0.06240	0.08500	0.00450	0.01060	0.22740	0.39530	0.04060	0.02470	0.02020	0.00900	0.02150	0.02930	0.01140	0.03300	0.02520	1.00010
LAWPh3-06	0.09019	0.06727	0.00583	0.00239	0.21267	0.35777	0.03327	0.10161	0.03253	0.00341	0.02895	0.02394	0.01138	0.02304	0.00575	1.00000
LAWPh3-07	0.09804	0.07610	0.00329	0.00525	0.23886	0.35064	0.03256	0.08843	0.00733	0.00557	0.03095	0.00782	0.00070	0.03050	0.02396	1.00000
LAWPh3-08	0.06672	0.06482	0.00468	0.00106	0.21243	0.43987	0.06288	0.06142	0.00569	0.00371	0.03291	0.01515	0.00185	0.00050	0.02631	1.00000
LAWPh3-09	0.07822	0.08597	0.00305	0.00842	0.21285	0.35513	0.05090	0.09226	0.00236	0.00964	0.02289	0.05498	0.00205	0.00644	0.01484	1.00000
LAWPh3-10	0.08251	0.06361	0.00361	0.00789	0.23593	0.35502	0.06208	0.05579	0.01719	0.01103	0.03187	0.02626	0.00338	0.03836	0.00547	1.00000
LAWPh3-11	0.09337	0.09333	0.00565	0.00052	0.24759	0.35499	0.06429	0.03773	0.00746	0.00108	0.02187	0.01372	0.00817	0.03457	0.01566	1.00000
LAWPh3-12	0.11122	0.13512	0.00427	0.01071	0.21432	0.35137	0.03339	0.02761	0.00934	0.00295	0.02791	0.00229	0.01259	0.03846	0.01845	1.00000
LAWPh3-13	0.07122	0.06245	0.00580	0.00069	0.23038	0.39839	0.03214	0.08596	0.00272	0.01109	0.03501	0.03403	0.01251	0.00786	0.00975	1.00000
LAWPh3-14	0.06633	0.08264	0.00318	0.00033	0.25643	0.39559	0.03771	0.05296	0.02168	0.00917	0.02480	0.00209	0.00087	0.02139	0.02483	1.00000
LAWPh3-15	0.07298	0.09432	0.00430	0.01246	0.21708	0.35343	0.04499	0.08668	0.01692	0.00387	0.02942	0.04136	0.00008	0.01604	0.00607	1.00000
LAWPh3-16	0.06112	0.06919	0.00425	0.00333	0.23202	0.36558	0.05708	0.07417	0.00115	0.00165	0.03433	0.04082	0.00792	0.03623	0.01116	1.00000
LAWPh3-17	0.06166	0.06124	0.00392	0.01395	0.25366	0.38076	0.03652	0.09859	0.00753	0.00699	0.02374	0.00328	0.01327	0.02388	0.01101	1.00000
LAWPh3-18	0.08374	0.06075	0.00478	0.00394	0.22246	0.40785	0.04548	0.03578	0.03302	0.00324	0.03460	0.02946	0.01303	0.00403	0.01784	1.00000
LAWPh3-19 ^(a)	0.06703	0.06893	0.00373	0.01361	0.21427	0.40815	0.03056	0.08490	0.01079	0.01048	0.02112	0.03078	0.00211	0.02912	0.00442	1.00000
LAWPh3-19_mod1	0.06717	0.06907	0.00374	0.01364	0.21470	0.40897	0.03062	0.08507	0.01081	0.00848	0.02116	0.03084	0.00211	0.02918	0.00443	0.99999
LAWPh3-20	0.06035	0.08934	0.00409	0.01122	0.22432	0.41198	0.03530	0.04758	0.02863	0.00730	0.03388	0.00127	0.00074	0.03639	0.00761	1.00000

(a) Composition was modified due to issues during processing (Section 2.2); the modified composition will be used in the following sections.

(b) The original 20-glass SFD (i.e. the matrix of un-modified glasses) was generated with component values to five decimal places, summing to 1.00000 exactly.

Table 2.4. Concentrations in mass fractions of the “Others” components for all glasses, including the mods.

Glass ID	Cl	F	P ₂ O ₅	Total
LAWPh3-01	0.00137	0.00208	0.00446	0.00791
LAWPh3-02	0.00074	0.00112	0.00240	0.00426
LAWPh3-03	0.00443	0.00672	0.01438	0.02553
LAWPh3-04	0.00201	0.00305	0.00652	0.01158
LAWPh3-05 ^(a)	0.00432	0.00656	0.01420	0.02492
LAWPh3-05_mod6	0.00440	0.00660	0.01420	0.02520
LAWPh3-06	0.00100	0.00151	0.00324	0.00575
LAWPh3-07	0.00415	0.00631	0.01350	0.02396
LAWPh3-08	0.00456	0.00693	0.01482	0.02631
LAWPh3-09	0.00257	0.00391	0.00836	0.01484
LAWPh3-10	0.00095	0.00144	0.00308	0.00547
LAWPh3-11	0.00272	0.00412	0.00882	0.01566
LAWPh3-12	0.00320	0.00486	0.01039	0.01845
LAWPh3-13	0.00169	0.00257	0.00549	0.00975
LAWPh3-14	0.00430	0.00654	0.01399	0.02483
LAWPh3-15	0.00105	0.00160	0.00342	0.00607
LAWPh3-16	0.00193	0.00294	0.00629	0.01116
LAWPh3-17	0.00191	0.00290	0.00620	0.01101
LAWPh3-18	0.00309	0.00470	0.01005	0.01784
LAWPh3-19 ^(a)	0.00077	0.00116	0.00249	0.00442
LAWPh3-19_mod1	0.00077	0.00116	0.00250	0.00443
LAWPh3-20	0.00132	0.00200	0.00429	0.00761

(a) Composition was modified due to issues during processing (Section 2.2); the modified composition will be used in the following sections.

2.1.2 Glass Batching and Melting

Glass fabrication was performed according to the PNNL procedure *Glass Batching and Melting* (WFDL-GBM-1, Rev. 2).¹ Single metal oxides, single metal carbonates, and sodium salts were weighed out in the appropriate masses to form the target glass composition for each glass and then placed into a plastic bag. After thoroughly mixing in the plastic bag for at least 30 s until a uniform color developed, the powders were transferred into an agate milling chamber and milled for 4 min in an Angstrom vibratory mill. The powders were then transferred to a clean Pt-10%Rh crucible for melting using a two-step melt process. The first melt was of the raw materials after mixing in the agate milling chamber. Initial melting was performed at a temperature of 1150°C for 1 h to facilitate the formation of macroscopically homogenous glasses. A second melt of the glass was performed after the first melt was quenched and the glass was ground to a fine powder in a tungsten carbide vibratory mill. Some glasses required a third melt or more to be performed. Generally, the second melt and subsequent melts were at the same temperature, or 50°C to 100°C higher, than the initial melt, and 1 h in duration. See Table 2.5 for specific melt times and temperatures used for each glass. Two glasses were modified (mods) to achieve a macroscopically homogeneous glass; they are described in Section 2.2.

¹Russell RL. 2016. *Glass Batching and Melting*. WFDL-GBM-1, Rev. 2, Pacific Northwest National Laboratory, Richland, WA.

Table 2.5. Melt temperatures and times for all glasses prepared in this study.

Glass_ID	Melt 1		Melt 2		Melt 3		Melt 4	
	Temp (°C)	Time (h)						
LAWPh3-01	1150	1	1150	1	NA	NA	NA	NA
LAWPh3-02	1150	1	1150	1	NA	NA	NA	NA
LAWPh3-03	1150	1	1150	1	NA	NA	NA	NA
LAWPh3-04	1150	1	1150	1	NA	NA	NA	NA
LAWPh3-05_mod6 ^(a)	1150	1	1250	1	NA	NA	NA	NA
LAWPh3-06	1150	1	1150	1	1250	1	NA	NA
LAWPh3-07	1150	1	1150	1	NA	NA	NA	NA
LAWPh3-08	1150	1	1150	1	NA	NA	NA	NA
LAWPh3-09	1150	1	1150	1	NA	NA	NA	NA
LAWPh3-10	1150	1	1200	1	1200	1	NA	NA
LAWPh3-11	1150	1	1150	1	NA	NA	NA	NA
LAWPh3-12	1150	1	1150	1	1250	1	NA	NA
LAWPh3-13	1150	1	1200	1	NA	NA	NA	NA
LAWPh3-14	1150	1	1150	1	NA	NA	NA	NA
LAWPh3-15	1150	1	1150	1	NA	NA	NA	NA
LAWPh3-16	1150	1	1150	1	NA	NA	NA	NA
LAWPh3-17	1150	1	1150	1	NA	NA	NA	NA
LAWPh3-18	1150	1	1200	1	1250	1	NA	NA
LAWPh3-19_mod1 ^(a)	1150	1	1150	1	NA	NA	NA	NA
LAWPh3-20	1150	1	1150	1	1150	1	1250	1

NA = not applicable

(a) See Section 2.2 for details of modified glasses.

Of the 20 glasses, 3 required a second melt at 1200°C and 1 required a second melt at 1250°C. In addition, five of the glasses required three or more melts to achieve an acceptable glass with minimal inhomogeneities and appropriate pour viscosity. Pictures of the glasses prepared in this work are shown in Appendix A.

The laboratory crucible-scale fabrication of glasses is not intended to mimic the actual melter process or feed processing. Rather, it is intended to fabricate a glass sample with a controlled composition for property testing. Composition is the primary variable in determining glass properties. The other primary impact of temperature history of glass melts is the impact on phase assemblage. Both liquid and crystalline phase separation may occur in some glasses.

2.2 Compositional Modifications

During melting, LAWPh3-05 and LAWPh3-19 showed significant inhomogeneities and, therefore, were modified from their original compositions. The modifications to these glasses are discussed in detail in the following sections. The two modified compositions, LAWPh3-05_mod6 and LAWPh3-19_mod1, both formed clear and homogeneous glasses, which were used in the rest of the research described in this report.

2.2.1 LAWPh3-05

LAWPh3-05 exhibited phase separation upon initial melting. After four melts at increasing melt temperatures to prepare a homogeneous glass, phase separation was still detected upon pouring the fourth

melt (1250°C for 1 h). After melting, while the melt was cooling on the stainless-steel quench plate, there was clear evidence of various parts of the melt cooling at different rates and the resulting glass showed clear striations, presumably caused by phases changes under different temperature histories (Figure 2.1). It is interesting to note that the surface in direct contact with the pour plate has a thin layer that is a homogeneous green glass.

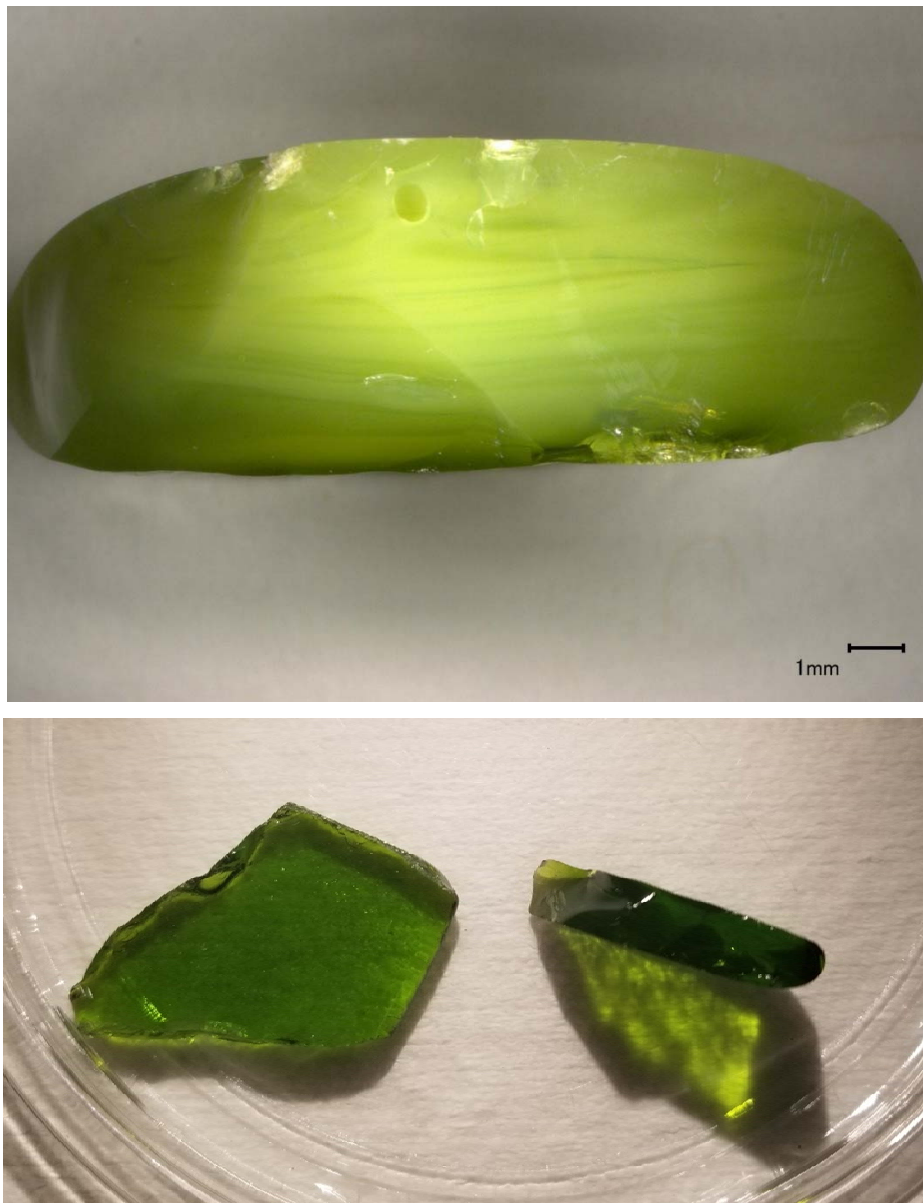


Figure 2.1. Cross-section image of LAWPh3-05 after third melt (top), and image of LAWPh3-05_mod6 after the second melt (bottom).

This glass composition was modified six times before a homogeneous glass was formed. An image of the sixth iteration of modifications is shown in Figure 2.1 (bottom). Full compositions of the modification iterations are shown in Table 2.6.

Table 2.6. Compositions, in mass fraction, of the original glass LAWPh3-05 and the corresponding modifications that were melted during this work.

Glass ID	Al ₂ O ₃	B ₂ O ₃	Cr ₂ O ₃	Fe ₂ O ₃	Na ₂ O	SiO ₂	ZrO ₂	CaO	SnO ₂
LAWPh3-05	0.06186	0.06195	0.00557	0.01051	0.22524	0.39153	0.06059	0.02442	0.03024
LAWPh3-05mod 2	0.07190	0.07190	0.00540	0.01030	0.22010	0.38260	0.05920	0.02390	0.02950
LAWPh3-05_mod 3	0.07190	0.07190	0.00560	0.01060	0.22720	0.37500	0.05800	0.02460	0.02600
LAWPh3-05_mod 4	0.06390	0.06400	0.00580	0.01090	0.23270	0.40440	0.04060	0.02520	0.02020
LAWPh3-05_mod 5	0.06240	0.08500	0.00560	0.01060	0.22710	0.39470	0.04060	0.02460	0.02020
LAWPh3-05_mod 6	0.06240	0.08500	0.00450	0.01060	0.22740	0.39530	0.04060	0.02470	0.02020

Glass ID	SO ₃	ZnO	K ₂ O	MgO	V ₂ O ₅	P ₂ O ₅	Cl	F
LAWPh3-05	0.00895	0.02126	0.02903	0.01126	0.03267	0.01404	0.00432	0.00656
LAWPh3-05_mod 2	0.0087	0.0208	0.0284	0.011	0.0319	0.0137	0.0042	0.0064
LAWPh3-05_mod 3	0.009	0.0214	0.0293	0.0114	0.0329	0.0142	0.0044	0.0066
LAWPh3-05_mod 4	0.0092	0.022	0.03	0.0116	0.0337	0.0145	0.0045	0.0068
LAWPh3-05_mod 5	0.009	0.0214	0.0293	0.0114	0.0329	0.0142	0.0044	0.0066
LAWPh3-05_mod 6	0.009	0.0215	0.0293	0.0114	0.033	0.0142	0.0044	0.0066

Mod1 of LAWPh3-05 was not prepared and melting modified compositions started with Mod2. The modifications explored were aimed at reducing and determining if any of the following components were the cause of the phase separation, in order of what was believed to be the initial cause: SnO₂, ZrO₂, B₂O₃, Al₂O₃, and Cr₂O₃. Table 2.6 shows how the components of interest were changed for the modifications. All other components not listed were kept at the same ratios as are found in the original composition by renormalizing the composition to account for the specific component changes. The unchanged values varied by less than 10% from the maximum value to the minimum value of a given component across all modifications. It was determined that Cr₂O₃ had a significant impact on the phase separation; further work should be done to explore these results.

2.2.2 LAWPh3-19

Salt segregation was observed in the LAWPh3-19 quenched glass. LAWPh3-19 was melted three times, and after each melt there was clear evidence of salt segregation. As a result, the SO₃ concentration was reduced from 1.05 to 0.85 wt%, while maintaining the ratios of the other components. The full composition is shown in Table 2.7.

Table 2.7. Compositions, in mass fraction, of the original LAWPh3-19 and the corresponding modification that was melted during this work.

	Al ₂ O ₃	B ₂ O ₃	Cr ₂ O ₃	Fe ₂ O ₃	Na ₂ O	SiO ₂	ZrO ₂	CaO	SnO ₂
LAWPh3-19	0.06703	0.06893	0.00373	0.01361	0.21427	0.40815	0.03056	0.08490	0.01079
LAWPh3-19mod1	0.06717	0.06907	0.00374	0.01364	0.21470	0.40897	0.03062	0.08507	0.01081

	Cl	F	SO ₃	ZnO	K ₂ O	MgO	P ₂ O ₅	V ₂ O ₅
LAWPh3-19	0.00077	0.00116	0.01048	0.02112	0.03078	0.00211	0.00249	0.02912
LAWPh3-19mod1	0.00077	0.00116	0.00848	0.02116	0.03084	0.00211	0.00250	0.02918

Images of the original glass and the post-modification glass are shown in Figure 2.2.

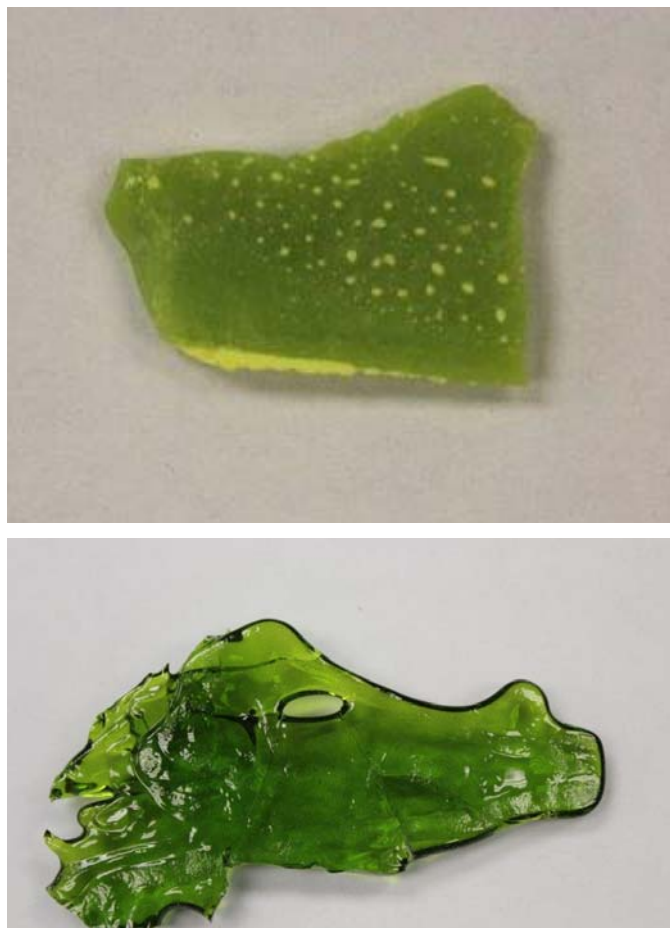


Figure 2.2. Images of LAWPh3-19 after the 3rd melt (top) and LAWPh3-19_mod1 after the second melt (bottom).

It was evident after one modification that the compositional change was effective, and further modifications were not pursued.

2.3 Chemical Composition Analysis

To confirm that the “as-fabricated” glasses corresponded to the target compositions, each glass was analyzed at the Savannah River National Laboratory (SRNL) Process Science Analytical Laboratory (PSAL). Three preparation techniques, including sodium peroxide fusion (PS), lithium metaborate fusion (LM), and potassium hydroxide fusion (KH), were used to prepare each of the glass samples for analysis, in duplicate. Descriptions of the dissolution processes can be found in Fox et al. (2020).

Each of the duplicate samples was analyzed twice by inductively coupled plasma atomic emission spectroscopy (ICP-AES) or ion chromatography (IC), which resulted in a total of four chemical analysis measurements per element for each of the glasses. These measurements were then averaged, and the average value was reported.

Glass composition standards were also intermittently prepared and analyzed to assess the performance of the ICP-AES and IC instruments/procedures over the course of these analyses. Specifically, several samples of the Low-Activity Reference Material (LRM) (Ebert and Wolfe 1999) were included as part of

the SRNL-PSAL analytical plan. The preparation and measurement methods used for each of the reported glass elements are listed in Table 2.8.

A detailed data analysis of the chemical composition measurements is published elsewhere (Fox et al. 2020). A short summary of these data analyses is included in Section 3.1.

Table 2.8. Preparation and measurement methods used in reporting the measured concentrations of each of the elements of the study glasses (Fox et al. 2020).

Analyte	Quenched Glasses Preparation Method	Measurement Method
Al	PS	ICP-AES
B	PS	ICP-AES
Ca	PS	ICP-AES
Cl	KH	IC
Cr	LM	ICP-AES
F	KH	IC
Fe	LM, PS	ICP-AES
K	LM	ICP-AES
Mg	LM	ICP-AES
Na	LM	ICP-AES
P	PS	ICP-AES
S	LM	ICP-AES
Si	PS	ICP-AES
Sn	PS	ICP-AES
V	LM	ICP-AES
Zn	LM	ICP-AES
Zr	PS	ICP-AES

2.4 Density Measurements

The room temperature density for each glass was measured using the Archimedes' method with an aluminum slug as the reference material. Deionized water (DIW) was used as the immersion liquid and three separate pieces were measured for each glass, with the final value being the average of all measurements. The density of water versus temperature was obtained from the *CRC Handbook of Chemistry and Physics* and the density was calculated using the following equation from ASTM C693-93:

$$\rho = \frac{W_A \rho_W - W_W \rho_A}{W_A - W_W} \quad (2.1)$$

where:

W_A = weight of glass specimen in air

ρ_W = density of water

W_W = weight of glass specimen in water

ρ_A = density of air (values provided in ASTM C693)

The results are discussed in Section 3.2.

2.5 Viscosity Measurements

Glass viscosity (η) was measured as a function of temperature according to the PNNL procedure *High Temperature Viscosity Measurement using Anton Paar FRS1600* (EWG-OP-0046, Rev. 0.0).¹ Quenched glasses were crushed such that dimensions were between 0.5 mm and 1 cm, and 30 mL of glass was measured out via the ethanol displacement method. Measurements were performed in a Pt-10%Rh cup with Pt-10%Rh cylindrical bob measuring geometry. Glass was heated at 5 K min⁻¹ from room temperature to 1150°C and allowed to melt before the measuring bob was lowered into the cup. The measuring bob remained in position and spinning at a shear rate of 10 s⁻¹ for most of the test, including during temperature ramps and equilibration steps.

Measurements were made over a series of temperatures, beginning at 1150°C, then cooling to 1050°C and 950°C before reheating to 1150°C, heating to 1250°C, and cooling to 1150°C for a final measurement. All temperature ramps were conducted over a 35-min window, and upon reaching temperature the glass was allowed to equilibrate for 1 h before measurements were performed. At each temperature, 100-torque readings were performed every 3 s for a 5-min iso-shear measurement window at a constant shear rate of 10 s⁻¹. Once at each temperature, a series of measurements was performed where shear rate increased from 0-20 s⁻¹ and then decreased from 20-0 s⁻¹ to confirm Newtonian behavior of the glass melt. Over the duration of the test, three measurements were performed at 1150°C. The first measurement should represent the quenched glass whereas the second and third measurements may give different values if the glass was altered (i.e., crystal formation, significant volatilization) during the test. Before, during, and after the set of tests covered in this report, viscosity of Defense Waste Processing Facility (DWPF) Environmental Assessment (EA) startup frit (Crum et al. 2012) was measured with the same measurement conditions as were used for all glasses in this study and was confirmed to be within the allowable tolerance as defined in the operating procedure.²

2.6 Electrical Conductivity Measurements

The electrical conductivities (ECs, σ) of the quenched glasses were measured with an Anton Parr FRS 1600 Furnace Rheometer System and a Solartron Analytical 1470E potentiostat and 1400 frequency analyzer (Solartron Analytical, Oak Ridge, TN). Testing was completed according to PNNL procedure EWG-OP-0047, Rev. 0.0. Platinum plates (1.3 in. long by 0.28 in. wide) were placed parallel to each other with a separation of 0.367 in. A 30-mL glass sample was used for EC measurement in a Pt-alloy crucible, typically after measuring glass viscosity. Before measuring ECs of the test matrix glasses, cell constant (k) for the measurement cell was determined. Impedance values for two room temperature conductivity reference solutions (1 S/m and 0.5 S/m) were measured over a range of frequencies. The real and imaginary components of impedance (Z' and Z'') were plotted and fit to determine solution resistance (R_s). Cell constant is then determined according to the equation:

$$\sigma = k/R_s \quad (2.2)$$

The calibration was then checked with DWPF standard glass at the temperatures of interest (950°C to 1250°C). For each glass measurement, the sample was first heated to ~1150°C and the probe was slowly lowered into the molten glass to a depth of 12.7 mm. The glass was held at temperature for 20 min, then two scans from 1 MHz to 0.1 Hz, each conducted for 3 min, were taken. The glass was then cooled to 1050°C at 10K/min and allowed to equilibrate for 20 min prior to two more scans being taken, with the

¹ McCarthy B. 2017. *High-Temperature Viscosity Measurement Using Anton Paar FRS1600*. EWG-OP-0046, Rev. 0.0. Pacific Northwest National Laboratory, Richland, WA.

same steps being followed to conduct measurements at 950°C. The real and imaginary components of impedance were plotted and fit to determine Rs. These results are discussed in Section 3.4.

2.7 Crystal Fraction Determination at 950°C (isothermal heat treatment)

Equilibrium crystal fraction at a fixed temperature was measured in Pt-10%Rh crucibles and boats with tight-fitting lids (to minimize volatility) according to the ASTM International standard procedure *Standard Test Method for Determining Liquidus Temperature of Immobilized Waste Glasses and Simulated Waste Glasses* (ASTM C1720). The heat treatment times and temperatures were 24 ± 2 h at 950°C to ensure equilibrium was achieved without excessive volatility. The samples were then quenched and analyzed by XRD.

The crystal fraction formed during heat treatment was analyzed by XRD according to Section 12.4.4 of ASTM C1720. Powdered glass samples were prepared using 5-wt% CeO₂ as an internal standard phase with between 1.5 and 2.5 g of glass powder. Glass and CeO₂ were milled together for 2 min in a 10-cm³ tungsten carbide disc mill. The powdered samples were loaded into XRD sample holders and scanned at a 0.04° 2θ step size, 4-s dwell time, from 10° to 70° 2θ scan range. XRD spectra were analyzed with TOPAS[®] 4.2 software (Bruker AXS Inc., Madison, Wisconsin) for phase identification and Rietveld refinement to semi-quantify the amounts of crystal phases in some samples with high crystalline content. These results are discussed in Section 3.5.

2.8 Crystal Fraction in Container Centerline Cooling Samples

A portion (~30 g) of each test glass was subjected to the simulated CCC temperature profile shown in Table 2.9 and Figure 2.3. This profile is the temperature schedule of CCC heat treatment for Hanford LAW glasses planned for use at WTP¹ and modified by PNNL. Pieces of quenched glass, <1 cm in length, were placed in a Pt-10%Rh crucible and covered with a Pt-10%Rh lid. The glass samples were brought to a target melt temperature, typically the highest temperature used to melt the glass during preparation, and held for 30 min. Then they were quickly cooled to 1114°C. The cooling profile was then started from 1114°C to room temperature based on nine cooling segments (see Table 2.9).

Table 2.9. Container centerline cooling profile for LAW glass.¹

Segment	Time (min)	Start Temp. (°C)	Rate (°C/min)
1	-30	Melt temp.	0
2	0	1114	-7.125
3	0-16	1000	-1.754
4	16-73	900	-0.615
5	73-195	825	-0.312
6	195-355	775	-0.175
7	355-640	725	-0.130
8	640-1600	600	-0.095
9	1600-3710	Room temp.	NA

¹ Memorandum, "Container Centerline Cooling Data," Rev. 1, CCN: 074181, RPP-WTP, October 29, 2003. Bechtel National, Inc., Richland, WA.

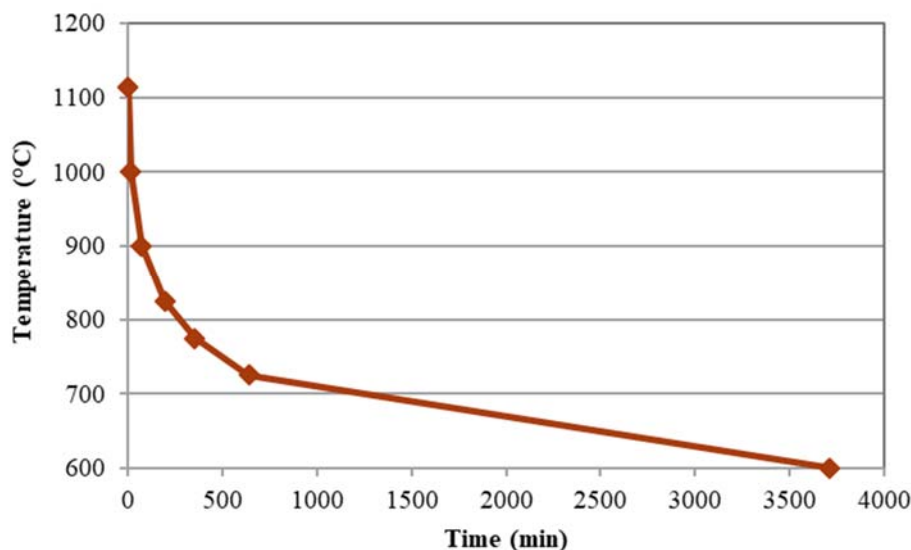


Figure 2.3. Plot of temperature schedule during CCC heat treatment of Hanford LAW glasses.

The amounts and types of crystalline phases that formed during CCC heat treatment were analyzed by XRD according to Section 12.4.4 of ASTM C1720. Powdered glass samples were prepared using 5-wt% CeO₂ as an internal standard phase with 1.5-2.5 g of powdered glass. Glass and CeO₂ were milled together for 2 min in a 10-cm³ tungsten carbide milling chamber. The powdered glass samples were loaded into XRD sample holders and scanned at a 0.04° 2θ step size, 4-s dwell time, from 10° to 70° 2θ scan range. XRD spectra were analyzed with TOPAS® 4.2 Software (Bruker AXS Inc., Madison, Wisconsin) for phase identification and Rietveld refinement to semi-quantify the amounts of crystal phases in some samples with high crystalline content. These results are discussed in Section 3.5.

2.9 Product Consistency Testing Analysis

PCT responses were measured in triplicate for quenched and CCC samples of each glass using Method A of ASTM C1285. Also included in the PCT experimental test matrix and tested in triplicate were the DWPF EA glass and blanks. Glass samples were ground, sieved to -100 +200 mesh, washed, and prepared according to the ASTM C1285 procedure. The prepared glass was added to DIW in a 1 g to 10 mL ratio, resulting in a surface area-to-solution volume ratio of approximately 2000 m⁻¹. The vessels used were desensitized Type 304L stainless steel. The vessels were closed, sealed, and placed into an oven at 90 ± 2°C for 7 days ± 3 h.

After the 7 days at 90°C, the vessels were removed from the oven and allowed to cool to room temperature. The final mass of the vessel and the solution pH were measured. Each test solution was then filtered through a 0.45-μm filter and acidified at a ratio of 1 mL leachate to 10 mL 2 vol% HNO₃ (prepared from concentrated, high-purity HNO₃) to ensure that the cations present remained in solution. The resulting solutions were analyzed by SRNL for Si, Na, and B. Samples of a multi-element, standard solution were also analyzed as a check on the accuracy of the ICP-AES instrument and procedure. Normalized releases (g/m²) were calculated based on target compositions using the leachate concentrations averaged by three ICP-AES measurements. Normalized losses (g/m²) were calculated by using a density of 2.65 g/cm³, the target mass fraction of the element in the unleached glass, and an assumed surface area over volume of 2000 m⁻¹. Results from the PCT work are published elsewhere (Fox et al. 2020); a short summary of these results is included in Section 3.6.

2.10 Vapor Hydration Testing Analysis

In the VHT, monolithic glass samples were exposed to water vapor at 200°C in sealed stainless-steel vessels according to ASTM C1663. Quenched VHT samples were prepared by pouring the melted glass into a mold and annealing at 500°C for 2 h, followed by slow cooling to room temperature (achieved by shutting the furnace off and allowing to cool naturally). If the samples originated from CCC heat-treated glass, no annealing step was performed. Samples of approximately 1.5 mm by 10 mm by 10 mm were cut from annealed or CCC-treated LAW glass bars using a diamond-impregnated saw. Actual thicknesses are reported in Section 3.7. All sides of the cut sample were polished to 600-grit surface finishes with silicon carbide paper.

Polished samples were hung from stainless-steel supports on Pt wire within the stainless-steel vessels (see Figure 2.4). DIW was added to the bottom of the vessel so that enough water was present to react with the specimen without enough water to reflux during testing (0.25 g). The samples were heated and held at 200°C in a convection oven for either 7 or 24 days. All samples were initially tested for 24 days. Samples found to fully react in 24 days were then tested for shorter times to enable the estimation of a numerical alteration rate.

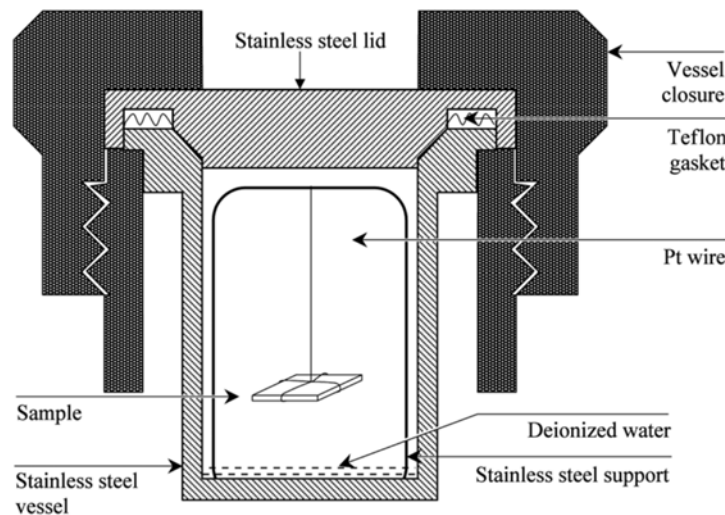


Figure 2.4. General setup for conducting VHTs as shown in ASTM C1663.

After removal from the oven, vessels were weighed and then quenched in cold water. The specimens were removed from the vessels and cross-sectioned with or without epoxy (depending on the stability of each sample) for analysis by optical microscopy. After optical images were taken, the specimens were analyzed to determine the amount of glass altered during the test.

The remaining glass thickness of the VHT specimen was determined by performing at least 10 measurements distributed (roughly equally) across the cross section of the sample. Images of cross sections may be found in Appendix B. Then, the average and standard deviations of the 10 measurements of the remaining glass were calculated. The amount of glass altered per unit surface area of specimen was determined from the average thickness of unaltered glass according to Eq. (2.3) (Equation 3 from Section 13 in ASTM C1663):

$$m_a = \frac{1}{2} \rho (d_i - d_r) = \frac{m_i}{2w_i l_i} \left(1 - \frac{d_r}{d_i} \right) \quad (2.3)$$

where:

w_i, d_i, l_i = initial width, thickness, and length of the specimen, respectively (m)

d_r = average thickness of remaining glass layer (m)

m_i = initial specimen mass (g)

m_a = mass of glass converted to alteration products per unit surface area (g/m^2)

ρ = glass density g/m^3

The average rate of corrosion was calculated as $r_a = m_a/t$, where t is the corrosion time. Vienna et al. (2001) showed that, if the average rate of corrosion at 200°C is

$$r_a = \frac{m_a}{t} < 50 \text{ [g}/(\text{m}^2 \cdot \text{d})] \quad (2.4)$$

then the final rate of corrosion, $r_{\infty} < 50 \text{ g}/(\text{m}^2 \cdot \text{d})$, meets the current ORP requirement for LAW glass performance according to the WTP contract (DOE 2000).

These results are discussed in Section 3.7.

2.11 Sulfate Solubility Determination

Sulfur solubility was measured on the quenched glass samples. The procedure was developed by PNNL and can be found in Jin et al. 2019. There are three primary phases of testing with each glass:

(1) saturation with sodium sulfate, (2) DIW wash, and (3) analysis. Each phase is described below.

1. Saturation with sodium sulfate was performed by taking 100 g of each glass, grinding it, and then sieving through a #120 sieve (125 μm). Then, 7.64 g of Na_2SO_4 per 100 g of glass was added to the sieved powdered glass to maintain 4 mass% SO_3 added to the glass/salt system, and the combination was mixed for homogeneity. The mixture of baseline glass and Na_2SO_4 was melted at 1150°C for 1 h in a Pt-10%Rh crucible with a tight-fitting lid. After melting, the mixture was poured onto a steel plate and quenched. The mixture was again mixed by crushing and sieving through a #120 sieve (125 μm) and placed back into the Pt-10%Rh crucible to melt at 1150°C for 1 h the second time. After the second melting, the mixture was quenched by pouring onto a steel plate, mixed by crushing and sieving, and melted under the same conditions for the third time. The glass, after three times re-melting and re-mixing, was crushed and sieved through the #120 sieve (125 μm).
2. The sieved samples after the third melt were washed with DIW to remove excess salt prior to further analysis. This was done by adding 2 g of glass/salt mixture to a centrifuge filter in a centrifuge tube and adding 20 g of DIW to the tube. The tube was capped and shaken by hand for 2 min. Samples were placed in a balanced centrifuge which was set to 3175 rpm for 5 min. The solution was decanted through a low-density polyethylene bottle, after the filter was removed, and then the filter was reinserted into the tube. A second wash was performed following the same steps and then the glass was weighed and dried at 80°C overnight. To ensure there was enough sample for analysis, a fresh 2 g of the same glass was obtained and the procedure described above was done again and the resulting solutions combined.
3. The washed and filtered glasses and the wash solutions recovered from filtering were then analyzed by ICP-AES and IC at SRNL. A representative sample was taken from each of the wash solutions generated from the preparation of the sulfate saturated melt (SSM) samples. The sample was diluted according to expected concentrations of the species of interest in each of the solutions, and each sample was analyzed in triplicate by ICP-AES and IC. Blanks and standards

were used intermittently to assess the performance of each of the instruments and procedures. Methods of measurement are shown in Table 2.10.

Table 2.10. Measurement methods used in reporting the concentrations of each of the analytes of the wash solutions (Fox et al. 2020).

Analyte	Measurement Method
Al	ICP-AES
B	ICP-AES
Ca	ICP-AES
Cl ⁻	IC
Cr	ICP-AES
F ⁻	IC
Fe	ICP-AES
K	ICP-AES
Mg	ICP-AES
Na	ICP-AES
P	ICP-AES
PO ₄ ⁻	IC
S	ICP-AES
SO ₄ ²⁻	IC
Si	ICP-AES
Sn	ICP-AES
V	ICP-AES
Zn	ICP-AES
Zr	ICP-AES

The results are discussed in Section 3.8.

3.0 Results and Discussion

This section describes the test results for the chemical composition, density, viscosity, EC, crystal fraction, secondary phase identification, PCT, VHT, and sulfate solubility for the LAW glasses studied.

3.1 Chemical Analysis of Glass Composition (performed by SRNL)

The targeted and average measured component concentrations (wt%) in the quenched glasses are presented in Appendix C along with the relative percent differences (RPDs). The composition analyses of the glass samples were performed as described in Section 2.3. The purpose of these comparisons was to determine whether (1) any LAW Phase 3 glasses were mis-batched, or (2) there was substantive volatility in any component(s) during glass melting.

The results presented in this section are summarized from the report by Fox et al. (2020). They reviewed the analytical sequences of the measurements, determined the average chemical composition for each glass, and compared the measured and targeted compositions of the glasses.

Plots of the wt% glass component concentrations measured for each sample by oxide and analytical block are provided in Appendix A of Fox et al. (2020). These plots are presented in analytical sequence within each calibration block, with different symbols and colors used to represent each of the study and standard glasses, and include all the measurement data. Plotting the data in this format provides an opportunity to identify gross trends in performance of the analytical instruments/procedures within and among calibration blocks. A review of these plots did not identify any gross patterns or trends in the analytical process over the course of these measurements. Only minor, block-to-block calibration shifts were seen. In all cases, the instrument check standards were within specification. These small calibration effects are typical of ICP-AES analyses and are “averaged out” by taking the mean of the measurements for each element. There were no indications of an error in glass preparation that had to be addressed in treatment of the data.

A comparison of the LRM results to their acceptability limits was performed by SRNL. The review was in the form of plots of the measurements arranged by preparation method and element, framed by upper and lower acceptability limits for the concentration of the element in question. The results show that all the measurements for the elements present in the LRM standard glass were within the acceptability limits used by SRNL in conducting instrument and procedure assessments during the execution of these analyses.

The four measurements (duplicates of two glass preparations) for each oxide in each glass were averaged by SRNL to determine an analyzed chemical composition for each glass. A sum of oxide wt% values was computed for each glass based on the averaged, measured values. The following observations were noted based on these results:

- The measured concentrations of Cl and F were below the targeted values for most of the study glasses. This is most likely due to volatility during melting.
- The measured values for Al₂O₃, Cr₂O₃, Na₂O, P₂O₅, and ZrO₂ were somewhat below the targeted values for some of the study glasses.
- The measured concentrations of K₂O were below the targeted values for glasses with higher targeted concentrations of K₂O.
- All the sums of measured oxides for the study glasses fell within the interval of 95 to 100 wt% for the glasses, indicating acceptable recovery of the glass components.

Based on the observations above, along with the RPDs shown in Appendix C, it was determined that analyzed glass compositions are subject to biased analyses and volatility. Hence, analyzed glass compositions are useful only for assessing whether (1) glasses were correctly batched according to their targeted compositions, and (2) any components were subject to substantive volatility during melting. It was concluded from the data that the glasses had been batched correctly and there were no components subject to substantive, or unexpected, volatility.

Hence, it was decided that the targeted values of components were best used in the subsequent calculations, specifically, the glass compositions used to calculate normalized PCT releases of those components. For sulfate solubility, the measured SO₃ concentrations were used for data assessment.

3.2 Density

This section presents and discusses the results of the glass density measurements for the Phase 3 enhanced LAW glasses obtained using the methods discussed in Section 2.4. The results of the glass density measurements are shown in Table 3.1.

Table 3.1. Densities of Phase 3 enhanced LAW glasses. Each glass was measured on three different samples (except LAWPh3-06, LAWPh3-18, and LAWPh3-20, each of which was measured on six different samples).

Glass ID	Measured Density (g/cm ³)	Standard Deviation (g/cm ³)
LAWPh3-01	2.6851	0.0003
LAWPh3-02	2.6630	0.0002
LAWPh3-03	2.6820	0.0016
LAWPh3-04	2.6509	0.0002
LAWPh3-05-mod6	2.6344	0.0049
LAWPh3-06	2.7236	0.0019
LAWPh3-07	2.6733	0.0016
LAWPh3-08	2.6772	0.0004
LAWPh3-09	2.6715	0.0003
LAWPh3-10	2.7174	0.0069
LAWPh3-11	2.6589	0.0012
LAWPh3-12	2.6123	0.0020
LAWPh3-13	2.6635	0.0008
LAWPh3-14	2.6629	0.0016
LAWPh3-15	2.7042	0.0012
LAWPh3-16	2.6944	0.0025
LAWPh3-17	2.6927	0.0004
LAWPh3-18	2.6976	0.0014
LAWPh3-19-mod1	2.6456	0.0034
LAWPh3-20	2.6913	0.0026

Three to six samples were prepared and measured for each of the glasses and the average value of the three to six samples was reported. The density values are in a range of 2.61 to 2.72 g/cm³. The standard deviations (SDs) were also calculated, which showed very good reproducibility of the density measurement (SDs ranged from 0.0002 to 0.0069 g/cm³).

3.3 Viscosity (η)

This section presents and discusses the viscosity results for the Phase 3 enhanced LAW glasses obtained using the methods discussed in Section 2.5. The results of the viscosity measurements at various temperatures are listed in Appendix D and summarized in Table 3.2. The measured values for each glass, represented by the first measured 1150°C value, are shown in poise (P).

Equations are widely used to fit viscosity-temperature data for a given waste glass. In this work, only the Vogel-Fulcher-Tammann (VFT) equation was used, which is given by:

$$\ln(\eta) = E + \frac{F}{T-T_0}, \quad (3.1)$$

where E, F, and T_0 are temperature independent and potentially composition dependent coefficients and T is the temperature in K.

This equation can be used to estimate the effect of temperature on viscosity over a wide range of temperatures for silicate-based glasses. The corresponding E, F, and T_0 coefficients were determined using least-squares regression and are shown in Table 3.2.

Using the VFT coefficients and $T = 1150$, the VFT-predicted values of η_{1150} for each of the Phase 3 enhanced LAW glasses are shown in Table 3.2. These values range from 10.47 P to 59.26 P for the Phase 3 enhanced LAW glasses.

Table 3.2. The measured viscosities at 1150°C, the VFT viscosity coefficients from fitting measured data, and the VFT equation calculated viscosity values at 1150°C.

Glass ID	Mean Measured	VFT Coefficients (P)			VFT Calculated
	Viscosity at 1150°C (P)	E (lnP)	F (lnP·K)	T_0 (K)	Viscosity η_{1150} (P)
LAWPh3-01	13.25	-5.3253	7671.2	453.64	13.29
LAWPh3-02	12.15	-5.8245	8885.1	357.85	12.38
LAWPh3-03	34.14	-5.9048	9897.1	376.59	34.88
LAWPh3-04	10.30	-4.3638	5997.8	529.57	10.47
LAWPh3-05 mod6	27.01	-6.1219	10674	292.56	27.64
LAWPh3-06	21.14	-5.4148	8087.8	468.91	21.35
LAWPh3-07	19.30	-5.0861	7881.2	445.59	19.61
LAWPh3-08	58.48	-5.6117	9546.8	438.30	59.26
LAWPh3-09	17.10	-6.3789	9950.7	344.10	17.16
LAWPh3-10	24.17	-6.2819	9676.4	401.80	24.34
LAWPh3-11	30.26	-7.1752	13268	169.45	30.20
LAWPh3-12	26.76	-4.8496	8308.7	403.21	27.02
LAWPh3-13	21.97	-5.4894	8687.1	412.04	22.25
LAWPh3-14	19.50	-5.4241	8742.2	384.32	19.91
LAWPh3-15	15.62	-10.247	19712	-95.440	15.39
LAWPh3-16	14.30	-5.4069	8113.5	420.50	14.66
LAWPh3-17	13.70	-7.3986	12039	220.29	13.60
LAWPh3-18	53.81	-6.0774	10407	390.70	54.74
LAWPh3-19 mod1	25.56	-6.2767	10566	314.23	25.83
LAWPh3-20	29.58	-7.7470	13345	222.20	28.94

3.4 Electrical Conductivity (σ)

This section presents the results of the electrical conductivity (EC, σ) measurements, as described in Section 2.6. Only a subset of glasses in this study were measured. The results of the measurements are summarized in Table 3.3 and in Appendix E.

Table 3.3. Electrical conductivity measurements, and the corresponding temperatures, for select glasses in LAW Phase 3.

Glass ID	T1 (°C)	EC value for T1 [S/m]	T2 (°C)	EC value for T2 [S/m]	T3 (°C)	EC value for T3 [S/m]	T4 (°C)	EC value for T4 [S/m]
LAWPh3-01-1	1050	50.07	1150	65.69	1173	68.56	NM	NM
LAWPh3-03	1050	54.80	1150	71.17	1159	71.65	NM	NM
LAWPh3-04	1050	43.16	1150	58.31	1164	59.33	NM	NM
LAWPh3-05_mod6	950	37.61	1050	50.93	1150	56.46	1170	63.15
LAWPh3-06	1050	38.62	1150	53.04	1184	58.32	NM	NM
LAWPh3-07	950	39.81	1050	54.42	1150	69.71	1198	75.84
LAWPh3-10	950	38.31	1050	53.53	1150	69.18	1210	76.50
LAWPh3-11	950	30.30	1050	43.60	1150	57.67	1189	62.69
LAWPh3-13	1050	45.46	1150	61.07	1176	64.74	NM	NM
LAWPh3-14	950	40.31	1050	53.99	1150	67.70	1200	74.23
LAWPh3-20	950	28.74	1050	39.95	1150	52.16	1192	56.43

NM = No additional EC-temperature pairs were measured.

The EC values measured at temperatures near 1150°C ($\pm 10^\circ\text{C}$) ranged from 52.16 to 71.65 S/m. As EC values were measured at varying temperatures, the VFT equation (equation 3.1) was also fit to the data for each glass and an EC value at 1150°C ($\sigma_{1150^\circ\text{C}}$) was calculated. The corresponding E, F and T_0 coefficients were determined and are shown in Table 3.4. The resulting estimated conductivities for the Phase 3 enhanced LAW glasses at 1150°C ranged from 51.78 to 71.17 S/m.

Table 3.4. VFT model coefficients and calculated electrical conductivity values for select glasses in LAW Phase 3 with measured EC data.

Glass ID	VFT model coefficients (S/m)			VFT calculated values @ T=1150°C
	E [ln(S/m)]	A [ln(S/m)*K]	T ₀ [K]	σ_{1150C} [S/m]
LAWPh3-01-1	0.3052	-266.33	782.84	65.69
LAWPh3-03	-0.2261	-16.367	1006.4	71.17
LAWPh3-04	-0.2994	-43.154	970.22	58.31
LAWPh3-05_mod6	-9.8289	-41181	5578.7	58.84
LAWPh3-06	2.4754	-3358.5	69.937	53.04
LAWPh3-07	1.3176	-1360.6	342.41	69.27
LAWPh3-10	1.0655	-1002.8	455.04	68.56
LAWPh3-11	1.3741	-1546.8	347.78	57.46
LAWPh3-13	0.6871	-589.95	650.16	61.07
LAWPh3-14	1.3132	-1463.3	291.36	67.64
LAWPh3-20	1.2915	-1679.5	288.55	51.78

3.5 Crystal Fraction of Heat-Treated Glasses

This section presents and discusses the crystal fraction results for the Phase 3 enhanced LAW glasses obtained using the methods discussed in Sections 2.7 and 2.8. For each of the 20 glasses, the as-melted (quenched) sample was first analyzed by optical microscope and XRD for crystallinity. Two heat-treated samples were then prepared from each quenched glass by the isothermal (950°C, 24 h) and CCC heat-treatment methods, respectively. These heat-treated samples were then analyzed by optical microscope and XRD. A total of 60 samples (quenched, isothermal at 950°C, and CCC for each of the 20 Phase 3 glasses) were analyzed by optical microscope and XRD. All the quenched samples had no crystals or very few crystals observed by optical microscope or detected by XRD. However, crystals were detected in heat-treated (CCC and isothermal) samples.

Each heat-treated glass was photographed (see Appendix F) and the crystals were analyzed by XRD (see Appendix G).

Table 3.5 summarizes the XRD quantitative analysis results of crystallinity in wt% of the heat-treated glasses. All but three glasses were amorphous after treatment at 950°C for 24 h. All crystallized glasses contained nasicon ($\text{Na}_4\text{Zr}_2\text{Si}_3\text{O}_{12}$), while one glass contained grossular ($\text{Ca}_3\text{Al}_2(\text{SiO}_4)_3$) and combeite ($\text{Na}_2\text{Ca}_2\text{Si}_3\text{O}_9$). The wt% total crystallinity ranged from 0 to 13.4 wt%.

Table 3.5. Crystal amount and type for the LAW Phase 3 glasses after heat treatments. This table only lists the glasses with crystal phases detected after heat treatments. The glasses not listed were amorphous after both isothermal and CCC treatments.

Glass ID	Isothermal (950°C, 24 h)		CCC	
	Crystal Fraction (wt%)	Crystal Phase	Crystal Fraction (wt%)	Crystal Phase
LAWPh3-09	0	Amorphous	25.24	Sodium phosphate – 8.79 wt% Nepheline – 6.53 wt% Sodium calcium silicate – 6.29 wt% Huayne – 1.23 wt% Potassium chromium oxide fluoride – 1.23 wt% Tin oxide – 1.18 wt%
LAWPh3-10	13.4	Nasicon	0	Amorphous
LAWPh3-13	0	Amorphous	46.45	Combeite – 45.38 wt% Potassium aluminosilicate – 1.07 wt%
LAWPh3-15	1.5	Nasicon	0	Amorphous
LAWPh3-16	3.5	Nasicon – 0.54 wt%, Combeite – 1.38 wt%, Grossular – 1.46 wt%	0	Amorphous
LAWPh3-17	0	Amorphous	4.66	Huayne – 3.38 wt% Aluminum phosphate – 0.80 wt% Potassium chromium oxide fluoride – 0.45 wt%
LAWPh3-19 mod1	0	Amorphous	11.84	Combeite – 11.84 wt%,

Nasicon = Na₄Zr₂Si₃O₁₂; Combeite = Na₂Ca₂Si₃O₉; Grossular = Ca₃Al₂(SiO₄)₃; Nepheline = K(Na,K)₃Al₄Si₄O₁₆; Huayne = (Na_{4.5}K_{1.1}Ca_{2.4})(Si₆Al₆O₂₄)(SO₄)₂.

For the CCC-treated samples, all but three glasses had crystal content of less than 5 wt%, while the other three glasses had crystal content greater than 25 wt%. The major crystalline phases appearing in the glasses containing crystals were nepheline (LAWPh3-09-CCC), nasicon (LAWPh3-09-950, LAWPh3-15-950, LAWPh3-16-950), and combeite (LAWPh3-16-950, LAWPh3-13-CCC, LAWPh3-19_mod1-CCC).

3.6 PCT Response

This section presents and discusses the PCT results for the Phase 3 enhanced LAW glasses obtained using the methods discussed in Section 2.9. The PCT results are published elsewhere (Fox et al. 2020) and are summarized here. The PCT results were normalized to the target values of the glasses and they are shown in

Table 3.6.

Table 3.6. Normalized release values of B, Na, and Si (in g/m²) for all LAW Phase 3 glasses.

Glass ID	Quenched Samples			CCC Samples		
	B (g/m ²)	Na (g/m ²)	Si (g/m ²)	B (g/m ²)	Na (g/m ²)	Si (g/m ²)
LAWPh3-01	4.505	3.734	0.503	3.289	2.773	0.506
LAWPh3-02	7.529	6.559	0.807	6.551	5.267	0.764
LAWPh3-03	3.751	3.257	0.717	2.097	1.807	0.517
LAWPh3-04	1.282	1.628	0.377	0.730	0.940	0.236
LAWPh3-05_mod6	6.640	5.190	1.015	5.563	4.123	0.939
LAWPh3-06	< 0.321	0.993	0.172	0.534	1.786	0.266
LAWPh3-07	0.501	1.168	0.259	0.635	0.928	< 0.132
LAWPh3-08	0.344	0.654	0.178	0.354	0.607	0.112
LAWPh3-09	1.138	1.653	0.308	17.445	10.341	0.568
LAWPh3-10	0.835	1.234	0.249	1.143	1.353	0.298
LAWPh3-11	1.623	1.471	0.240	1.452	1.276	0.246
LAWPh3-12	1.360	0.960	0.085	0.780	0.575	0.065
LAWPh3-12-2	1.558	1.075	0.110	NM	NM	NM
LAWPh3-13	0.405	1.287	0.236	9.45	9.06	0.92
LAWPh3-14	0.797	1.320	0.359	0.816	1.131	0.342
LAWPh3-15	0.873	1.475	0.267	1.069	1.452	0.282
LAWPh3-16	2.747	3.408	0.692	2.266	2.657	0.414
LAWPh3-17	0.532	1.713	0.353	8.853	6.191	0.519
LAWPh3-17-2	0.591	1.324	0.293	NM	NM	NM
LAWPh3-18	0.451	0.841	0.221	0.521	0.779	0.155
LAWPh3-19-mod	0.502	1.096	0.210	0.715	1.530	0.242
LAWPh3-20	0.481	0.741	0.215	9.220	7.397	1.006

NM = not measured.

SRNL measured PCT release for B, Na, and Si. Na and B are of interest to WTP, with a contract limit of 2 g/m² for both B and Na (DOE 2000).

A review of the PCT data for the 20 Phase 3 LAW glass compositions show that 5 of the quenched glasses and 9 of the CCC glasses had normalized releases for boron (NR [B]) that were greater than 2 g/m², the WTP contract limit. The same 5 quenched glasses and 8 CCC glasses had normalized release rates for sodium (NR [Na]) that were higher than the WTP contract limit of 2 g/m². It should be remembered that because these data will be used to develop PCT-composition models, it is desirable to have some glasses with PCT releases above the contract limit.

The NRs for B and Na are compared (in ln[NR, g/m²] units) for quenched and CCC glasses in Figure 3.1. It appears that many glasses exhibit congruent dissolution of B and Na at higher release rates, while Na is released faster than B for many glasses at lower release rates, especially for quenched glasses.

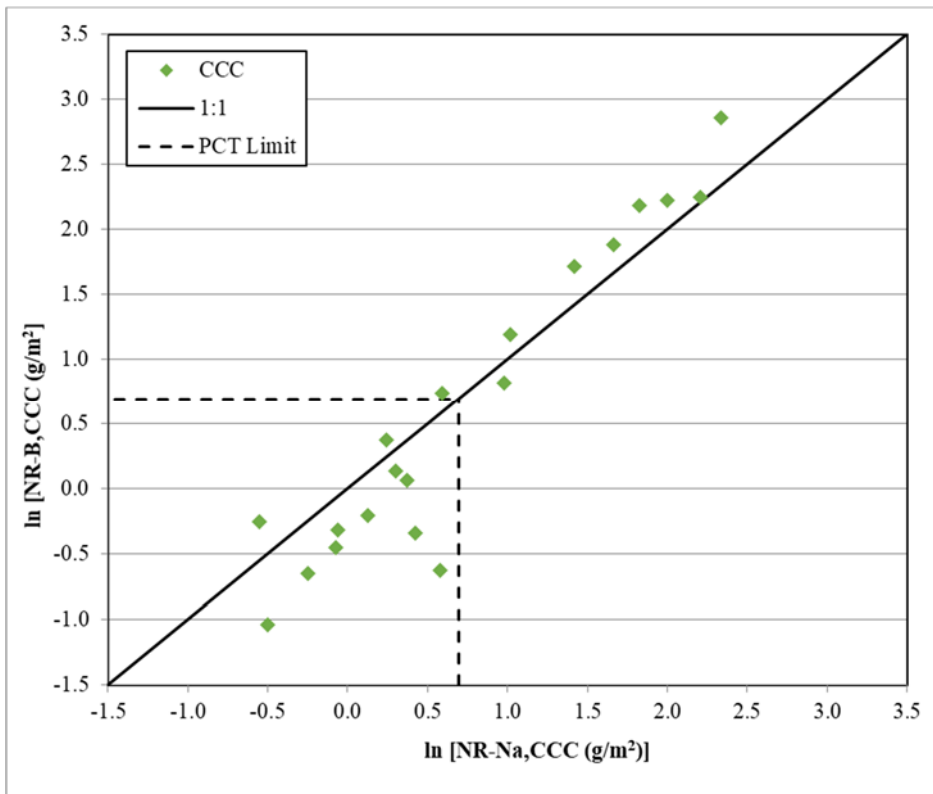
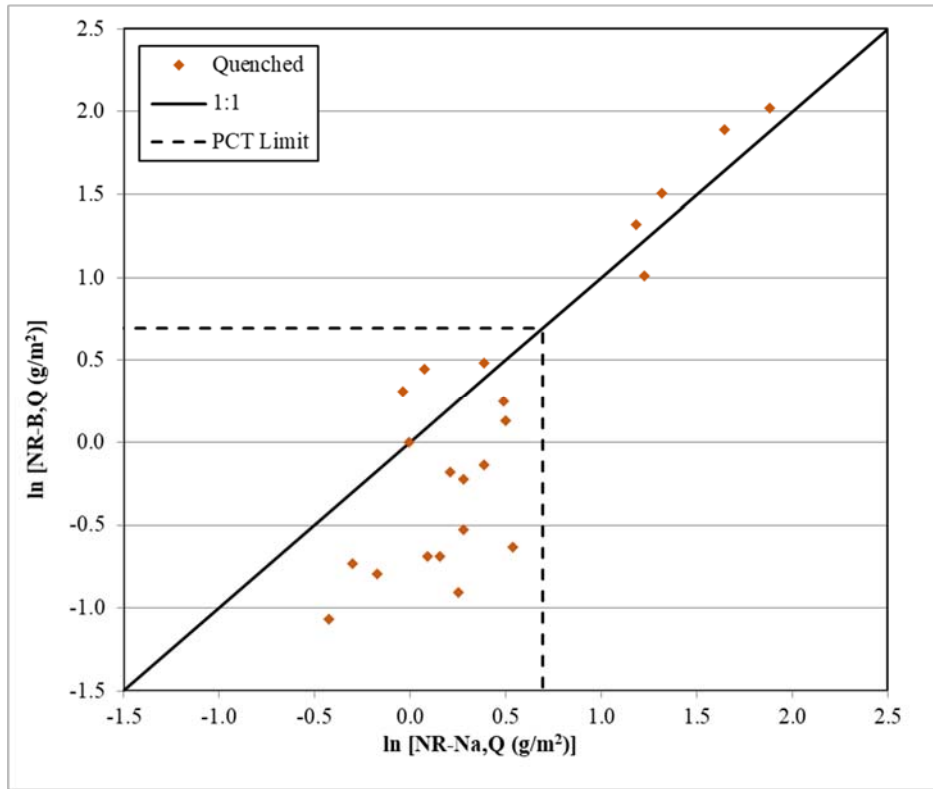


Figure 3.1. $\ln[\text{NR}]$ for B compared to Na for quenched (top) and CCC (bottom) glasses (solid line = 1:1; dashed line = the WTP contract limit).

Figure 3.2 compares the natural logarithms of normalized PCT releases (g/m^2) for the quenched and CCC glasses. There is no clear trend in PCT responses for CCC and quenched glasses. This may be due to only a few glasses precipitating crystals upon CCC-treatment.

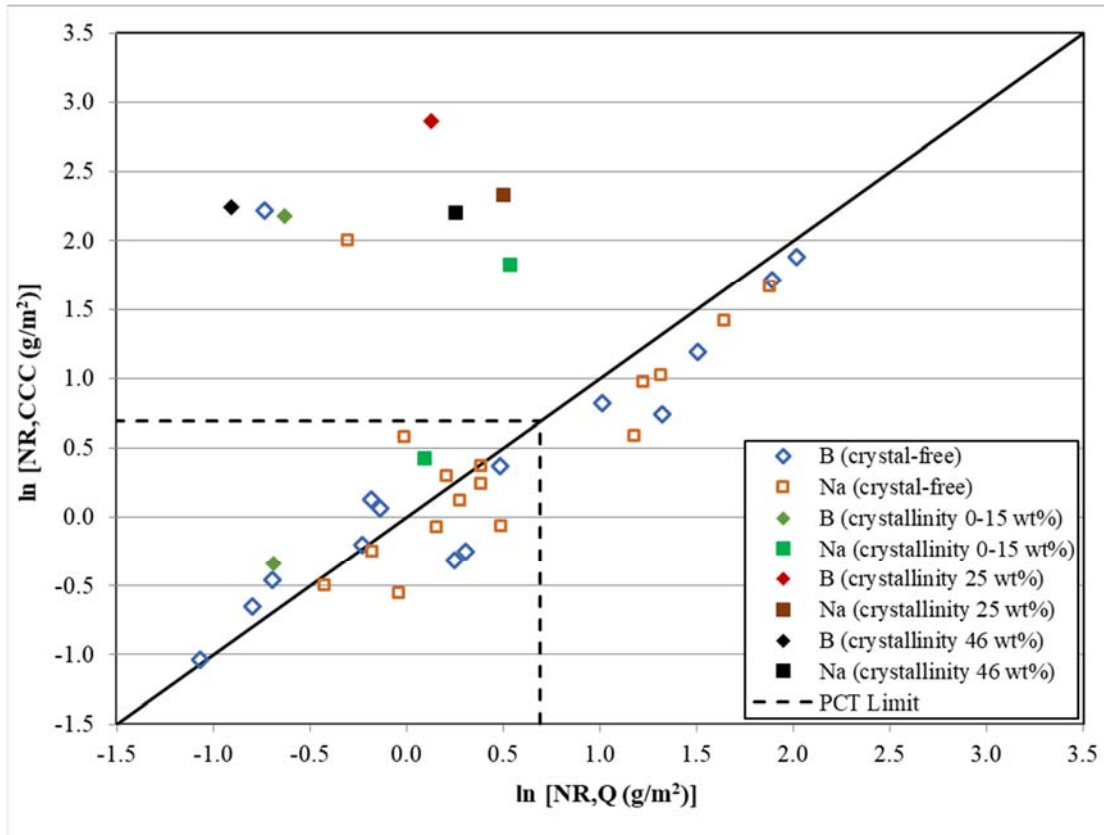


Figure 3.2. Comparison of $\ln[\text{NR} (\text{g/m}^2)]$ of B and Na for quenched versus CCC-treated samples of Phase 3 enhanced LAW glasses.

3.7 VHT Response

This section presents and discusses the VHT results obtained using the methods discussed in Section 2.10. Table 3.7 shows the corrosion rate ($\text{g/m}^2/\text{d}$) and alteration thickness (μm) of each glass based on the VHT. For samples that (i) were fully corroded (i.e. had no remaining unaltered glass after testing), or (ii) did not have even corrosion across the sample, the alteration thickness is indicated as greater than half the initial thickness. The alteration rate is also shown as a “greater than” value, based on the original thickness. See Appendix B for photos of the glass samples after the VHT.

Table 3.7. Measured alteration rate ($\text{g/m}^2/\text{d}$) and alteration thickness (μm) from the VHT for quenched and CCC glasses.

Glass_ID	Time (d)		Initial Thickness (mm)		Measured Alteration Rate ($\text{g/m}^2/\text{d}$)		Measured Alteration Thickness (D), μm	
	Quenched	CCC	Quenched	CCC	Quenched	CCC	Quenched	CCC
LAWPh3-01-1	24	24	1.29	1.56	>68.3	>85.5	>645	>780
LAWPh3-02	24	24	1.47	1.52	>77.8	>80.2	>735	>760
LAWPh3-03	24	7	1.55	1.55	>80.0	>278	>775	>775
LAWPh3-04	24	24	1.42	1.46	30.1	46.5	272	421
LAWPh3-05_mod6	7	7	1.50	1.49	241	>273	640	>745
LAWPh3-06	24	7	1.53	1.54	6.48	28.1	57.1	72.3
LAWPh3-07	24	7	1.55	1.42	>85.5	238	>775	623
LAWPh3-08	24	7	1.45	1.54	0.59	20.9	5.24	54.8
LAWPh3-09	24	7	1.51	1.44	55.7	4.69	501	12.3
LAWPh3-10	24	7	1.31	1.43	48.2	89.5	426	230
LAWPh3-11	7	7	1.47	1.48	>270	>329	>735	>740
LAWPh3-12	7	7	1.48	1.47	78.6	69.4	211	186
LAWPh3-13	7	7	1.42	1.51	>262	>275	>710	>755
LAWPh3-14	7	7	1.53	1.49	54.2	>277	143	>745
LAWPh3-15	7	7	1.43	1.38	33.5	56.1	86.8	145
LAWPh3-16	7	7	1.47	1.52	207	>281	538	>760
LAWPh3-17	7	7	1.46	1.52	39.8	18.7	103	48.5
LAWPh3-18	24	24	1.52	1.50	3.43	32.1	30.6	286
LAWPh3-19_mod1	7	7	1.51	1.52	38.9	17.0	103	44.9
LAWPh3-20	7	7	1.52	1.56	8.90	3.54	23.1	9.22

A total of 6 of the 20 quenched glasses and 8 of the 20 CCC glasses were fully altered after their corresponding test. Of the resulting alteration rates for quenched glasses, 11 exceeded the VHT limit, with a corrosion rate $>50 \text{ g/m}^2/\text{d}$ (Table 3.7). A total of 12 of the 20 CCC glasses exceeded the VHT limit, with a corrosion rate $>50 \text{ g/m}^2/\text{d}$ (Table 3.7). However, glasses with VHT corrosion rates larger than the limit are necessary for property-composition model development.

3.8 Sulfur Solubility

This section presents and discusses the chemical analysis results of the sulfate-saturated glasses obtained using the methods discussed in Section 2.11. For each glass, the “baseline” sample (quenched matrix glass) and the “sulfate-saturated melt” (SSM) sample were analyzed by ICP-AES and IC. The chemical analysis results of the baseline glasses are presented and discussed in Section 3.1. More detailed chemical analysis results have been reported by Fox et al. (2020).

A total of 20 glass samples were prepared based on the glasses listed in Table 2.3 and Table 2.4, including 18 original matrix glasses and 2 modified glasses. There were no indications of errors in glass preparation that had to be addressed in using the data, as discussed in Section 3.1. Table 3.8 and Figure 3.3 summarize the measured SO₃ concentrations in the baseline and the sulfate-saturated glasses. The measured SO₃ values in the sulfate-saturated glasses are taken to be the SO₃ solubility values for the SSM versions of the Phase 3 LAW glasses.

Table 3.8. Target and measured baseline values of SO₃ and SO₃ solubility values for samples of Phase 3 LAW glasses.

Sample ID	SO ₃ wt%		
	Target Baseline	Measured Baseline	Solubility (SSM)
LAWPh3-01-1	0.528	0.552	1.714
LAWPh3-02	0.447	0.478	1.950
LAWPh3-03	0.538	0.525	1.290
LAWPh3-04	1.274	1.203	2.416
LAWPh3-05_mod6	0.900	0.953	1.580
LAWPh3-06	0.341	0.355	1.592
LAWPh3-07	0.557	0.532	1.905
LAWPh3-08	0.371	0.359	1.317
LAWPh3-09	0.964	0.951	1.641
LAWPh3-10	1.103	1.074	1.557
LAWPh3-11	0.108	0.138	1.559
LAWPh3-12	0.295	0.315	1.353
LAWPh3-13	1.109	1.111	1.628
LAWPh3-14	0.917	0.883	2.010
LAWPh3-15	0.387	0.409	1.749
LAWPh3-16	0.165	0.192	1.950
LAWPh3-17	0.699	0.675	2.076
LAWPh3-18	0.324	0.363	1.143
LAWPh3-19_mod1	0.850	1.100	1.960
LAWPh3-20	0.730	0.743	1.727

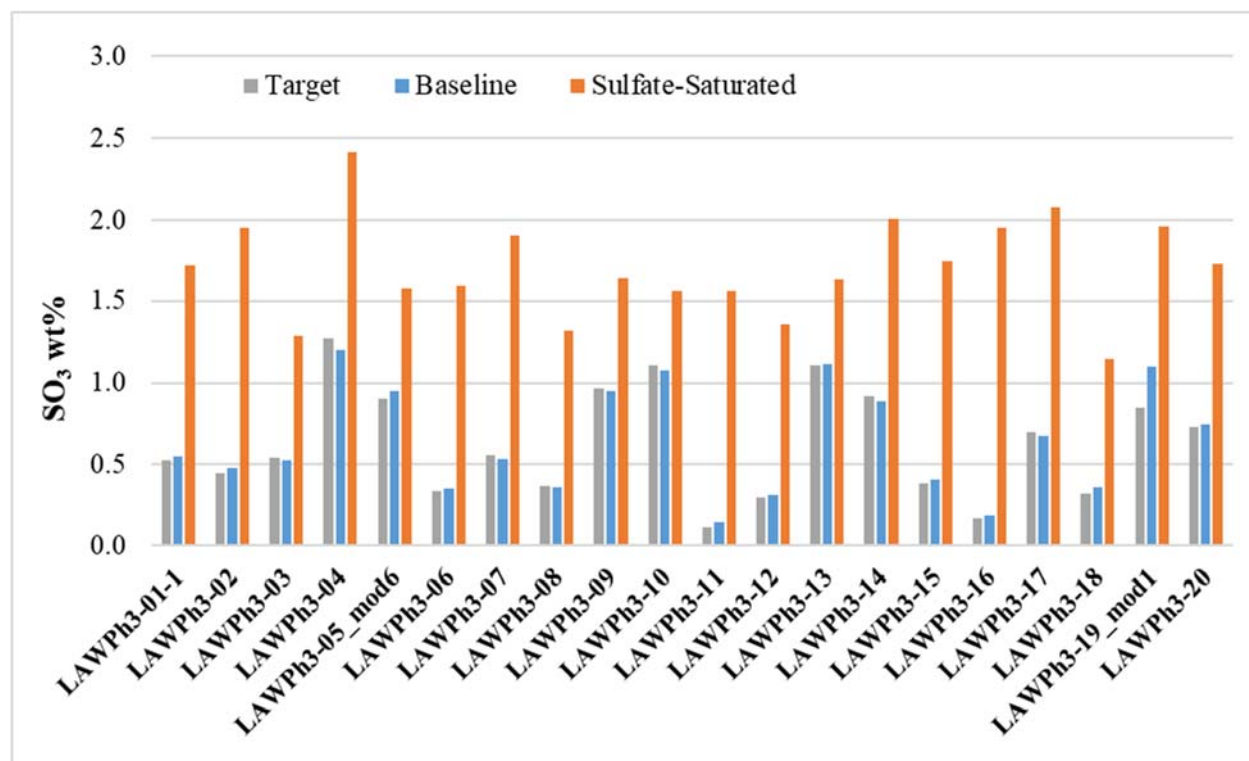


Figure 3.3. Target sulfur concentration and analyzed sulfate concentration in the baseline and the sulfate-saturated Phase 3 LAW glasses.

The SO₃ concentrations in the target baseline glasses were all below 1.5 wt%. After saturation, there was a significant increase of SO₃, which is considered the experimentally determined SO₃ solubility of the glass. In most glasses, the SO₃ solubility (i.e., the saturated SO₃ concentrations) was between 1.0 wt% and 2.0 wt%. Three glasses had a SO₃ solubility slightly above 2.0 wt%, with the highest SO₃ solubility being 2.42 wt% in glass LAWPh3-04.

Appendix H shows the full compositions after normalization of measured compositions for the sulfur-saturated glass samples. However, care must be taken in considering these compositions because some of the measured component values used to calculate these compositions may have statistically significant biases. Such biases can impart biases to other components whose measured values were unbiased. Comparisons between baseline glass compositions (Appendix C) and a sulfur-saturated glass (Appendix H) showed that after the sulfur-saturation, other major glass components only have negligible changes except when the SO₃ reaches high concentrations. For the minor components, K₂O decreases, which may be due to the salt phase, and the losses of the Cl, F, and P₂O₅ may be due to volatilization during multiple times of melting and/or extraction into the salt.

4.0 Summary

The objective of the task described in this report was to generate data on enhanced LAW glass compositions to ultimately support the development, validation, and implementation of glass property-composition models. The goal was to study LAW glasses that expand the compositional region of LAW vitrification operation (including higher waste loading and higher tolerance for recycle streams) for the full region of Hanford LAW compositions. Fifteen LAW glass components were selected for variation in the experimental work, including an “Others” component mix. Certain components were chosen for variation in the experimental work for specific reasons.

A statistical space-filling experimental design approach was used to generate a test matrix of 20 Phase 3 enhanced LAW glass compositions. Two of the matrix glasses needed some modification to their compositions to form homogeneous glasses. The chemical compositions of the glasses were analyzed to determine (1) whether any Phase 3 enhanced LAW glass(es) was(were) mis-batched, (2) if there was substantive volatility in any component(s) during glass melting, or (3) whether there were any component(s) that was(were) not completely incorporated into the glass melts. All the measured sums of oxides for the study glasses fell within the interval of 95 to 100 wt%, indicating reasonable recovery of the glass components. Some degree of scatter among the Al_2O_3 , B_2O_3 , Na_2O , K_2O , SiO_2 , P_2O_5 , and ZrO_2 measurements was noted for the study glasses.

In measuring the crystal fraction of the glasses after isothermal treatment at 950°C for 24 ± 2 h, all but three glasses were found to be XRD amorphous. All three of the crystal-containing glasses contained nasicon (ideally $\text{Na}_2\text{Zr}_2\text{SiP}_2\text{O}_{12}$), and one of the glasses also contained combeite (ideally $\text{Na}_2\text{Ca}_2\text{Si}_3\text{O}_9$) and grossular (ideally $\text{Ca}_3\text{Al}_2(\text{SiO}_4)_3$), for a total crystallinity ranging from 0 to 13.4 wt%.

For crystal analysis after the CCC profile, XRD scans of CCC glass samples identified several crystal types in four different glasses. The major crystalline phases appearing (in the glasses containing crystals) were combeite and nepheline (ideally $\text{NaAlSi}_3\text{O}_8$).

The density values ranged from 2.61 to 2.72 g/cm^3 . The viscosity values, as determined the VFT equation for a temperature of 1150°C , ranged from 10.47 to 59.26 poise. This range falls within the 10 to 100 P limits that were set for the design of the glasses for LAW Phase 3. The measured values for electrical conductivity, as well as those determined by the Arrhenius fit, at 1150°C ranged from 52 to 71 S/m.

A review of the PCT data shows that 5 of the quenched glasses and 9 of the CCC glasses had normalized release values for boron (NR [B]) that are higher than the WTP contract limit of 2 g/m^2 , while 5 of the quenched glasses and 8 of the CCC glasses had normalized release values for sodium (NR [Na]) that are higher than the WTP contract limit. The test matrix was developed in this way so that PCT-composition models would be able to predict whether a given glass meets the PCT limits. It appeared that the CCC heat treatment had little impact on the PCT results as compared to the quenched versions of the study glasses.

A total of 6 of the 20 quenched glasses and 8 of the 20 CCC glasses were fully altered during the VHT. Of the quenched glasses, 11 exceeded the 50 $\text{g}/\text{m}^2/\text{d}$ VHT limit. There was a wide distribution of corrosion rates, with values varying from 0.59 to >270 $\text{g}/\text{m}^2/\text{d}$ for quenched glasses and from 3.54 to >329 $\text{g}/\text{m}^2/\text{d}$ for CCC glasses.

The SO_3 concentrations measured in the baseline glasses varied from 0.138 to 1.203 wt%. After sulfur-saturation, there was a significant increase of SO_3 , which is considered the experimentally determined SO_3 solubility of the glass. The SO_3 solubility (i.e., the saturated SO_3 concentrations) ranged between 1.143 and 2.416 wt%.

5.0 References

10 CFR 830, *Energy/Nuclear Safety Management*. U.S. Code of Federal Regulations.

ASME NQA-1-2012, *Quality Assurance Requirements for Nuclear Facility Applications*. American Society of Mechanical Engineers, New York, NY.

ASTM C1285, *Standard Test Methods for Determining Chemical Durability of Nuclear, Hazardous, and Mixed Waste Glasses and Multiphase Glass Ceramics: The Product Consistency Test (PCT)*. ASTM International, West Conshohocken, PA.

ASTM C1663, *Standard Test Method for Measuring Waste Glass or Glass Ceramic Durability by Vapor Hydration Test*. ASTM International, West Conshohocken, PA.

ASTM C1720, *Standard Test Method for Determining Liquidus Temperature of Immobilized Waste Glasses and Simulated Waste Glasses*. ASTM International, West Conshohocken, PA.

ASTM C693-93, *Standard Test Method for Density of Glass by Buoyancy*. ASTM International, West Conshohocken, PA.

Borkowski JJ and GF Piepel. 2009. "Uniform designs for highly constrained mixture experiments." *Journal of Quality Technology* 41(1):35-47.

CRC Handbook of Chemistry and Physics, 89th ed, Taylor & Francis, 2008-2009.

Crum JV, TB Edwards, RL Russell, PJ Workman, MJ Schweiger, RF Schumacher, DE Smith, DK Peeler, and JD Vienna. 2012. "DWPF Startup Frit Viscosity Measurement Round Robin Results." *Journal of the American Ceramic Society* 95(7):2196-2205.

DOE. 2000. *Design, Construction, and Commissioning of the Hanford Tank Waste Treatment and Immobilization Plant*. Contract DE-AC27-01RV14136, as amended, U.S. Department of Energy, Office of River Protection, Richland, WA.

DOE. 2020. Amendment 18 to Memorandum "Enhanced WTP Glass Composition Envelope Development," signed by F Taylor. Inter-Entity Work Order M0ORV00129, U.S. Department of Energy, Office of River Protection, Richland, WA.

DOE Order 414.1D, *Quality Assurance*. U.S. Department of Energy, Washington, D.C.

Ebert WL and SF Wolfe. 1999. *Round-robin Testing of a Reference Glass for Low-Activity Waste Forms*. ANL-99/22, Argonne National Laboratory, Argonne, IL.

Fox KM, TB Edwards, MC Riley, and WT Riley. 2020. *Characterization of Hanford LAW Phase 3 Glasses*. SRNL-STI-2018-00649, Rev. 2, Westinghouse Savannah River Company, Aiken, SC.

Jin T, DS Kim, LP Darnell, BL Weese, NL Canfield, M Bliss, MJ Schweiger, JD Vienna, and AA Kruger. 2019. "A Crucible Salt Saturation Method for Determining Sulfur Solubility in Glass Melt." *International Journal of Applied Glass Science* 10:92-102.

Joseph R, E Gui, and S Ba. 2015. "Maximum projection designs for computer experiments." *Biometrika*. 102(2):371-380.

Piepel GF, SK Cooley, IS Muller, H Gan, I Joseph, and IL Pegg. 2007. *ILAW PCT, VHT, Viscosity, and Electrical Conductivity Model Development*. VSL-07R1230-1, Rev. 0, Vitreous State Laboratory, The Catholic University of America, Washington, D.C.

Piepel GF, SK Cooley, JD Vienna, and JV Crum. 2015. "Designing a Mixture Experiment when the Components are Subject to a Nonlinear Multiplecomponent Constraint." *Quality Engineering*. doi:10.1080/08982112.2015.1086003.

Piepel GF, SK Cooley, JD Vienna, and JV Crum. 2016. *Experimental Design for Hanford Low-Activity Waste Glasses with High Waste Loading*. PNNL-24391, Rev. 1, Pacific Northwest National Laboratory, Richland, WA.

Russell RL, T Jin, BP McCarthy, LP Darnell, DE Rinehart, CC Bonham, V Gervasio, JM Mayer, CL Arendt, JB Lang, MJ Schweiger, and JD Vienna. 2017. *Enhanced Hanford Low-Activity Waste Glass Property Data Development: Phase 1*. PNNL-26630, Rev. 0, Pacific Northwest National Laboratory, Richland, WA.

Russell RL, BP McCarthy, SK Cooley, GF Piepel, EA Cordova, SE Sannoh, V Gervasio, MJ Schweiger, JB Lang, CH Skidmore, CE Lonergan, BA Stanfill, JM Meline, and JD Vienna. 2020. *Enhanced Hanford Low-Activity Waste Glass Property Data Development: Phase 2*. PNNL-28838, Rev. 2, Pacific Northwest National Laboratory, Richland, WA.

Vienna JD, P Hrma, A Jiricka, DE Smith, TH Lorier, IA Reamer, and RL Schultz. 2001. *Hanford Immobilized LAW Product Acceptance Testing: Tanks Focus Area Results*. PNNL-13744, Pacific Northwest National Laboratory, Richland, WA.

Vienna JD, DS Kim, IS Muller, GF Piepel, and AA Kruger. 2014. "Toward Understanding the Effect of Low-Activity Waste Glass Composition on Sulfur Solubility." *Journal of the American Ceramic Society* 97(10):3135-3142.

Appendix A – Images of As-Quenched Glasses

The photos in this appendix show quenched samples of each Phase 3 enhanced low-activity waste (LAW) glass after melting in a Pt 10%Rh crucible twice at the specified melt temperature. The two modified glasses, LAWPh3-05_mod6 and LAWPh3-19_mod1, are shown in Section 2.2.

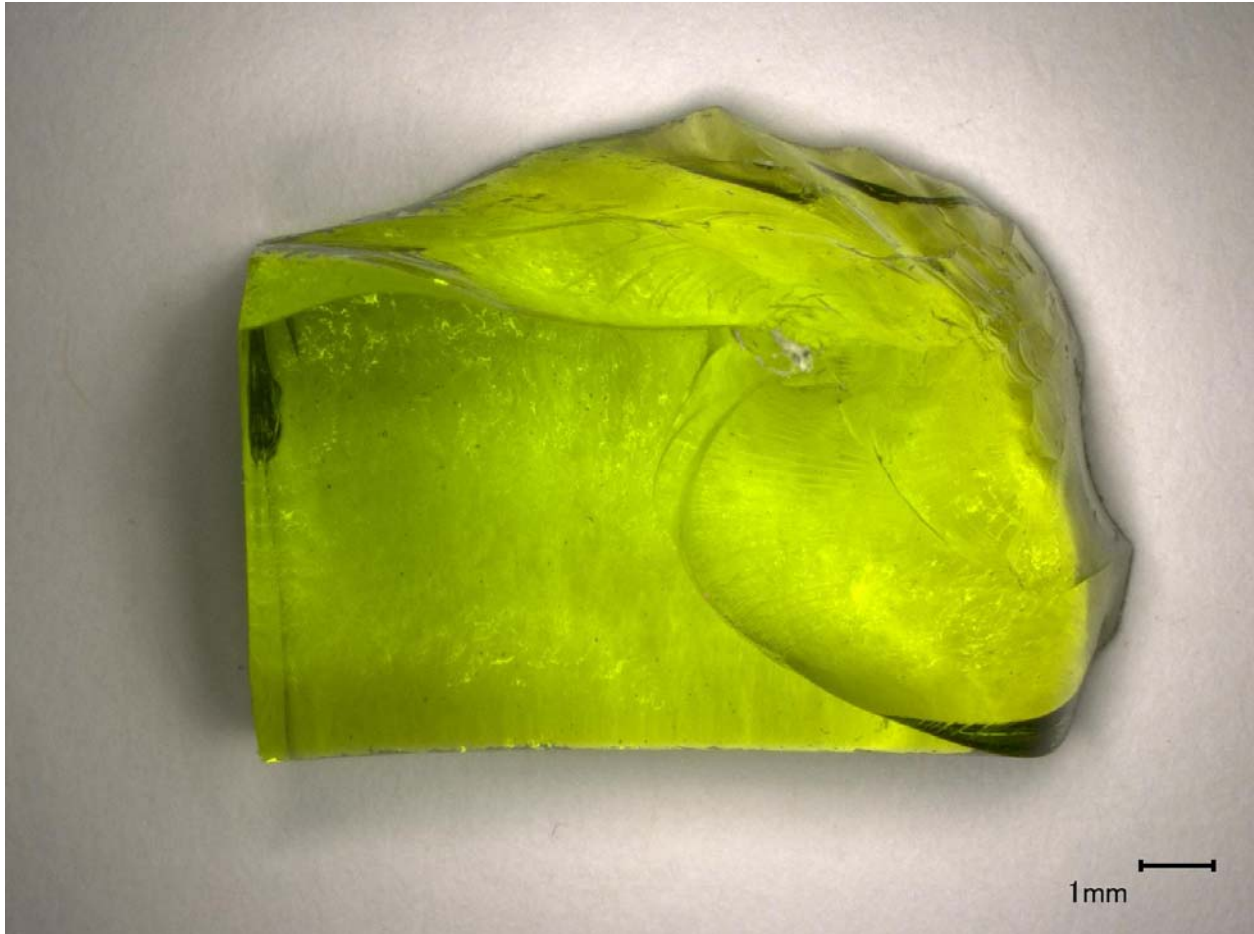


Figure A.1. Image of glass LAWPh3-01-1-Q after the second melt at 1150°C for 1 h.

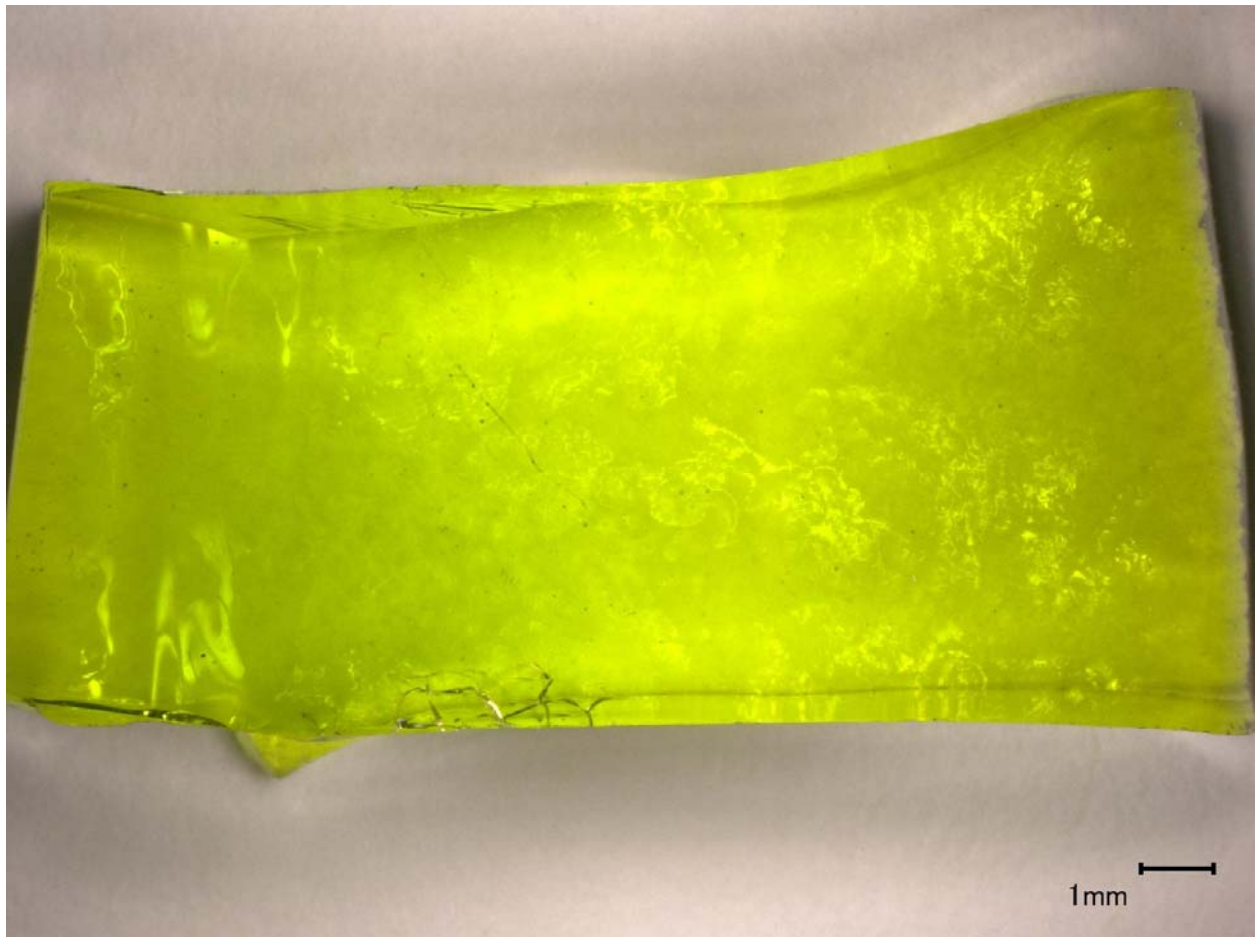


Figure A.2. Image of LAWPh3-02-Q, morphology of second melt at 1150°C for 1 h.

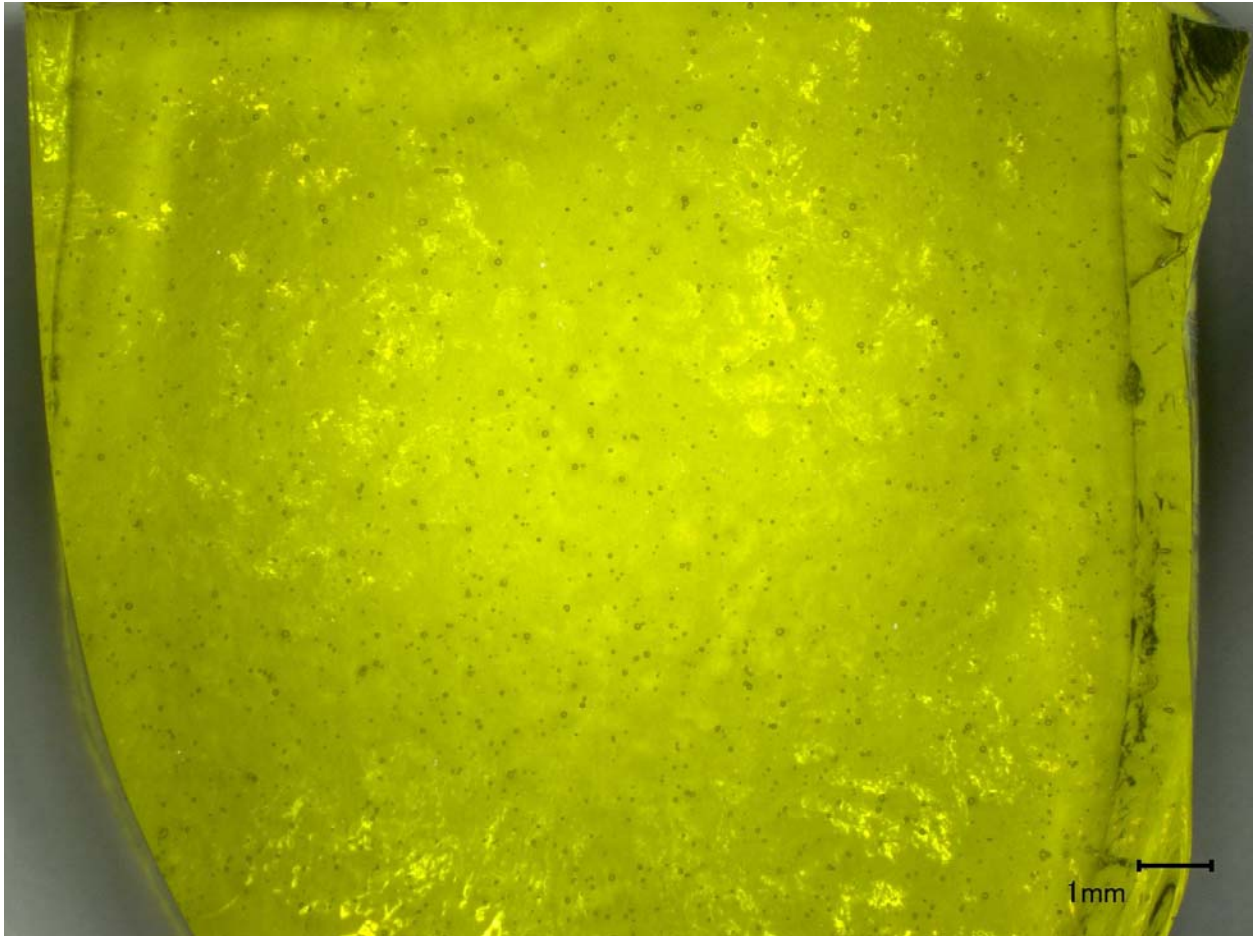


Figure A.3. Image of LAWPh3-03-Q, morphology of second melt at 1150°C for 1 h.

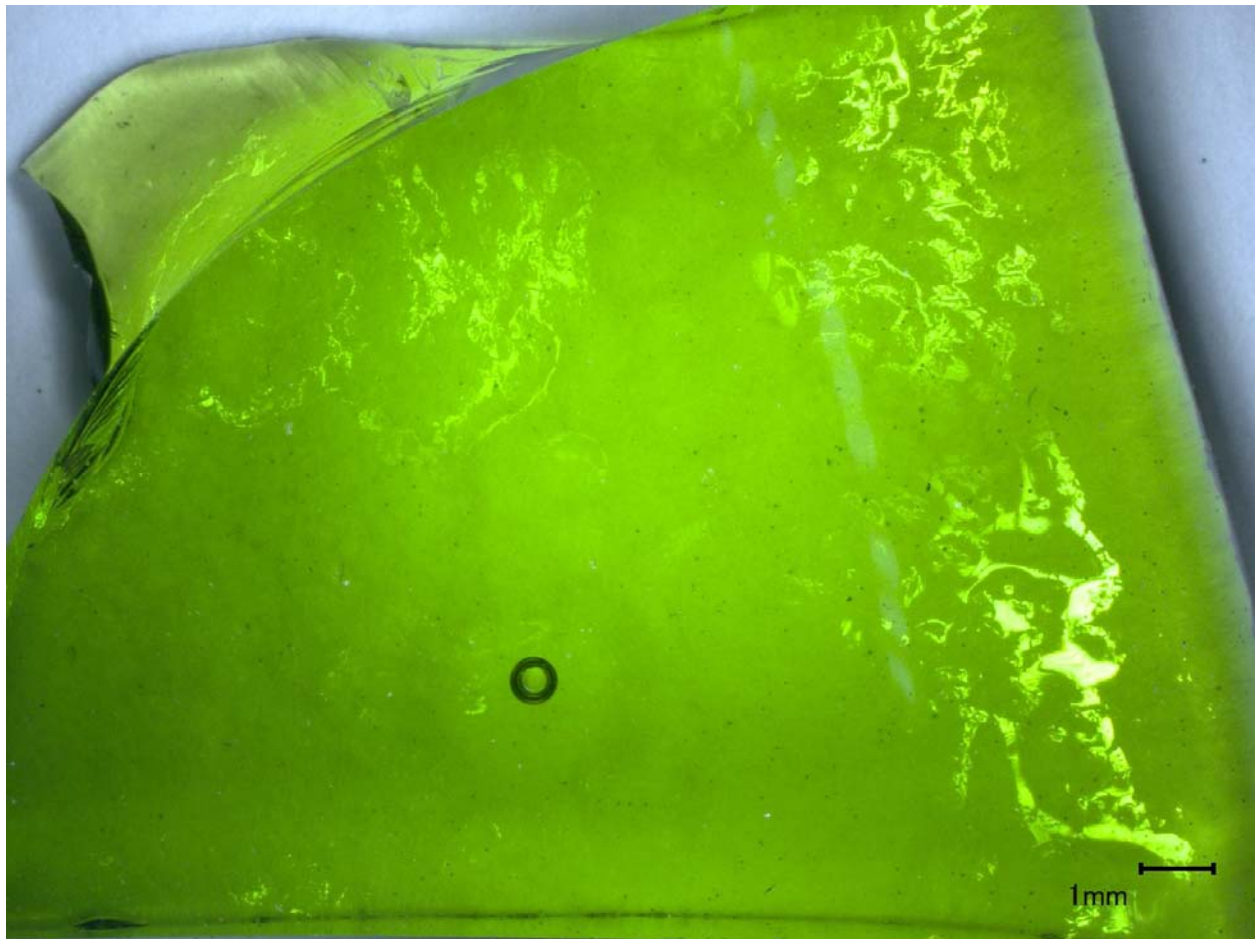


Figure A.4. Image of LAWPh3-04-Q, morphology of second melt at 1150°C for 1 h.

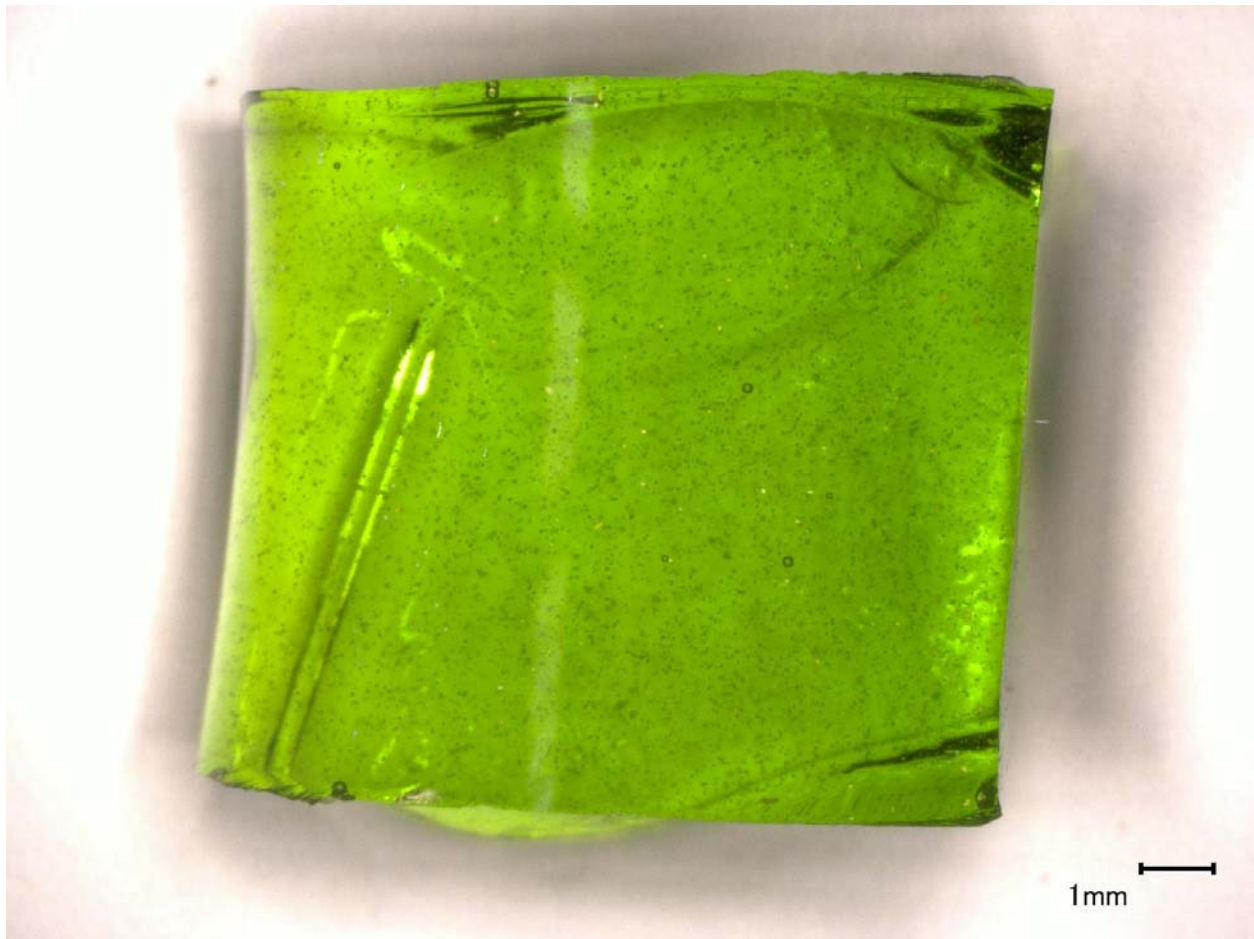


Figure A.5. Image of LAWPh3-06-Q, morphology of second melt at 1150°C for 1 h.

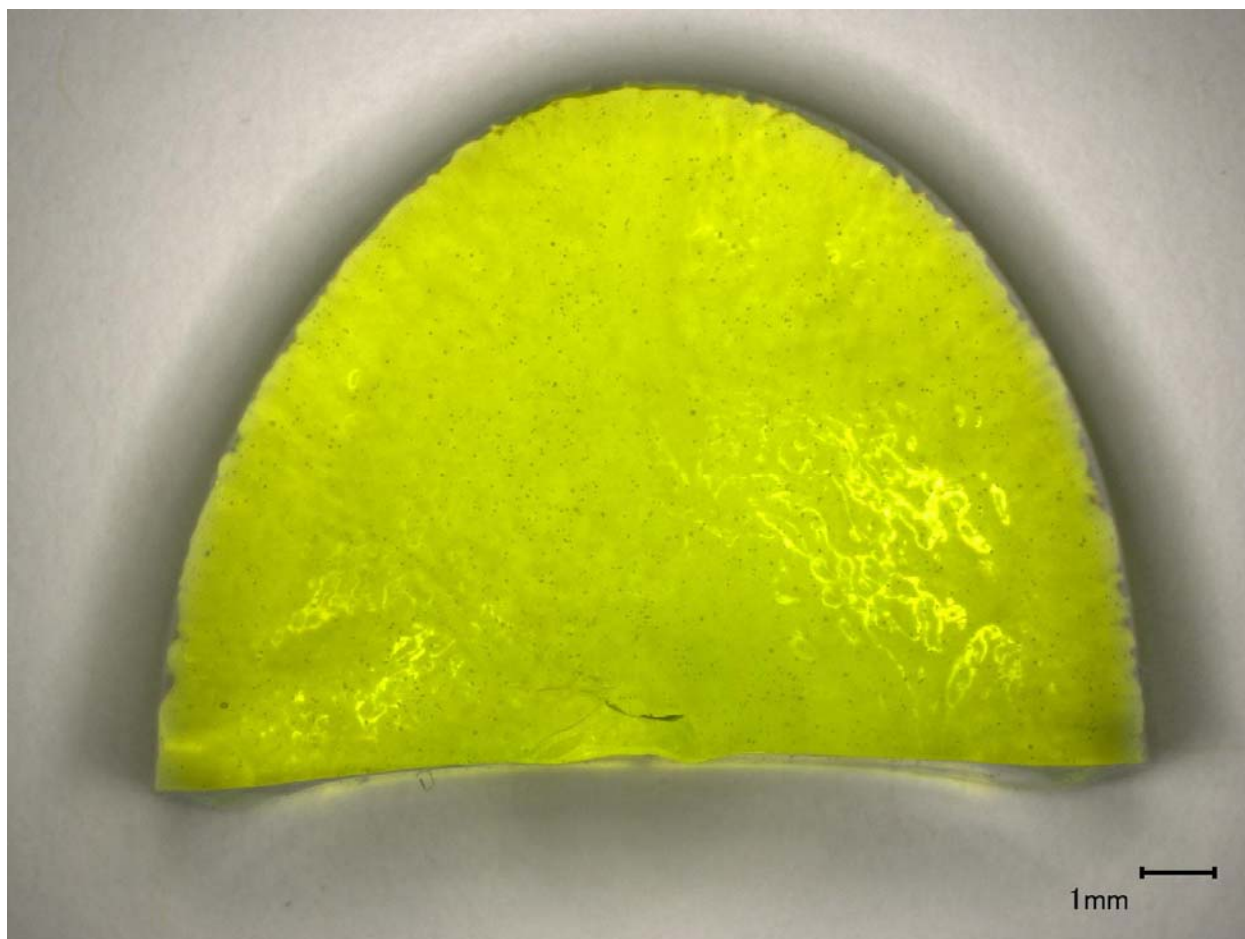


Figure A.6. Image of LAWPh3-07-Q, morphology of second melt at 1150°C for 1 h.

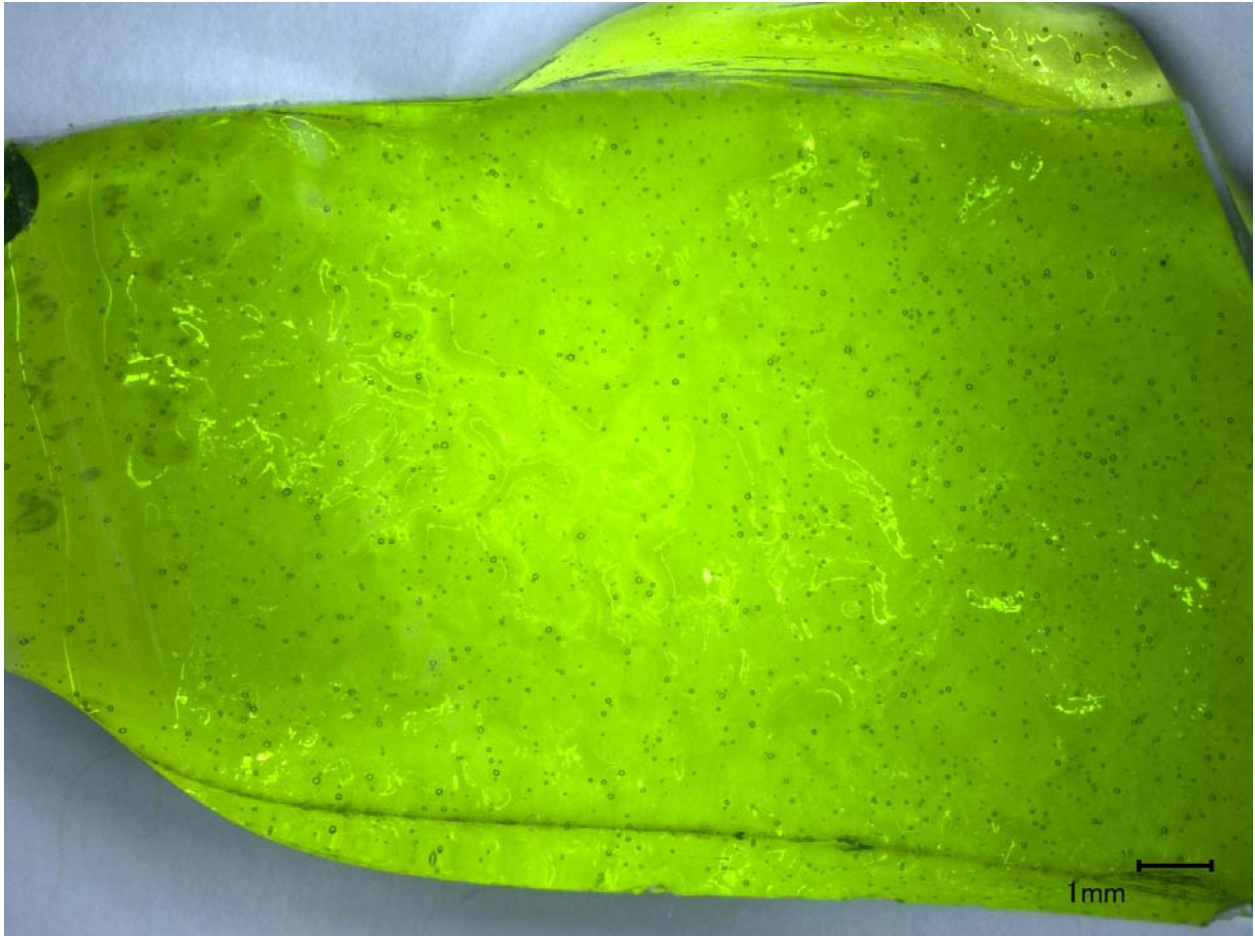


Figure A.7. Image of LAWPh3-08-Q, morphology of second melt at 1150°C for 1 h.



Figure A.8. Image of LAWPh3-09-Q, morphology of second melt at 1150°C for 1 h.

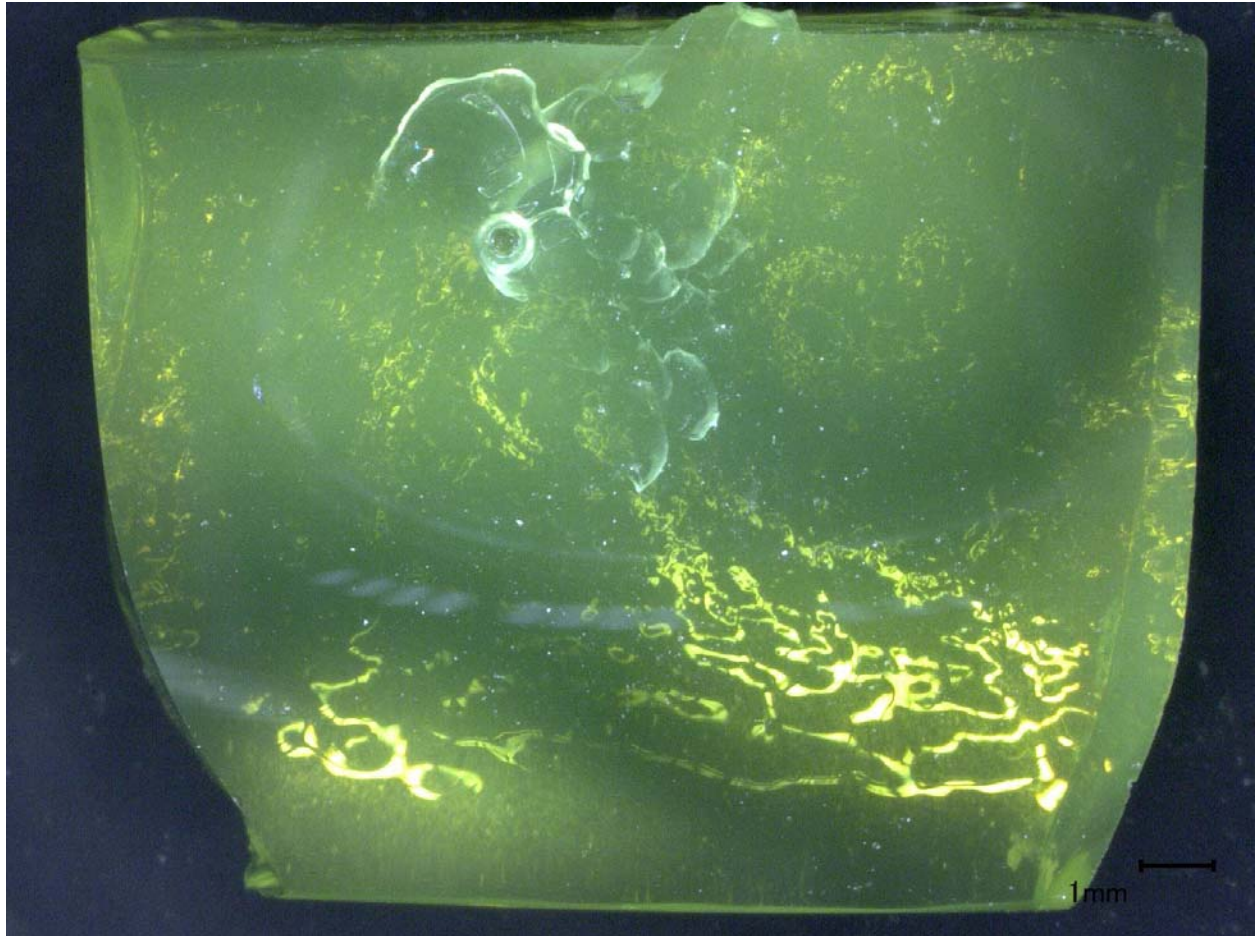


Figure A.9. Image of LAWPh3-10-Q, morphology of third melt at 1200°C for 1 h.

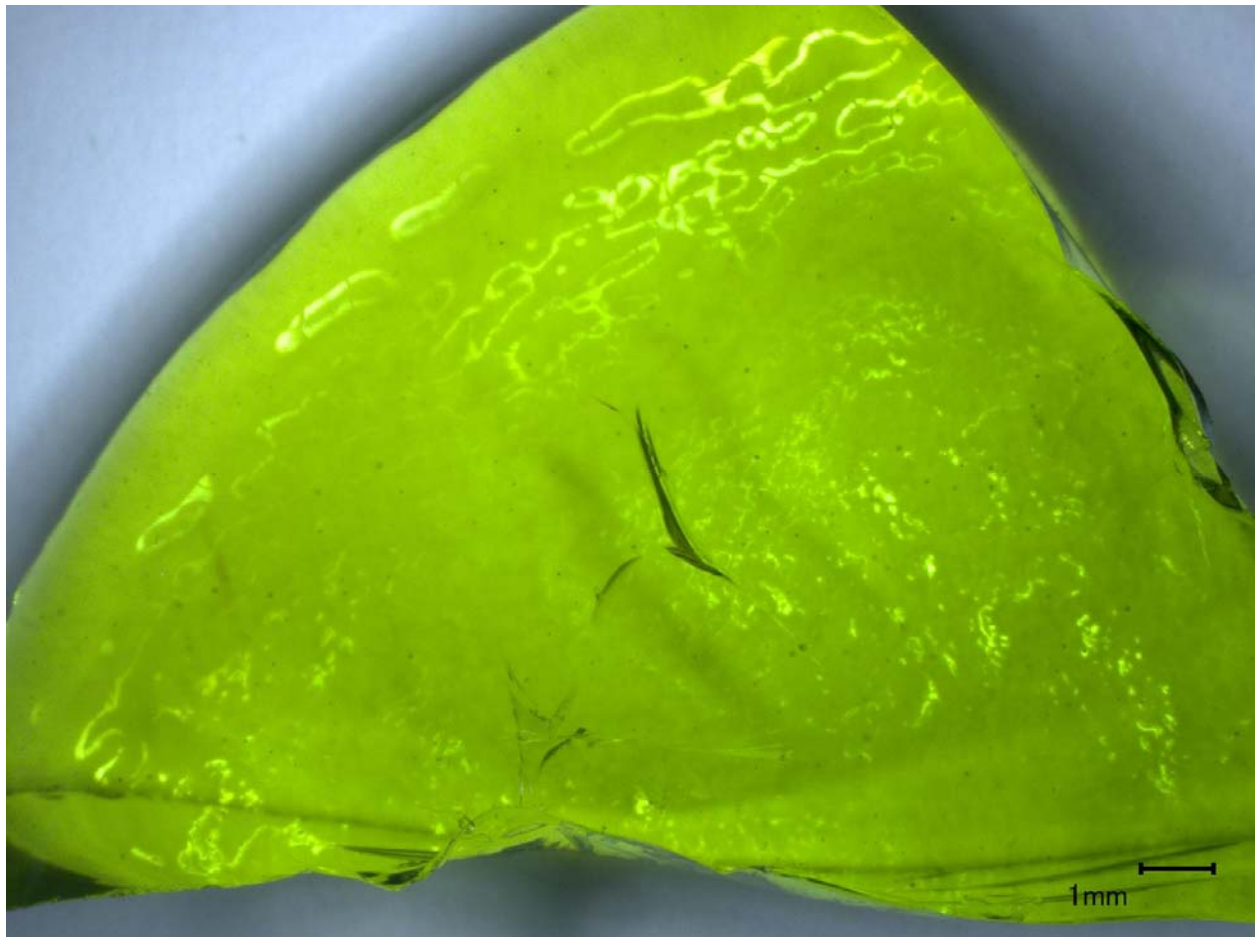


Figure A.10. Image of LAWPh3-11-Q, morphology of second melt at 1150°C for 1 h.



Figure A.11. Image of LAWPh3-12-Q, morphology of second melt at 1250°C for 1 h.

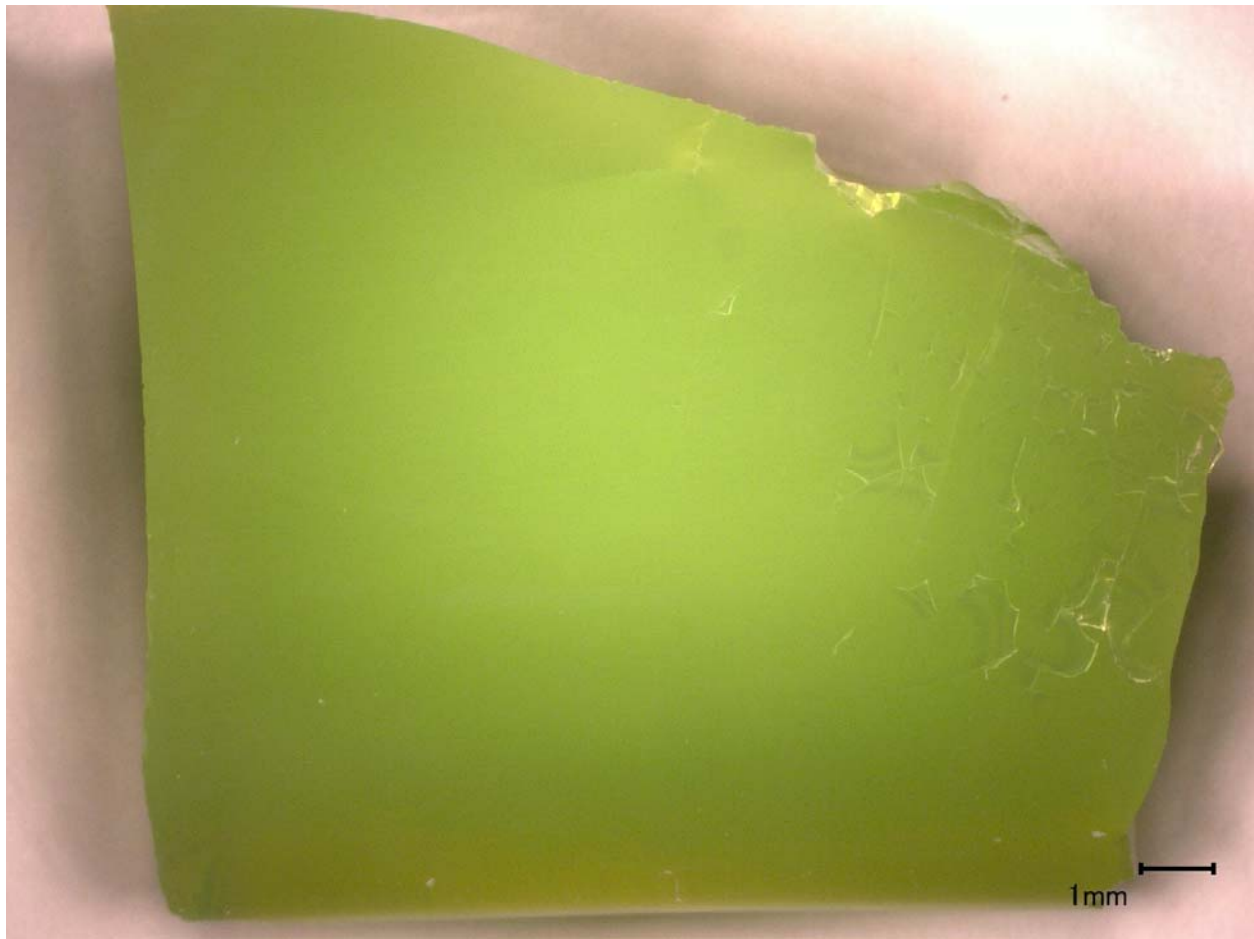


Figure A.12. Image of LAWPh3-13-Q, morphology of second melt at 1150°C for 1 h.

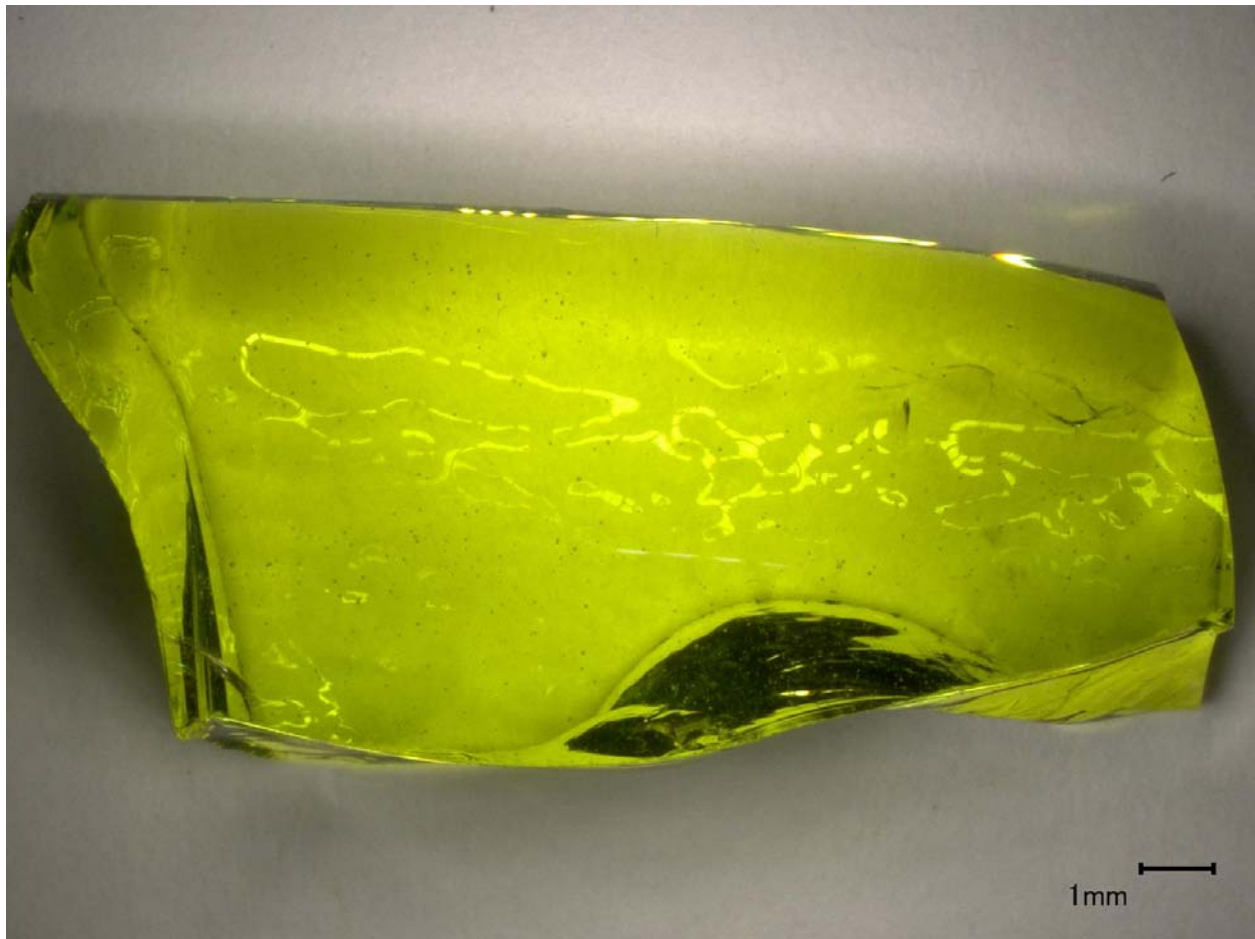


Figure A.13. Image of LAWPh3-14-Q, morphology of second melt at 1150°C for 1 h.

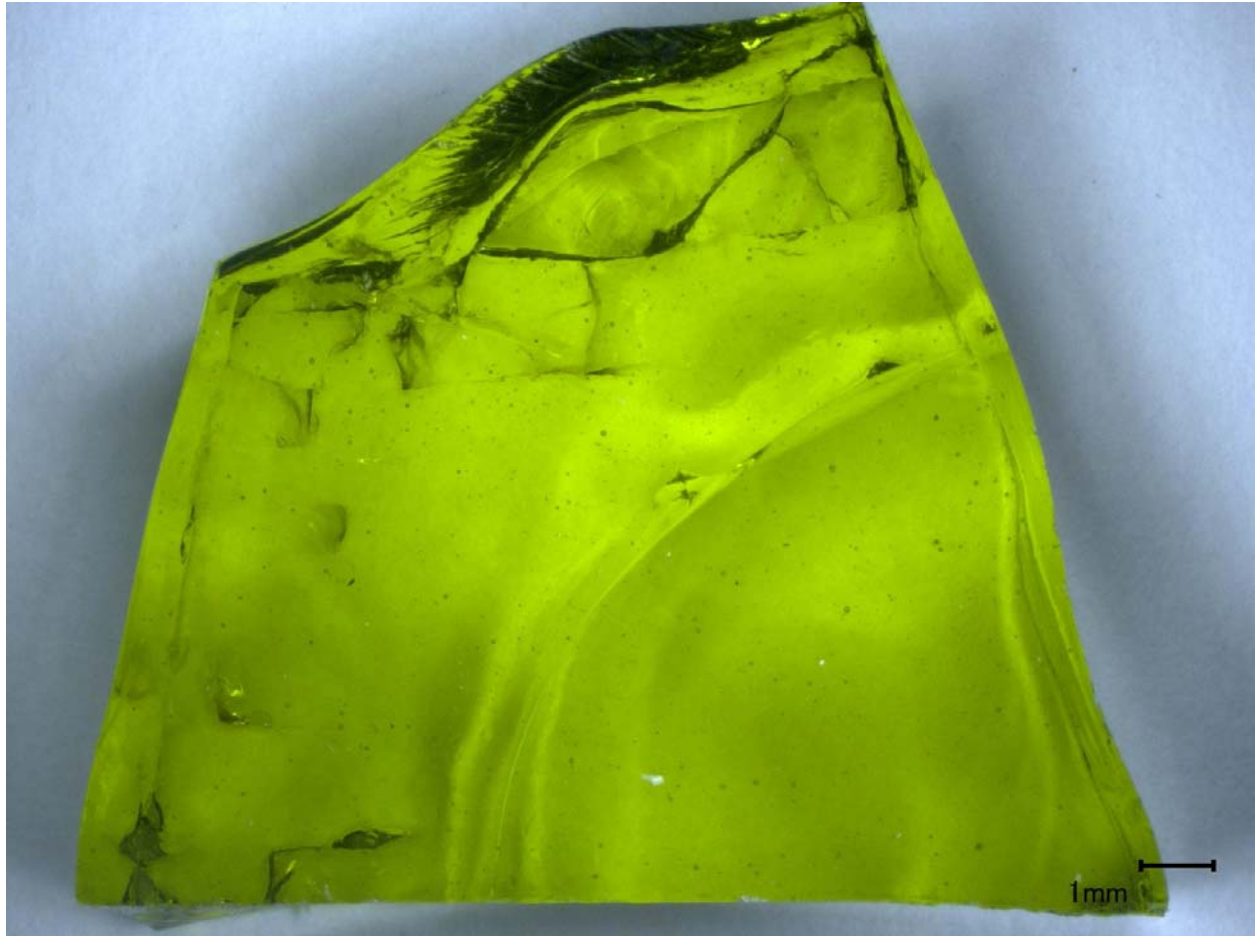


Figure A.14. Image of LAWPh3-15-Q, morphology of second melt at 1150°C for 1 h.

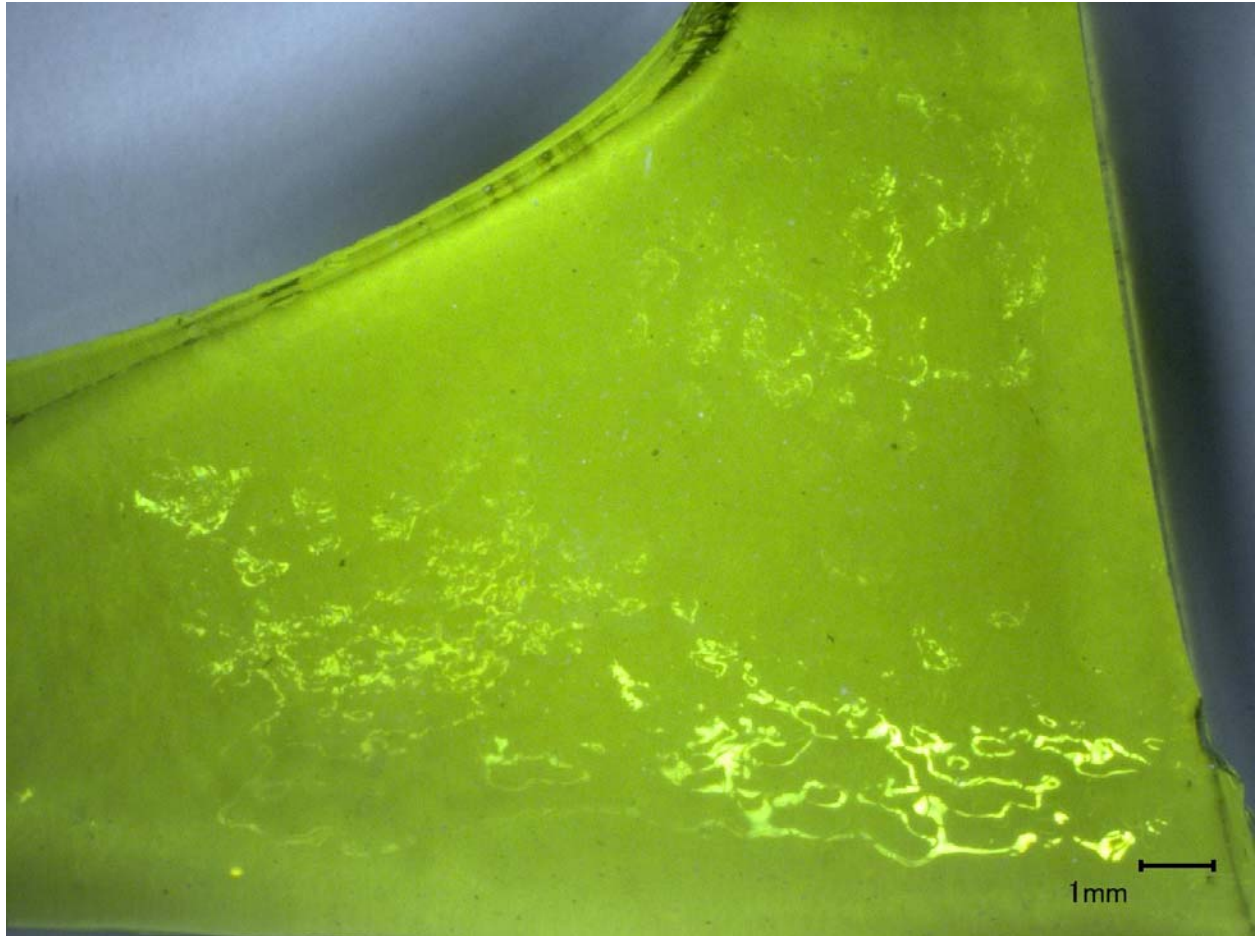


Figure A.15. Image of LAWPh3-16-Q, morphology of second melt at 1150°C for 1 h.



Figure A.16. Image of LAWPh3-17-Q, morphology of second melt at 1150°C for 1 h.



Figure A.17. Image of LAWPh3-18-Q, morphology of second melt at 1250°C for 1 h.

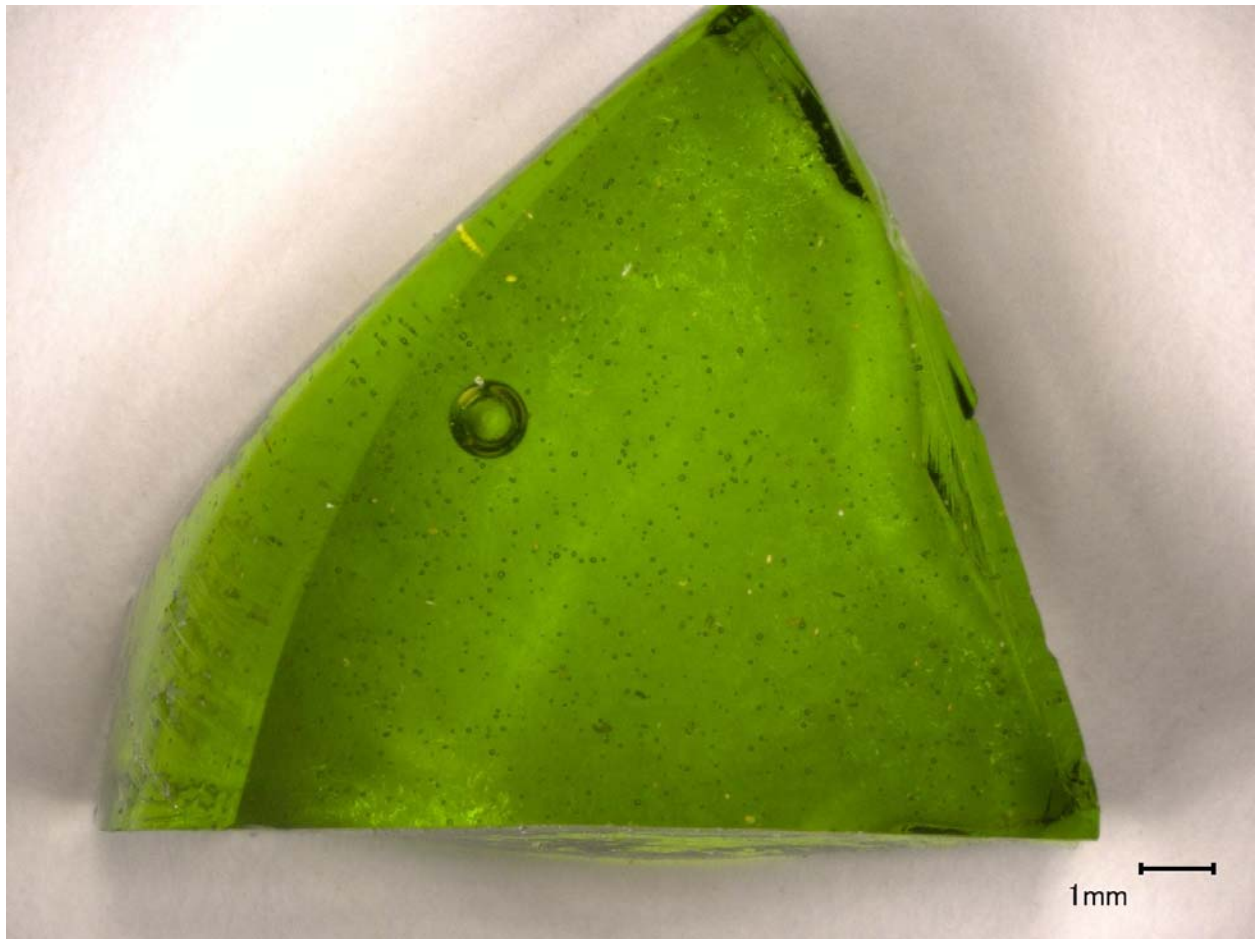


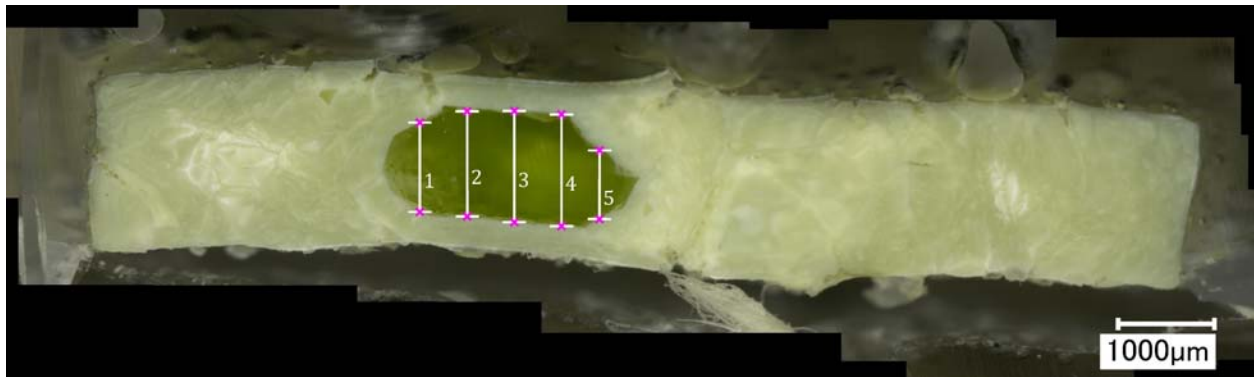
Figure A.18. Image of LAWPh3-20-Q, morphology of fourth melt at 1250°C for 1 h.

Appendix B – Images of Samples Post-Vapor Hydration Test

This appendix shows cross-section photos of both quenched (Q) and container centerline cooling (CCC) samples after Vapor Hydration Test (VHT). These photos show the variation in corrosion with the samples. Many of the tested samples were extensively corroded with unmeasurable VHT corrosion depth.

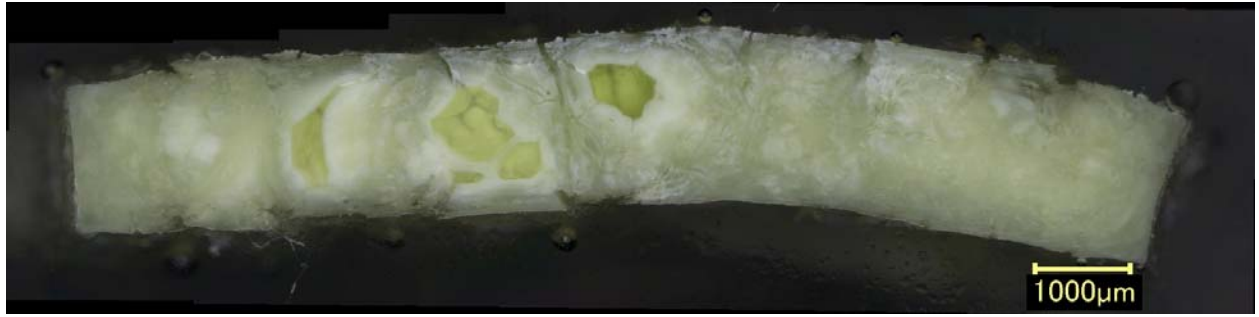


(a) Quenched



(b) CCC

Figure B.1. LAWPh3-01 samples after VHT for 24 days.

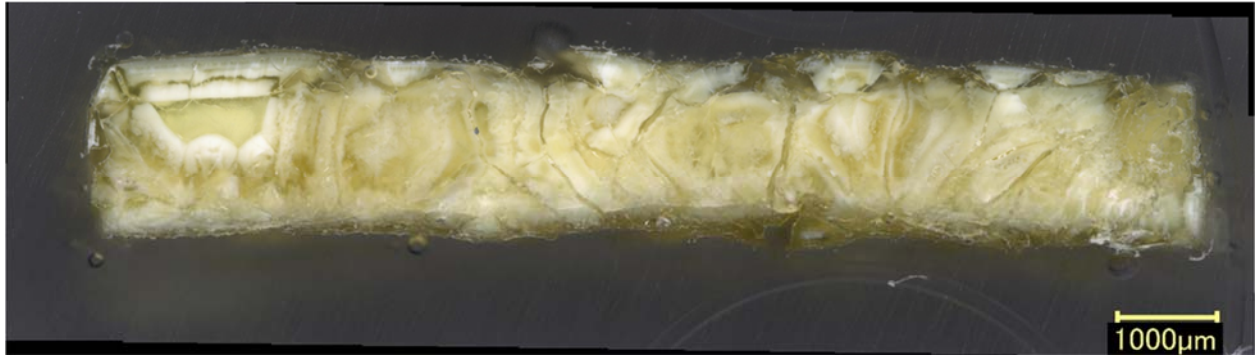


(a) Quenched

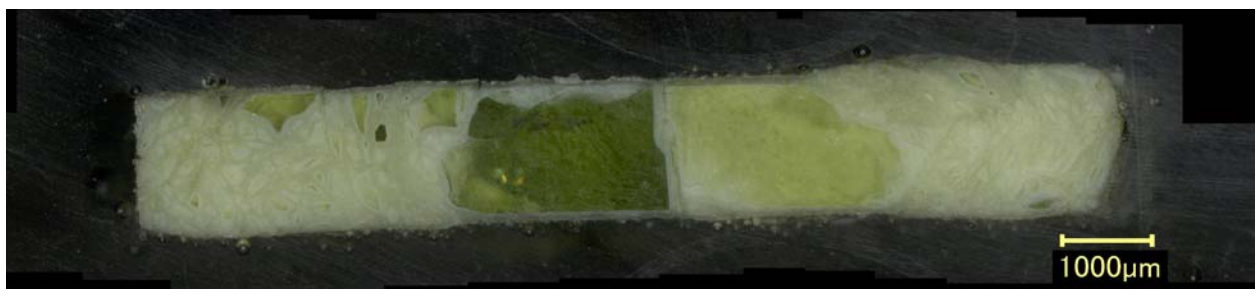


(b) CCC

Figure B.2. LAWPh3-02 samples after VHT for 7 days.

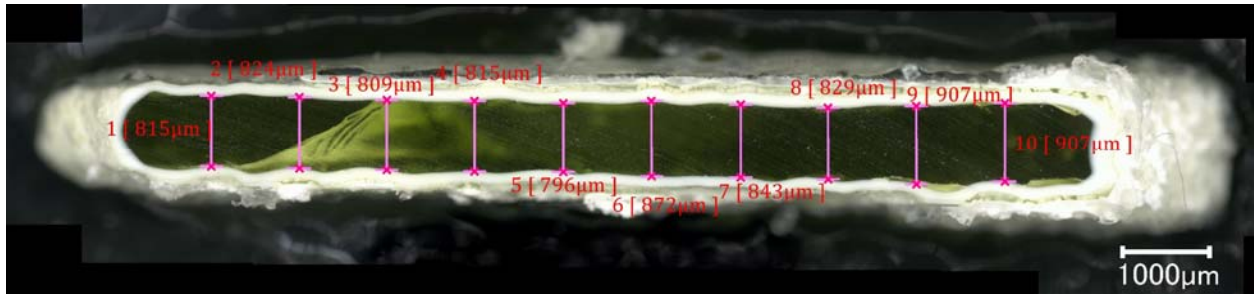


(a) Quenched

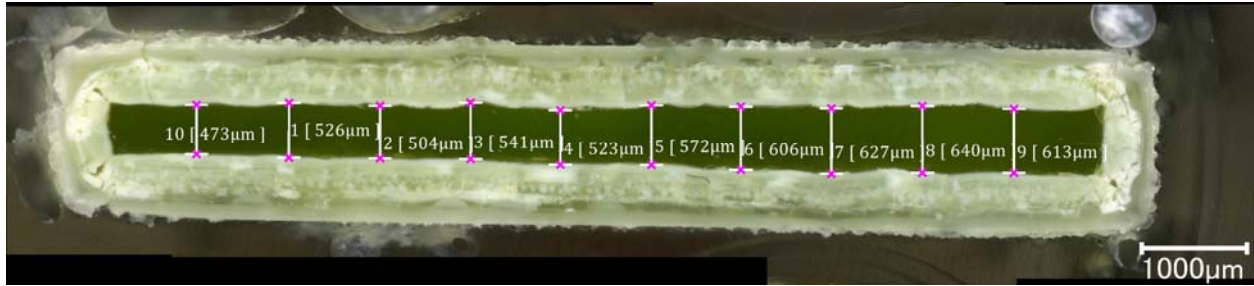


(b) CCC

Figure B.3. LAWPh3-03 samples after VHT for 7 days.

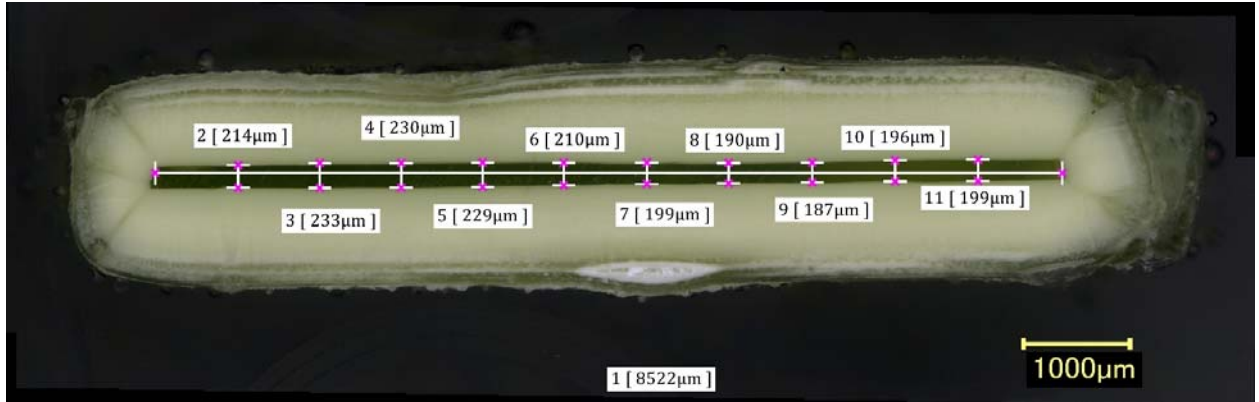


(a) Quenched

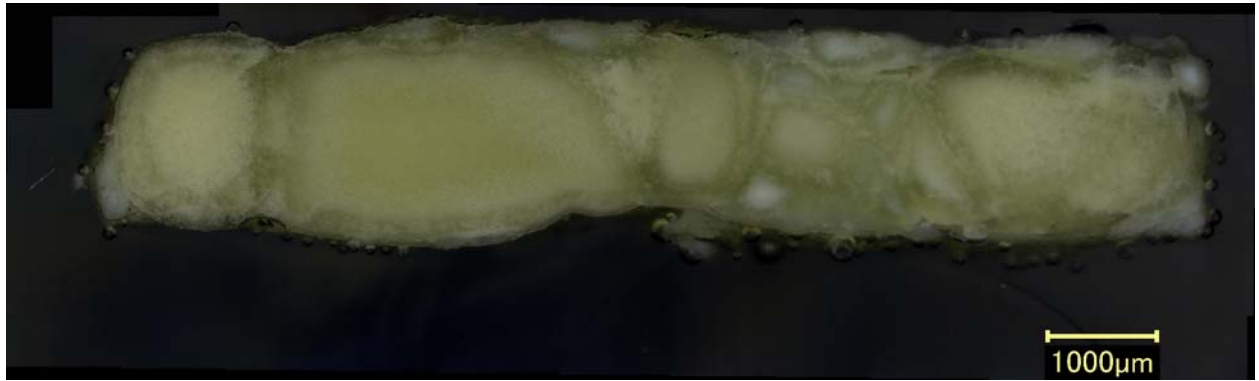


(b) CCC

Figure B.4. LAWPh3-04 samples after VHT for 24 days.

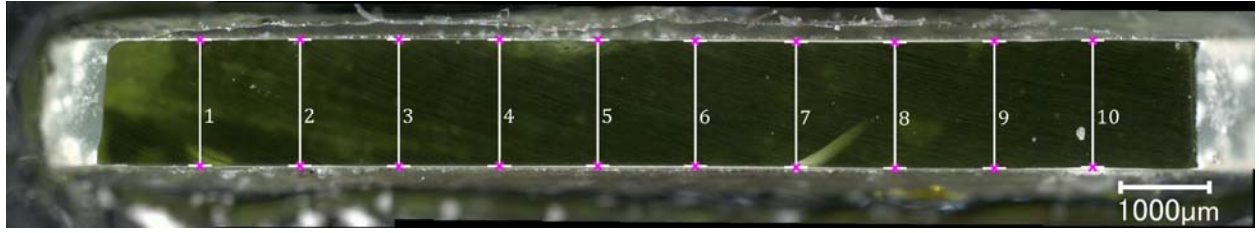


(a) Quenched

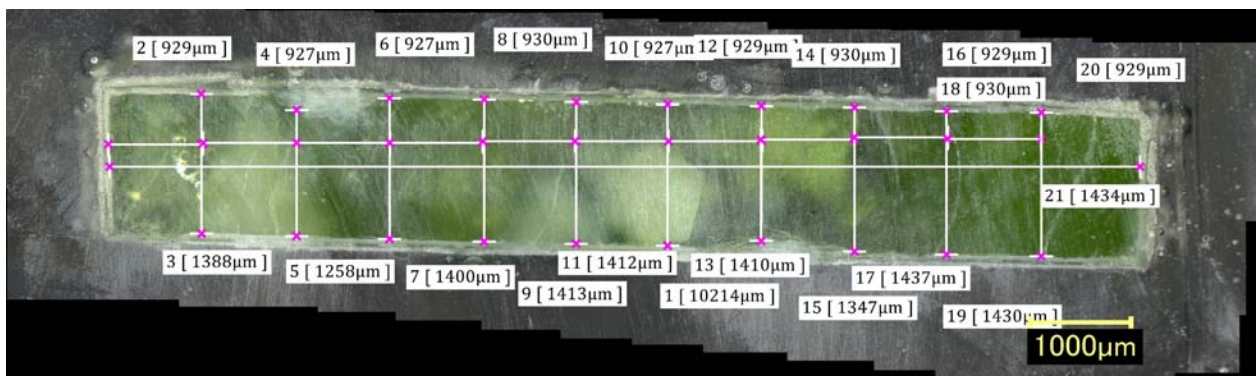


(b) CCC

Figure B.5. LAWPh3-05_mod6 samples after VHT for 24 days.

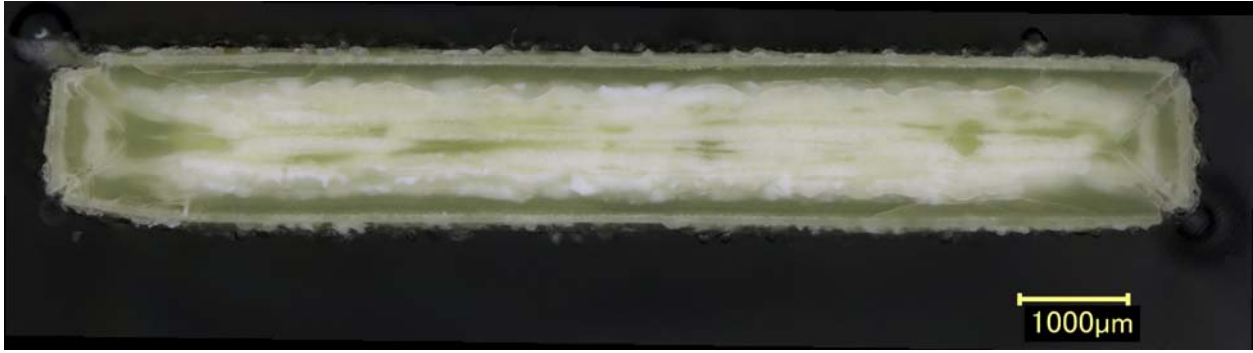


(a) Quenched

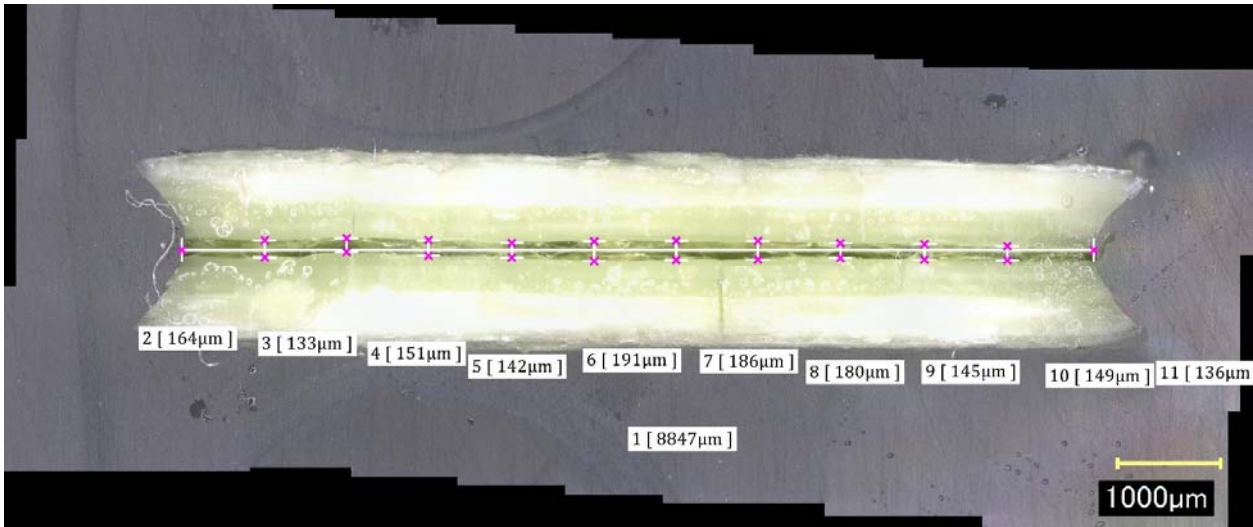


(b) CCC

Figure B.6. LAWPh3-06 samples after VHT for 24 days.

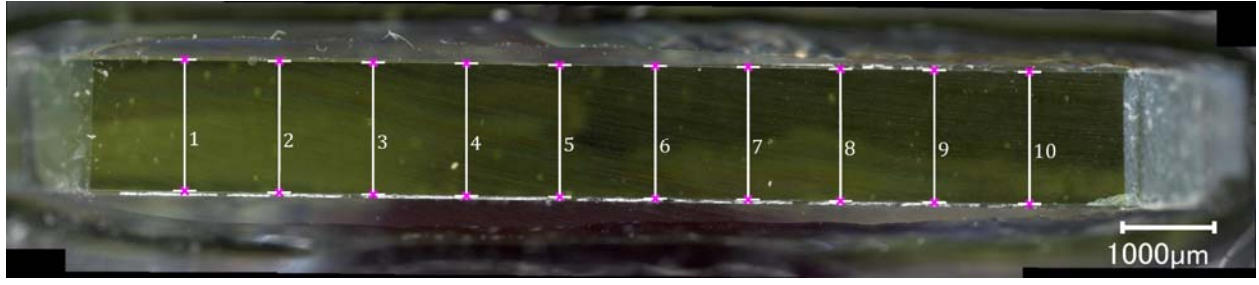


(a) Quenched

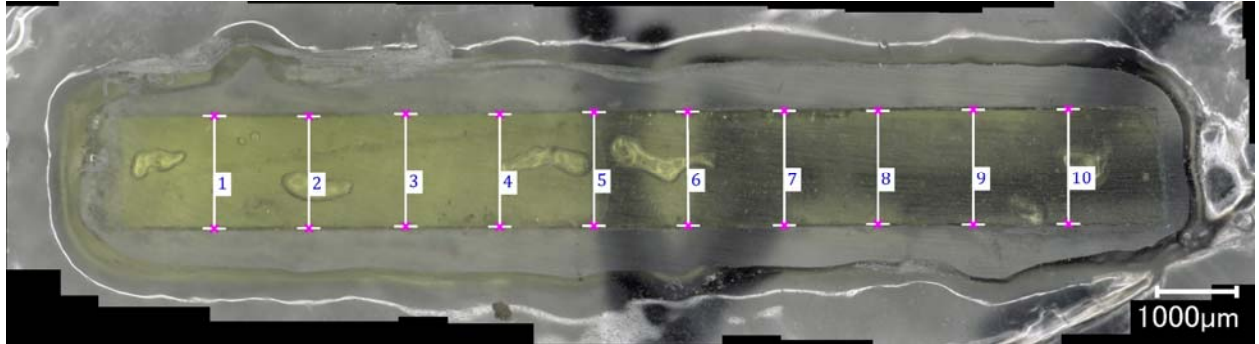


(b) CCC

Figure B.7. LAWPh3-07 samples after VHT for 7 days.

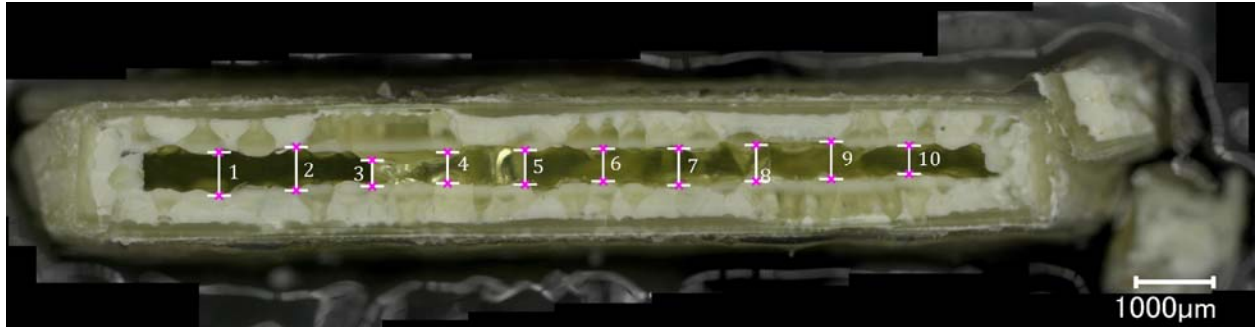


(a) Quenched

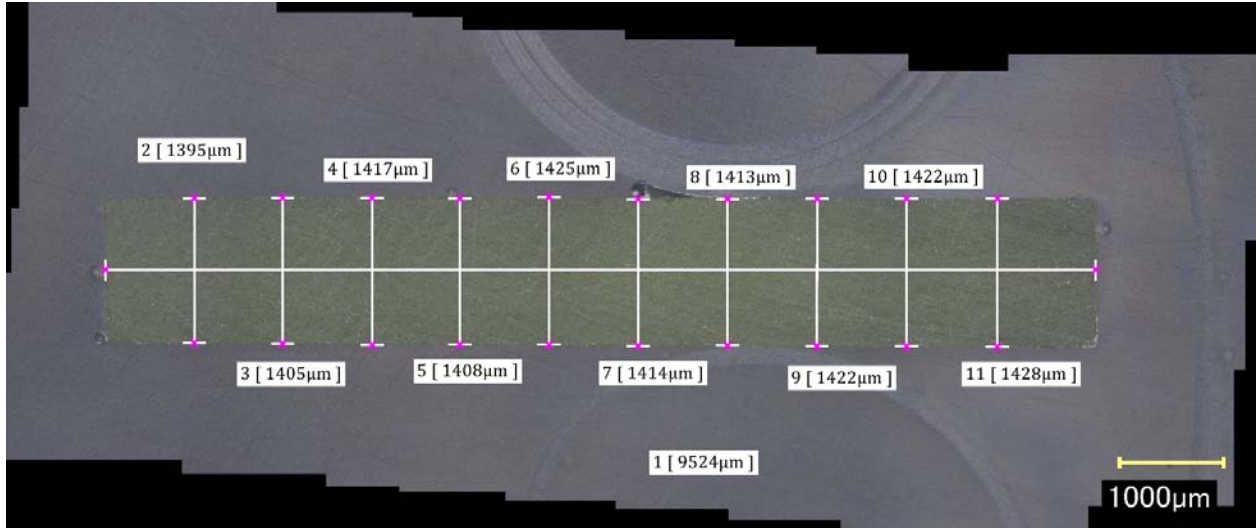


(b) CCC

Figure B.8. LAWPh3-08 samples after VHT for 24 days.

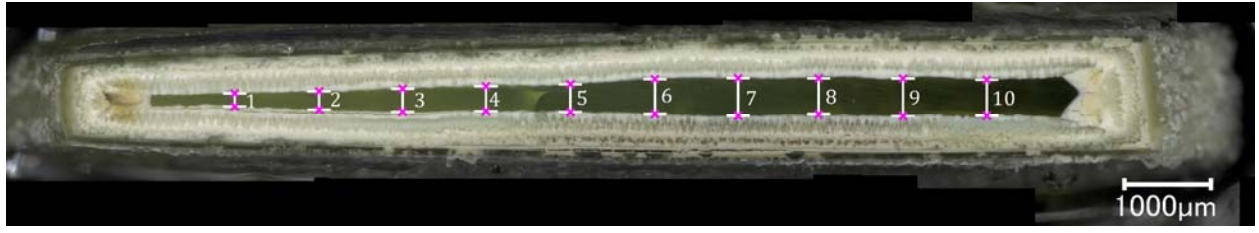


(a) Quenched

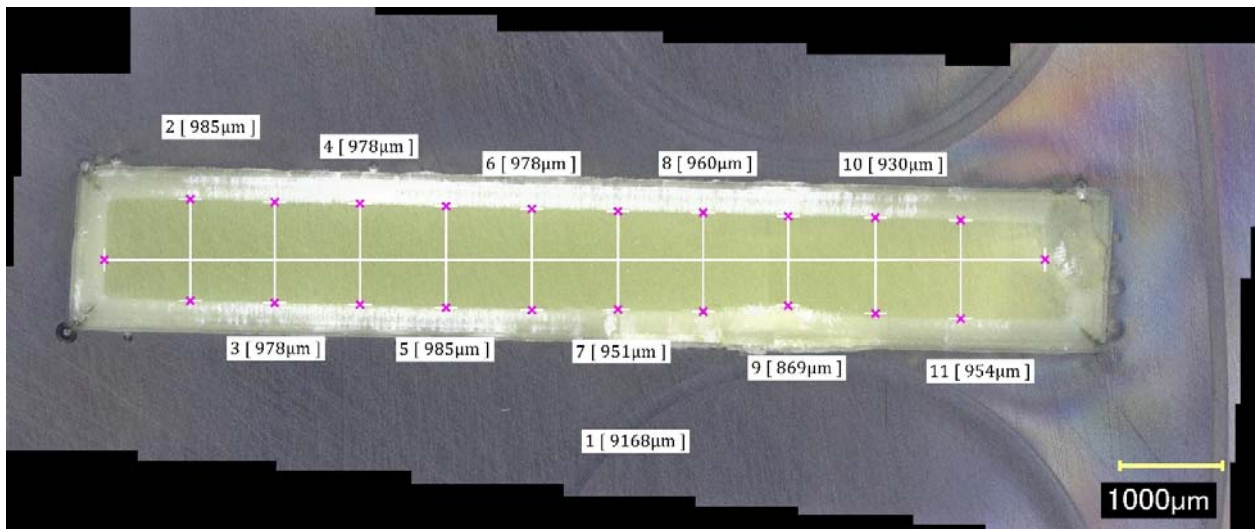


(b) CCC

Figure B.9. LAWPh3-09 samples after VHT for 7 days.



(a) Quenched



(b) CCC

Figure B.10. LAWPh3-10 samples after VHT for 24 days.

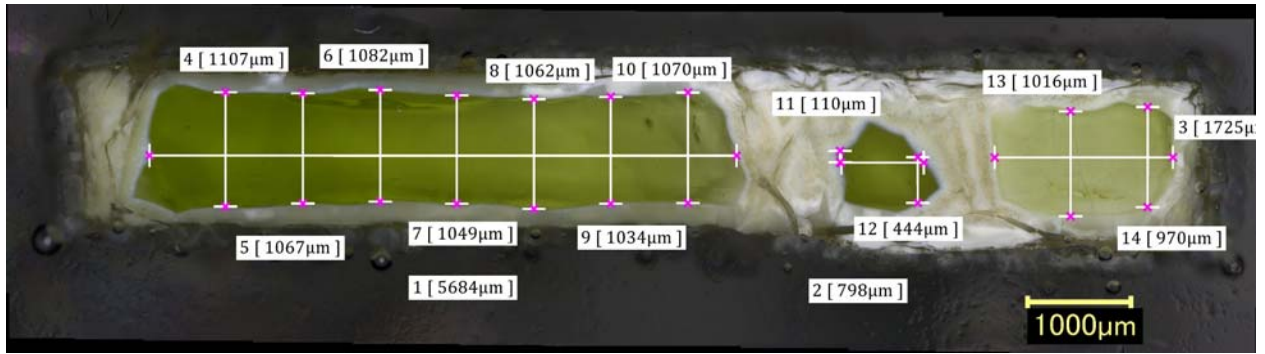


(a) Quenched

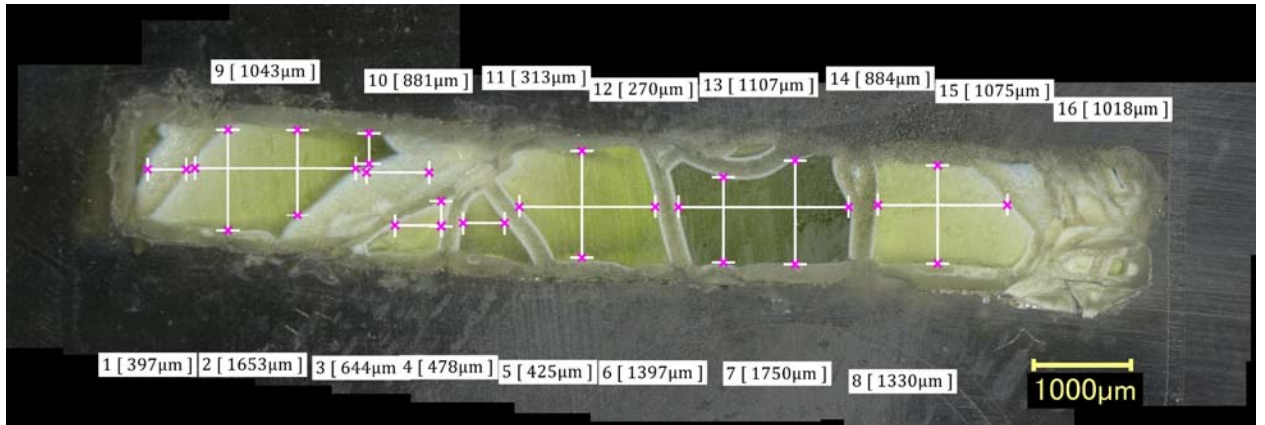


(b) CCC

Figure B.11. LAWPh3-11 samples after VHT for 7 days.

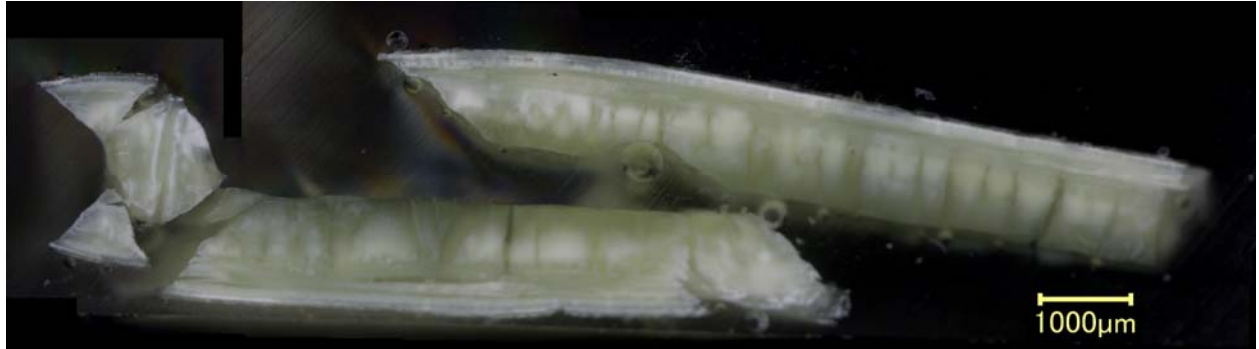


(a) Quenched



(b) CCC

Figure B.12. LAWPh3-12 samples after VHT for 7 days.

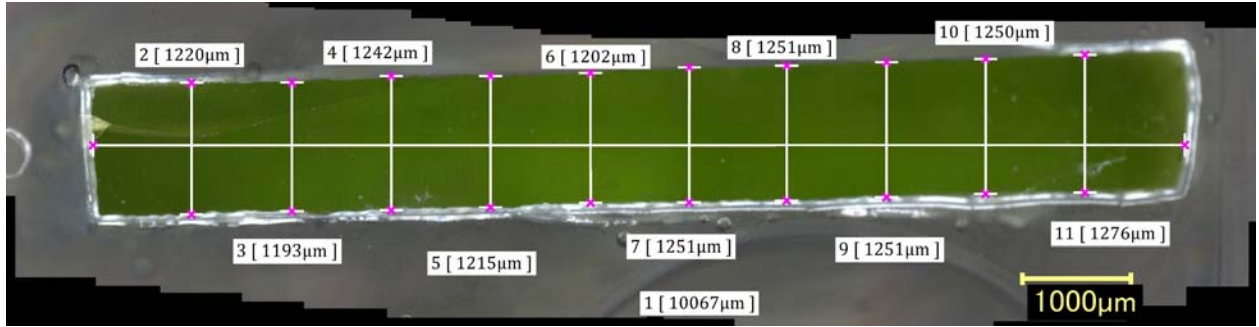


(a) Quenched

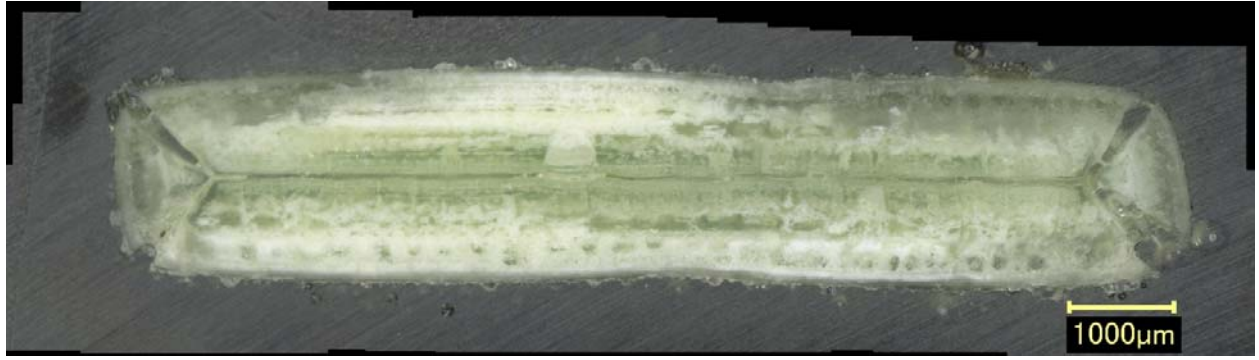


(b) CCC

Figure B.13. LAWPh3-013 samples after VHT for 7 days.

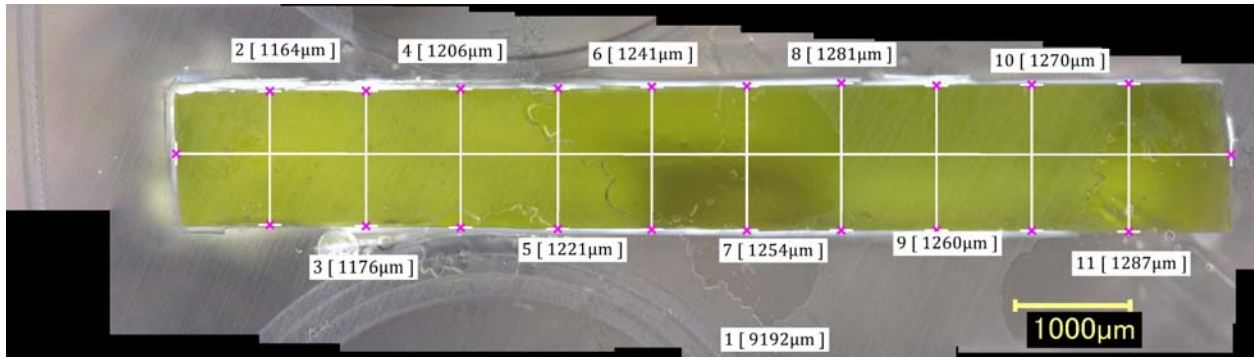


(a) Quenched

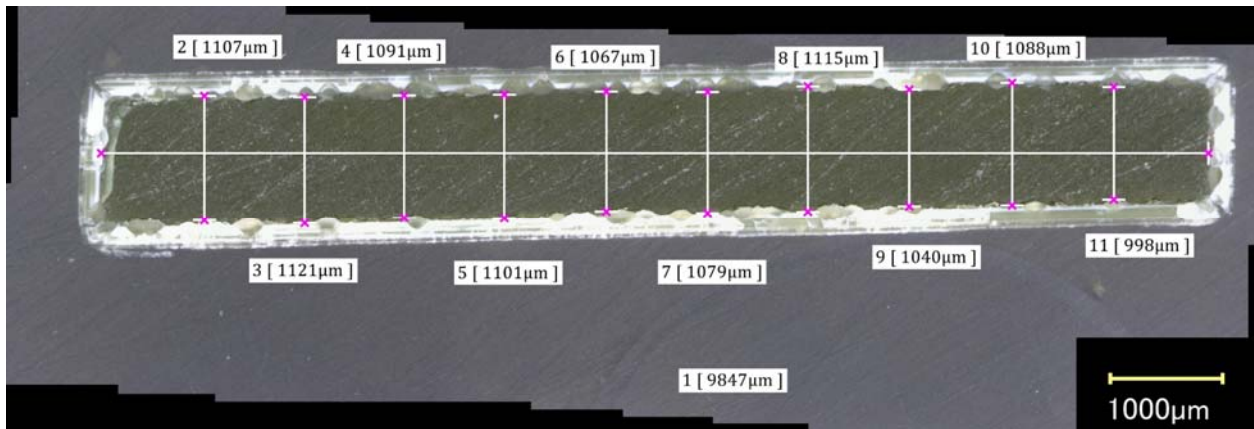


(b) CCC

Figure B.14. LAWPh3-014 samples after VHT for 7 days.

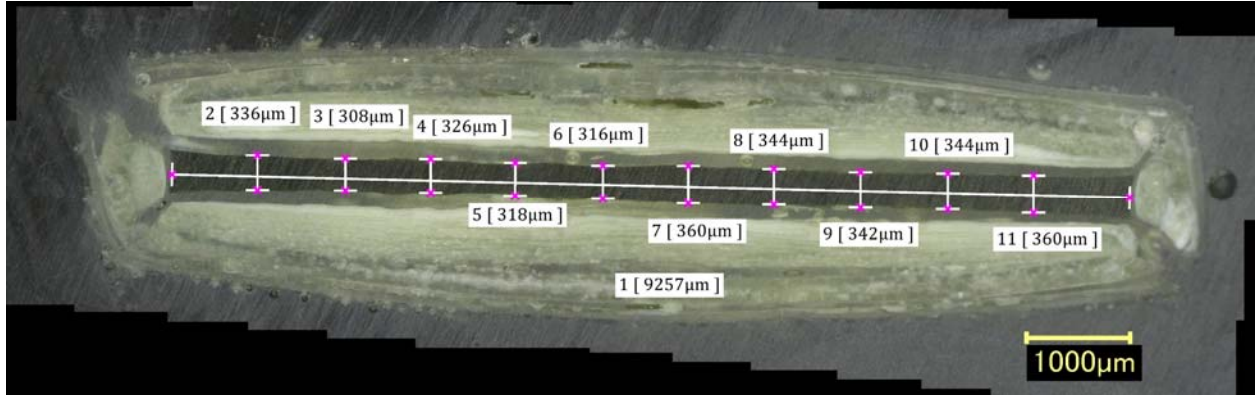


(a) Quenched



(b) CCC

Figure B.15. LAWPh3-015 samples after VHT for 24 days.

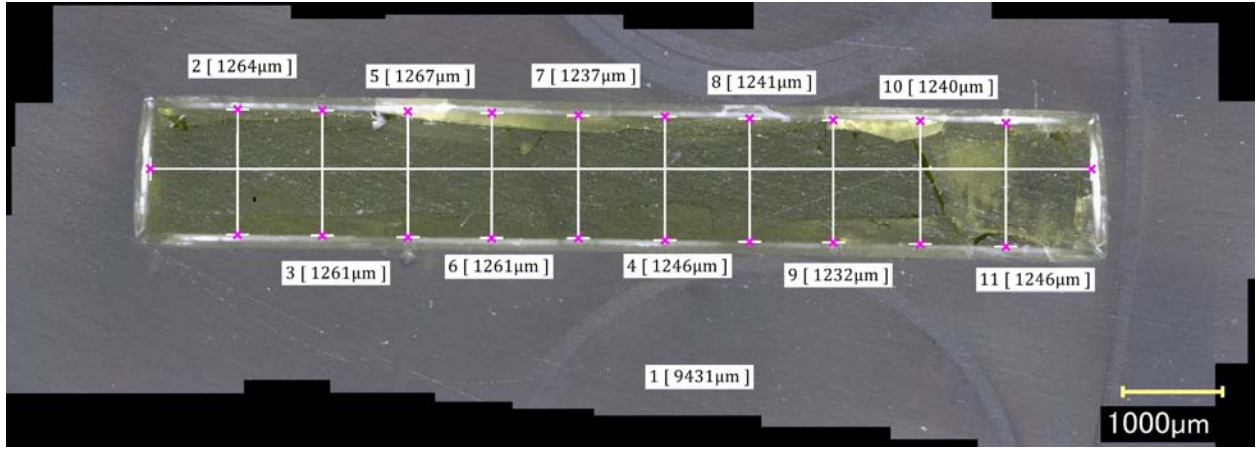


(a) Quenched

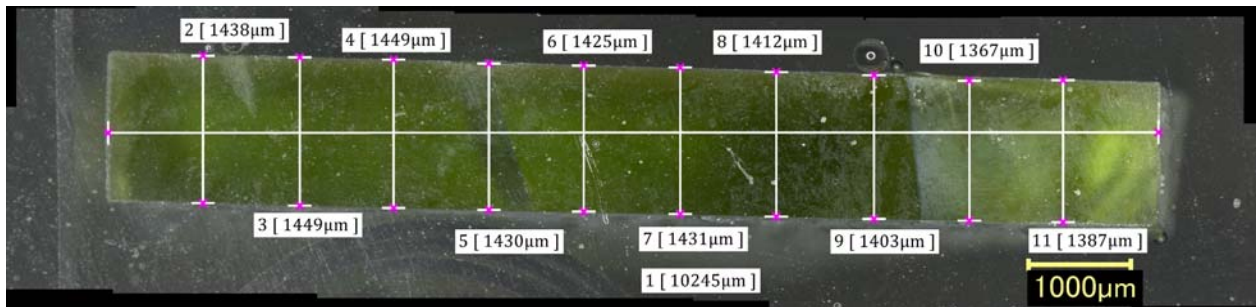


(b) CCC

Figure B.16. LAWPh3-02 samples after VHT for 7 days.

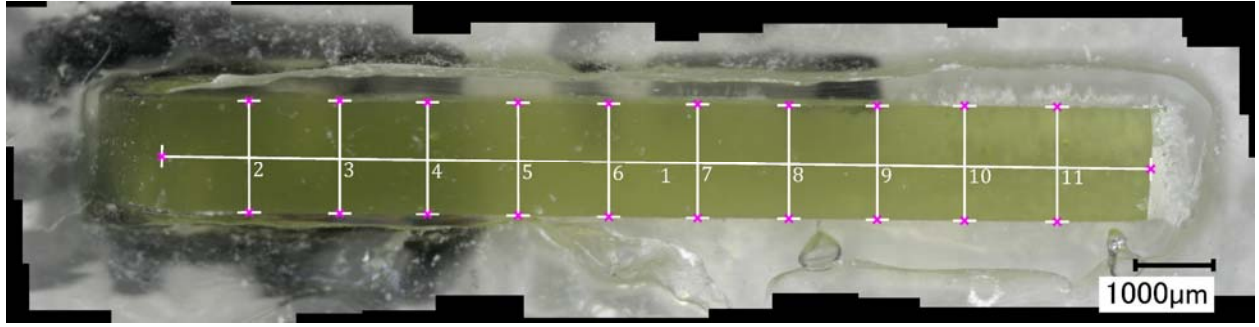


(a) Quenched

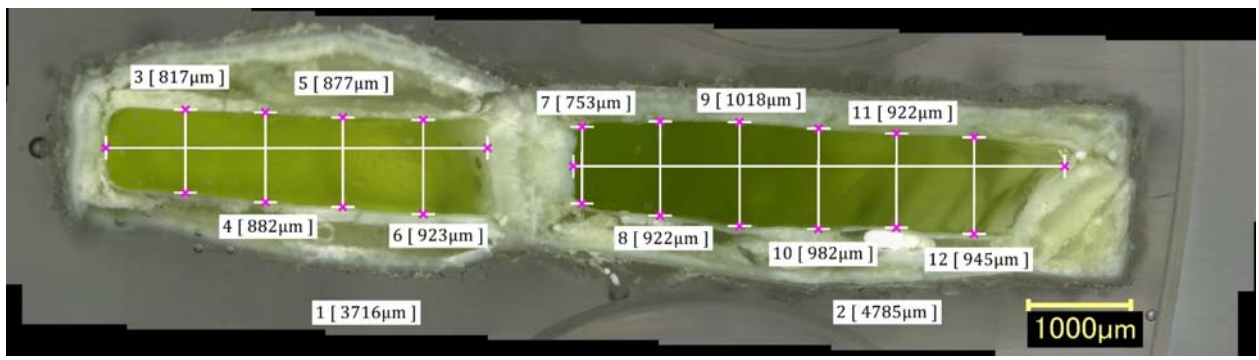


(b) CCC

Figure B.17. LAWPh3-17 samples after VHT for 7 days.



(a) Quenched

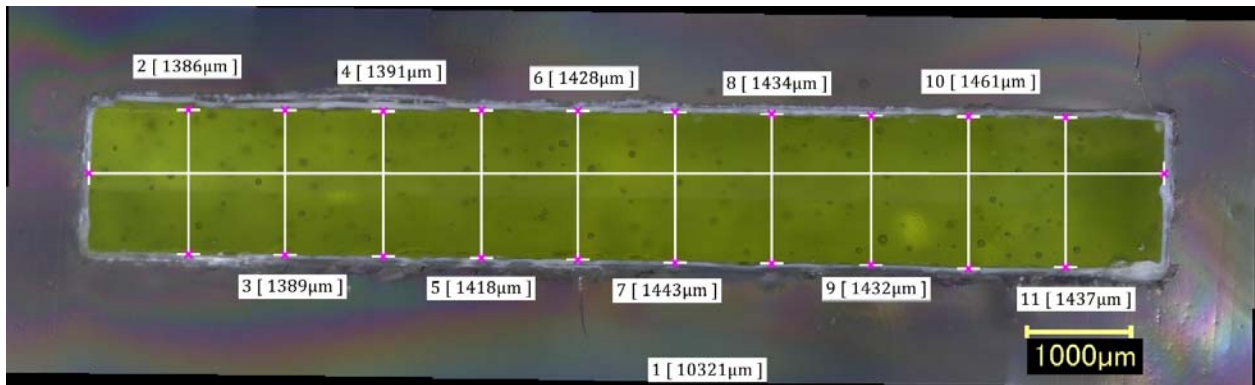


(b) CCC

Figure B.18. LAWPh3-18 samples after VHT for 24 days.

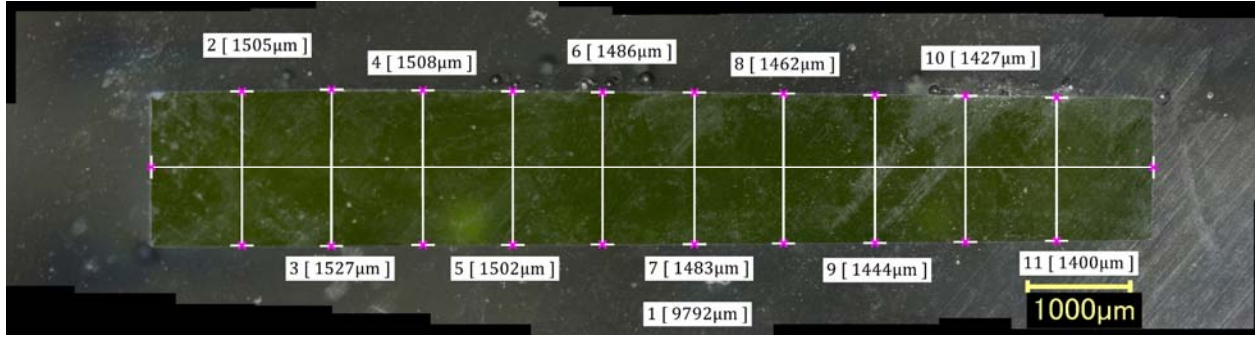


(a) Quenched

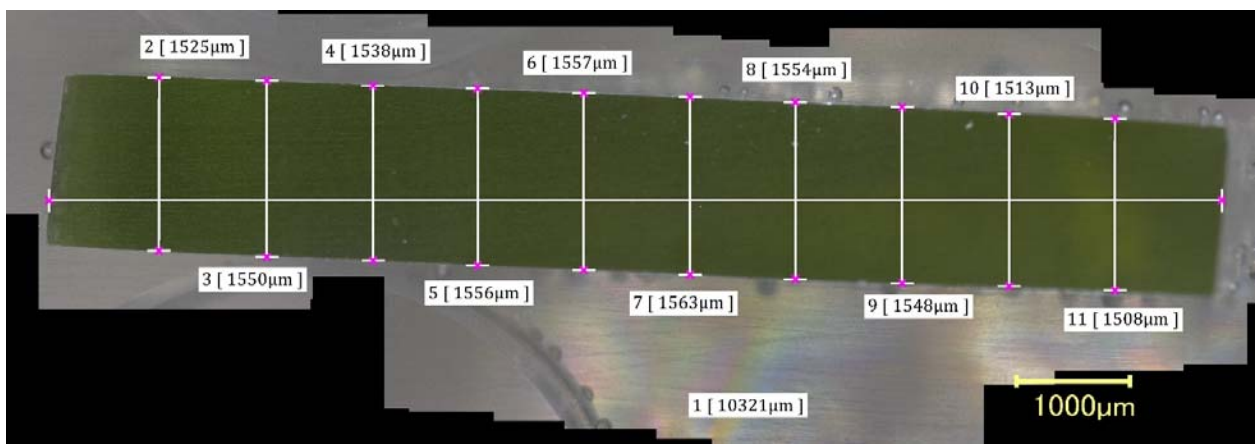


(b) CCC

Figure B.19. LAWPh3-19_mod samples after VHT for 7 days.



(a) Quenched



(b) CCC

Figure B.20. LAWPh3-20 samples after VHT for 7 days.

Appendix C – Analyzed Compositions for As-Quenched Glasses

This appendix provides the averaged measured values for all components of each glass study during this work. The data originate from SRNL-STI-2018-00649, Rev. 2 (Fox et al. 2020). There were two main purposes for analyzing the compositions of these glasses. First, the analyzed SO₃ values estimate the concentrations of that component incorporated into the glass melts. Second, comparing target and analyzed values of components provides for detecting glasses that were mis-batched, or components subject to volatilization during melting.

The tables in this appendix compare the targeted glass compositions with the analyzed glass compositions and their percent differences for the Phase 3 enhanced low-activity waste (LAW) glasses. Note that volatile components, and those with low concentrations, often have large changes between target and measured values. The relative percent difference (RPD) is calculated by the following equation:

$$RPD = (x_M - x_T) / x_M * 100 \quad (C.1)$$

Table C.1. Measured and target compositional values for LAWPh3-01-1. Relative percent difference between measured versus target values is included as well (BDL = below detection limit).

Glass ID	Oxide	BDL (<)	Measured (wt%)	Targeted (wt%)	% Difference of Measured versus Targeted
LAWPh3-01-1-Q	Al ₂ O ₃		6.405	6.576	-2.67
LAWPh3-01-1-Q	B ₂ O ₃		14.345	13.506	5.85
LAWPh3-01-1-Q	CaO		4.89	4.456	8.88
LAWPh3-01-1-Q	Cl		0.118	0.137	-16.10
LAWPh3-01-1-Q	Cr ₂ O ₃		0.51	0.574	-12.55
LAWPh3-01-1-Q	F		0.173	0.208	-20.23
LAWPh3-01-1-Q	Fe ₂ O ₃		0.498	0.537	-7.83
LAWPh3-01-1-Q	K ₂ O		0.81	0.676	16.54
LAWPh3-01-1-Q	MgO		1.121	1.235	-10.17
LAWPh3-01-1-Q	Na ₂ O		22.68	24.131	-6.40
LAWPh3-01-1-Q	P ₂ O ₅	<	0.233	0.446	-91.42
LAWPh3-01-1-Q	SiO ₂		35.994	35.582	1.14
LAWPh3-01-1-Q	SnO ₂		2.99	3.076	-2.88
LAWPh3-01-1-Q	SO ₃		0.552	0.528	4.35
LAWPh3-01-1-Q	V ₂ O ₅		0.258	0.281	-8.91
LAWPh3-01-1-Q	ZnO		1.97	2.07	-5.08
LAWPh3-01-1-Q	ZrO ₂		4.708	5.981	-27.04
LAWPh3-01-1-Q	Sum		98.254	100	-1.78

Table C.2. Measured and target compositional values for LAWPh3-02. Relative percent difference between measured versus target values is included as well (BDL = below detection limit).

Glass ID	Oxide	BDL (<)	Measured (wt%)	Targeted (wt%)	% Difference of Measured versus Targeted
LAWPh3-02-Q	Al ₂ O ₃		6.594	6.869	-4.17
LAWPh3-02-Q	B ₂ O ₃		12.429	13.158	-5.87
LAWPh3-02-Q	CaO		5.083	4.673	8.07
LAWPh3-02-Q	Cl		0.075	0.074	1.33
LAWPh3-02-Q	Cr ₂ O ₃		0.485	0.52	-7.22
LAWPh3-02-Q	F		0.076	0.112	-47.37
LAWPh3-02-Q	Fe ₂ O ₃	<	0.143	0.045	68.53
LAWPh3-02-Q	K ₂ O		2.608	2.886	-10.66
LAWPh3-02-Q	MgO		1.058	1.084	-2.46
LAWPh3-02-Q	Na ₂ O		21.366	22.707	-6.28
LAWPh3-02-Q	P ₂ O ₅	<	0.242	0.24	0.83
LAWPh3-02-Q	SiO ₂		33.32	34.922	-4.81
LAWPh3-02-Q	SnO ₂		1.603	1.553	3.12
LAWPh3-02-Q	SO ₃		0.478	0.447	6.49
LAWPh3-02-Q	V ₂ O ₅		2.651	2.854	-7.66
LAWPh3-02-Q	ZnO		2.894	3.091	-6.81
LAWPh3-02-Q	ZrO ₂		4.052	4.765	-17.60
LAWPh3-02-Q	Sum		95.158	100	-5.09

Table C.3. Measured and target compositional values for LAWPh3-03. Relative percent difference between measured versus target values is included as well (BDL = below detection limit).

Glass ID	Oxide	BDL (<)	Measured (wt%)	Targeted (wt%)	% Difference of Measured versus Targeted
LAWPh3-03-Q	Al ₂ O ₃		6.49	6.5	-0.15
LAWPh3-03-Q	B ₂ O ₃		7.076	6.62	6.44
LAWPh3-03-Q	CaO		4.589	4.093	10.81
LAWPh3-03-Q	Cl		0.368	0.443	-20.38
LAWPh3-03-Q	Cr ₂ O ₃		0.32	0.344	-7.50
LAWPh3-03-Q	F		0.586	0.672	-14.68
LAWPh3-03-Q	Fe ₂ O ₃		1.4	1.403	-0.21
LAWPh3-03-Q	K ₂ O		4.638	5.005	-7.91
LAWPh3-03-Q	MgO		1.124	1.176	-4.63
LAWPh3-03-Q	Na ₂ O		19.883	21.585	-8.56
LAWPh3-03-Q	P ₂ O ₅		1.071	1.438	-34.27
LAWPh3-03-Q	SiO ₂		42.679	39.958	6.38
LAWPh3-03-Q	SnO ₂		1.501	1.578	-5.13
LAWPh3-03-Q	SO ₃		0.525	0.538	-2.48
LAWPh3-03-Q	V ₂ O ₅		0.246	0.254	-3.25
LAWPh3-03-Q	ZnO		3	3.033	-1.10
LAWPh3-03-Q	ZrO ₂		4.508	5.358	-18.86
LAWPh3-03-Q	Sum		100.005	99.998	0.01

Table C.4. Measured and target compositional values for LAWPh3-04. Relative percent difference between measured versus target values is included as well (BDL = below detection limit).

Glass ID	Oxide	BDL (<)	Measured (wt%)	Targeted (wt%)	% Difference of Measured versus Targeted
LAWPh3-04-Q	Al ₂ O ₃		6.24	6.363	-1.97
LAWPh3-04-Q	B ₂ O ₃		12.485	12.757	-2.18
LAWPh3-04-Q	CaO		10.102	9.524	5.72
LAWPh3-04-Q	Cl		0.187	0.201	-7.49
LAWPh3-04-Q	Cr ₂ O ₃		0.448	0.494	-10.27
LAWPh3-04-Q	F		0.249	0.305	-22.49
LAWPh3-04-Q	Fe ₂ O ₃		0.361	0.367	-1.66
LAWPh3-04-Q	K ₂ O		0.863	0.895	-3.71
LAWPh3-04-Q	MgO		0.441	0.415	5.90
LAWPh3-04-Q	Na ₂ O		20.523	22.21	-8.22
LAWPh3-04-Q	P ₂ O ₅		0.626	0.652	-4.15
LAWPh3-04-Q	SiO ₂		35.566	35.803	-0.67
LAWPh3-04-Q	SnO ₂		0.496	0.349	29.64
LAWPh3-04-Q	SO ₃		1.203	1.274	-5.90
LAWPh3-04-Q	V ₂ O ₅		2.553	2.756	-7.95
LAWPh3-04-Q	ZnO		2.094	2.243	-7.12
LAWPh3-04-Q	ZrO ₂		2.955	3.392	-14.79
LAWPh3-04-Q	Sum		97.393	100	-2.68

Table C.5. Measured and target compositional values for LAWPh3-05_mod6. Relative percent difference between measured versus target values is included as well (BDL = below detection limit).

Glass ID	Oxide	BDL (<)	Measured (wt%)	Targeted (wt%)	% Difference of Measured versus Targeted
LAWPh3-05_mod6-Q	Al ₂ O ₃		6.24	5.78	7.37
LAWPh3-05_mod6-Q	B ₂ O ₃		8.5	10.2	-20.00
LAWPh3-05_mod6-Q	CaO		2.47	2.33	5.67
LAWPh3-05_mod6-Q	Cl		0.44	0.354	19.55
LAWPh3-05_mod6-Q	Cr ₂ O ₃		0.45	0.429	4.67
LAWPh3-05_mod6-Q	F		0.66	0.524	20.61
LAWPh3-05_mod6-Q	Fe ₂ O ₃		1.06	1.06	0.00
LAWPh3-05_mod6-Q	K ₂ O		2.93	2.68	8.53
LAWPh3-05_mod6-Q	MgO		1.14	1.06	7.02
LAWPh3-05_mod6-Q	Na ₂ O		22.7	20.6	9.25
LAWPh3-05_mod6-Q	P ₂ O ₅		1.42	1.32	7.04
LAWPh3-05_mod6-Q	SiO ₂		39.5	36.9	6.58
LAWPh3-05_mod6-Q	SnO ₂		2.02	2.16	-6.93
LAWPh3-05_mod6-Q	SO ₃		0.9	0.953	-5.89
LAWPh3-05_mod6-Q	V ₂ O ₅		3.3	3.18	3.64
LAWPh3-05_mod6-Q	ZnO		2.15	2.13	0.93
LAWPh3-05_mod6-Q	ZrO ₂		4.06	3.12	23.15
LAWPh3-05_mod6-Q	Sum		100	98.6	1.40

Table C.6. Measured and target compositional values for LAWPh3-06. Relative percent difference between measured versus target values is included as well (BDL = below detection limit).

Glass ID	Oxide	BDL (<)	Measured (wt%)	Targeted (wt%)	% Difference of Measured versus Targeted
LAWPh3-06-Q	Al ₂ O ₃		8.918	9.019	-1.13
LAWPh3-06-Q	B ₂ O ₃		7.446	6.727	9.66
LAWPh3-06-Q	CaO		10.581	10.161	3.97
LAWPh3-06-Q	Cl		0.081	0.1	-23.46
LAWPh3-06-Q	Cr ₂ O ₃		0.51	0.583	-14.31
LAWPh3-06-Q	F		0.125	0.151	-20.80
LAWPh3-06-Q	Fe ₂ O ₃		0.245	0.239	2.45
LAWPh3-06-Q	K ₂ O		2.364	2.394	-1.27
LAWPh3-06-Q	MgO		1.073	1.138	-6.06
LAWPh3-06-Q	Na ₂ O		20.018	21.267	-6.24
LAWPh3-06-Q	P ₂ O ₅	<	0.233	0.324	-39.06
LAWPh3-06-Q	SiO ₂		36.315	35.777	1.48
LAWPh3-06-Q	SnO ₂		3.18	3.253	-2.30
LAWPh3-06-Q	SO ₃		0.355	0.341	3.94
LAWPh3-06-Q	V ₂ O ₅		2.24	2.304	-2.86
LAWPh3-06-Q	ZnO		2.891	2.895	-0.14
LAWPh3-06-Q	ZrO ₂		2.472	3.327	-34.59
LAWPh3-06-Q	Sum		99.046	100	-0.96

Table C.7. Measured and target compositional values for LAWPh3-07. Relative percent difference between measured versus target values is included as well (BDL = below detection limit).

Glass ID	Oxide	BDL (<)	Measured (wt%)	Targeted (wt%)	% Difference of Measured versus Targeted
LAWPh3-07-Q	Al ₂ O ₃		9.23	9.804	-6.22
LAWPh3-07-Q	B ₂ O ₃		7.462	7.61	-1.98
LAWPh3-07-Q	CaO		9.224	8.843	4.13
LAWPh3-07-Q	Cl		0.345	0.415	-20.29
LAWPh3-07-Q	Cr ₂ O ₃		0.316	0.329	-4.11
LAWPh3-07-Q	F		0.527	0.631	-19.73
LAWPh3-07-Q	Fe ₂ O ₃		0.543	0.525	3.31
LAWPh3-07-Q	K ₂ O		0.734	0.782	-6.54
LAWPh3-07-Q	MgO	<	0.166	0.07	57.83
LAWPh3-07-Q	Na ₂ O		22.781	23.886	-4.85
LAWPh3-07-Q	P ₂ O ₅		1.21	1.35	-11.57
LAWPh3-07-Q	SiO ₂		34.015	35.064	-3.08
LAWPh3-07-Q	SnO ₂		0.56	0.733	-30.89
LAWPh3-07-Q	SO ₃		0.532	0.557	-4.70
LAWPh3-07-Q	V ₂ O ₅		3.035	3.05	-0.49
LAWPh3-07-Q	ZnO		3.093	3.095	-0.06
LAWPh3-07-Q	ZrO ₂		2.678	3.256	-21.58
LAWPh3-07-Q	Sum		96.452	100	-3.68

Table C.8. Measured and target compositional values for LAWPh3-08. Relative percent difference between measured versus target values is included as well (BDL = below detection limit).

Glass ID	Oxide	BDL (<)	Measured (wt%)	Targeted (wt%)	% Difference of Measured versus Targeted
LAWPh3-08-Q	Al ₂ O ₃		6.627	6.672	-0.68
LAWPh3-08-Q	B ₂ O ₃		6.778	6.482	4.37
LAWPh3-08-Q	CaO		6.786	6.142	9.49
LAWPh3-08-Q	Cl		0.363	0.456	-25.62
LAWPh3-08-Q	Cr ₂ O ₃		0.429	0.468	-9.09
LAWPh3-08-Q	F		0.577	0.693	-20.10
LAWPh3-08-Q	Fe ₂ O ₃	<	0.143	0.106	25.87
LAWPh3-08-Q	K ₂ O		1.373	1.515	-10.34
LAWPh3-08-Q	MgO		0.212	0.185	12.74
LAWPh3-08-Q	Na ₂ O		19.95	21.243	-6.48
LAWPh3-08-Q	P ₂ O ₅		1.186	1.482	-24.96
LAWPh3-08-Q	SiO ₂		45.514	43.987	3.36
LAWPh3-08-Q	SnO ₂		0.516	0.569	-10.27
LAWPh3-08-Q	SO ₃		0.359	0.371	-3.34
LAWPh3-08-Q	V ₂ O ₅	<	0.179	0.05	72.07
LAWPh3-08-Q	ZnO		3.289	3.291	-0.06
LAWPh3-08-Q	ZrO ₂		5.417	6.288	-16.08
LAWPh3-08-Q	Sum		99.698	100	-0.30

Table C.9. Measured and target compositional values for LAWPh3-09. Relative percent difference between measured versus target values is included as well (BDL = below detection limit).

Glass ID	Oxide	BDL (<)	Measured (wt%)	Targeted (wt%)	% Difference of Measured versus Targeted
LAWPh3-09-Q	Al ₂ O ₃		7.369	7.822	-6.15
LAWPh3-09-Q	B ₂ O ₃		8.01	8.597	-7.33
LAWPh3-09-Q	CaO		9.609	9.226	3.99
LAWPh3-09-Q	Cl		0.191	0.257	-34.55
LAWPh3-09-Q	Cr ₂ O ₃		0.28	0.305	-8.93
LAWPh3-09-Q	F		0.335	0.391	-16.72
LAWPh3-09-Q	Fe ₂ O ₃		0.81	0.842	-3.95
LAWPh3-09-Q	K ₂ O		4.858	5.498	-13.17
LAWPh3-09-Q	MgO		0.248	0.205	17.34
LAWPh3-09-Q	Na ₂ O		19.613	21.285	-8.52
LAWPh3-09-Q	P ₂ O ₅		0.787	0.836	-6.23
LAWPh3-09-Q	SiO ₂		35.994	35.513	1.34
LAWPh3-09-Q	SnO ₂		0.349	0.236	32.38
LAWPh3-09-Q	SO ₃		0.951	0.964	-1.37
LAWPh3-09-Q	V ₂ O ₅		0.617	0.644	-4.38
LAWPh3-09-Q	ZnO		2.079	2.289	-10.10
LAWPh3-09-Q	ZrO ₂		4.279	5.09	-18.95
LAWPh3-09-Q	Sum		96.377	100	-3.76

Table C.10. Measured and target compositional values for LAWPh3-10. Relative percent difference between measured versus target values is included as well (BDL = below detection limit).

Glass ID	Oxide	BDL (<)	Measured (wt%)	Targeted (wt%)	% Difference of Measured versus Targeted
LAWPh3-10-Q	Al ₂ O ₃		8.12	8.251	-1.61
LAWPh3-10-Q	B ₂ O ₃		6.544	6.361	2.80
LAWPh3-10-Q	CaO		6.216	5.579	10.25
LAWPh3-10-Q	Cl		0.069	0.095	-37.68
LAWPh3-10-Q	Cr ₂ O ₃		0.325	0.361	-11.08
LAWPh3-10-Q	F		0.122	0.144	-18.03
LAWPh3-10-Q	Fe ₂ O ₃		0.728	0.789	-8.38
LAWPh3-10-Q	K ₂ O		2.554	2.626	-2.82
LAWPh3-10-Q	MgO		0.348	0.338	2.87
LAWPh3-10-Q	Na ₂ O		22.175	23.593	-6.39
LAWPh3-10-Q	P ₂ O ₅	<	0.229	0.308	-34.50
LAWPh3-10-Q	SiO ₂		36.903	35.502	3.80
LAWPh3-10-Q	SnO ₂		1.663	1.719	-3.37
LAWPh3-10-Q	SO ₃		1.074	1.103	-2.70
LAWPh3-10-Q	V ₂ O ₅		3.722	3.836	-3.06
LAWPh3-10-Q	ZnO		3.124	3.187	-2.02
LAWPh3-10-Q	ZrO ₂		5.295	6.208	-17.24
LAWPh3-10-Q	Sum		99.212	100	-0.79

Table C.11. Measured and target compositional values for LAWPh3-11. Relative percent difference between measured versus target values is included as well (BDL = below detection limit).

Glass ID	Oxide	BDL (<)	Measured (wt%)	Targeted (wt%)	% Difference of Measured versus Targeted
LAWPh3-11-Q	Al ₂ O ₃		8.881	9.337	-5.13
LAWPh3-11-Q	B ₂ O ₃		9.418	9.333	0.90
LAWPh3-11-Q	CaO		3.935	3.773	4.12
LAWPh3-11-Q	Cl		0.235	0.272	-15.74
LAWPh3-11-Q	Cr ₂ O ₃		0.543	0.565	-4.05
LAWPh3-11-Q	F		0.349	0.412	-18.05
LAWPh3-11-Q	Fe ₂ O ₃	<	0.143	0.052	63.64
LAWPh3-11-Q	K ₂ O		1.259	1.372	-8.98
LAWPh3-11-Q	MgO		0.813	0.817	-0.49
LAWPh3-11-Q	Na ₂ O		24.23	24.759	-2.18
LAWPh3-11-Q	P ₂ O ₅		0.707	0.882	-24.75
LAWPh3-11-Q	SiO ₂		34.924	35.499	-1.65
LAWPh3-11-Q	SnO ₂		0.597	0.746	-24.96
LAWPh3-11-Q	SO ₃		0.138	0.108	21.74
LAWPh3-11-Q	V ₂ O ₅		3.347	3.457	-3.29
LAWPh3-11-Q	ZnO		2.343	2.187	6.66
LAWPh3-11-Q	ZrO ₂		5.39	6.429	-19.28
LAWPh3-11-Q	Sum		97.253	100	-2.82

Table C.12. Measured and target compositional values for LAWPh3-12. Relative percent difference between measured versus target values is included as well (BDL = below detection limit).

Glass ID	Oxide	BDL (<)	Measured (wt%)	Targeted (wt%)	% Difference of Measured versus Targeted
LAWPh3-12-Q	Al ₂ O ₃		10.676	11.122	-4.18
LAWPh3-12-Q	B ₂ O ₃		13.226	13.512	-2.16
LAWPh3-12-Q	CaO		3.05	2.761	9.48
LAWPh3-12-Q	Cl		0.263	0.32	-21.67
LAWPh3-12-Q	Cr ₂ O ₃		0.387	0.427	-10.34
LAWPh3-12-Q	F		0.391	0.486	-24.30
LAWPh3-12-Q	Fe ₂ O ₃		1.102	1.071	2.81
LAWPh3-12-Q	K ₂ O		0.236	0.229	2.97
LAWPh3-12-Q	MgO		1.144	1.259	-10.05
LAWPh3-12-Q	Na ₂ O		20.186	21.432	-6.17
LAWPh3-12-Q	P ₂ O ₅		1.011	1.039	-2.77
LAWPh3-12-Q	SiO ₂		34.336	35.137	-2.33
LAWPh3-12-Q	SnO ₂		1.019	0.934	8.34
LAWPh3-12-Q	SO ₃		0.315	0.295	6.35
LAWPh3-12-Q	V ₂ O ₅		3.374	3.846	-13.99
LAWPh3-12-Q	ZnO		2.452	2.791	-13.83
LAWPh3-12-Q	ZrO ₂		2.901	3.339	-15.10
LAWPh3-12-Q	Sum		96.069	100	-4.09

Table C.13. Measured and target compositional values for LAWPh3-13. Relative percent difference between measured versus target values is included as well (BDL = below detection limit).

Glass ID	Oxide	BDL (<)	Measured (wt%)	Targeted (wt%)	% Difference of Measured versus Targeted
LAWPh3-13-Q	Al ₂ O ₃		6.59	7.122	-8.07
LAWPh3-13-Q	B ₂ O ₃		5.731	6.245	-8.97
LAWPh3-13-Q	CaO		8.822	8.596	2.56
LAWPh3-13-Q	Cl		0.135	0.169	-25.19
LAWPh3-13-Q	Cr ₂ O ₃		0.558	0.58	-3.94
LAWPh3-13-Q	F		0.224	0.257	-14.73
LAWPh3-13-Q	Fe ₂ O ₃	<	0.143	0.069	51.75
LAWPh3-13-Q	K ₂ O		3.078	3.403	-10.56
LAWPh3-13-Q	MgO		1.226	1.251	-2.04
LAWPh3-13-Q	Na ₂ O		21.804	23.038	-5.66
LAWPh3-13-Q	P ₂ O ₅		0.408	0.549	-34.56
LAWPh3-13-Q	SiO ₂		38.882	39.839	-2.46
LAWPh3-13-Q	SnO ₂	<	0.179	0.272	-51.96
LAWPh3-13-Q	SO ₃		1.111	1.109	0.18
LAWPh3-13-Q	V ₂ O ₅		0.768	0.786	-2.34
LAWPh3-13-Q	ZnO		3.389	3.501	-3.30
LAWPh3-13-Q	ZrO ₂		2.59	3.214	-24.09
LAWPh3-13-Q	Sum		95.637	100	-4.56

Table C.14. Measured and target compositional values for LAWPh3-14. Relative percent difference between measured versus target values is included as well (BDL = below detection limit).

Glass ID	Oxide	BDL (<)	Measured (wt%)	Targeted (wt%)	% Difference of Measured versus Targeted
LAWPh3-14-Q	Al ₂ O ₃		6.429	6.633	-3.17
LAWPh3-14-Q	B ₂ O ₃		8.589	8.264	3.78
LAWPh3-14-Q	CaO		5.824	5.296	9.07
LAWPh3-14-Q	Cl		0.373	0.43	-15.28
LAWPh3-14-Q	Cr ₂ O ₃		0.302	0.318	-5.30
LAWPh3-14-Q	F		0.584	0.654	-11.99
LAWPh3-14-Q	Fe ₂ O ₃	<	0.143	0.033	76.92
LAWPh3-14-Q	K ₂ O		0.228	0.209	8.33
LAWPh3-14-Q	MgO	<	0.166	0.087	47.59
LAWPh3-14-Q	Na ₂ O		24.197	25.643	-5.98
LAWPh3-14-Q	P ₂ O ₅		1.104	1.399	-26.72
LAWPh3-14-Q	SiO ₂		39.256	39.559	-0.77
LAWPh3-14-Q	SnO ₂		2.088	2.168	-3.83
LAWPh3-14-Q	SO ₃		0.883	0.917	-3.85
LAWPh3-14-Q	V ₂ O ₅		2.013	2.139	-6.26
LAWPh3-14-Q	ZnO		2.346	2.48	-5.71
LAWPh3-14-Q	ZrO ₂		3.242	3.771	-16.32
LAWPh3-14-Q	Sum		97.767	100	-2.28

Table C.15. Measured and target compositional values for LAWPh3-15. Relative percent difference between measured versus target values is included as well (BDL = below detection limit).

Glass ID	Oxide	BDL (<)	Measured (wt%)	Targeted (wt%)	% Difference of Measured versus Targeted
LAWPh3-15-Q	Al ₂ O ₃		6.901	7.298	-5.75
LAWPh3-15-Q	B ₂ O ₃		8.911	9.432	-5.85
LAWPh3-15-Q	CaO		9.189	8.668	5.67
LAWPh3-15-Q	Cl		0.089	0.105	-17.98
LAWPh3-15-Q	Cr ₂ O ₃		0.393	0.43	-9.41
LAWPh3-15-Q	F		0.13	0.16	-23.08
LAWPh3-15-Q	Fe ₂ O ₃		1.243	1.246	-0.24
LAWPh3-15-Q	K ₂ O		3.578	4.136	-15.60
LAWPh3-15-Q	MgO	<	0.166	0.008	95.18
LAWPh3-15-Q	Na ₂ O		20.254	21.708	-7.18
LAWPh3-15-Q	P ₂ O ₅		0.324	0.342	-5.56
LAWPh3-15-Q	SiO ₂		33.694	35.343	-4.89
LAWPh3-15-Q	SnO ₂		1.736	1.692	2.53
LAWPh3-15-Q	SO ₃		0.409	0.387	5.38
LAWPh3-15-Q	V ₂ O ₅		1.513	1.604	-6.01
LAWPh3-15-Q	ZnO		2.648	2.942	-11.10
LAWPh3-15-Q	ZrO ₂		3.708	4.499	-21.33
LAWPh3-15-Q	Sum		94.887	100	-5.39

Table C.16. Measured and target compositional values for LAWPh3-16. Relative percent difference between measured versus target values is included as well (BDL = below detection limit).

Glass ID	Oxide	BDL (<)	Measured (wt%)	Targeted (wt%)	% Difference of Measured versus Targeted
LAWPh3-16-Q	Al ₂ O ₃		5.768	6.112	-5.96
LAWPh3-16-Q	B ₂ O ₃		6.81	6.919	-1.60
LAWPh3-16-Q	CaO		8.017	7.417	7.48
LAWPh3-16-Q	Cl		0.16	0.193	-20.63
LAWPh3-16-Q	Cr ₂ O ₃		0.385	0.425	-10.39
LAWPh3-16-Q	F		0.257	0.294	-14.40
LAWPh3-16-Q	Fe ₂ O ₃		0.327	0.333	-1.83
LAWPh3-16-Q	K ₂ O		3.593	4.082	-13.61
LAWPh3-16-Q	MgO		0.78	0.792	-1.54
LAWPh3-16-Q	Na ₂ O		22.242	23.202	-4.32
LAWPh3-16-Q	P ₂ O ₅		0.426	0.629	-47.65
LAWPh3-16-Q	SiO ₂		35.726	36.558	-2.33
LAWPh3-16-Q	SnO ₂	<	0.127	0.115	9.45
LAWPh3-16-Q	SO ₃		0.192	0.165	14.06
LAWPh3-16-Q	V ₂ O ₅		3.41	3.623	-6.25
LAWPh3-16-Q	ZnO		3.243	3.433	-5.86
LAWPh3-16-Q	ZrO ₂		4.762	5.708	-19.87
LAWPh3-16-Q	Sum		96.224	100	-3.92

Table C.17. Measured and target compositional values for LAWPh3-17. Relative percent difference between measured versus target values is included as well (BDL = below detection limit).

Glass ID	Oxide	BDL (<)	Measured (wt%)	Targeted (wt%)	% Difference of Measured versus Targeted
LAWPh3-17-Q	Al ₂ O ₃		6.056	6.166	-1.82
LAWPh3-17-Q	B ₂ O ₃		6.641	6.124	7.78
LAWPh3-17-Q	CaO		10.41	9.859	5.29
LAWPh3-17-Q	Cl		0.157	0.191	-21.66
LAWPh3-17-Q	Cr ₂ O ₃		0.344	0.392	-13.95
LAWPh3-17-Q	F		0.243	0.29	-19.34
LAWPh3-17-Q	Fe ₂ O ₃		1.407	1.395	0.85
LAWPh3-17-Q	K ₂ O		0.398	0.328	17.59
LAWPh3-17-Q	MgO		1.202	1.327	-10.40
LAWPh3-17-Q	Na ₂ O		23.624	25.366	-7.37
LAWPh3-17-Q	P ₂ O ₅		0.335	0.62	-85.07
LAWPh3-17-Q	SiO ₂		39.363	38.076	3.27
LAWPh3-17-Q	SnO ₂		0.711	0.753	-5.91
LAWPh3-17-Q	SO ₃		0.675	0.699	-3.56
LAWPh3-17-Q	V ₂ O ₅		2.263	2.388	-5.52
LAWPh3-17-Q	ZnO		2.275	2.374	-4.35
LAWPh3-17-Q	ZrO ₂		3.127	3.652	-16.79
LAWPh3-17-Q	Sum		99.231	100	-0.77

Table C.18. Measured and target compositional values for LAWPh3-18. Relative percent difference between measured versus target values is included as well (BDL = below detection limit).

Glass ID	Oxide	BDL (<)	Measured (wt%)	Targeted (wt%)	% Difference of Measured versus Targeted
LAWPh3-18-Q	Al ₂ O ₃		7.955	8.374	-5.27
LAWPh3-18-Q	B ₂ O ₃		5.892	6.075	-3.11
LAWPh3-18-Q	CaO		3.687	3.578	2.96
LAWPh3-18-Q	Cl		0.261	0.309	-18.39
LAWPh3-18-Q	Cr ₂ O ₃		0.464	0.478	-3.02
LAWPh3-18-Q	F		0.415	0.47	-13.25
LAWPh3-18-Q	Fe ₂ O ₃		0.408	0.394	3.43
LAWPh3-18-Q	K ₂ O		2.722	2.946	-8.23
LAWPh3-18-Q	MgO		1.284	1.303	-1.48
LAWPh3-18-Q	Na ₂ O		21.534	22.246	-3.31
LAWPh3-18-Q	P ₂ O ₅		0.824	1.005	-21.97
LAWPh3-18-Q	SiO ₂		39.684	40.785	-2.77
LAWPh3-18-Q	SnO ₂		3.133	3.302	-5.39
LAWPh3-18-Q	SO ₃		0.363	0.324	10.74
LAWPh3-18-Q	V ₂ O ₅		0.41	0.403	1.71
LAWPh3-18-Q	ZnO		3.436	3.46	-0.70
LAWPh3-18-Q	ZrO ₂		3.762	4.548	-20.89
LAWPh3-18-Q	Sum		96.233	100	-3.91

Table C.19. Measured and target compositional values for LAWPh3-19_mod1. Relative percent difference between measured versus target values is included as well (BDL = below detection limit).

Glass ID	Oxide	BDL (<)	Measured (wt%)	Targeted (wt%)	% Difference of Measured versus Targeted
LAWPh3-19_mod1-Q	Al ₂ O ₃		6.72	6.11	9.08
LAWPh3-19_mod1-Q	B ₂ O ₃		6.91	7.85	-13.60
LAWPh3-19_mod1-Q	CaO		8.51	7.88	7.40
LAWPh3-19_mod1-Q	Cl		0.08	0.0838	-4.75
LAWPh3-19_mod1-Q	Cr ₂ O ₃		0.37	0.354	4.32
LAWPh3-19_mod1-Q	F		0.12	0.0636	47.00
LAWPh3-19_mod1-Q	Fe ₂ O ₃		1.06	1.34	-26.42
LAWPh3-19_mod1-Q	K ₂ O		3.08	2.91	5.52
LAWPh3-19_mod1-Q	MgO		0.21	0.256	-21.90
LAWPh3-19_mod1-Q	Na ₂ O		21.5	19.1	11.16
LAWPh3-19_mod1-Q	P ₂ O ₅		0.25	0.256	-2.40
LAWPh3-19_mod1-Q	SiO ₂		40.9	38.6	5.62
LAWPh3-19_mod1-Q	SnO ₂		1.08	1.23	-13.89
LAWPh3-19_mod1-Q	SO ₃		0.85	1.1	-29.41
LAWPh3-19_mod1-Q	V ₂ O ₅		2.92	2.82	3.42
LAWPh3-19_mod1-Q	ZnO		2.12	2.1	0.94
LAWPh3-19_mod1-Q	ZrO ₂		3.06	2.45	19.93
LAWPh3-19_mod1-Q	Sum		99.7	98	1.71

Table C.20. Measured and target compositional values for LAWPh3-20. Relative percent difference between measured versus target values is included as well (BDL = below detection limit).

Glass ID	Oxide	BDL (<)	Measured (wt%)	Targeted (wt%)	% Difference of Measured versus Targeted
LAWPh3-20-Q	Al ₂ O ₃		5.881	6.035	-2.62
LAWPh3-20-Q	B ₂ O ₃		8.557	8.934	-4.41
LAWPh3-20-Q	CaO		5.23	4.758	9.02
LAWPh3-20-Q	Cl		0.131	0.132	-0.76
LAWPh3-20-Q	Cr ₂ O ₃		0.384	0.409	-6.51
LAWPh3-20-Q	F		0.148	0.2	-35.14
LAWPh3-20-Q	Fe ₂ O ₃		1.139	1.122	1.49
LAWPh3-20-Q	K ₂ O		0.148	0.127	14.19
LAWPh3-20-Q	MgO	<	0.166	0.074	55.42
LAWPh3-20-Q	Na ₂ O		21.164	22.432	-5.99
LAWPh3-20-Q	P ₂ O ₅		0.424	0.429	-1.18
LAWPh3-20-Q	SiO ₂		41.77	41.198	1.37
LAWPh3-20-Q	SnO ₂		2.828	2.863	-1.24
LAWPh3-20-Q	SO ₃		0.743	0.73	1.75
LAWPh3-20-Q	V ₂ O ₅		3.459	3.639	-5.20
LAWPh3-20-Q	ZnO		3.268	3.388	-3.67
LAWPh3-20-Q	ZrO ₂		3.056	3.53	-15.51
LAWPh3-20-Q	Sum		98.495	100	-1.53

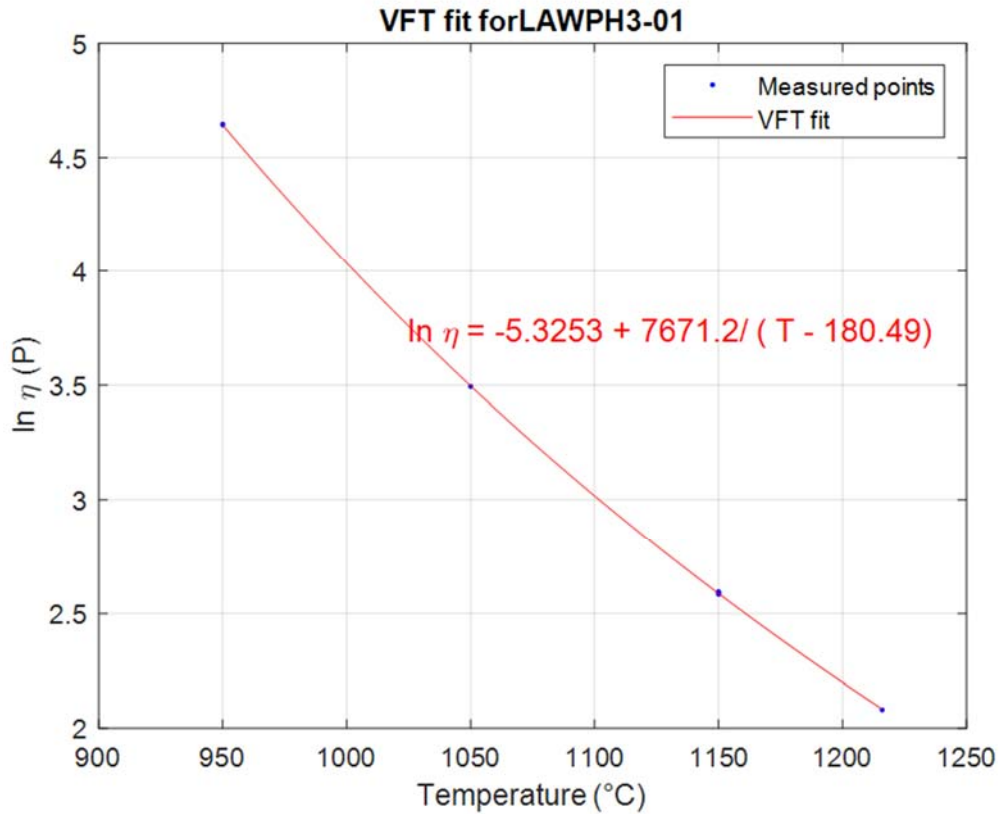
Table C.21. Measured and target compositional values for the reference glass (LRM) used during the testing. Relative percent difference between measured versus target values is included as well (BDL = below detection limit).

Glass ID	Oxide	BDL (<)	Measured (wt%)	Targeted (wt%)	% Difference of Measured versus Targeted
LRM	Al ₂ O ₃		9.228	9.51	-3.06
LRM	B ₂ O ₃		7.327	7.85	-7.14
LRM	CaO		0.322	0.54	-67.70
LRM	Cl	<	0.05	0	100.00
LRM	Cr ₂ O ₃		0.181	0.19	-4.97
LRM	F		0.896	0.86	4.02
LRM	Fe ₂ O ₃		1.304	1.38	-5.83
LRM	K ₂ O		1.384	1.48	-6.94
LRM	MgO	<	0.166	0.1	39.76
LRM	Na ₂ O		19.943	20.03	-0.44
LRM	P ₂ O ₅	<	0.369	0.54	-46.34
LRM	SiO ₂		55.871	54.2	2.99
LRM	SnO ₂	<	0.127	0	100.00
LRM	SO ₃		0.236	0.3	-27.12
LRM	V ₂ O ₅	<	0.179	0	100.00
LRM	ZnO	<	0.124	0	100.00
LRM	ZrO ₂		0.944	0.93	1.48
LRM	Sum		98.651	97.91	0.75

Appendix D – Viscosity Data

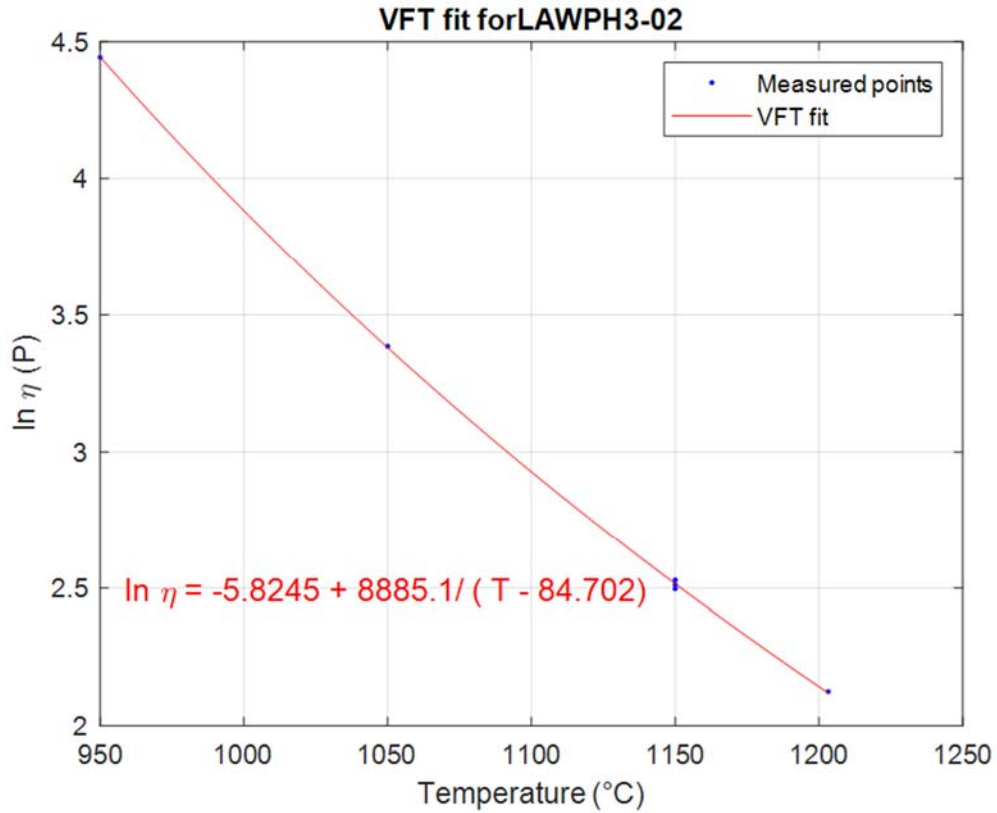
This appendix contains the measured viscosity data for each of the Phase 3 enhanced low-activity waste (LAW) glasses. The plots shown in this appendix were fitted to the Vogel-Fulcher-Tammann (VFT) model. The method and fitting coefficients are shown in Section 3.3.

The intent of the figures and fits shown in this appendix is mainly to assess trends of the data.



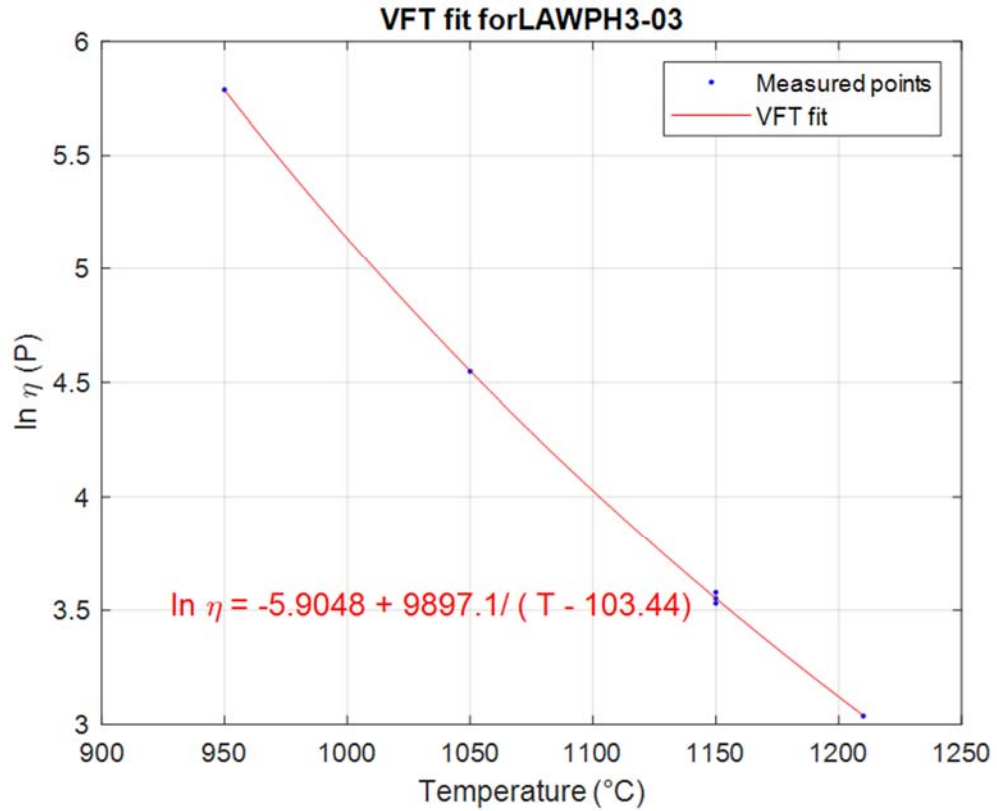
Temperature, °C	Viscosity, Pa s	Viscosity, P	ln Viscosity, Pa s	ln Viscosity, P
1150	1.32	13.25	0.28	2.58
1050	3.29	32.92	1.19	3.49
950	10.40	104.00	2.34	4.64
1150	1.33	13.30	0.29	2.59
1216	0.80	8.01	-0.22	2.08
1150	1.34	13.40	0.29	2.60

Figure D.1. Viscosity-temperature data and VFT fit for glass LAWPh3-01.



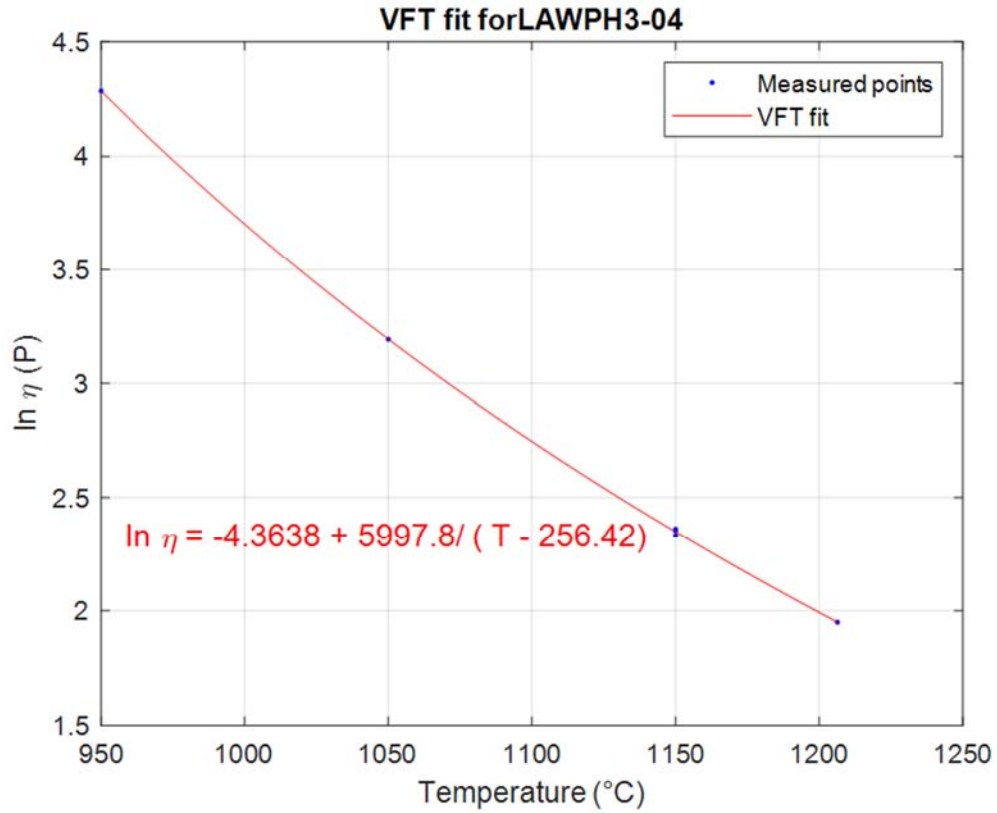
Temperature, °C	Viscosity, Pa s	Viscosity, P	ln Viscosity, Pa s	ln Viscosity, P
1150	1.21	12.15	0.19	2.50
1050	2.95	29.52	1.08	3.39
950	8.50	84.99	2.14	4.44
1150	1.23	12.33	0.21	2.51
1203	0.84	8.37	-0.18	2.12
1150	1.26	12.55	0.23	2.53

Figure D.2. Viscosity-temperature data and VFT fit for glass LAWPh3-02.



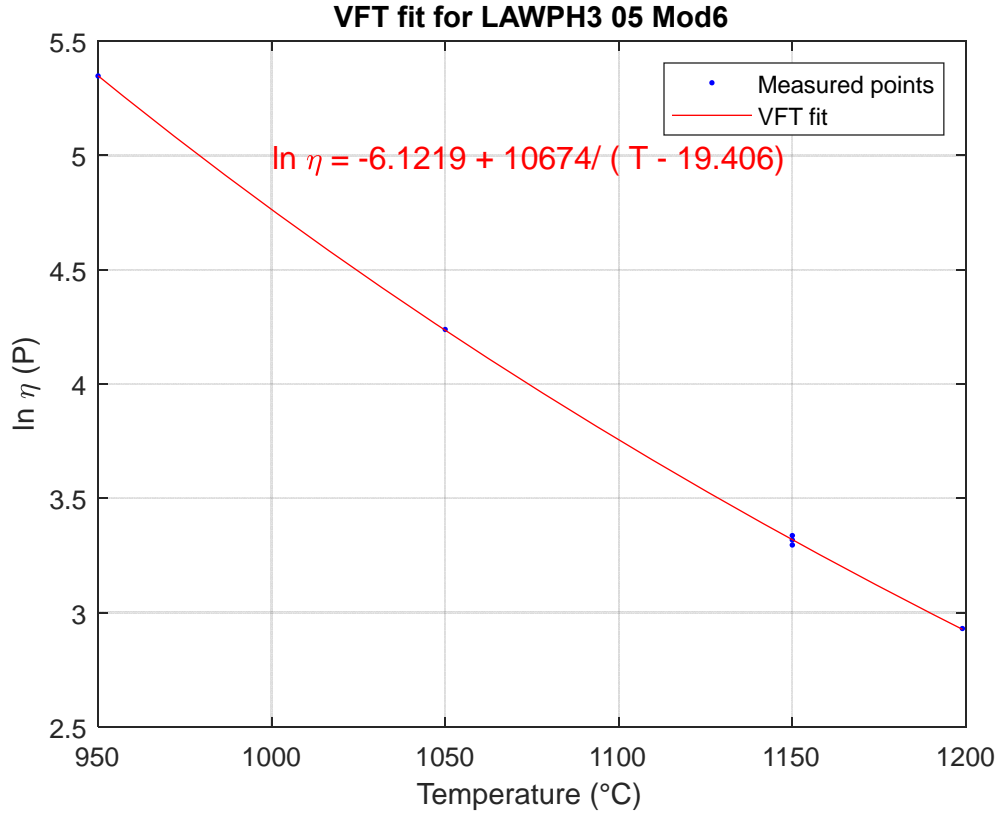
Temperature, °C	Viscosity, Pa s	Viscosity, P	ln Viscosity, Pa s	ln Viscosity, P
1150	3.41	34.14	1.23	3.53
1050	9.45	94.47	2.25	4.55
950	32.60	326.00	3.48	5.79
1150	3.49	34.88	1.25	3.55
1210	2.08	20.84	0.73	3.04
1150	3.58	35.81	1.28	3.58

Figure D.3. Viscosity-temperature data and VFT fit for glass LAWPh3-03.



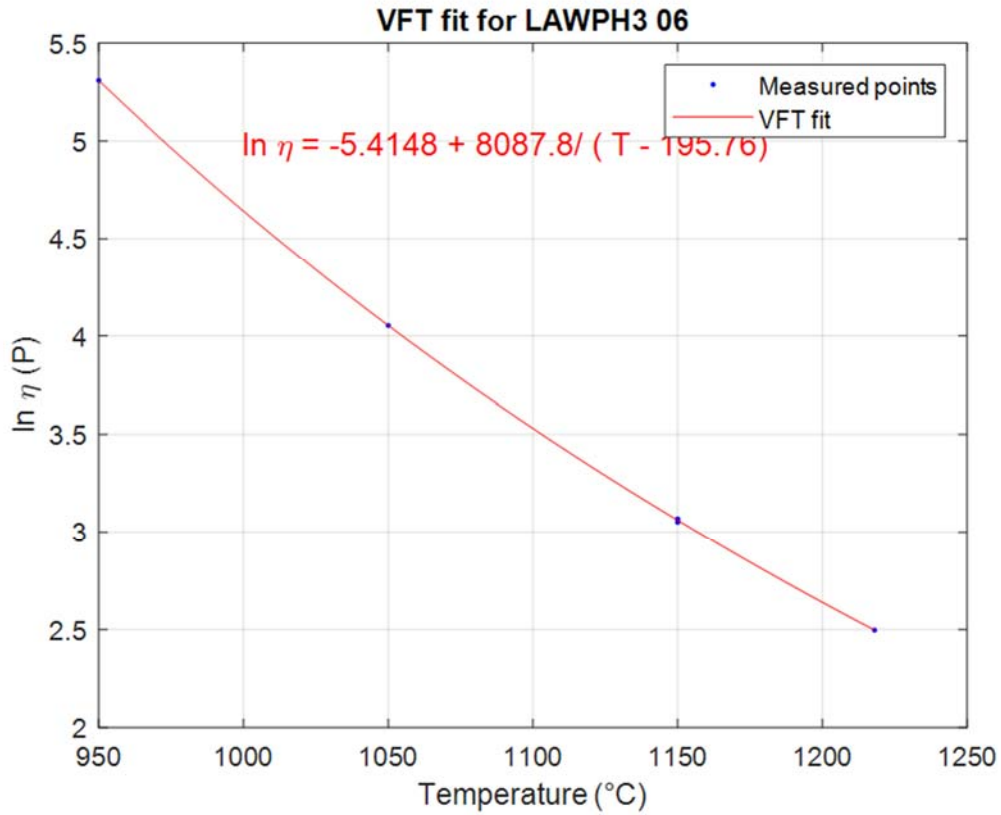
Temperature, °C	Viscosity, Pa s	Viscosity, P	ln Viscosity, Pa s	ln Viscosity, P
1150	1.03	10.30	0.03	2.33
1050	2.44	24.37	0.89	3.19
950	7.25	72.52	1.98	4.28
1150	1.05	10.51	0.05	2.35
1206	0.70	7.03	-0.35	1.95
1150	1.06	10.60	0.06	2.36

Figure D.4. Viscosity-temperature data and VFT fit for glass LAWPh3-04.



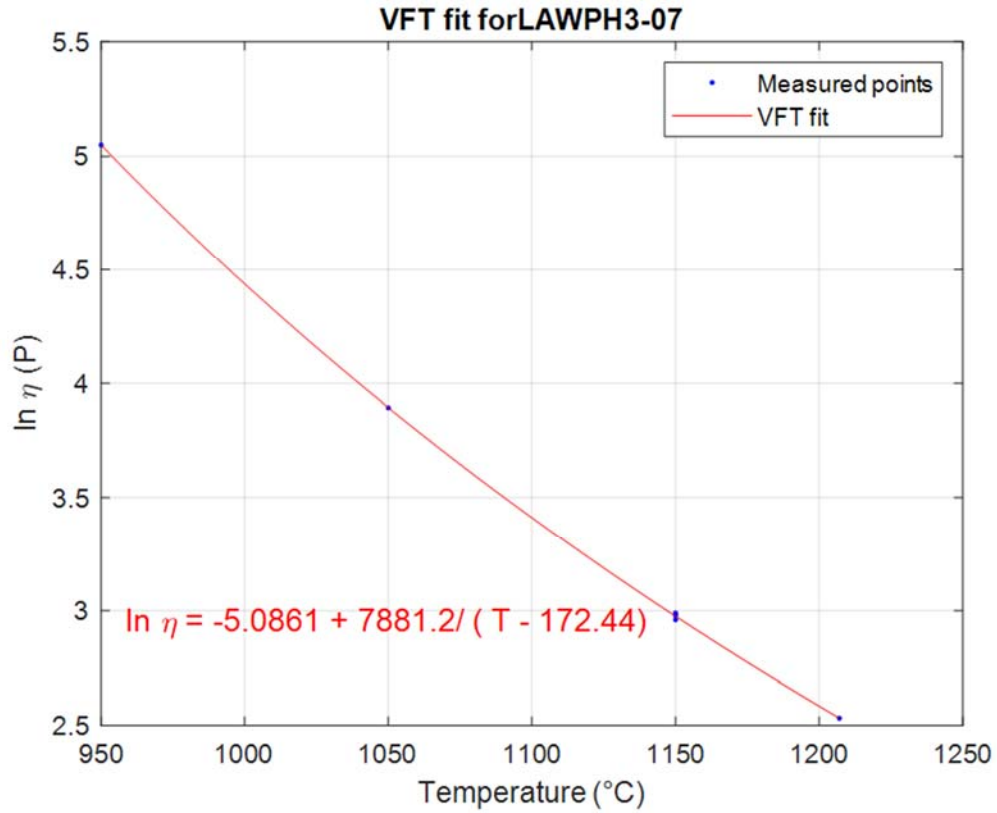
Temperature, °C	Viscosity, Pa s	Viscosity, P	ln Viscosity, Pa s	ln Viscosity, P
1150	2.70	27.01	0.99	3.30
1050	6.93	69.32	1.94	4.24
950	21.01	210.06	3.04	5.35
1150	2.76	27.61	1.02	3.32
1199	1.87	18.74	0.63	2.93
1150	2.81	28.15	1.03	3.34

Figure D.5. Viscosity-temperature data and VFT fit for glass LAWPh3-05_mod6.



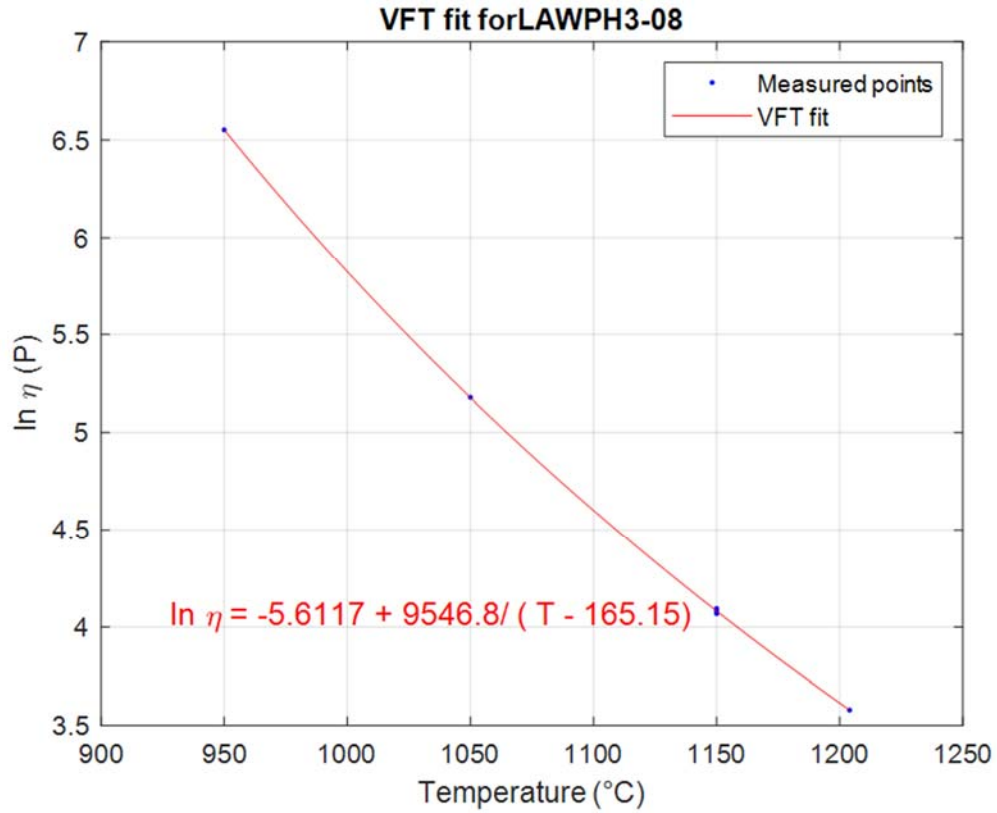
Temperature, °C	Viscosity, Pa s	Viscosity, P	ln Viscosity, Pa s	ln Viscosity, P
1150	2.11	21.14	0.75	3.05
1050	5.76	57.56	1.75	4.05
950	20.20	202.02	3.01	5.31
1150	2.14	21.39	0.76	3.06
1218	1.21	12.14	0.19	2.50
1150	2.15	21.51	0.77	3.07

Figure D.6. Viscosity-temperature data and VFT fit for glass LAWPh3-06.



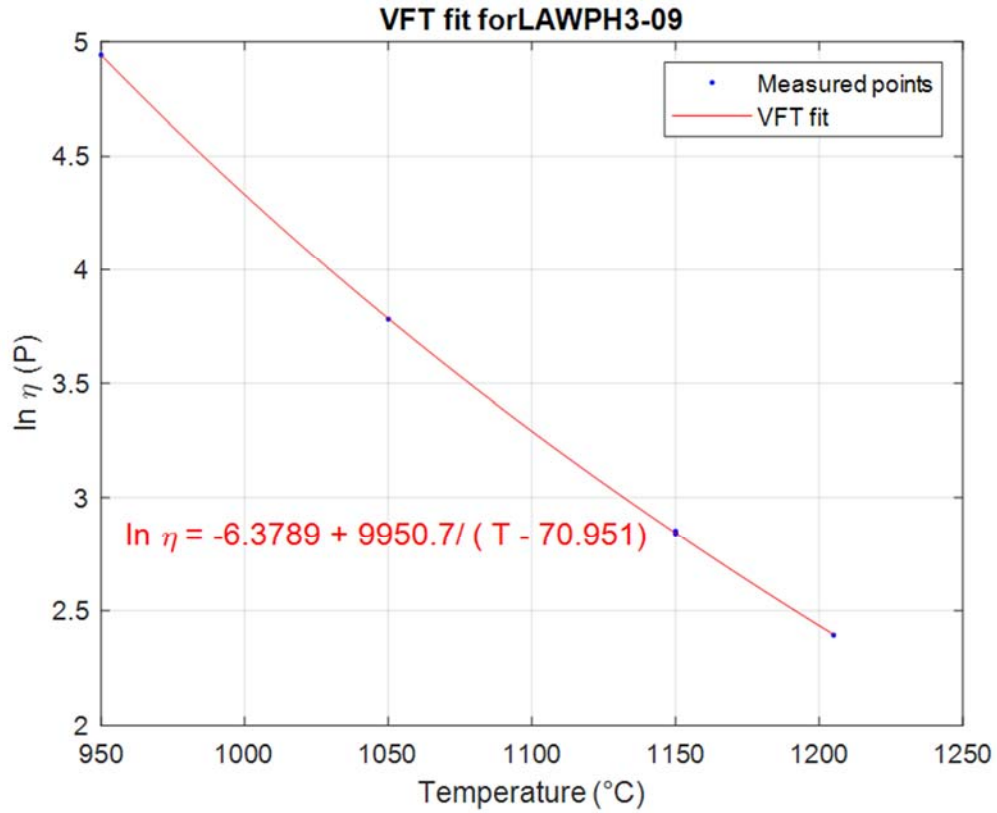
Temperature, °C	Viscosity, Pa s	Viscosity, P	ln Viscosity, Pa s	ln Viscosity, P
1150	1.93	19.30	0.66	2.96
1050	4.91	49.12	1.59	3.89
950	15.60	156.00	2.75	5.05
1150	1.97	19.67	0.68	2.98
1207	1.26	12.57	0.23	2.53
1150	1.99	19.88	0.69	2.99

Figure D.7. Viscosity-temperature data and VFT fit for glass LAWPh3-07.



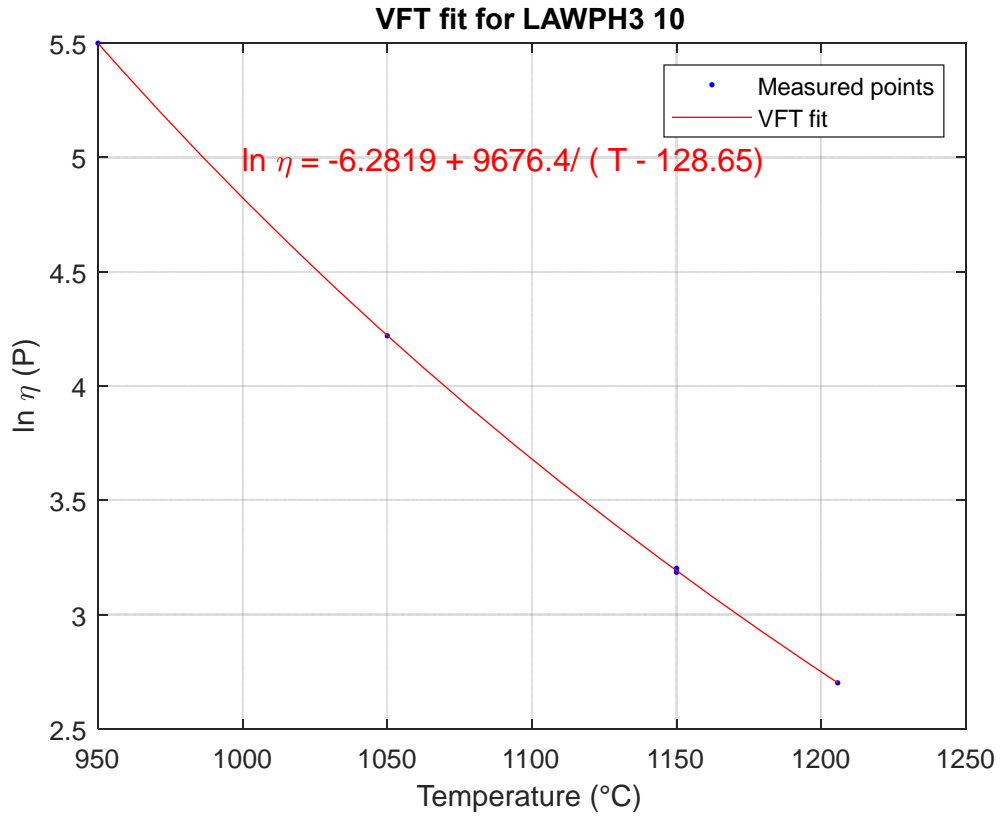
Temperature, °C	Viscosity, Pa s	Viscosity, P	ln Viscosity, Pa s	ln Viscosity, P
1150	5.85	58.48	1.77	4.07
1050	17.73	177.32	2.88	5.18
950	70.07	700.69	4.25	6.55
1150	5.93	59.26	1.78	4.08
1204	3.58	35.82	1.28	3.58
1150	6.00	60.00	1.79	4.09

Figure D.8. Viscosity-temperature data and VFT fit for glass LAWPh3-08.



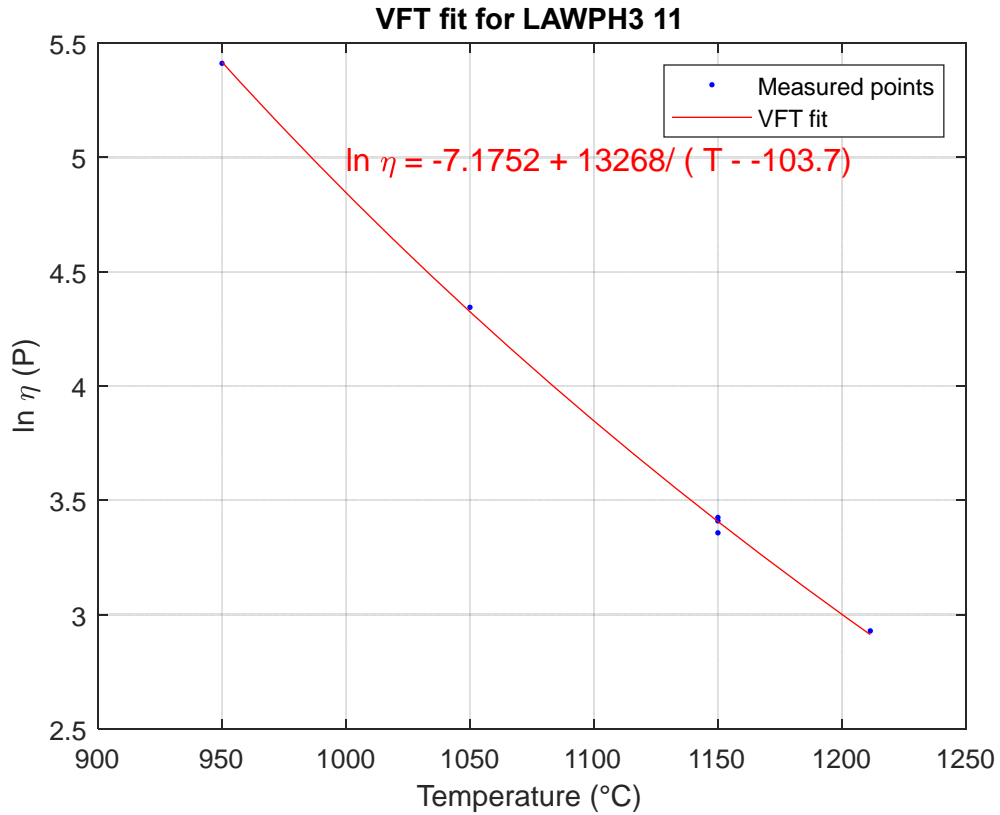
Temperature, °C	Viscosity, Pa s	Viscosity, P	ln Viscosity, Pa s	ln Viscosity, P
1150	1.71	17.10	0.54	2.84
1050	4.39	43.90	1.48	3.78
950	14.00	140.00	2.64	4.94
1150	1.73	17.33	0.55	2.85
1205	1.09	10.95	0.09	2.39
1150	1.72	17.15	0.54	2.84

Figure D.9. Viscosity-temperature data and VFT fit for glass LAWPh3-09.



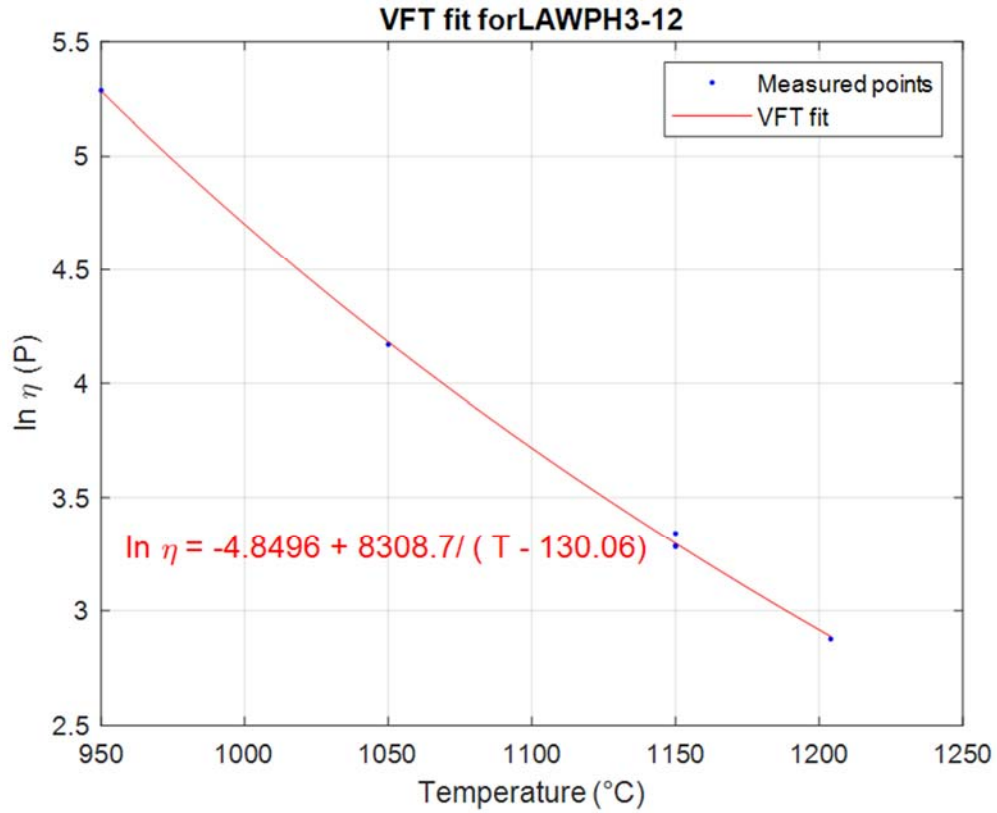
Temperature, °C	Viscosity, Pa s	Viscosity, P	ln Viscosity, Pa s	ln Viscosity, P
1150	2.42	24.17	0.88	3.19
1050	6.80	68.01	1.92	4.22
950	24.46	244.57	3.20	5.50
1150	2.43	24.30	0.89	3.19
1206	1.49	14.90	0.40	2.70
1150	2.46	24.60	0.90	3.20

Figure D.10. Viscosity-temperature data and VFT fit for glass LAWPh3-10.



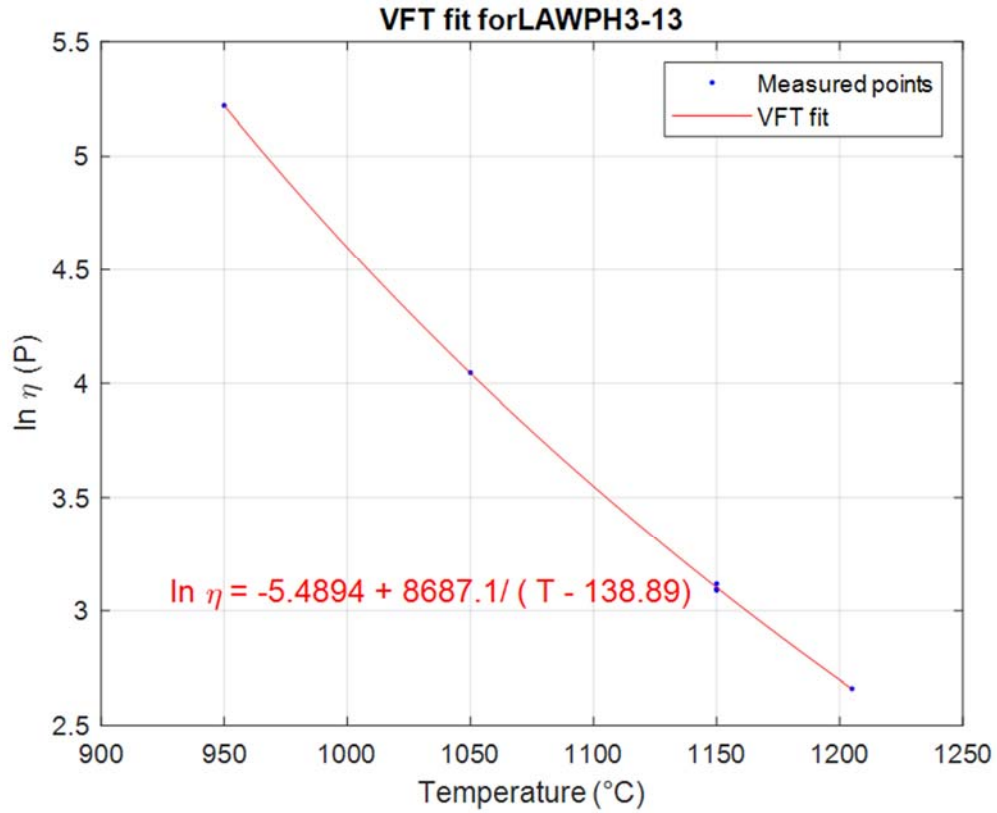
Temperature, °C	Viscosity, Pa s	Viscosity, P	ln Viscosity, Pa s	ln Viscosity, P
1150	3.03	30.26	1.11	3.41
1050	7.70	77.05	2.04	4.34
950	22.39	223.94	3.11	5.41
1150	2.87	28.73	1.06	3.36
1212	1.87	18.71	0.63	2.93
1150	3.07	30.73	1.12	3.43

Figure D.11. Viscosity-temperature data and VFT fit for glass LAWPh3-11.



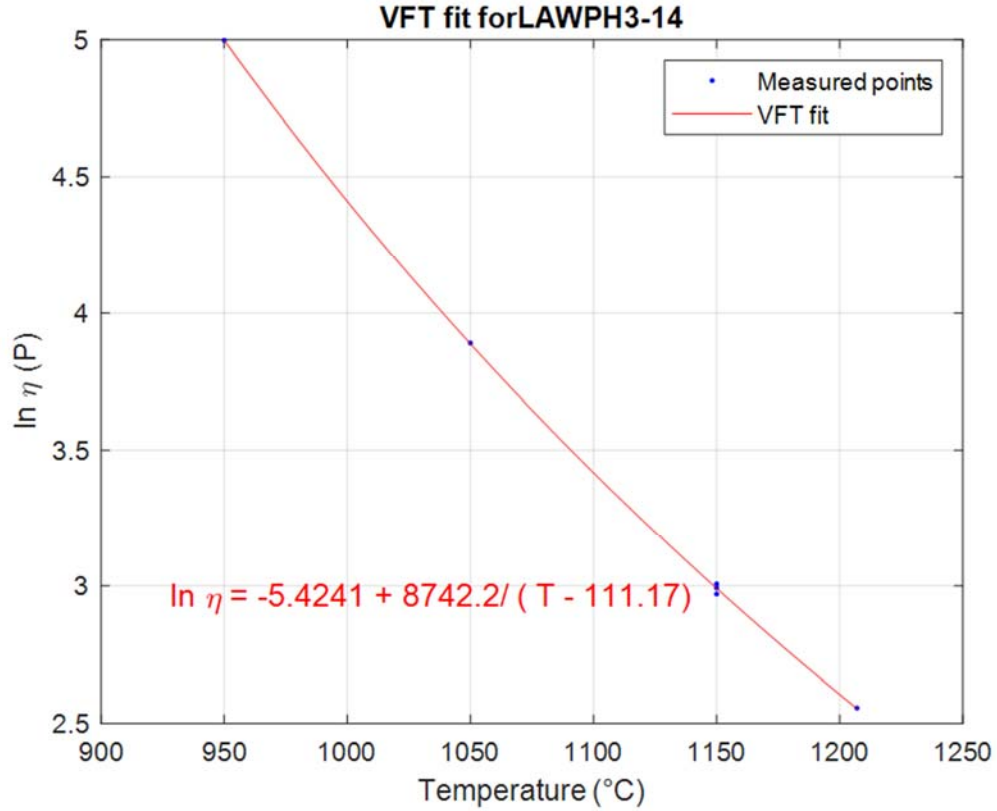
Temperature, °C	Viscosity, Pa s	Viscosity, P	ln Viscosity, Pa s	ln Viscosity, P
1150	2.68	26.76	0.98	3.29
1050	6.48	64.78	1.87	4.17
950	19.76	197.60	2.98	5.29
1150	2.66	26.62	0.98	3.28
1204	1.77	17.74	0.57	2.88
1150	2.83	28.25	1.04	3.34

Figure D.12. Viscosity-temperature data and VFT fit for glass LAWPh3-12.



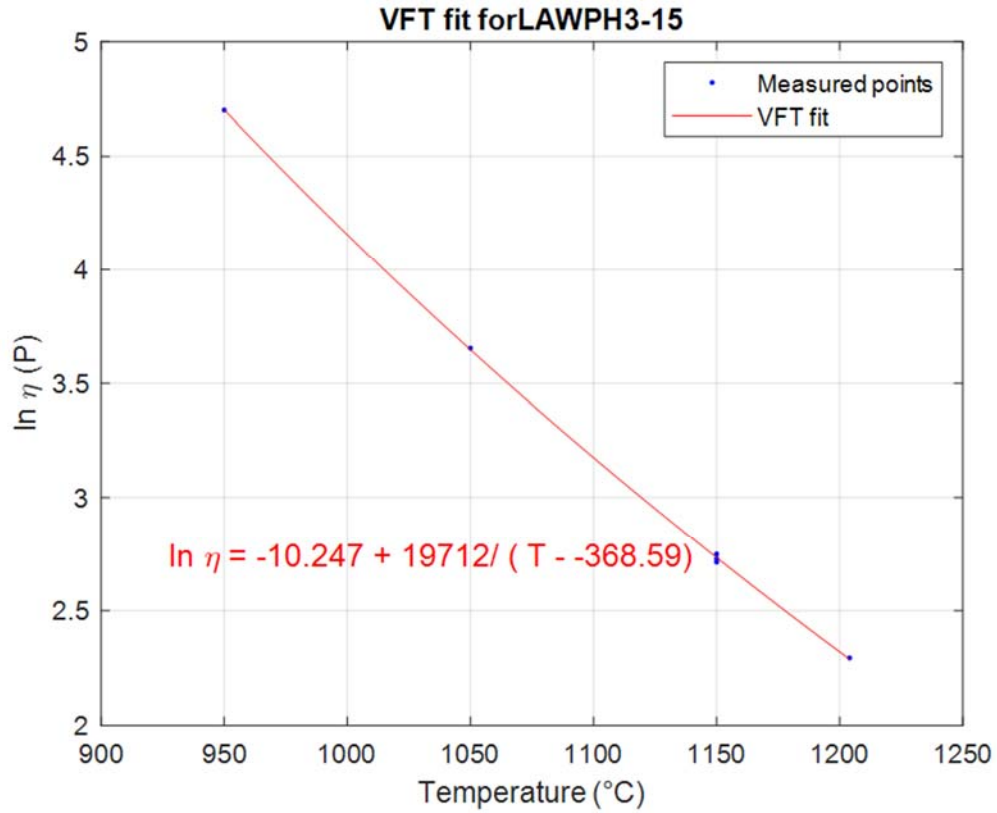
Temperature, °C	Viscosity, Pa s	Viscosity, P	ln Viscosity, Pa s	ln Viscosity, P
1150	2.20	21.97	0.79	3.09
1050	5.72	57.22	1.74	4.05
950	18.50	185.00	2.92	5.22
1150	2.21	22.10	0.79	3.10
1205	1.43	14.31	0.36	2.66
1150	2.26	22.61	0.82	3.12

Figure D.13. Viscosity-temperature data and VFT fit for glass LAWPh3-13.



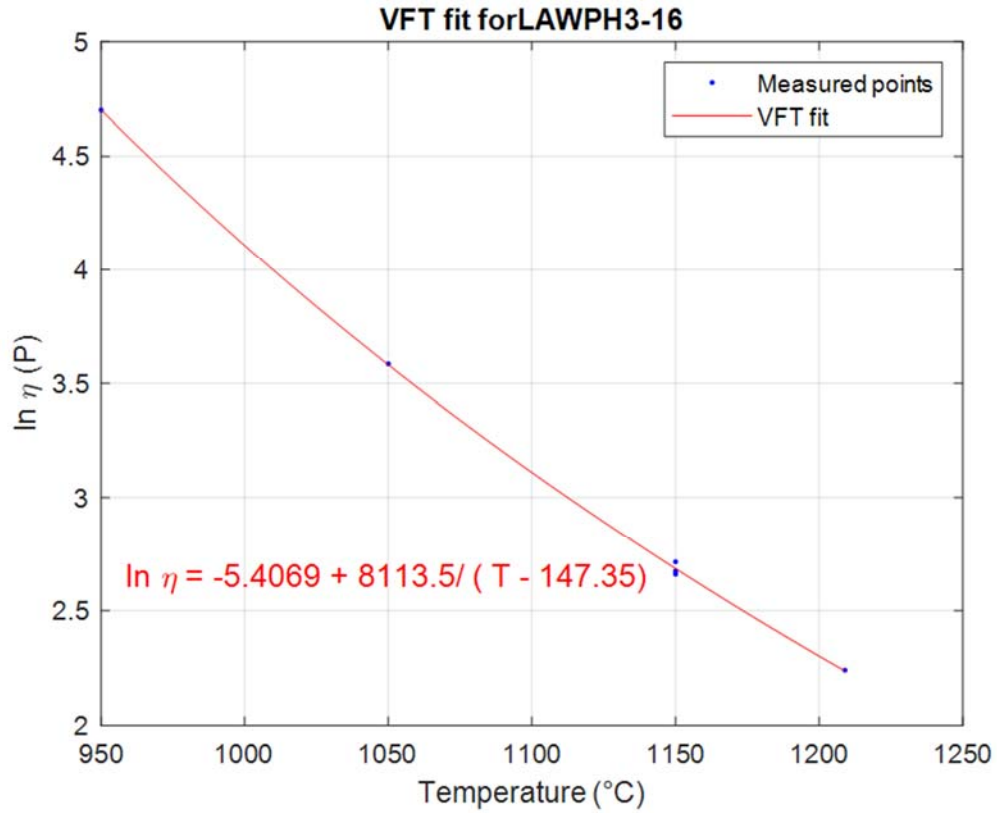
Temperature, °C	Viscosity, Pa s	Viscosity, P	ln Viscosity, Pa s	ln Viscosity, P
1150	1.95	19.50	0.67	2.97
1050	4.89	48.92	1.59	3.89
950	14.80	148.00	2.69	5.00
1150	1.99	19.93	0.69	2.99
1207	1.29	12.88	0.25	2.56
1150	2.02	20.23	0.70	3.01

Figure D.14. Viscosity-temperature data and VFT fit for glass LAWPh3-14.



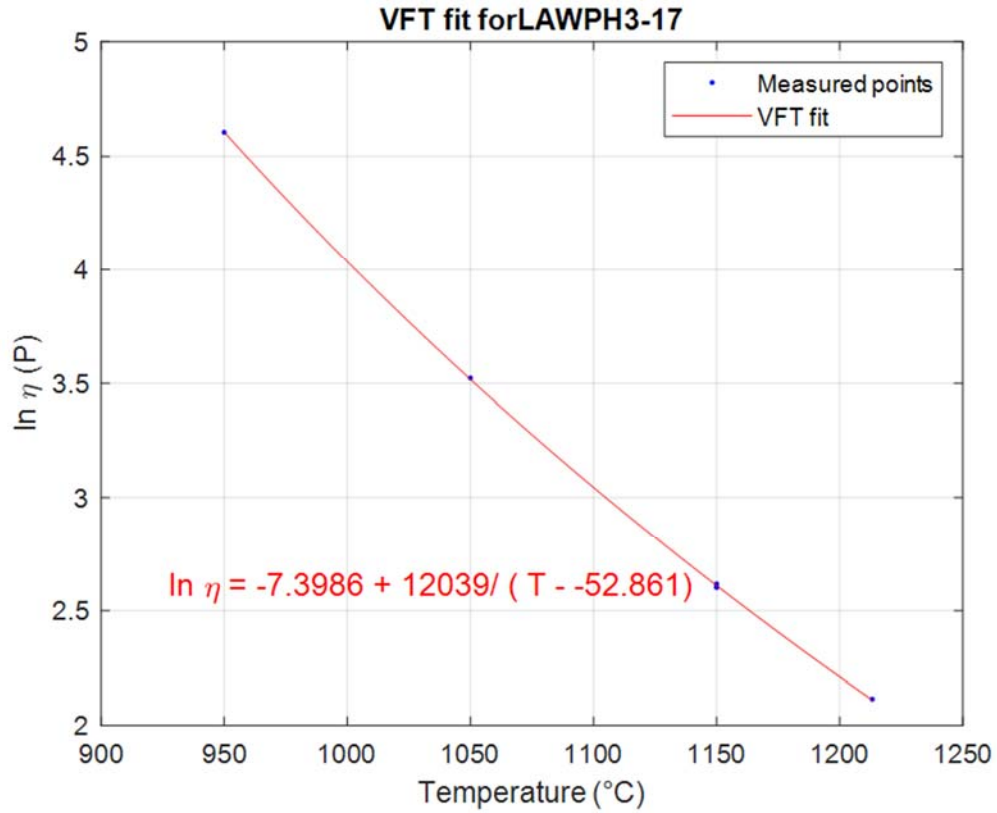
Temperature, °C	Viscosity, Pa s	Viscosity, P	ln Viscosity, Pa s	ln Viscosity, P
1150	1.56	15.62	0.45	2.75
1050	3.87	38.66	1.35	3.65
950	11.00	110.00	2.40	4.70
1150	1.51	15.07	0.41	2.71
1204	0.99	9.91	-0.01	2.29
1150	1.53	15.30	0.43	2.73

Figure D.15. Viscosity-temperature data and VFT fit for glass LAWPh3-15.



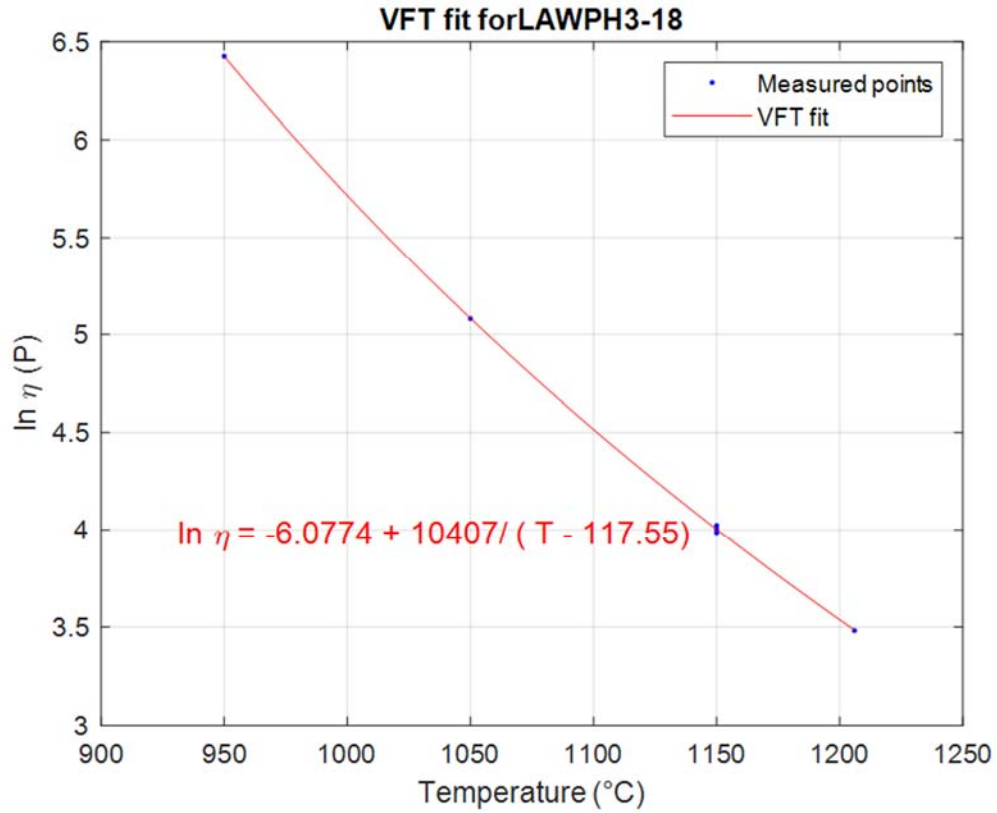
Temperature, °C	Viscosity, Pa s	Viscosity, P	ln Viscosity, Pa s	ln Viscosity, P
1150	1.43	14.30	0.36	2.66
1050	3.61	36.07	1.28	3.59
950	11.00	110.00	2.40	4.70
1150	1.45	14.50	0.37	2.67
1209	0.94	9.39	-0.06	2.24
1150	1.51	15.10	0.41	2.71

Figure D.16. Viscosity-temperature data and VFT fit for glass LAWPh3-16.



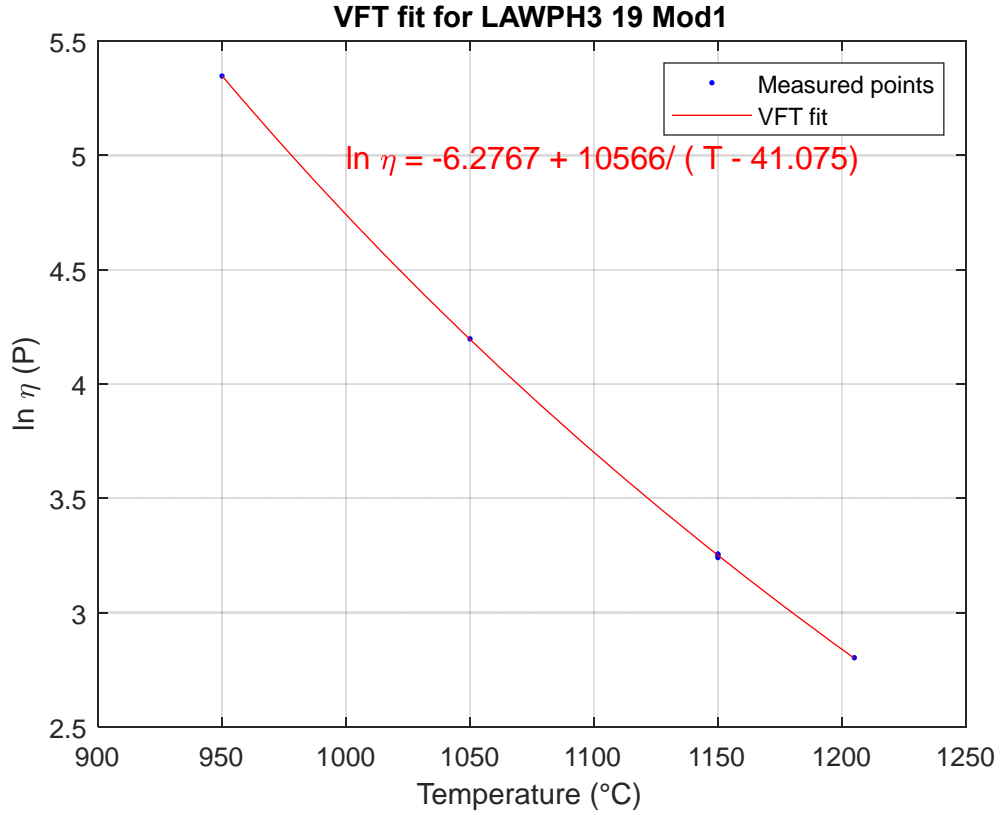
Temperature, °C	Viscosity, Pa s	Viscosity, P	ln Viscosity, Pa s	ln Viscosity, P
1150	1.37	13.70	0.31	2.62
1050	3.39	33.90	1.22	3.52
950	10.00	100.00	2.30	4.61
1150	1.35	13.50	0.30	2.60
1213.21	0.83	8.29	-0.19	2.12
1150	1.35	13.50	0.30	2.60

Figure D.17. Viscosity-temperature data and VFT fit for glass LAWPh3-17.



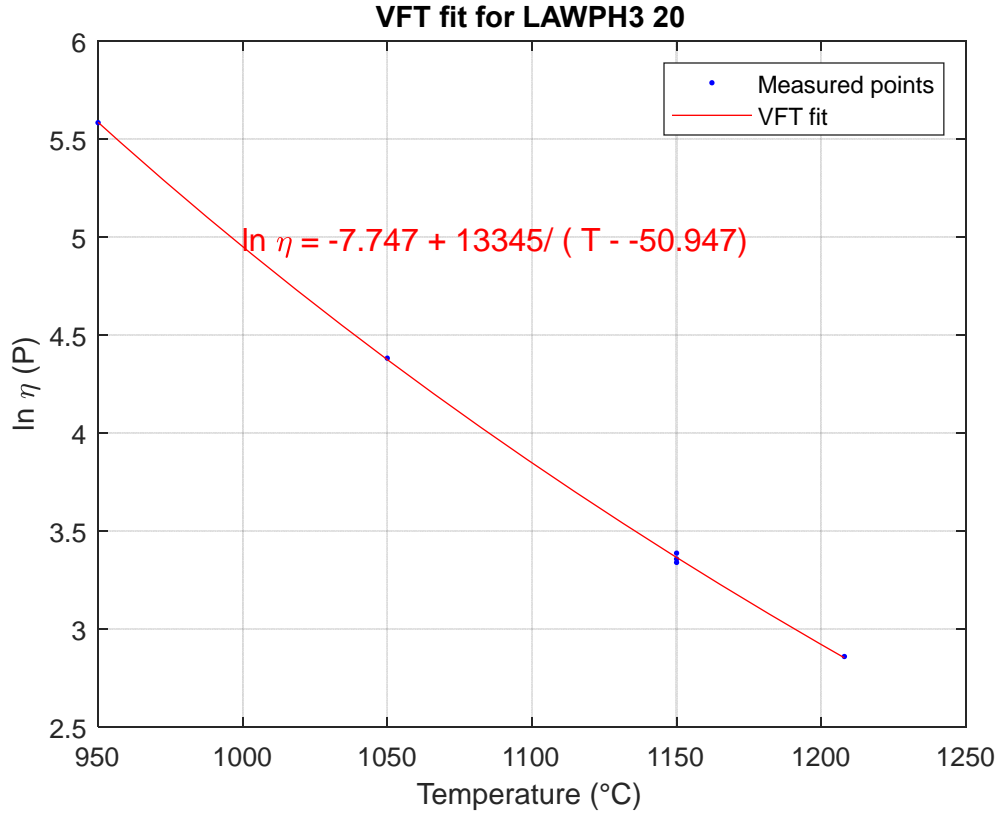
Temperature, °C	Viscosity, Pa s	Viscosity, P	ln Viscosity, Pa s	ln Viscosity, P
1150	5.38	53.81	1.68	3.99
1050	16.10	161.00	2.78	5.08
950	61.72	617.21	4.12	6.43
1150	5.48	54.83	1.70	4.00
1206	3.25	32.52	1.18	3.48
1150	5.59	55.86	1.72	4.02

Figure D.18. Viscosity-temperature data and VFT fit for glass LAWPh3-18.



Temperature, °C	Viscosity, Pa s	Viscosity, P	ln Viscosity, Pa s	ln Viscosity, P
1150	2.56	25.56	0.94	3.24
1050	6.65	66.52	1.89	4.20
950	21.00	210.00	3.04	5.35
1150	2.59	25.85	0.95	3.25
1205	1.65	16.49	0.50	2.80
1150	2.60	25.95	0.95	3.26

Figure D.19. Viscosity-temperature data and VFT fit for glass LAWPh3-19_mod1.



Temperature, °C	Viscosity, Pa s	Viscosity, P	ln Viscosity, Pa s	ln Viscosity, P
1150	2.96	29.58	1.08	3.39
1050	8.00	79.99	2.08	4.38
950	26.60	266.02	3.28	5.58
1150	2.82	28.20	1.04	3.34
1208	1.75	17.46	0.56	2.86
1150	2.87	28.71	1.05	3.36

Figure D.20. Viscosity-temperature data and VFT fit for glass LAWPh3-20.

Appendix E – Electrical Conductivity Data

This appendix presents the $\ln(\text{EC})$ versus inverse temperature (in Kelvin) for the glasses with electrical conductivity data. The plots result in an Arrhenius relationship and the A (intercept) and B (slope) coefficients.

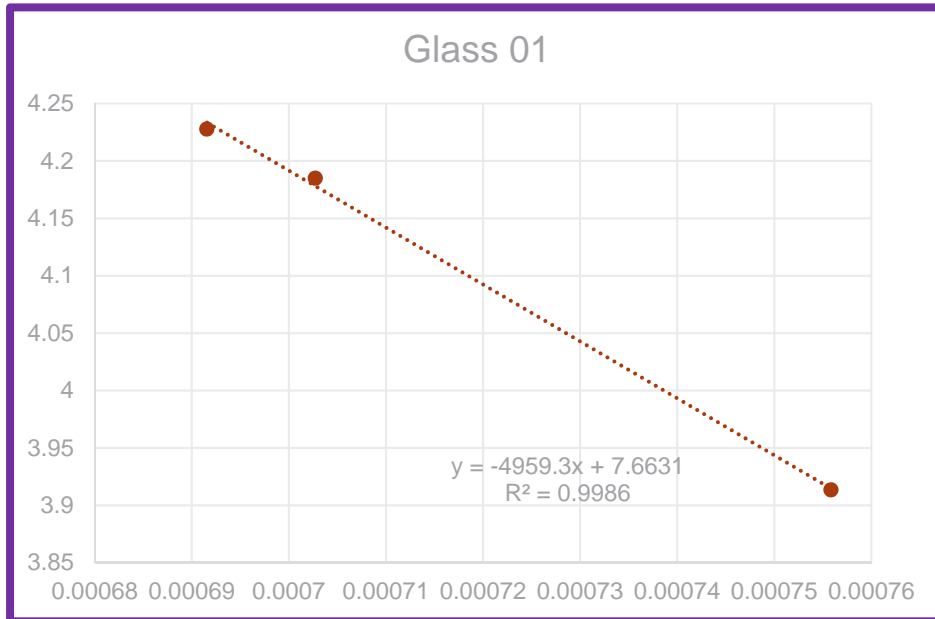


Figure E.1. Electrical conductivity data ($\ln(\text{EC}, \text{S/m})$) versus inverse temperature in Kelvin) for LAWPh3-01-1.

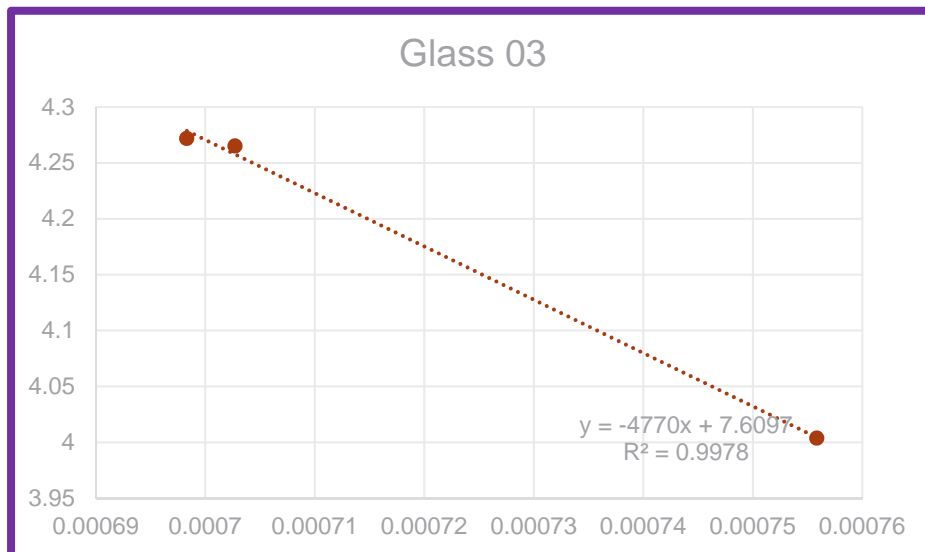


Figure E.2. Electrical conductivity data ($\ln(\text{EC}, \text{S/m})$) versus inverse temperature in Kelvin) for LAWPh3-03.

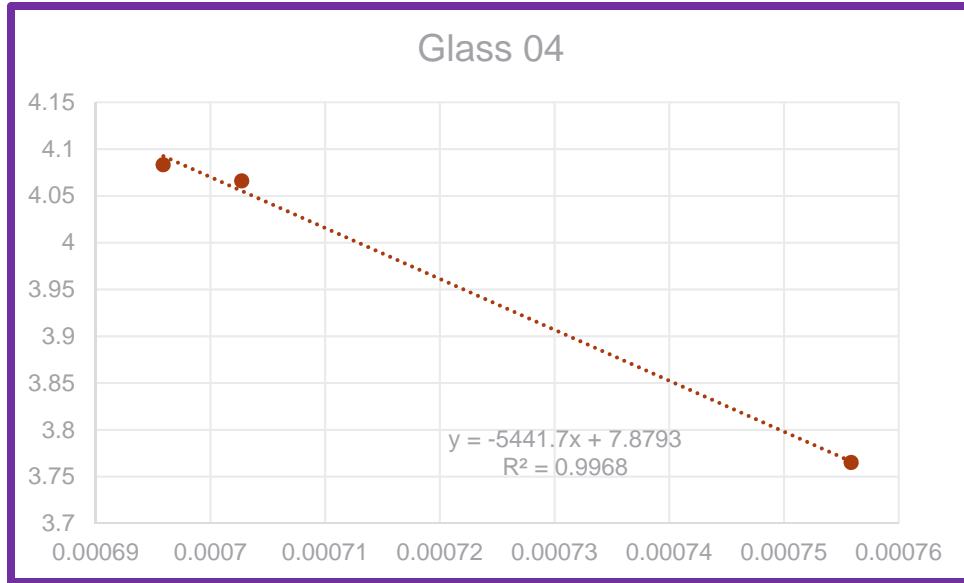


Figure E.3. Electrical conductivity data (ln(EC, S/m) versus inverse temperature in Kelvin) for LAWPh3-04.



Figure E.4. Electrical conductivity data (ln(EC, S/m) versus inverse temperature in Kelvin) for LAWPh3-05_mod6.



Figure E.5. Electrical conductivity data (ln(EC, S/m) versus inverse temperature in Kelvin) for LAWPh3-06.

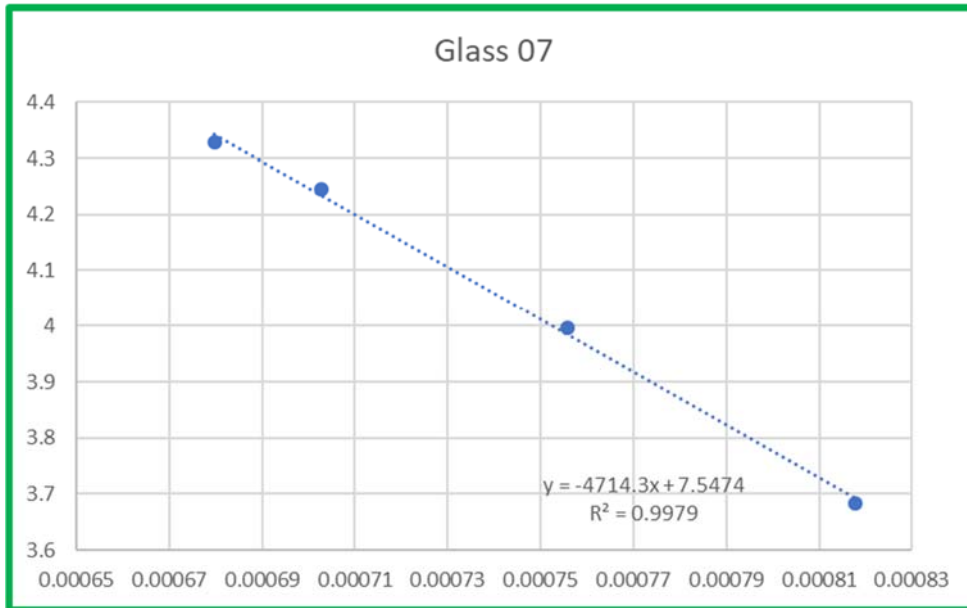


Figure E.6. Electrical conductivity data (ln(EC, S/m) versus inverse temperature in Kelvin) for LAWPh3-07.

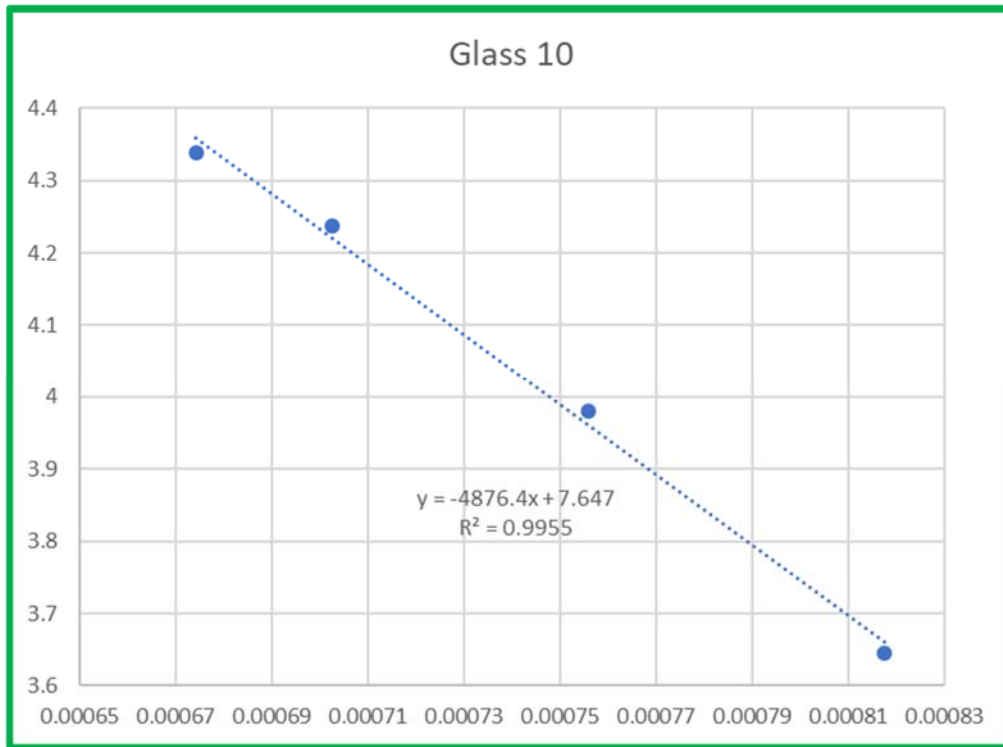


Figure E.7. Electrical conductivity data ($\ln(\text{EC}, \text{S/m})$) versus inverse temperature in Kelvin) for LAWPh3-10.

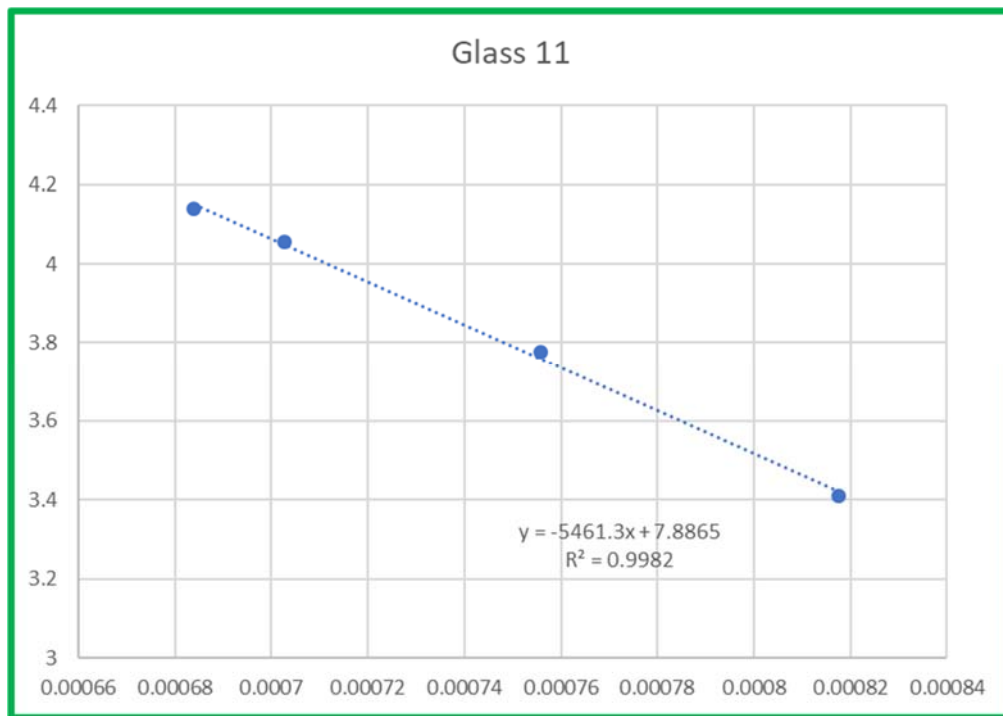


Figure E.8. Electrical conductivity data ($\ln(\text{EC}, \text{S/m})$) versus inverse temperature in Kelvin) for LAWPh3-11.

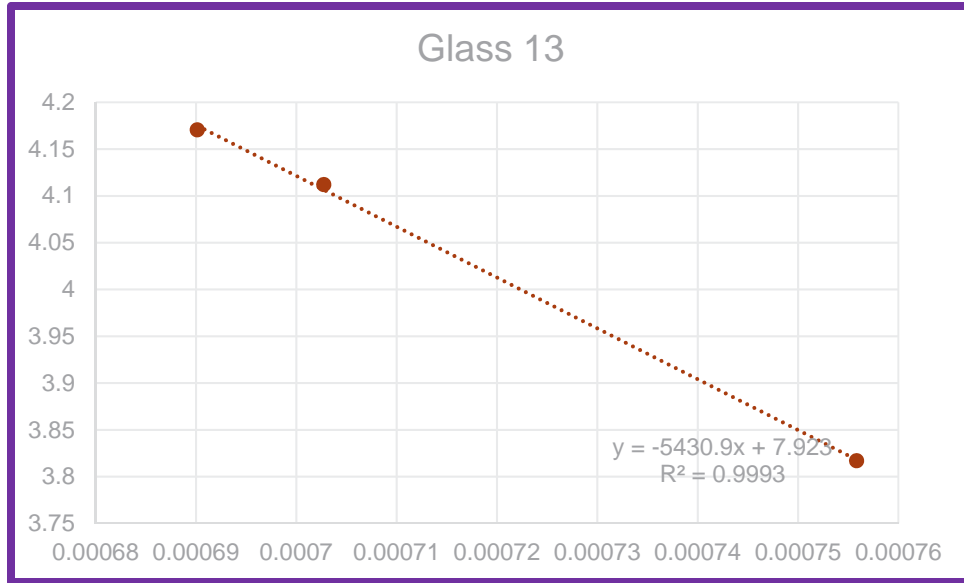


Figure E.9. Electrical conductivity data (ln(EC, S/m) versus inverse temperature in Kelvin) for LAWPh3-13.

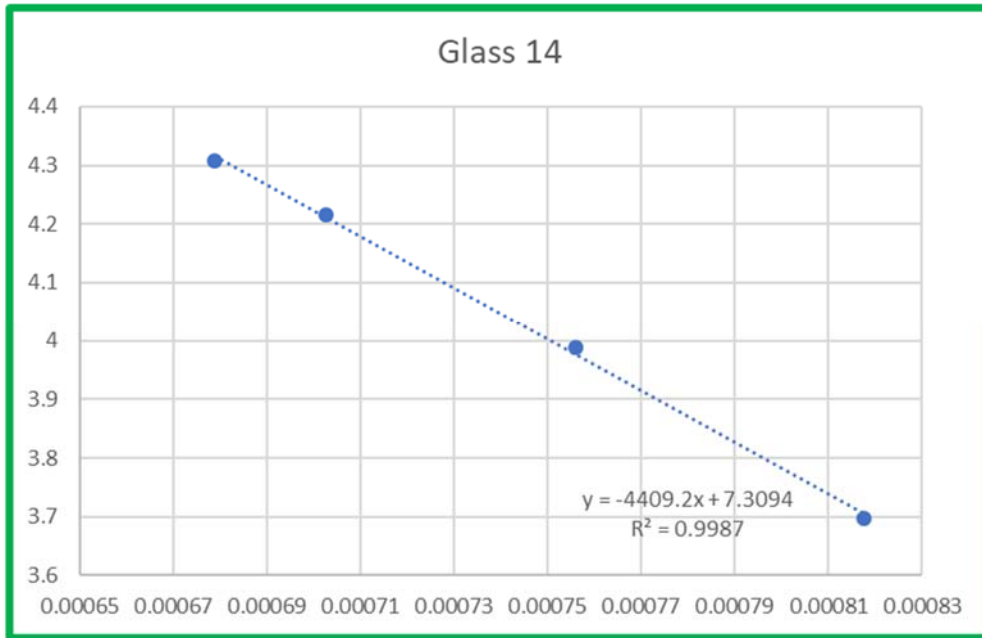


Figure E.10. Electrical conductivity data (ln(EC, S/m) versus inverse temperature in Kelvin) for LAWPh3-14.

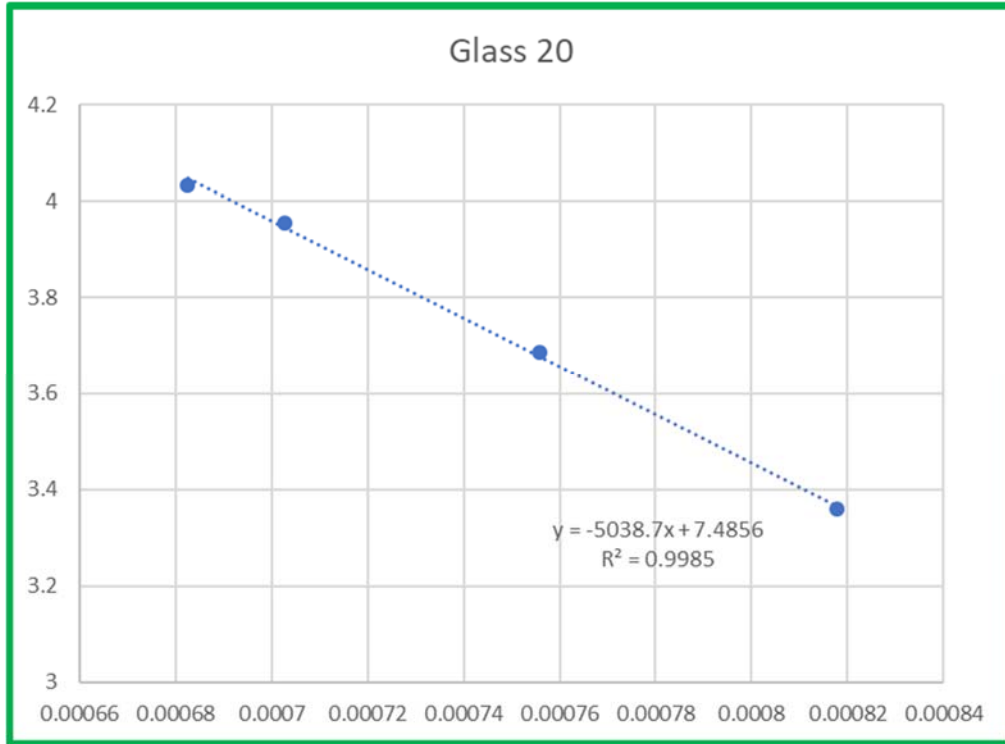


Figure E.11. Electrical conductivity data (ln(EC, S/m) versus inverse temperature in Kelvin) for LAWPh3-20.

Appendix F – Images of Crystal-Containing Heat-Treated Glasses (after isothermal holds at 950°C and CCC)

This appendix contains images of the glass compositions that contained crystals in the glass after heat treatments. These heat treatments are the crystal fraction determination (isothermal at 950°C for 24 h) as well as the container centerline cooling (CCC) profile. The images of quenched samples before heat treatments are in Appendix A. Images for the modified glasses after CCC were not taken.



Figure F.1(a). Optical micrograph of glass LAWPh3-01 after isothermal treatment at 950°C for 24 h magnified 20X.



Figure F.1(b). Photograph of glass LAWPh3-01 after CCC heat treatment (top).

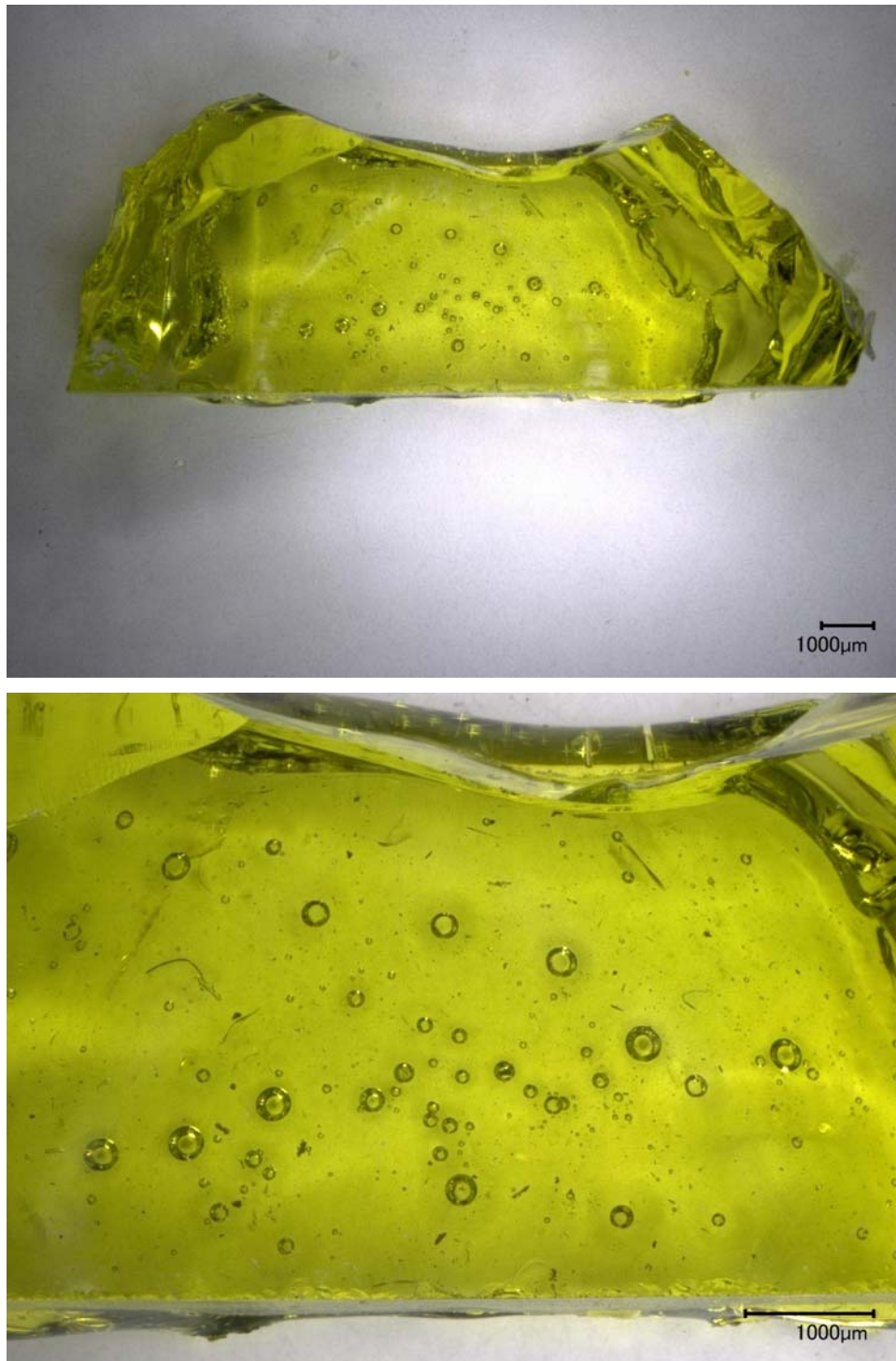


Figure F.2(a). Optical micrograph of glass LAWPh3-02 after isothermal treatment at 950°C for 24 h magnified 20X (top) and 50X (bottom).



Figure F.2(b). Photograph of glass LAWPh3-02 after CCC heat treatment (top).



Figure F.3(a). Optical micrograph of glass LAWPh3-03 after isothermal treatment at 950°C for 24 h.



Figure F.3(b). Photograph of glass LAWPh3-03 after CCC heat treatment (top).

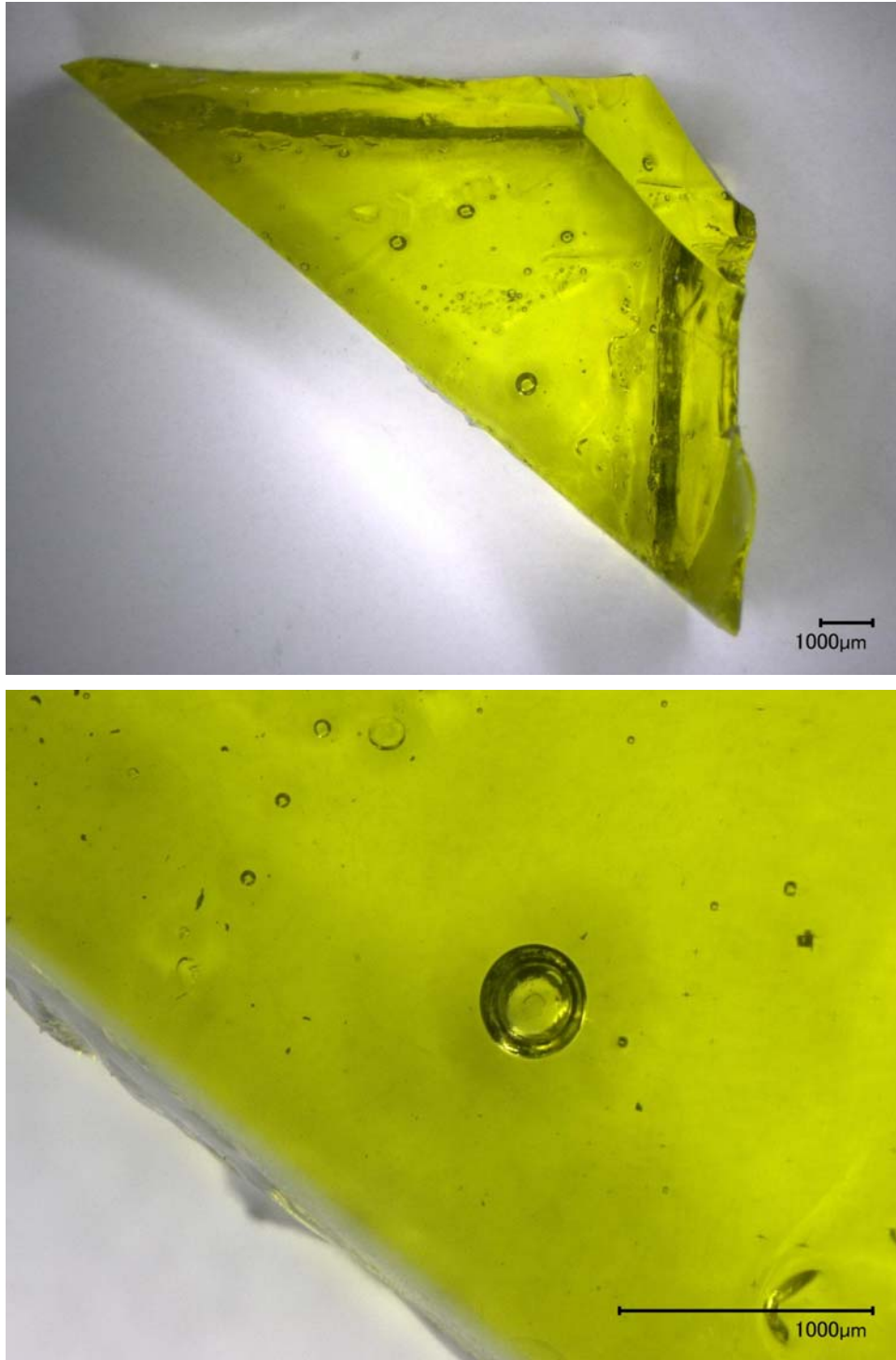


Figure F.4(a). Optical micrograph of glass LAWPh3-04 after isothermal treatment at 950°C for 24 h magnified 20X (top) and 100X (bottom).



Figure F.4(b). Photograph of glass LAWPh3-04 after CCC heat treatment (top).

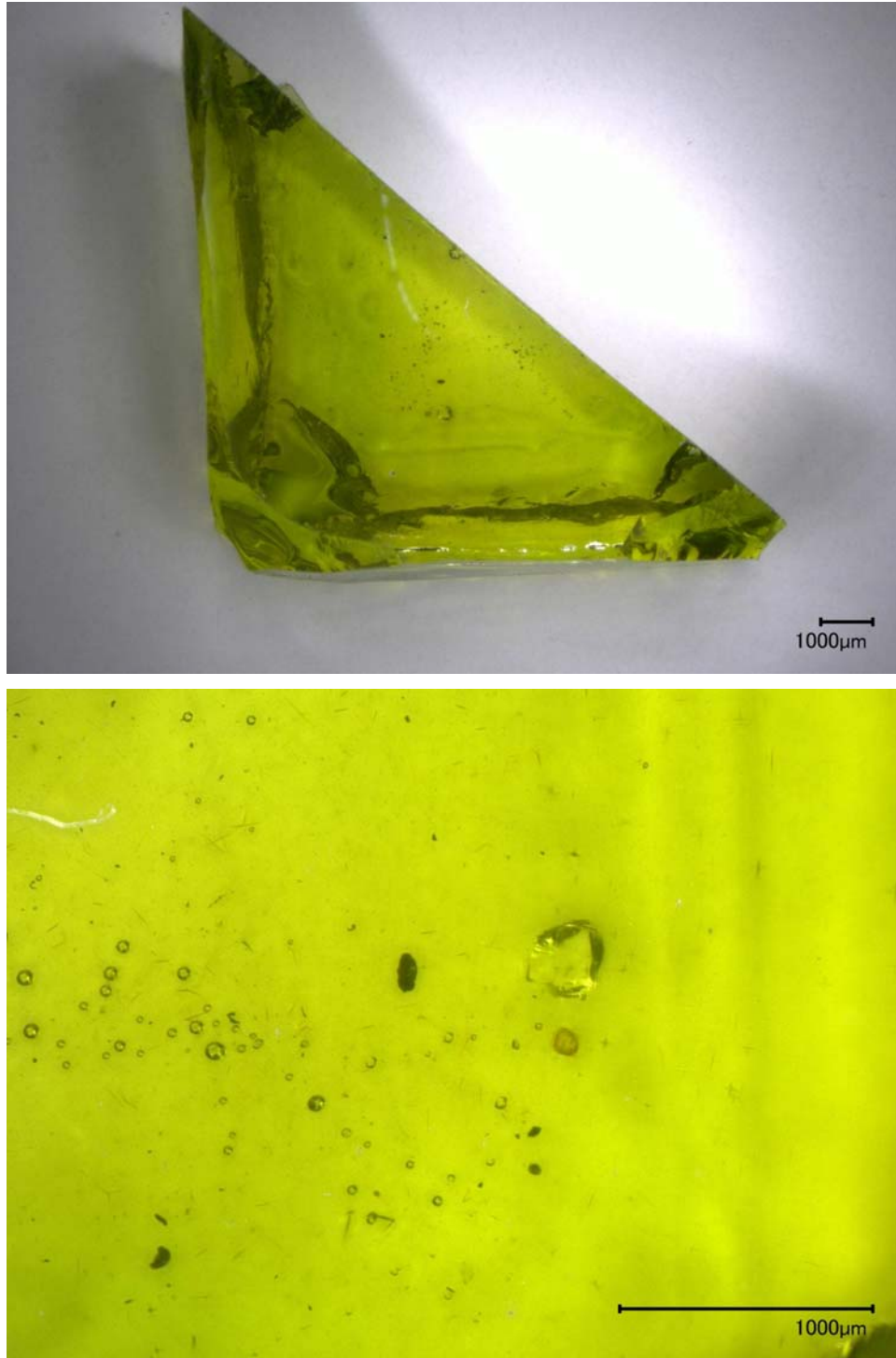


Figure F.5(a). Optical micrograph of glass LAWPh3-06 after isothermal treatment at 950°C for 24 h magnified 20X (top) and 100X (bottom).

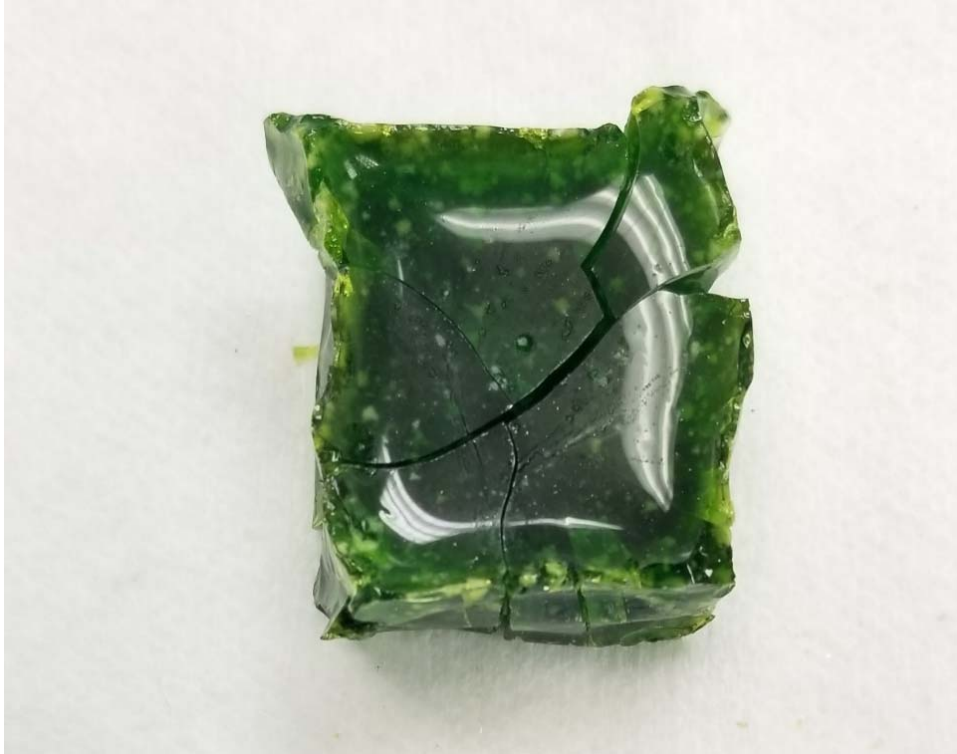


Figure F.5(b). Photograph of glass LAWPh3-06 after CCC heat treatment.

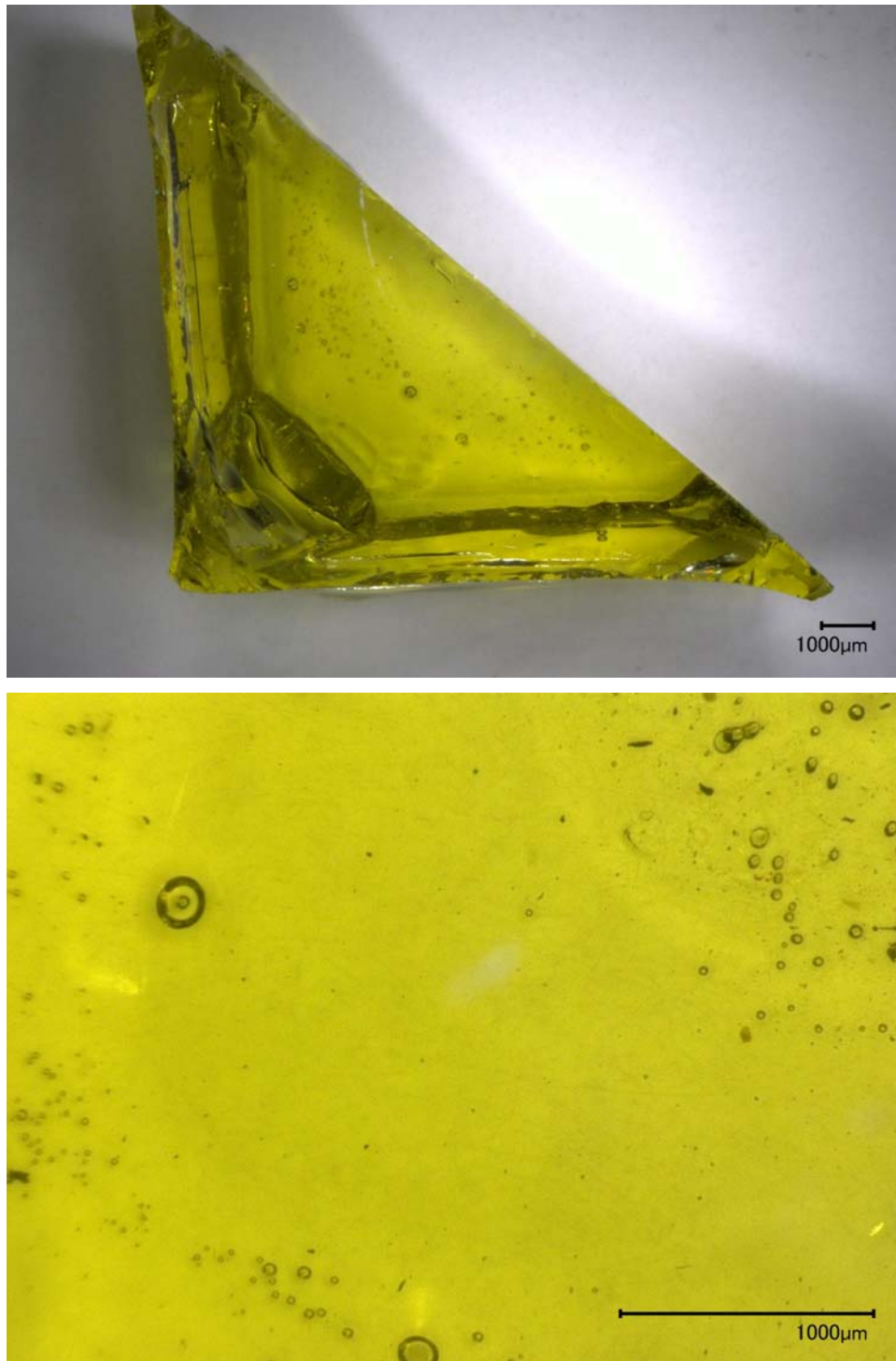


Figure F.6(a). Optical micrograph of glass LAWPh3-07 after isothermal treatment at 950°C for 24 h magnified 20X (top) and 100X (bottom).

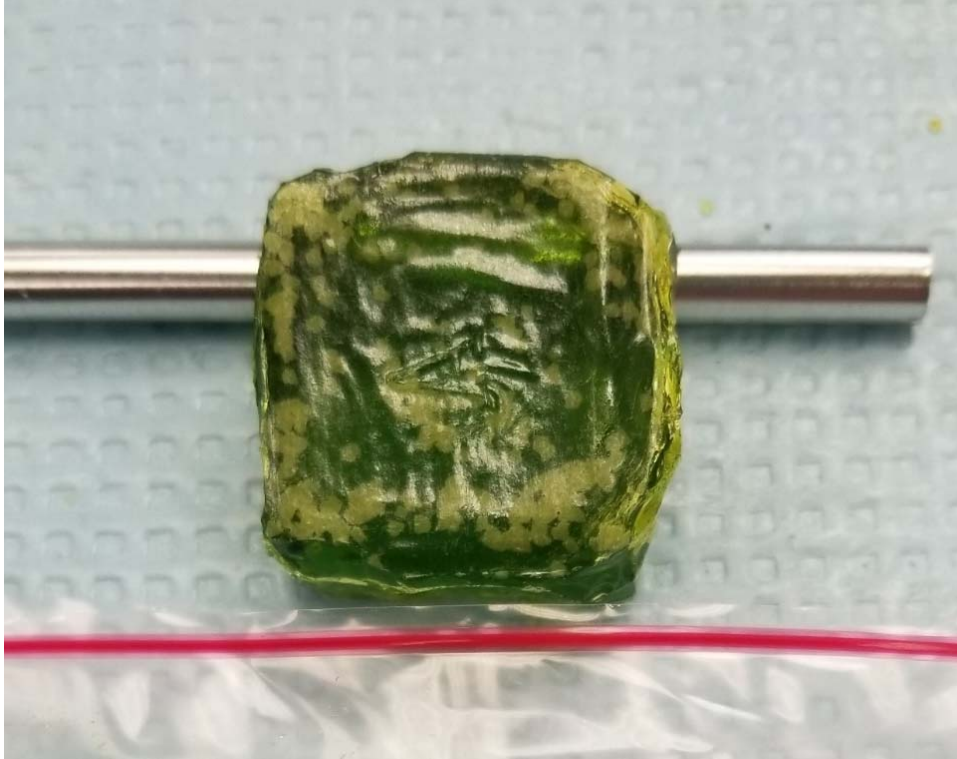


Figure F.6(b). Photograph of glass LAWPh3-07 after CCC heat treatment.

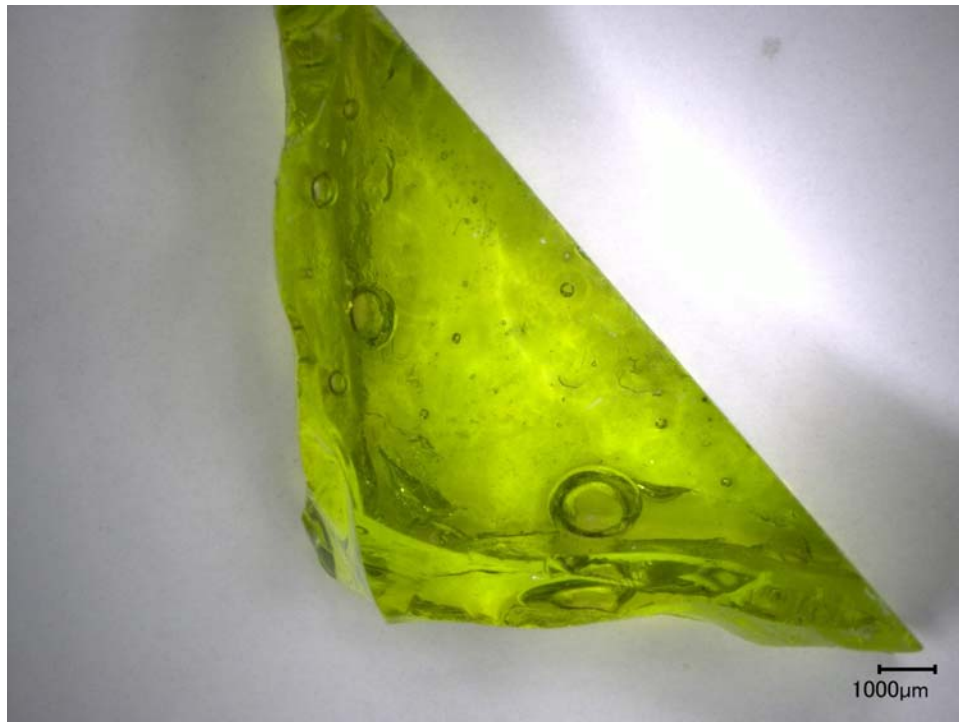


Figure F.7(a). Optical micrograph of glass LAWPh3-08 after isothermal treatment at 950°C for 24 h magnified 20X.

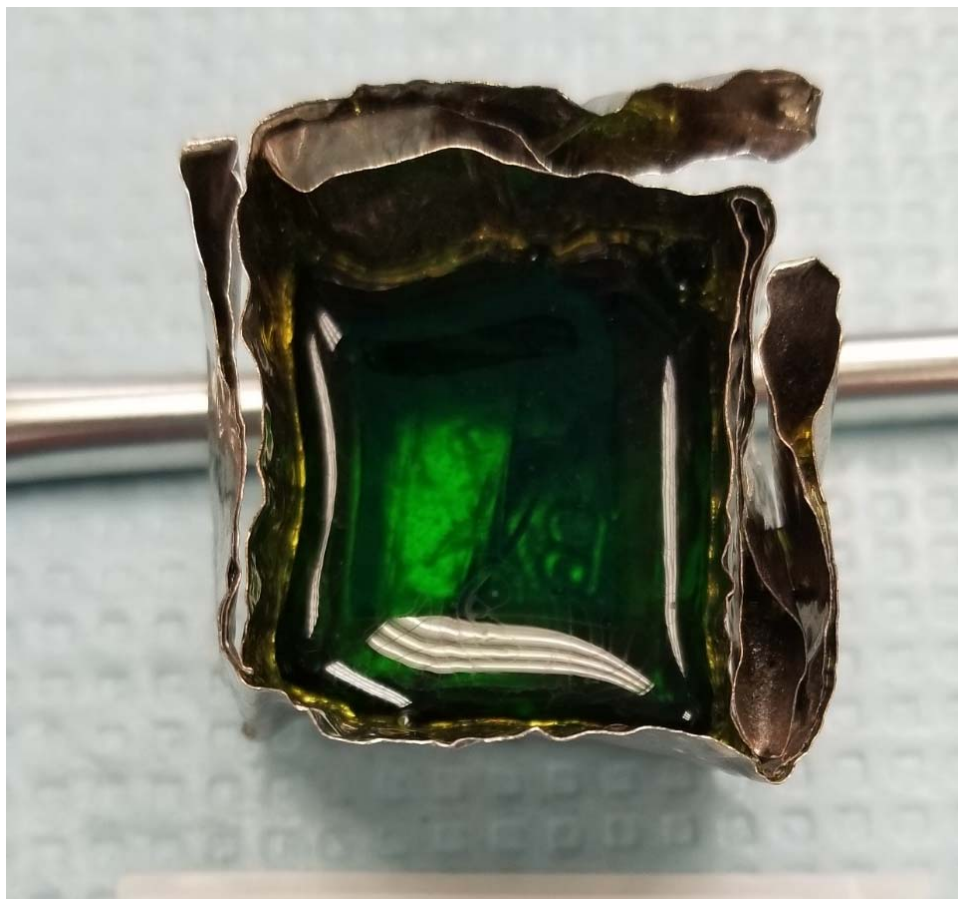


Figure F.7(b). Photograph of glass LAWPh3-08 after CCC heat treatment.

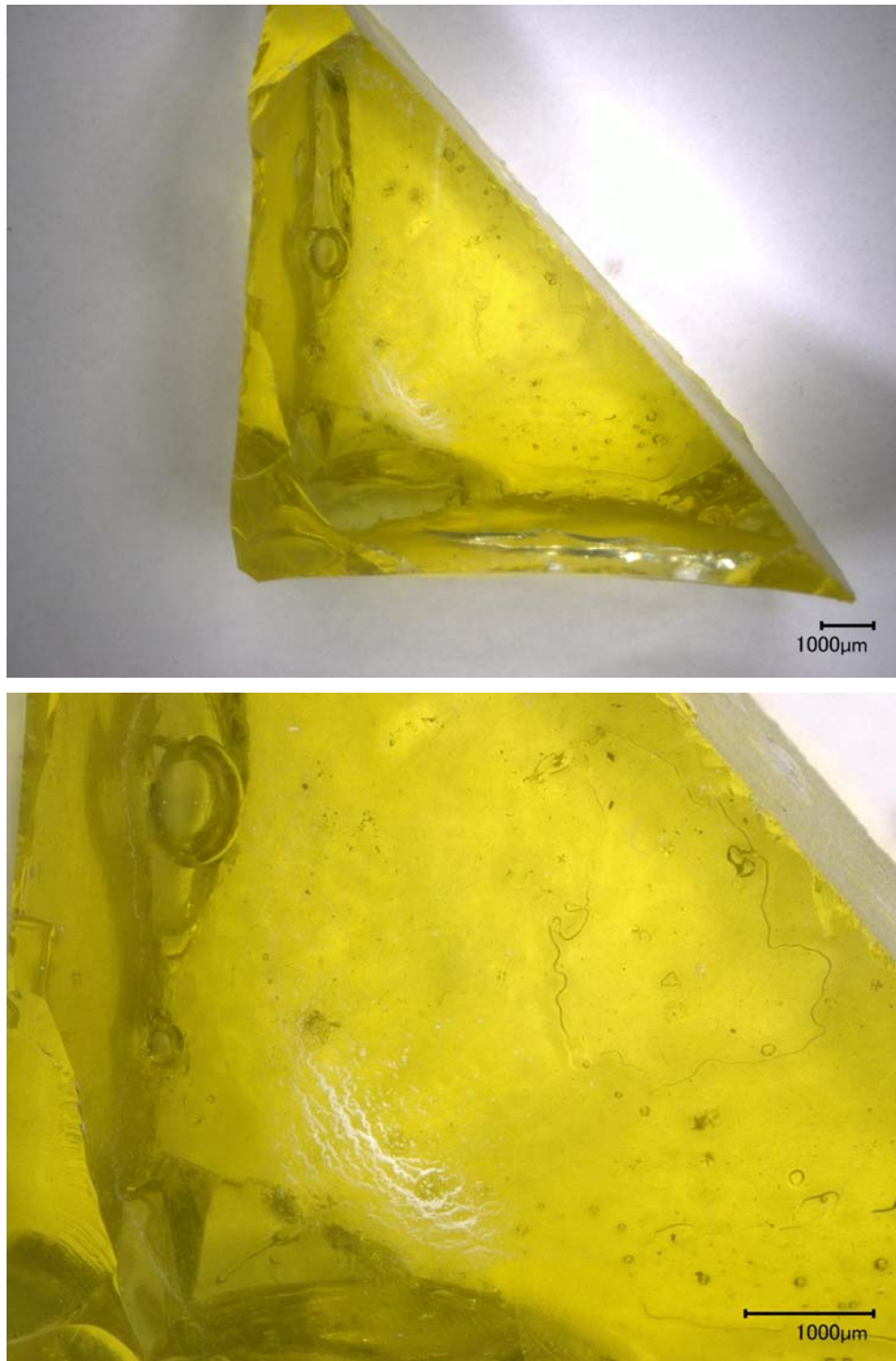


Figure F.8(a). Optical micrograph of glass LAWPh3-09 after isothermal treatment at 950°C for 24 h magnified 20X (top) and 50X (bottom).



Figure F.8(b). Photograph of glass LAWPh3-09 after CCC heat treatment.

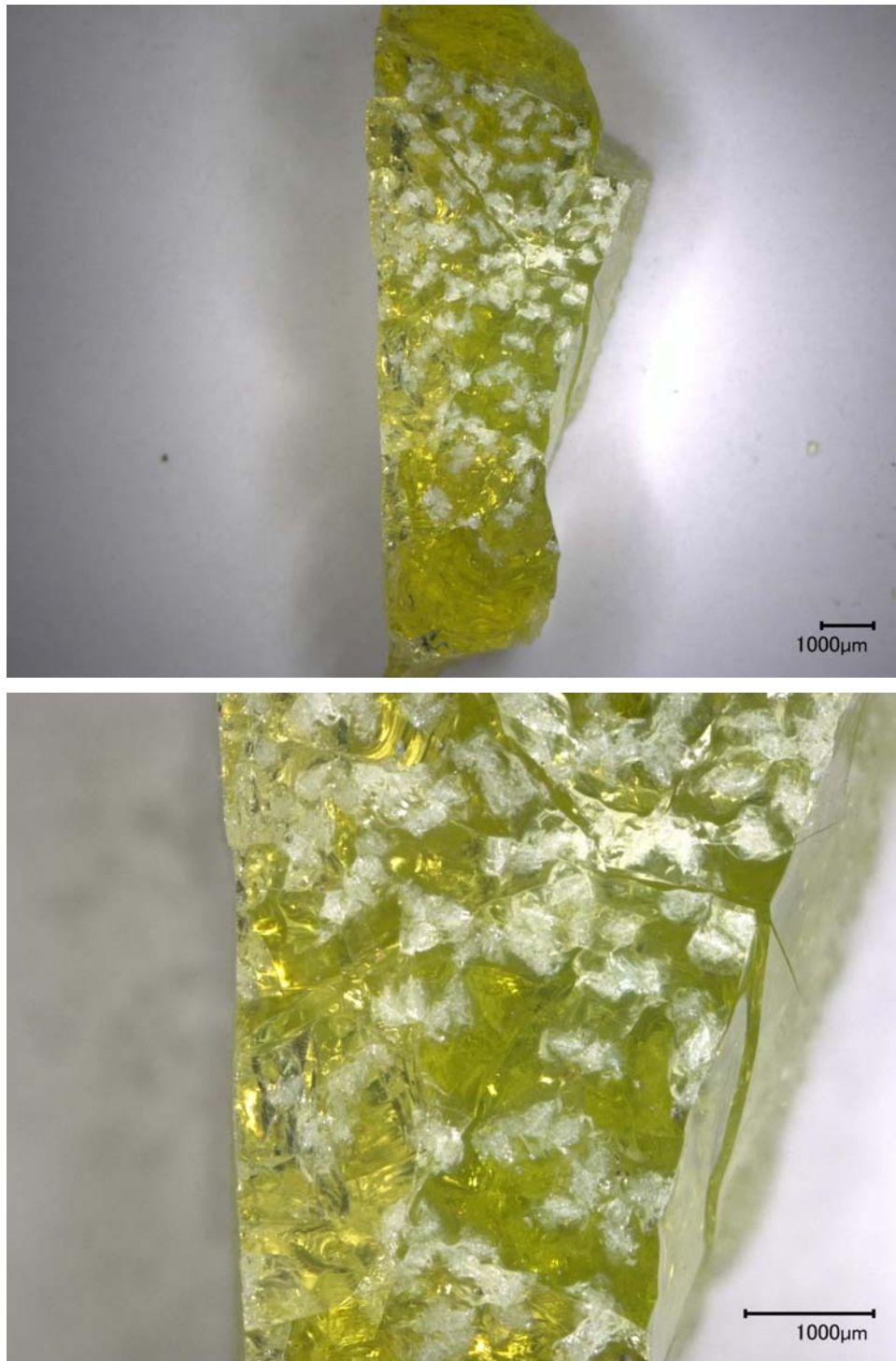


Figure F.9(a). Optical micrograph of glass LAWPh3-10 after isothermal treatment at 950°C for 24 h magnified 20X (top) and 50X (bottom).

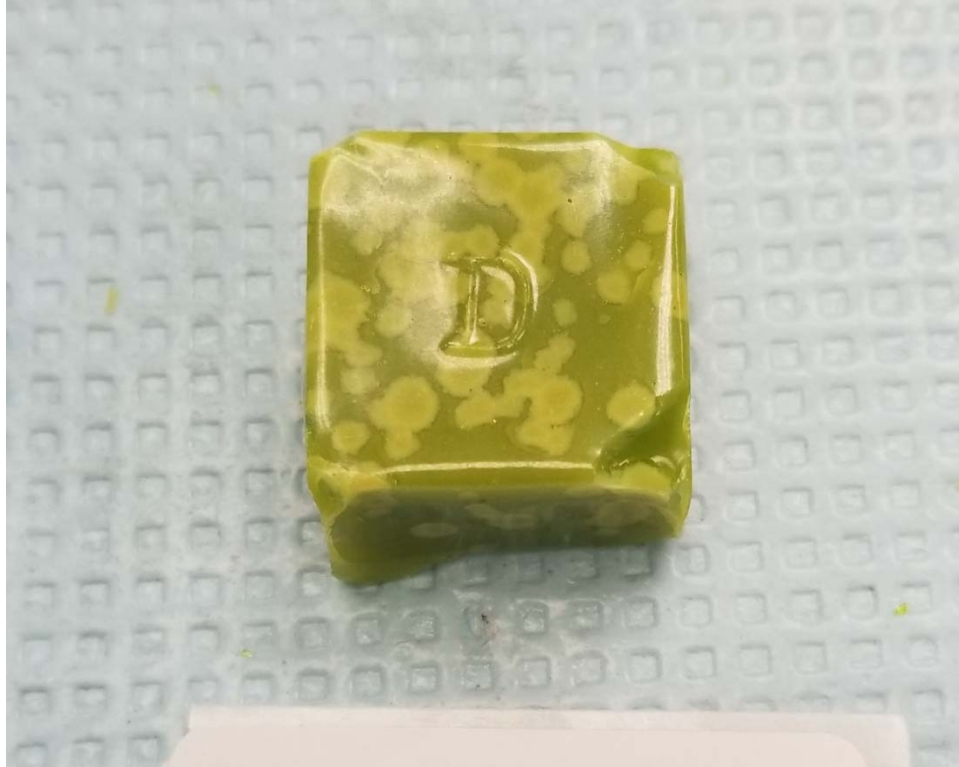


Figure F.9(b). Photograph of glass LAWPh3-10 after CCC heat treatment.

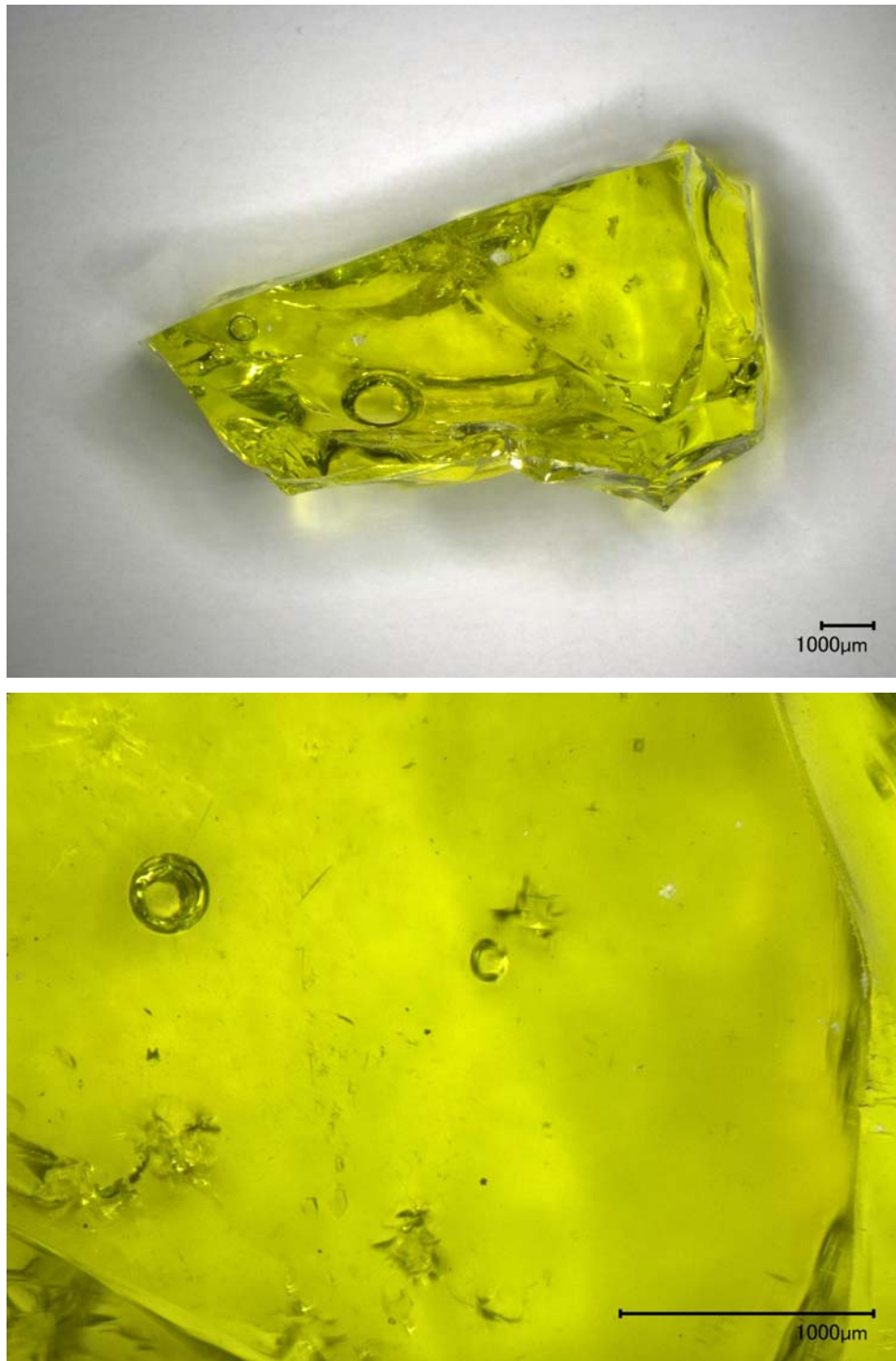


Figure F.10(a). Optical micrograph of glass LAWPh3-11 after isothermal treatment at 950°C for 24 h magnified 20X (top) and 100X (bottom).



Figure F.10(b). Photograph of glass LAWPh3-11 after CCC heat treatment.

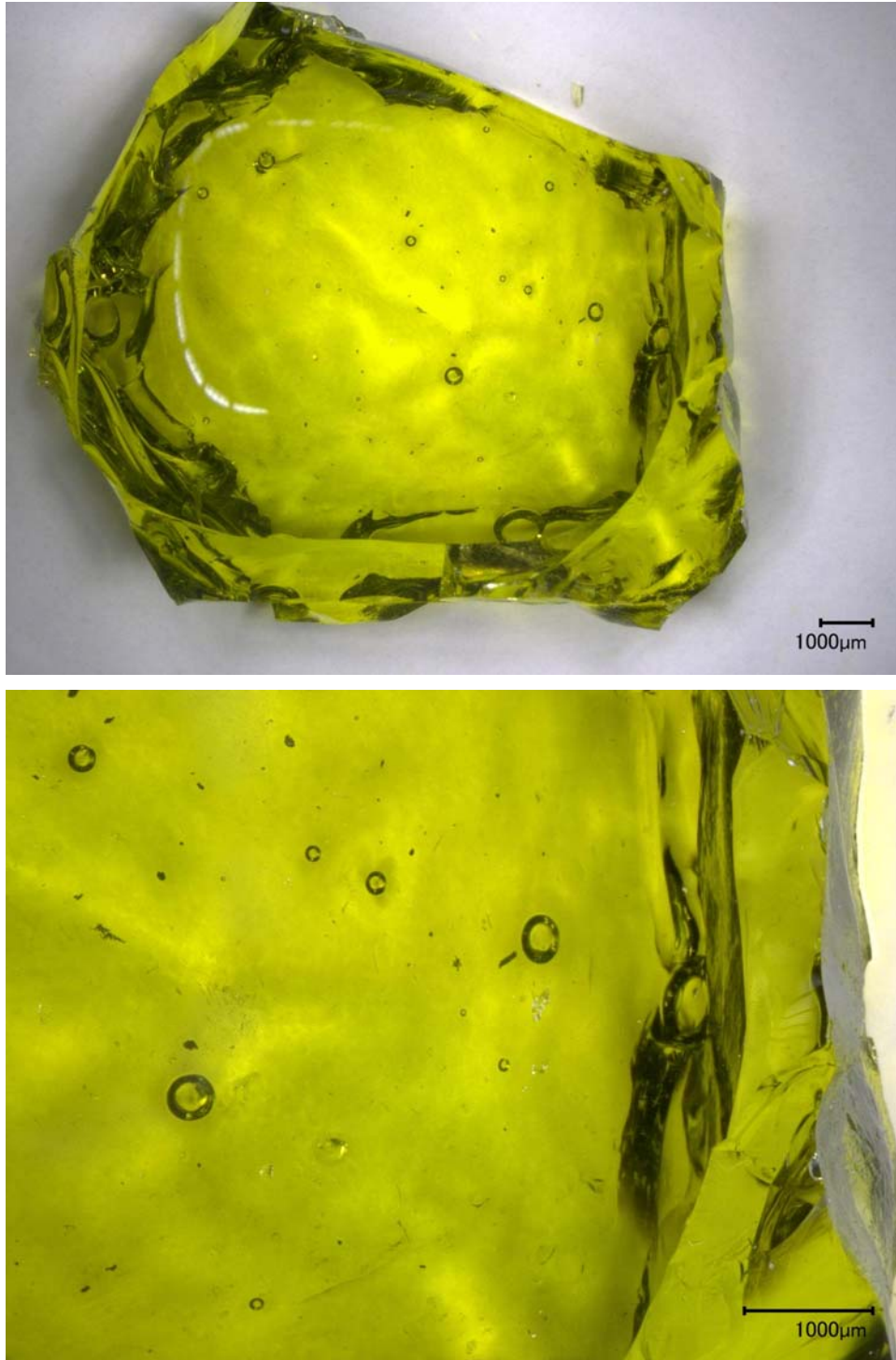


Figure F.11(a). Optical micrograph of glass LAWPh3-12 after isothermal treatment at 950°C for 24 h magnified 20X (top) and 50X (bottom).



Figure F.11(b). Photograph of glass LAWPh3-12 after CCC heat treatment.

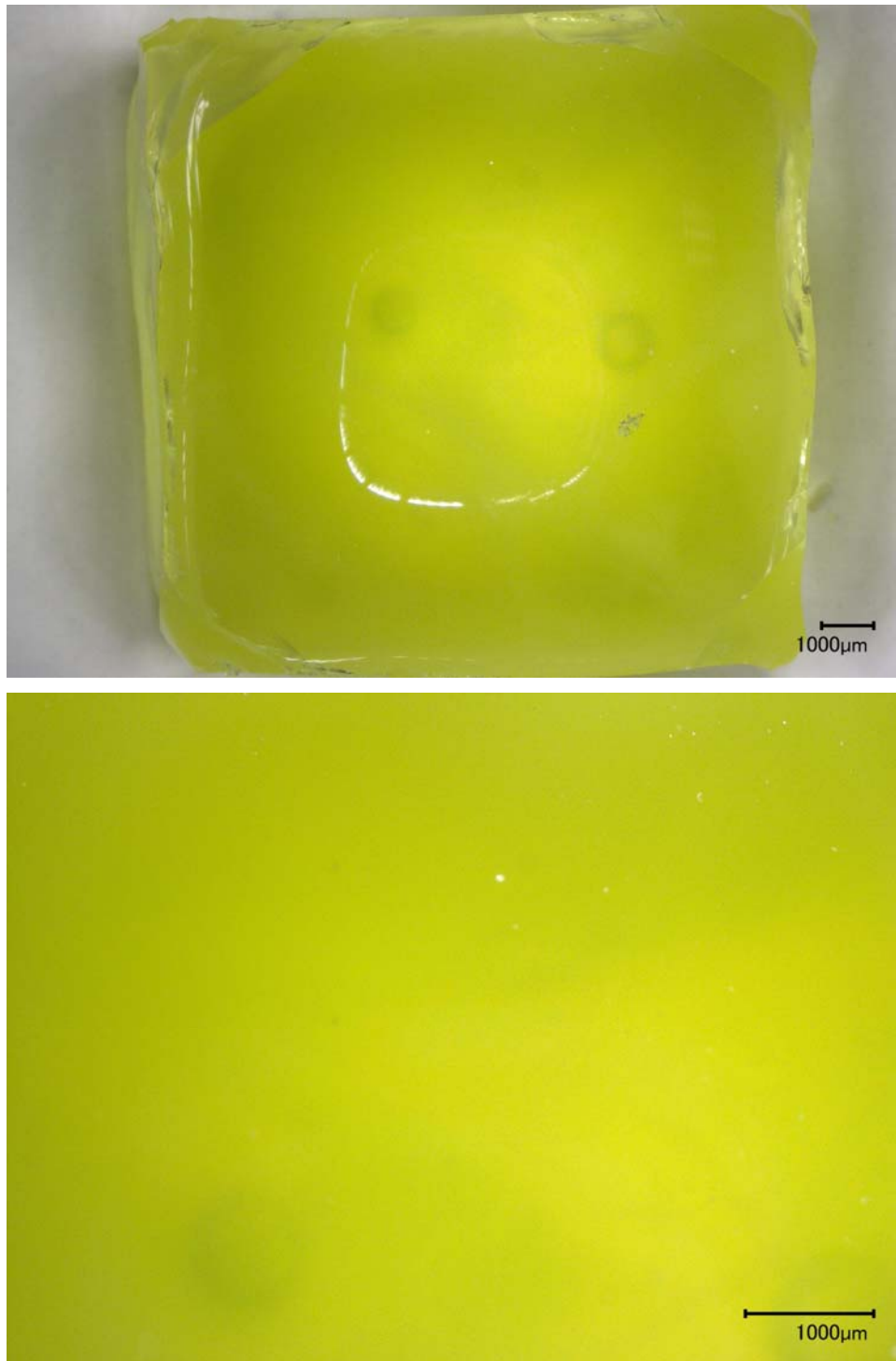


Figure F.12(a). Optical micrograph of glass LAWPh3-13 after isothermal treatment at 950°C for 24 h magnified 20X (top) and 50X (bottom).



Figure F.12(b). Photograph of glass LAWPh3-13 after CCC heat treatment.



Figure F.13(a). Optical micrograph of glass LAWPh3-14 after isothermal treatment at 950°C for 24 h magnified 20X.

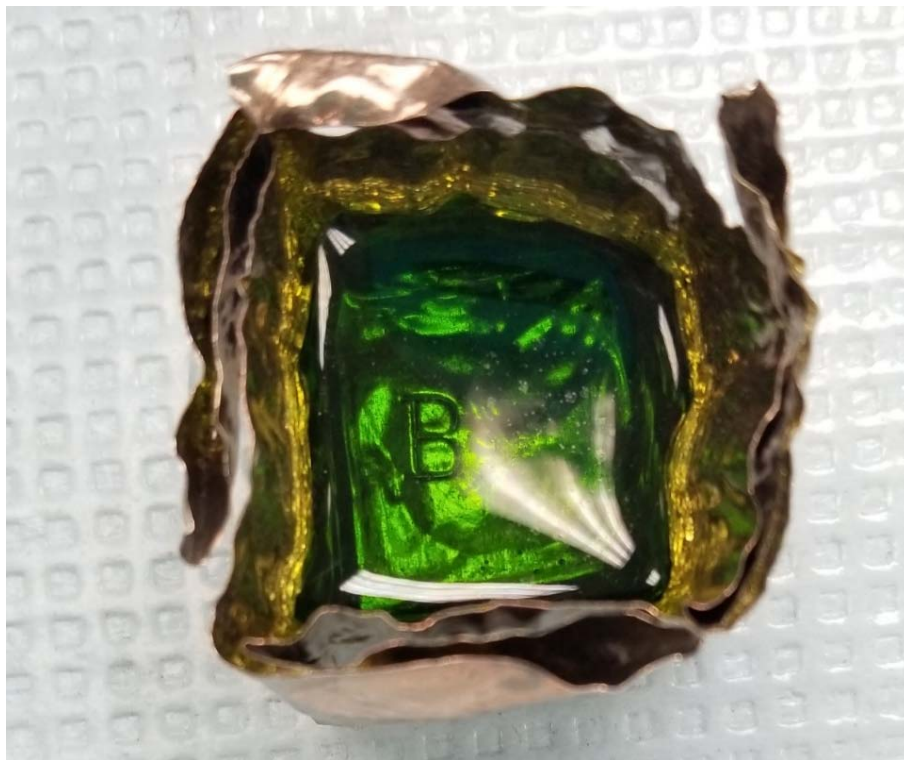


Figure F.13(b). Photograph of glass LAWPh3-14 after CCC heat treatment.

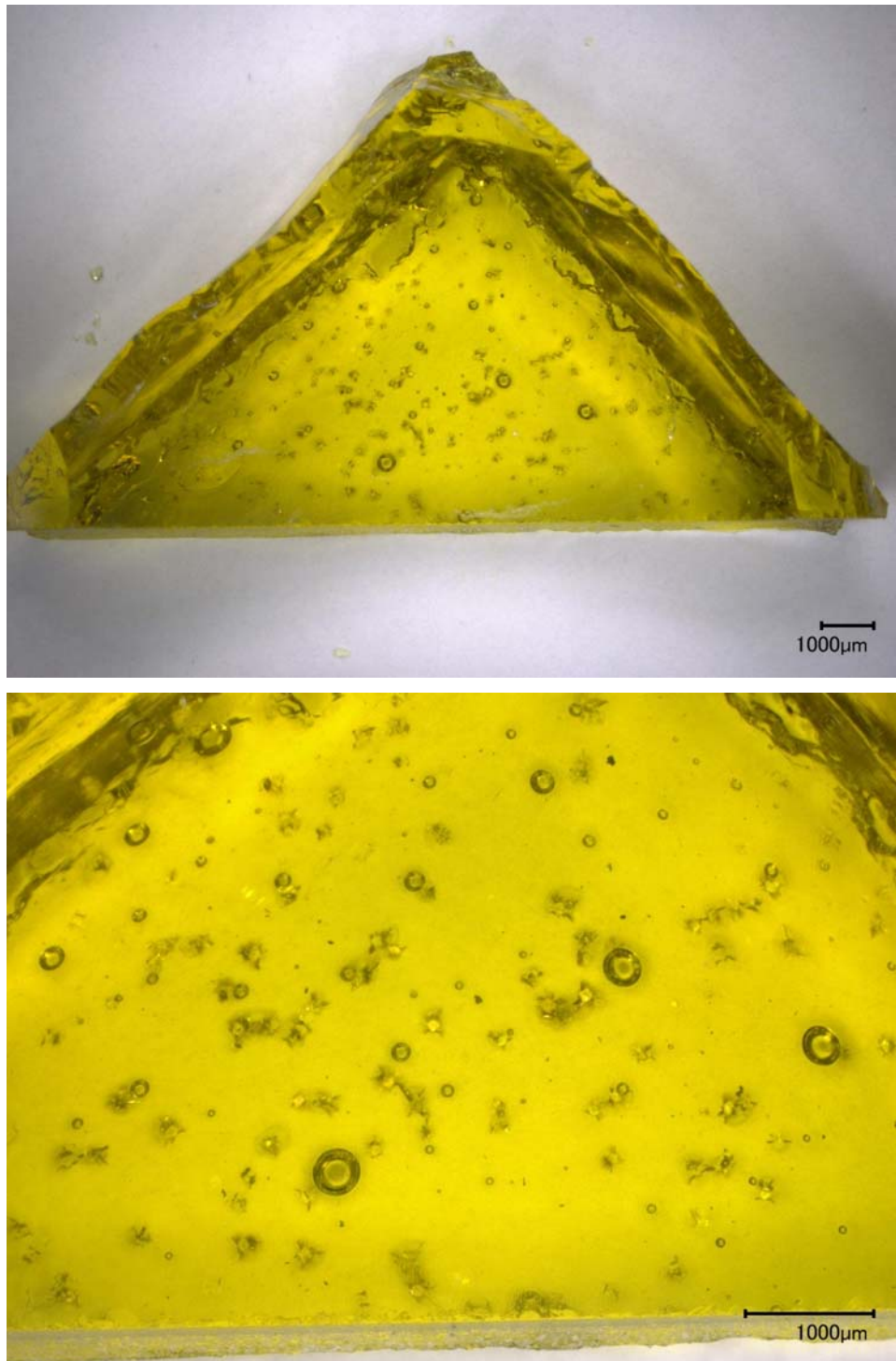


Figure F.14(a). Optical micrograph of glass LAWPh3-15 after isothermal treatment at 950°C for 24 h magnified 20X (top) and 50X (bottom).



Figure F.14(b). Photograph of glass LAWPh3-15 after CCC heat treatment.

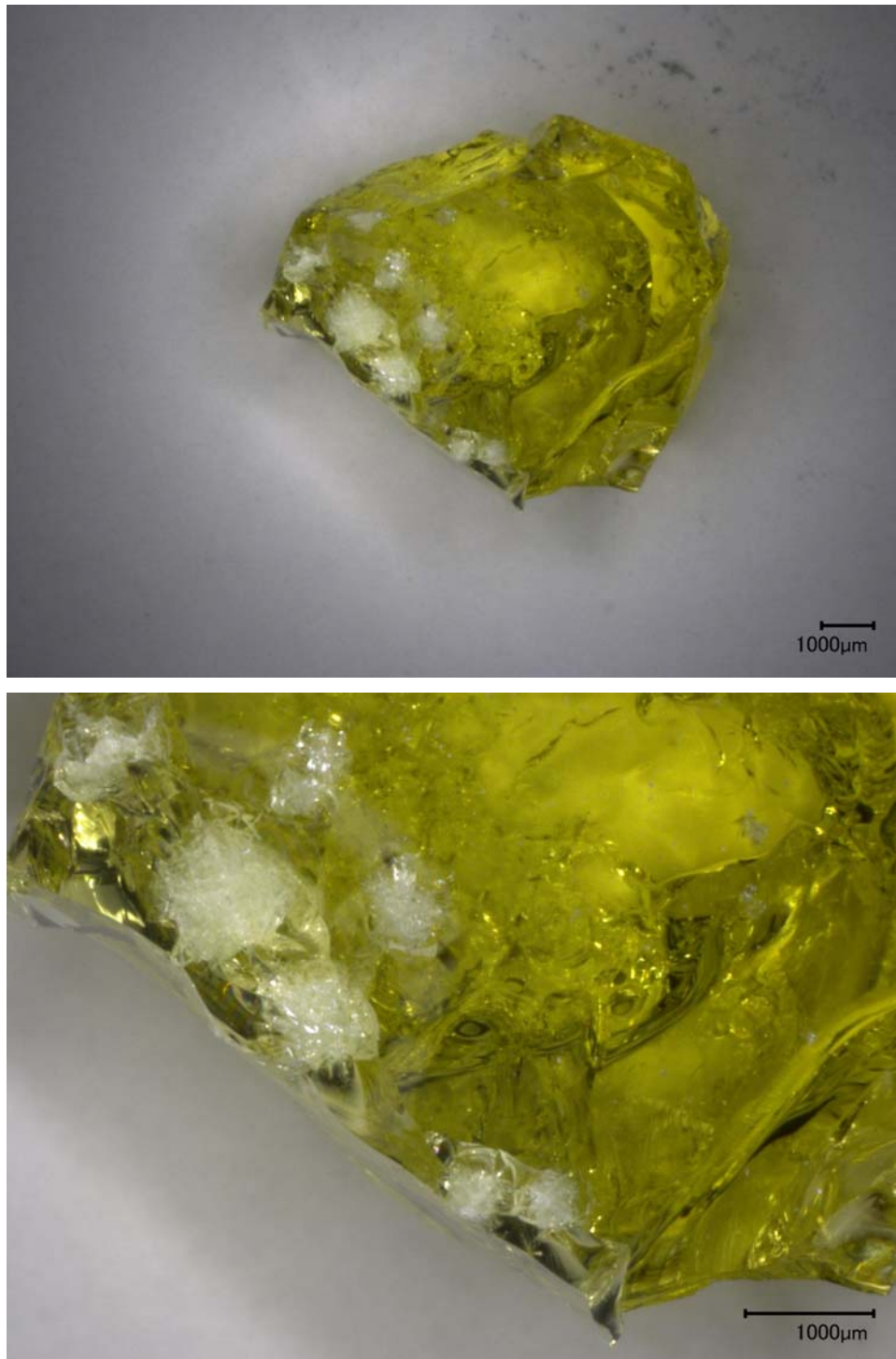


Figure F.15(a). Optical micrograph of glass LAWPh3-16 after isothermal treatment at 950°C for 24 h magnified 20X (top) and 50X (bottom).

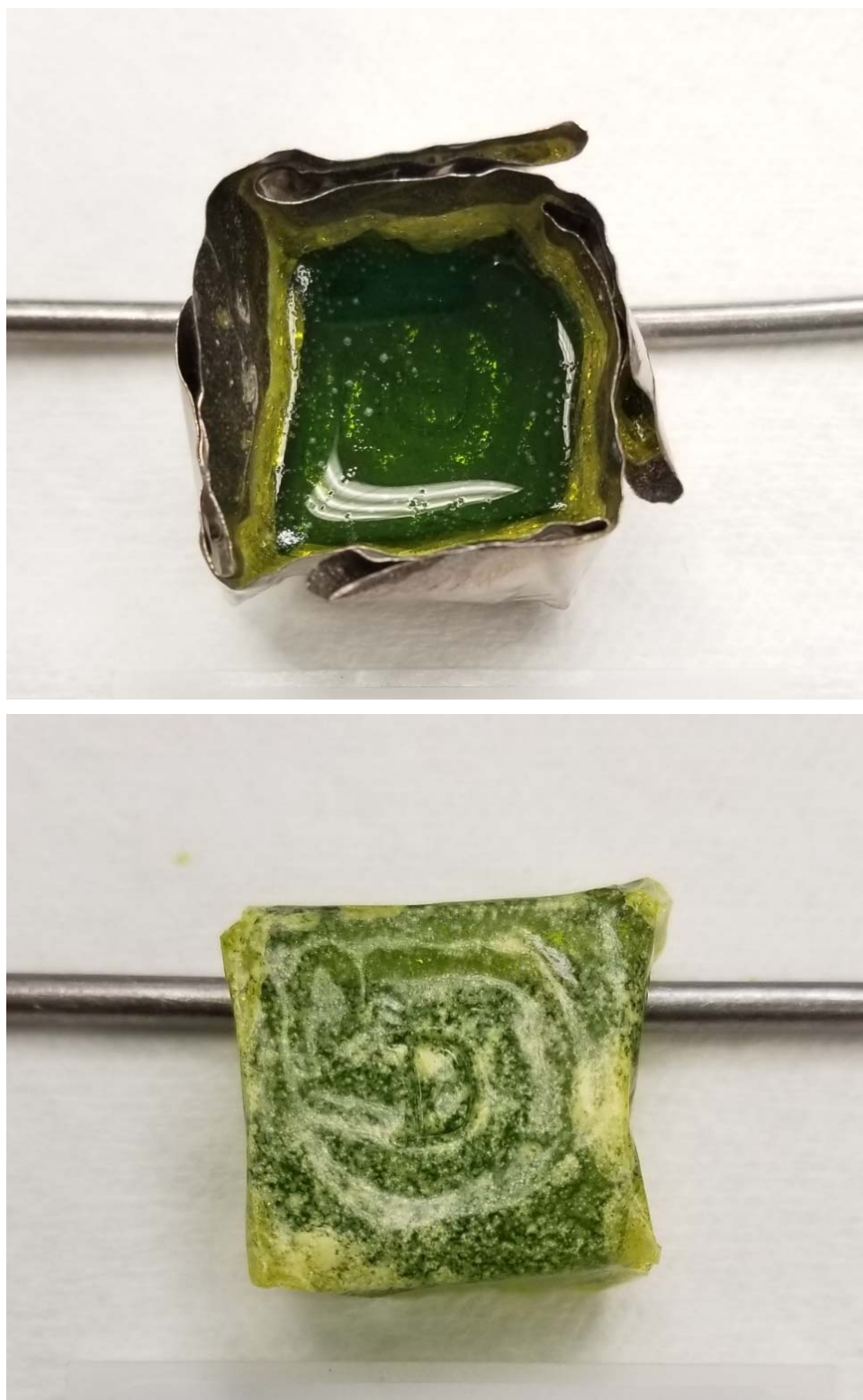


Figure F.15(b). Photograph of glass LAWPh3-16 after CCC heat treatment in crucible (top) and bottom portion out of crucible (bottom).



Figure F.16(a). Optical micrograph of glass LAWPh3-17 after isothermal treatment at 950°C for 24 h magnified 10X (top) and 100X (bottom).



Figure F.16(b). Photograph of glass LAWPh3-17 after CCC heat treatment in crucible (top) and bottom out of crucible (bottom).

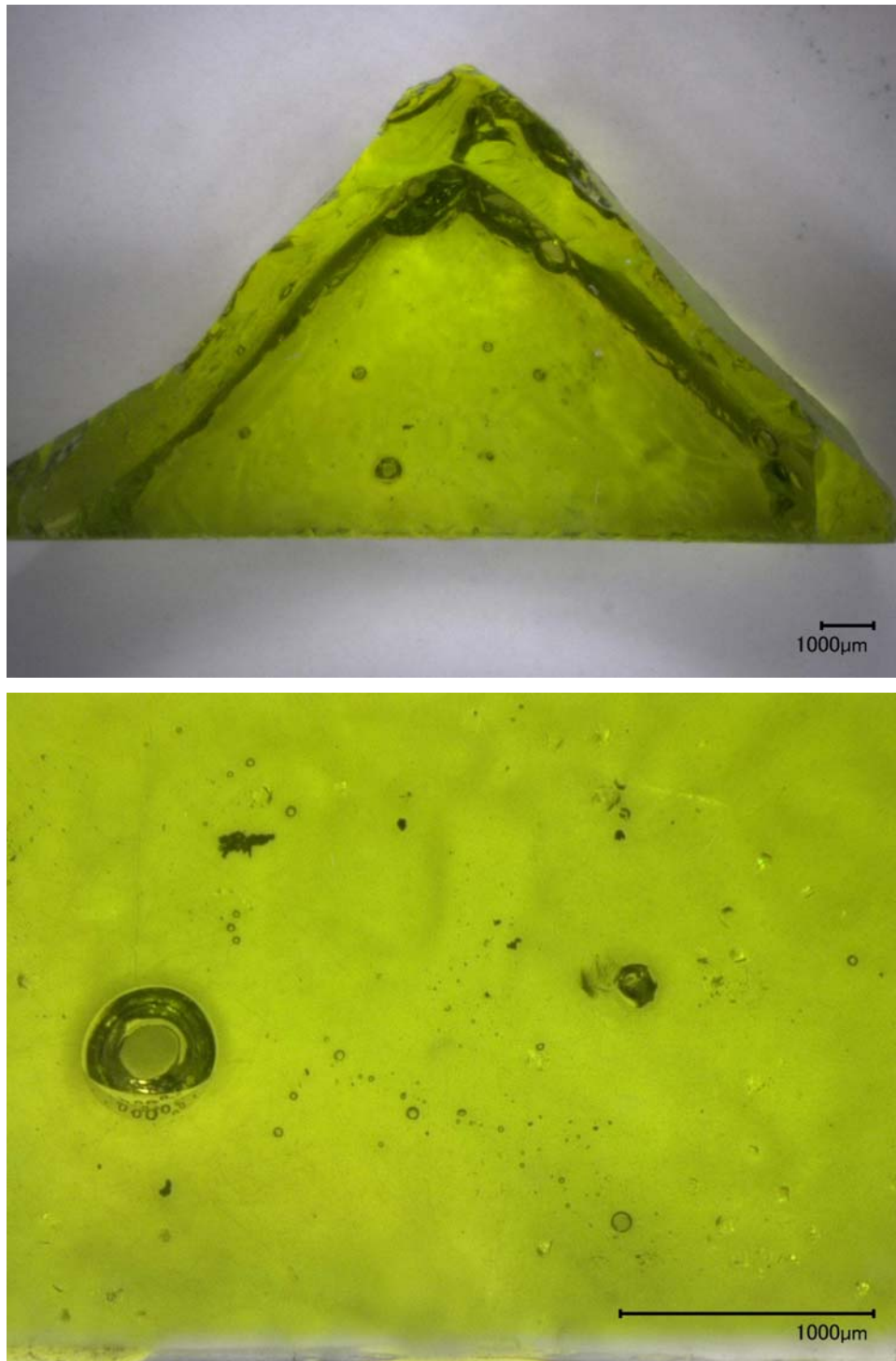


Figure F.17(a). Optical micrograph of glass LAWPh3-18 after isothermal treatment at 950°C for 24 h magnified 20X (top) and 100X (bottom).



Figure F.17(b). Photograph of glass LAWPh3-18 after CCC heat treatment.

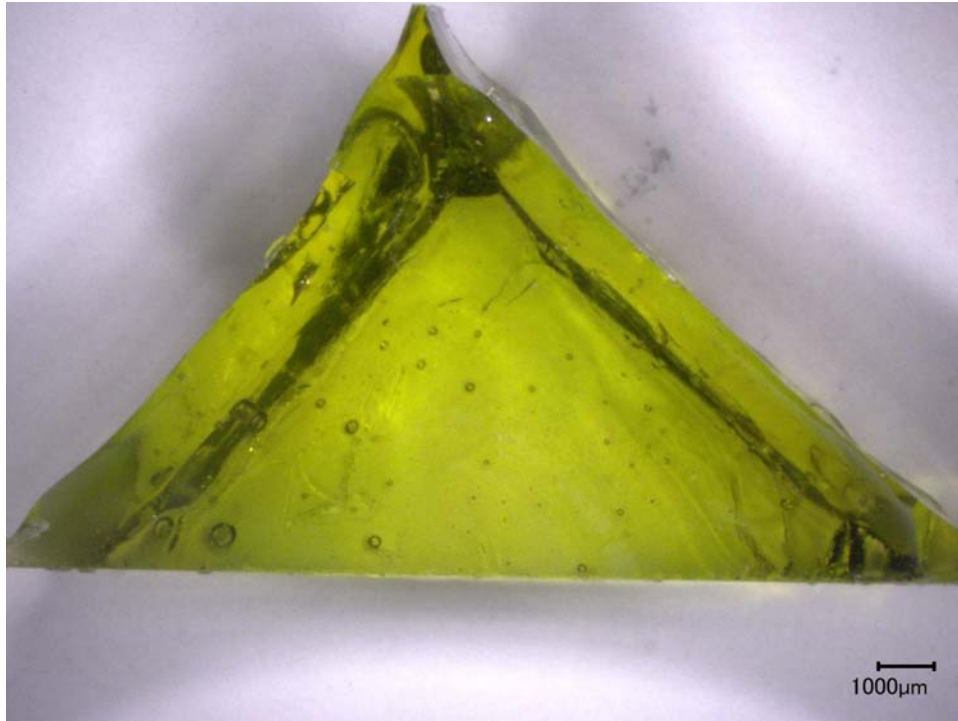


Figure F.18(a). Glass LAWPh3-20 after isothermal treatment at 950°C for 24 h magnified 20X.



Figure F.18(b). Photograph of glass LAWPh3-20 after CCC heat treatment.

Appendix G – XRD Data for All LAW Phase 3 Glasses

This appendix shows the X-ray diffraction (XRD) plots of Phase 3 glasses as quenched (Q), isothermally heat treated (CF) for 24 h at 950°C, and container centerline cooling (CCC) heat treated. No crystal phase was seen from XRD patterns of the as-quenched samples. Some heat-treated samples crystallized as shown by the following patterns.

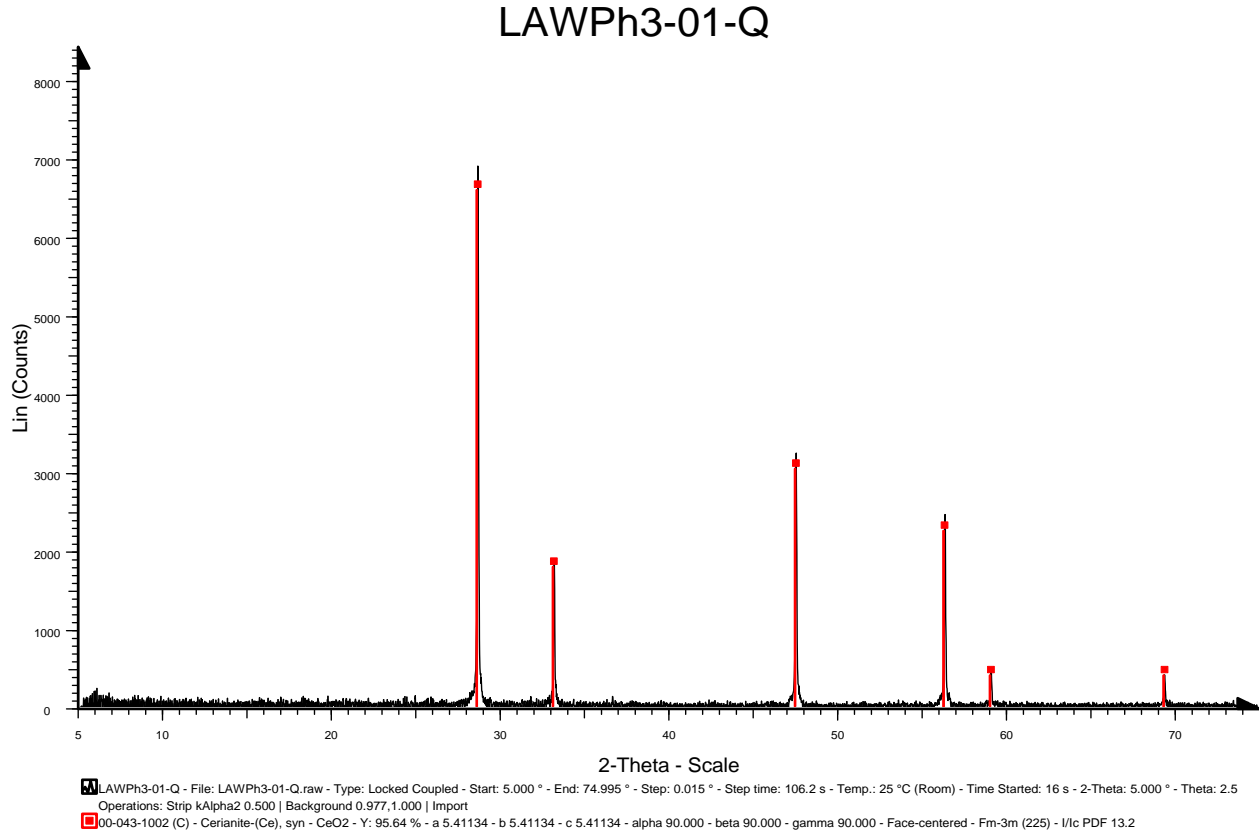


Figure G.1(a). XRD spectrum for LAWPh3-01-Q.

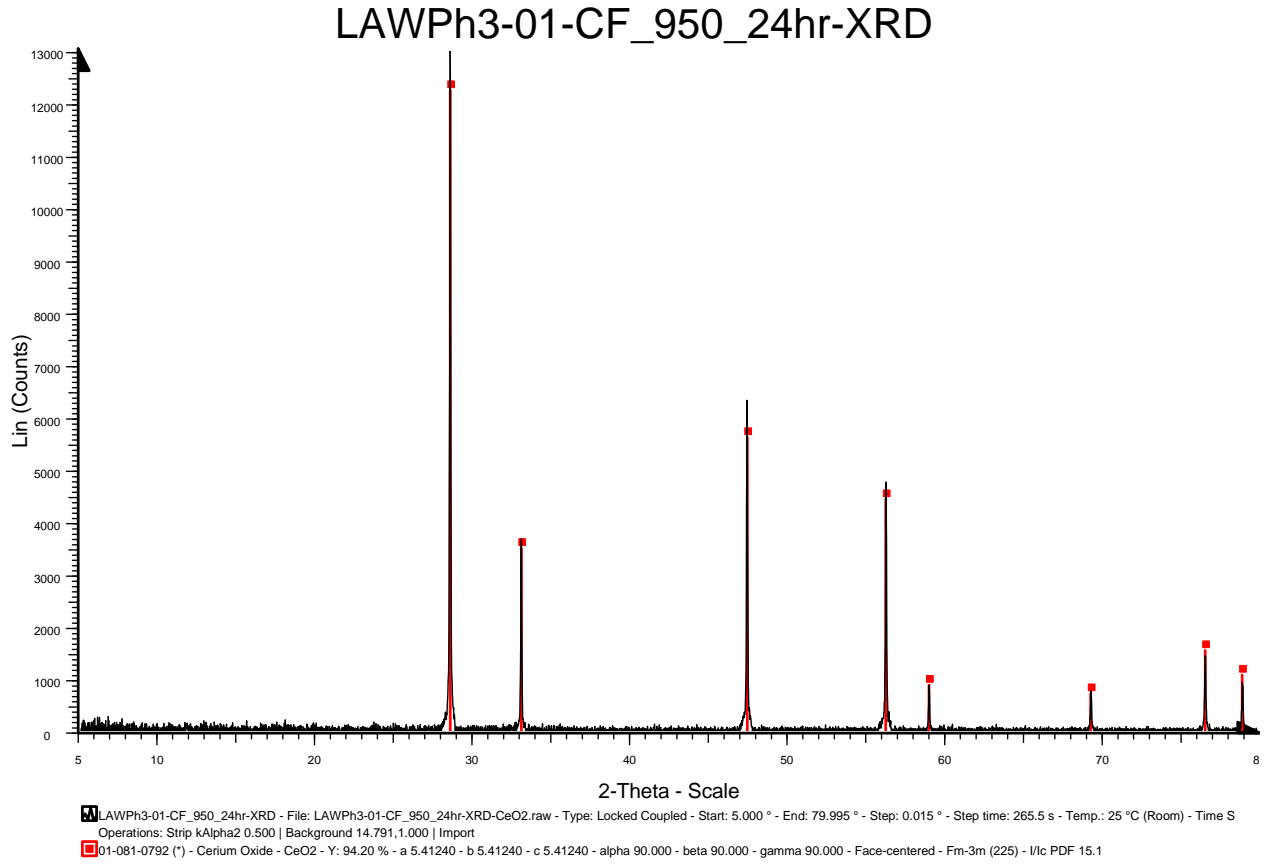


Figure G.1(b). XRD spectrum for LAWPh3-01-CF.

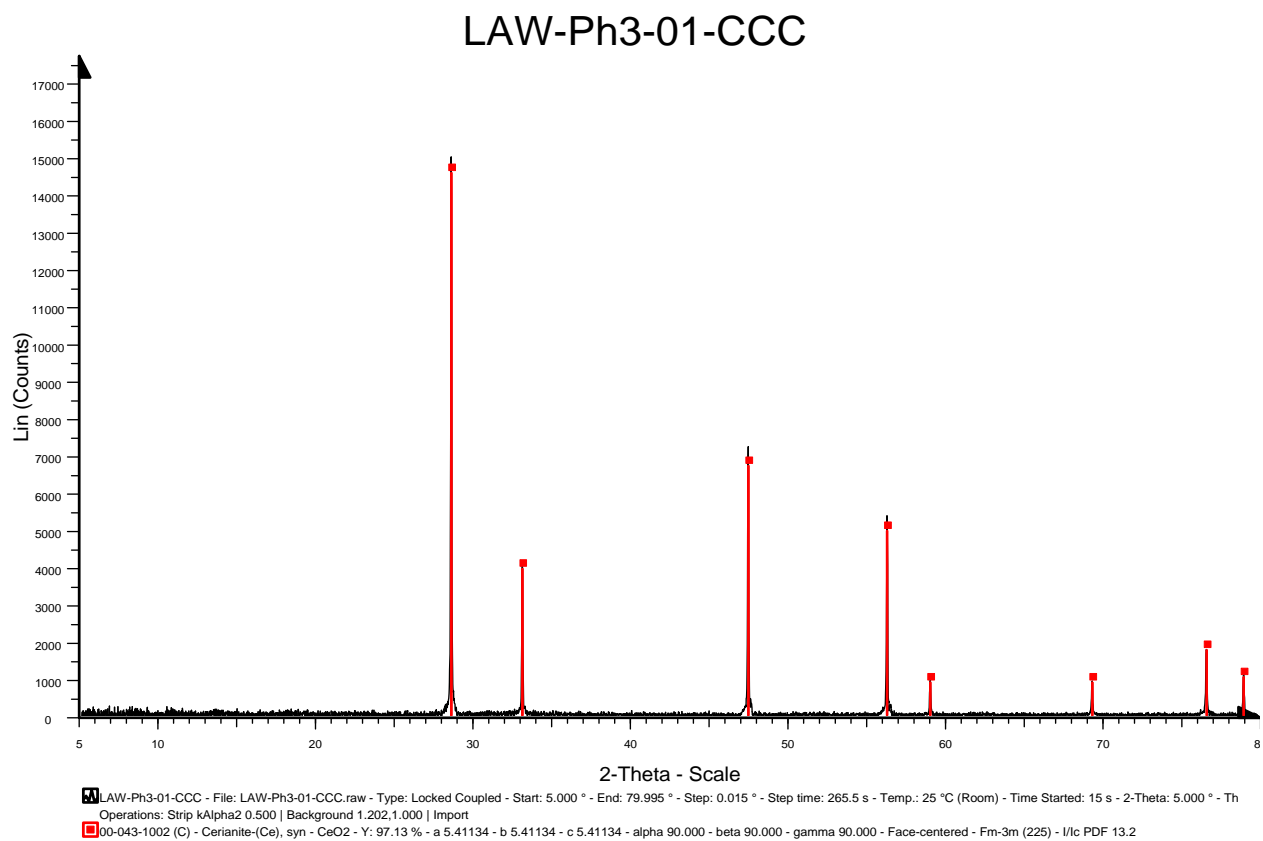


Figure G.1(c). XRD spectrum for LAWPh3-01-CCC.

LAWPh3-02-Q

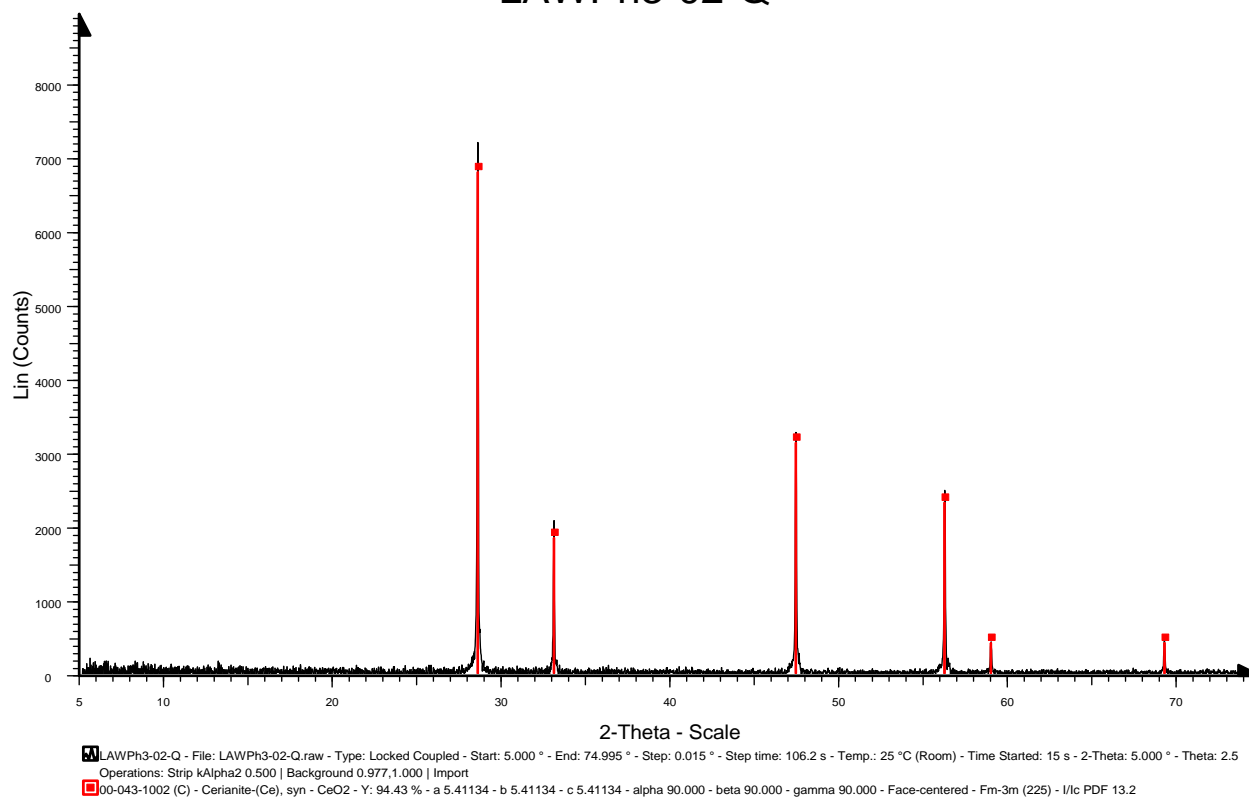


Figure G.2(a). XRD spectrum for LAWPh3-02-Q.

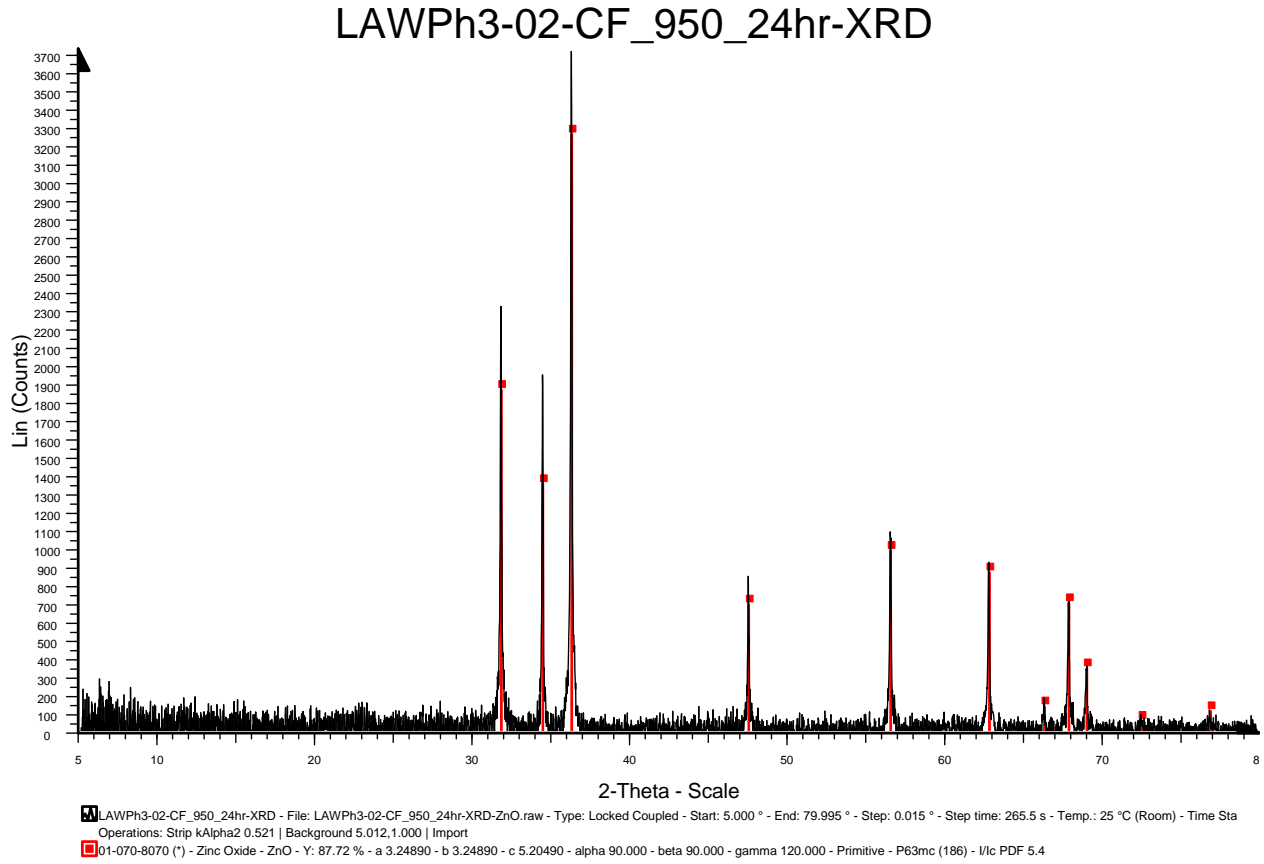


Figure G.2(b). XRD spectrum for LAWPh3-02-CF.

LAW-Ph3-02-CCC

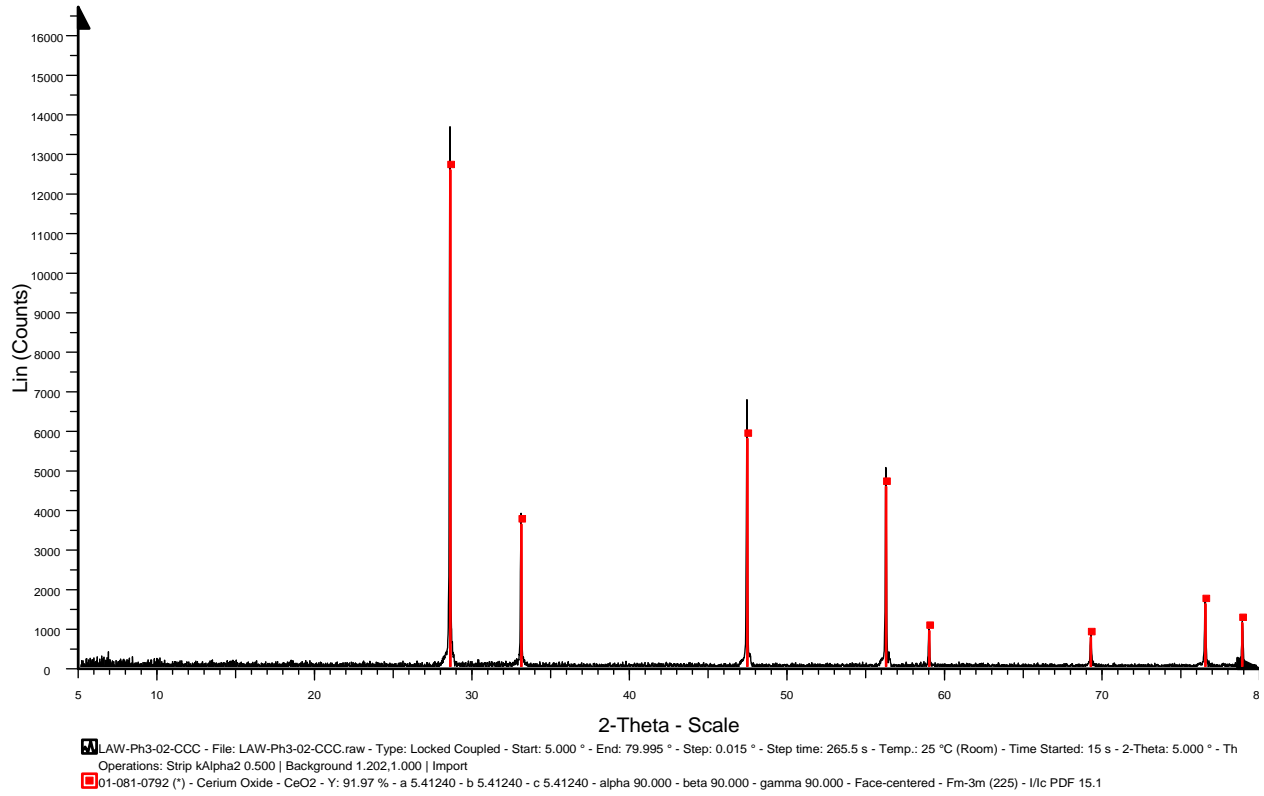


Figure G.2(c). XRD spectrum for LAWPh3-02-CCC.

LAWPh3-03-Q

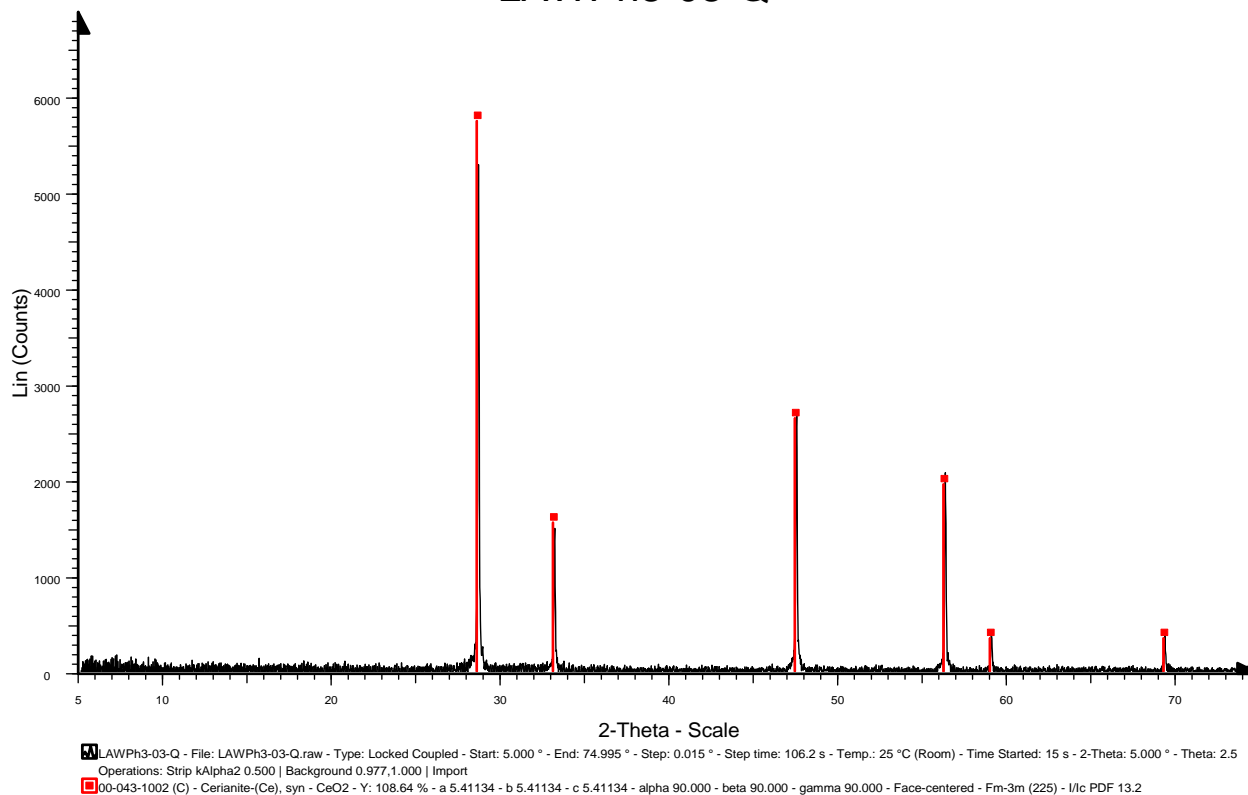


Figure G.3(a). XRD spectrum for LAWPh3-03-Q.

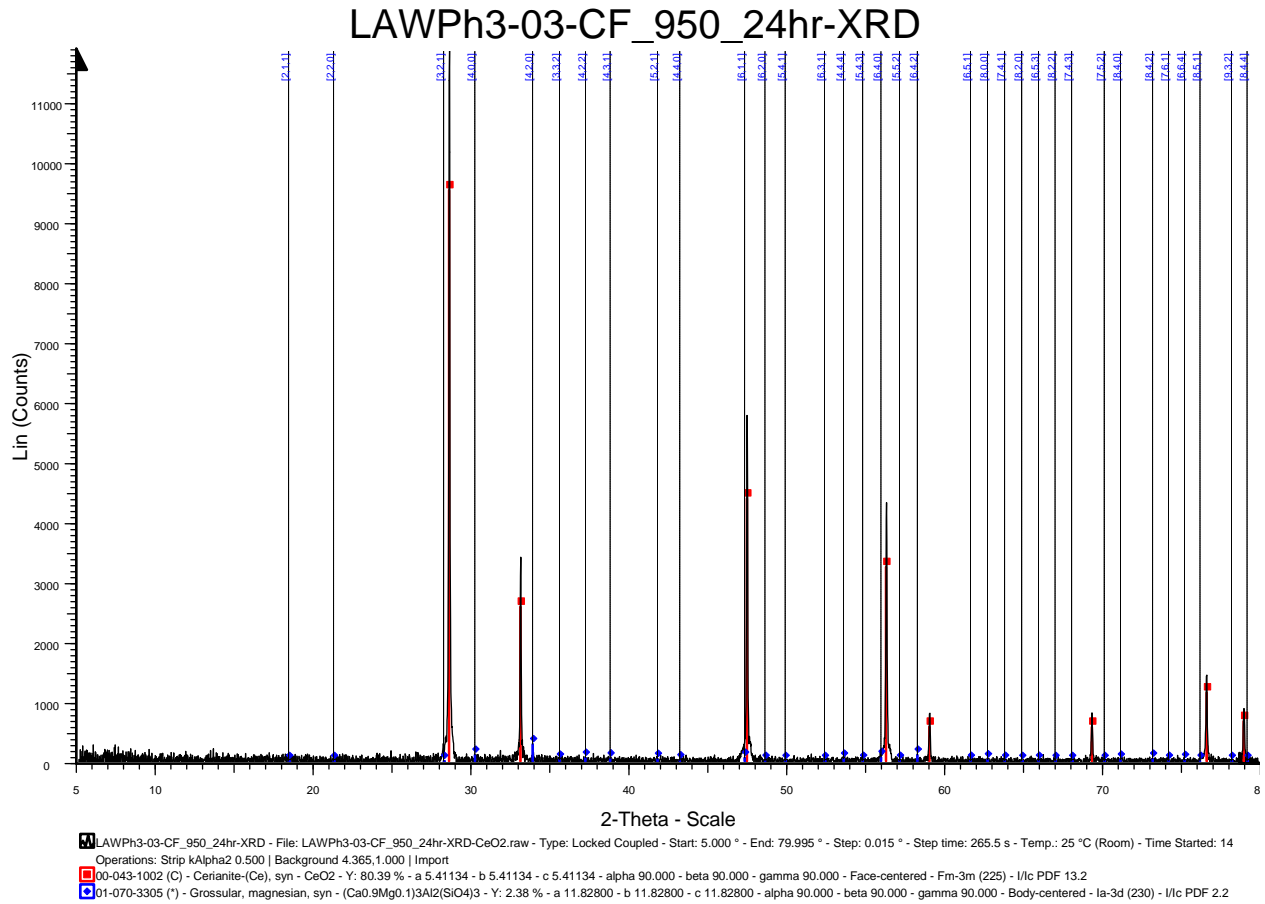


Figure G.3(b). XRD spectrum for LAWPh3-03-CF.

LAW-Ph3-03-CCC

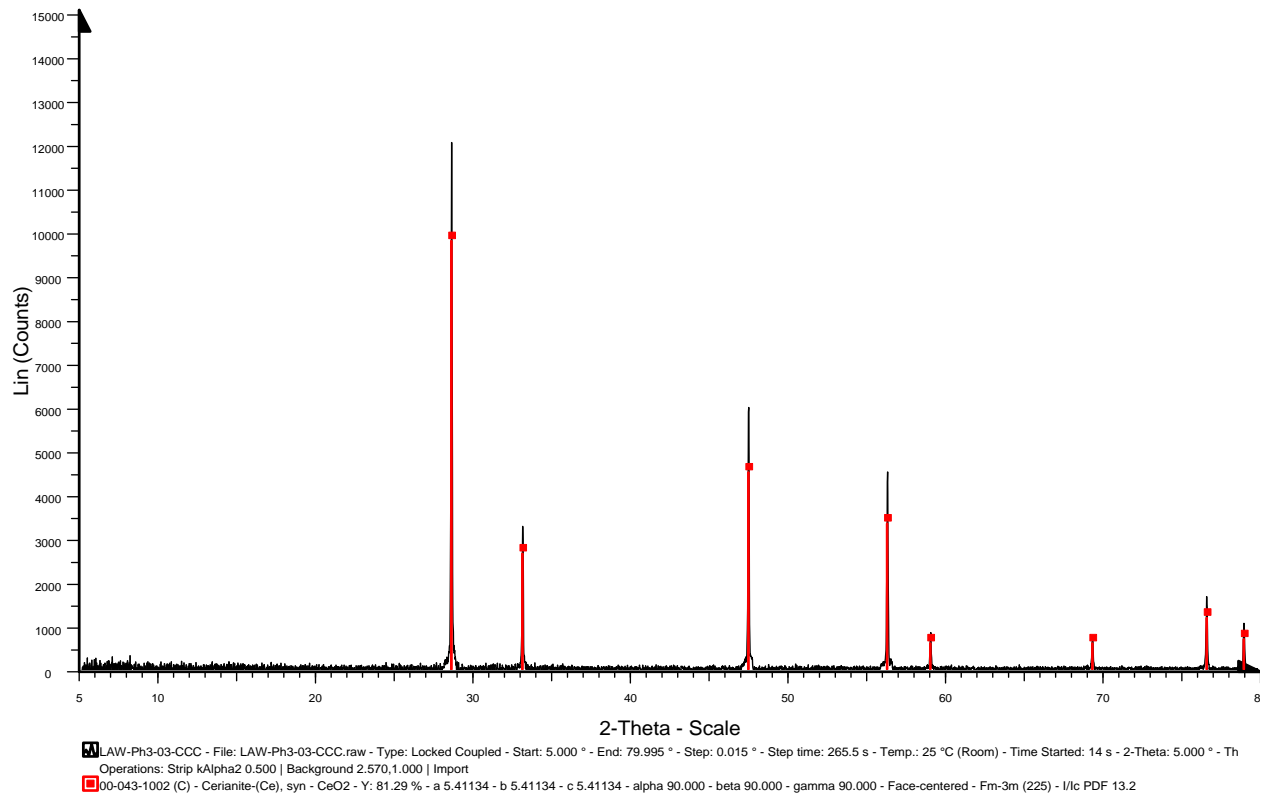


Figure G.3(c). XRD spectrum for LAWPh3-02-CCC.

LAWPh3-04-Q

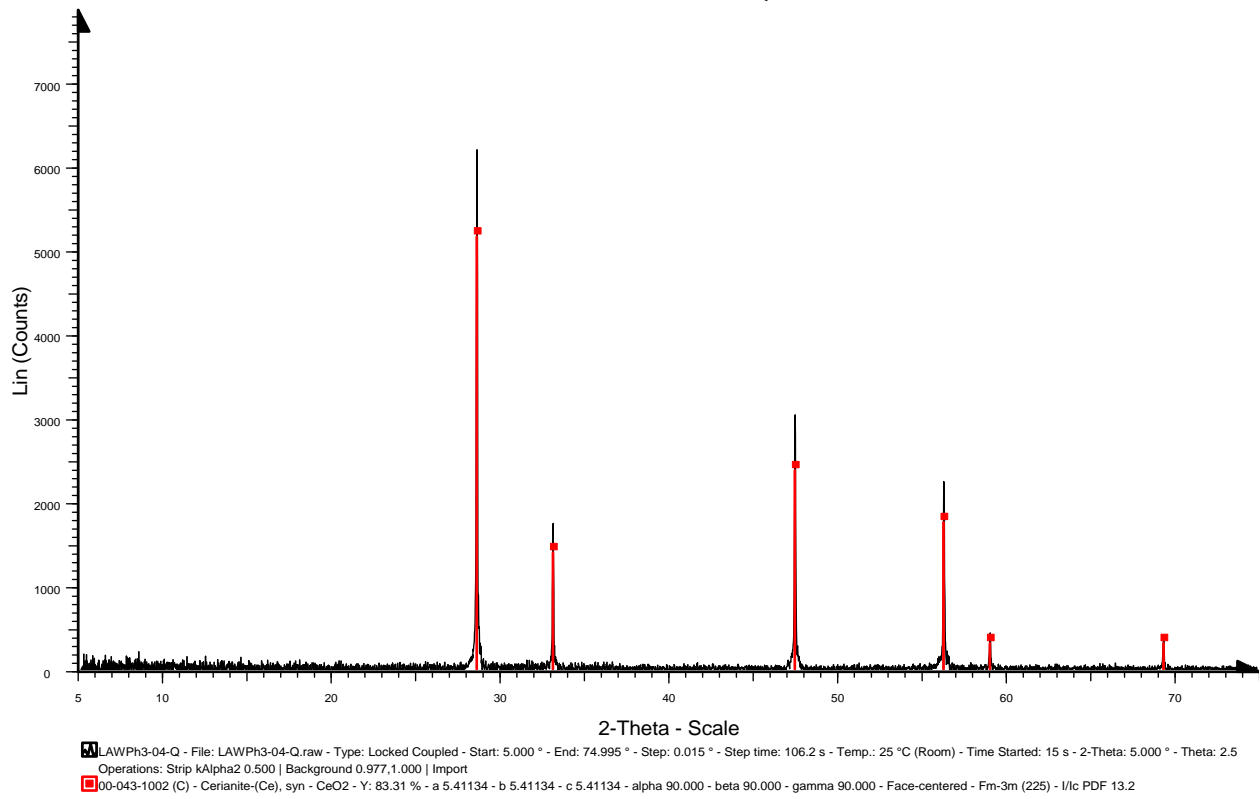


Figure G.4(a). XRD spectrum for LAWPh3-04-Q.

LAWPh3-04-CF_950_24hr-XRD

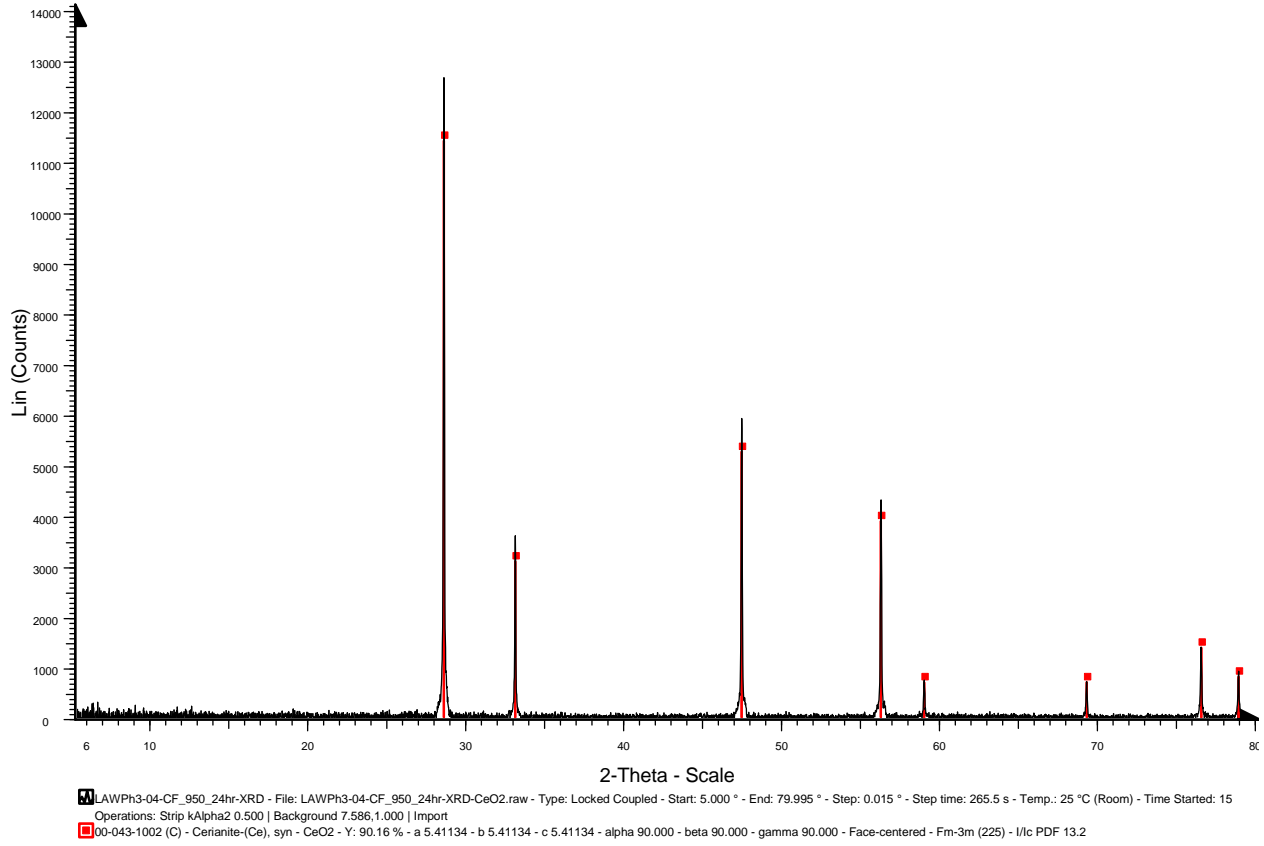


Figure G.4(b). XRD spectrum for LAWPh3-04-CF.

LAW-Ph3-04-CCC

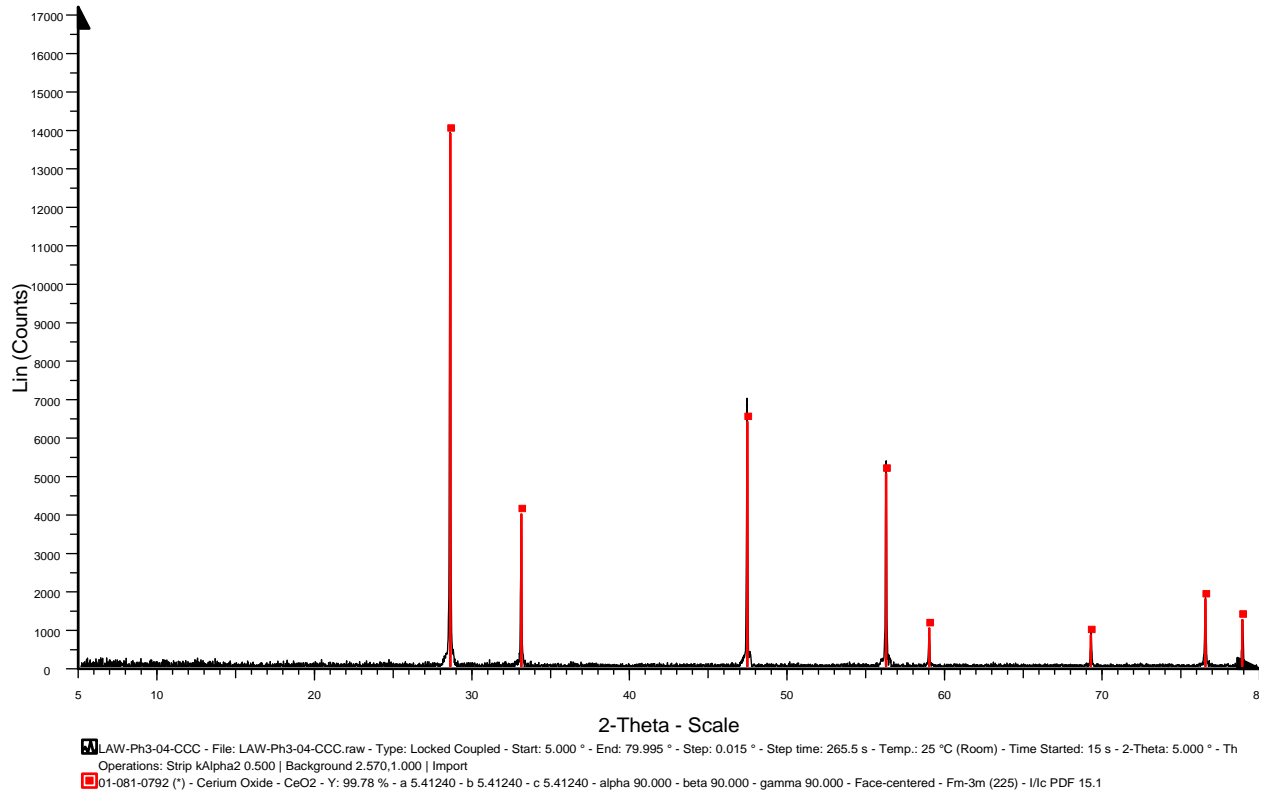


Figure G.4(c). XRD spectrum for LAWPh3-04-CCC.

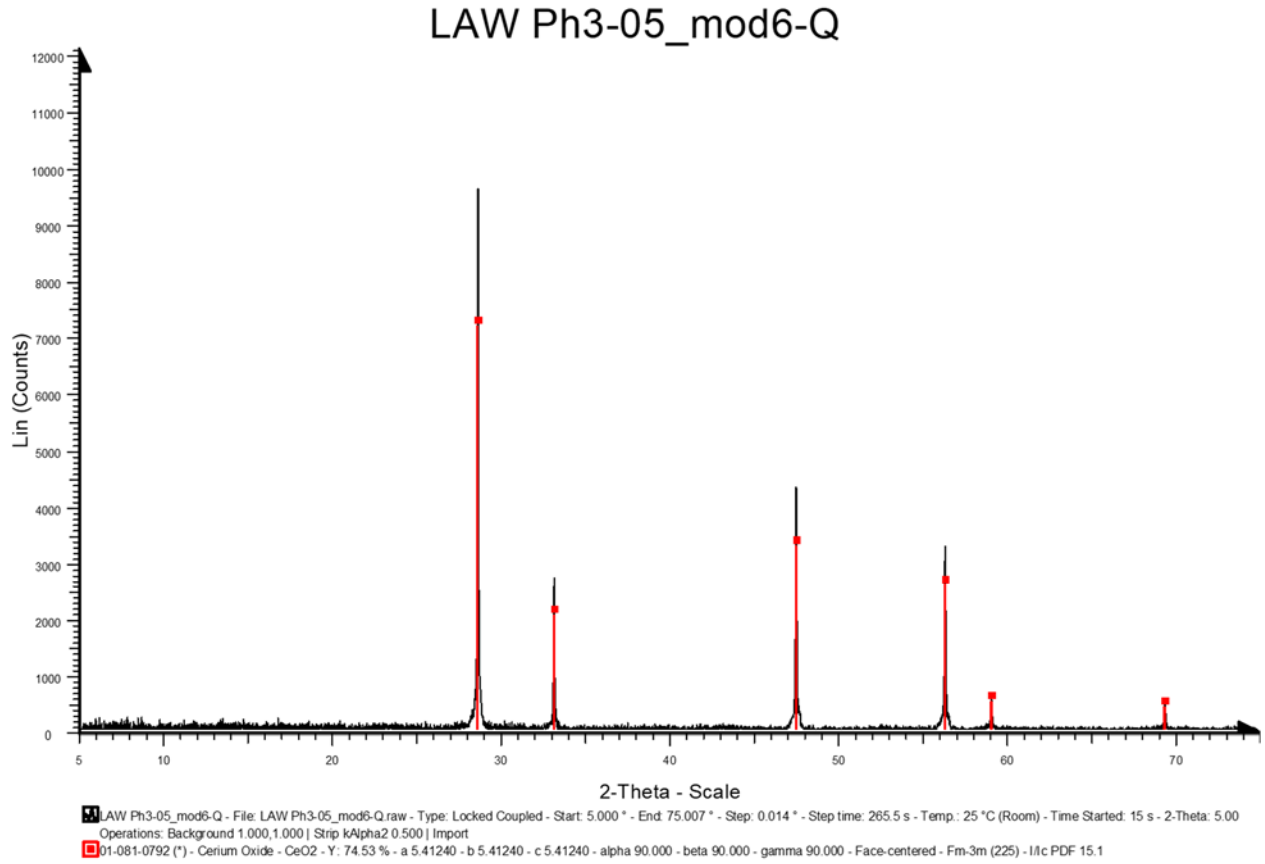


Figure G.5(a). XRD spectrum for LAWPh3-05_mod6-Q.

LAW Ph3-05_mod6-CF

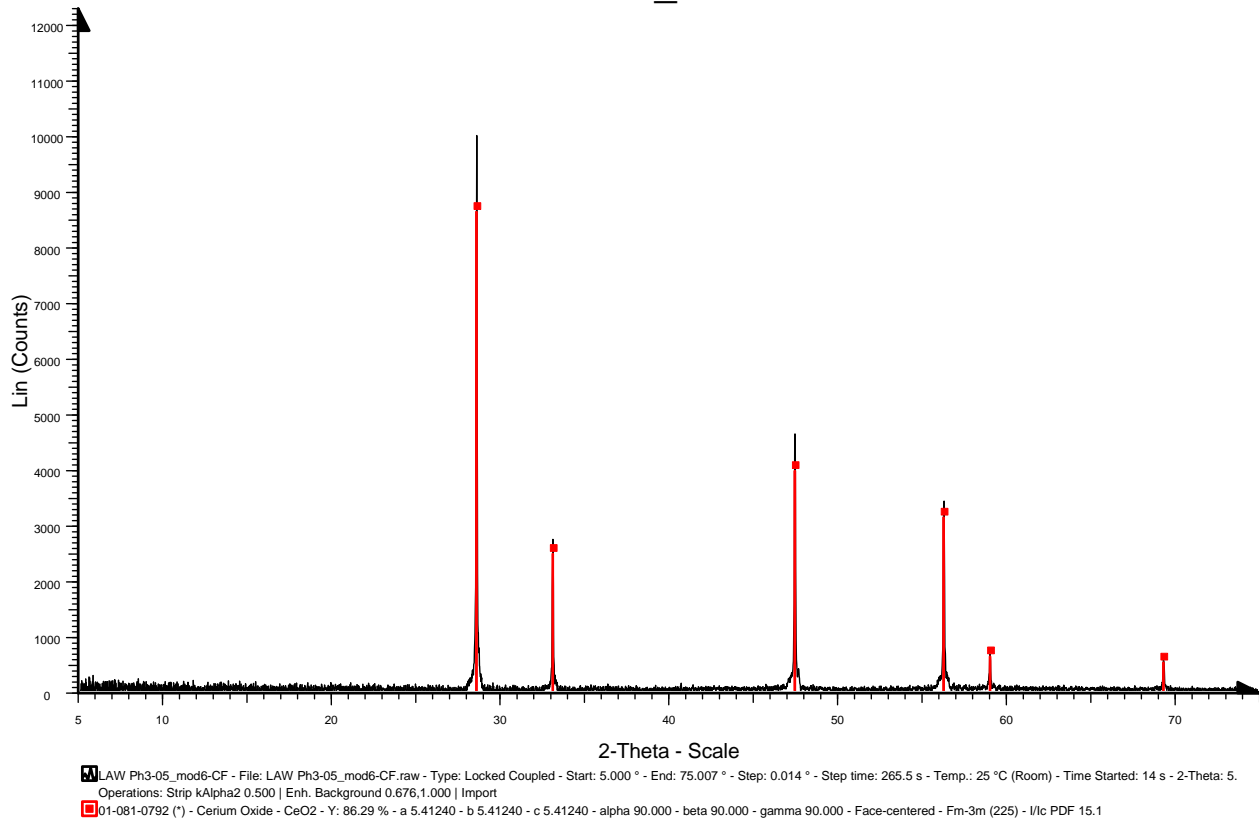


Figure G.5(b). XRD spectrum for LAWPh3-05_mod6-CF.

LAW Ph3-05_mod6-CCC

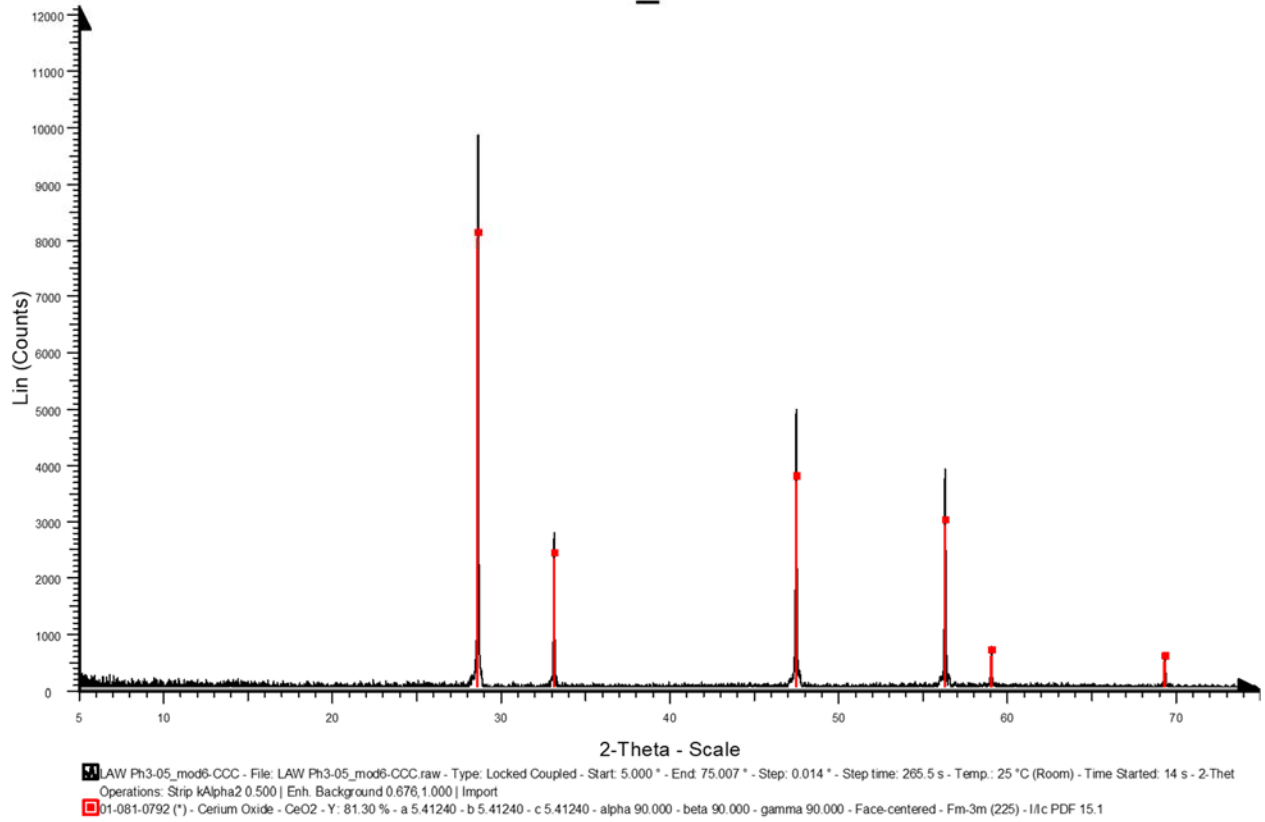


Figure G.5(c). XRD spectrum for LAWPh3-05_mod6-CCC.

LAWPh3-06-Q

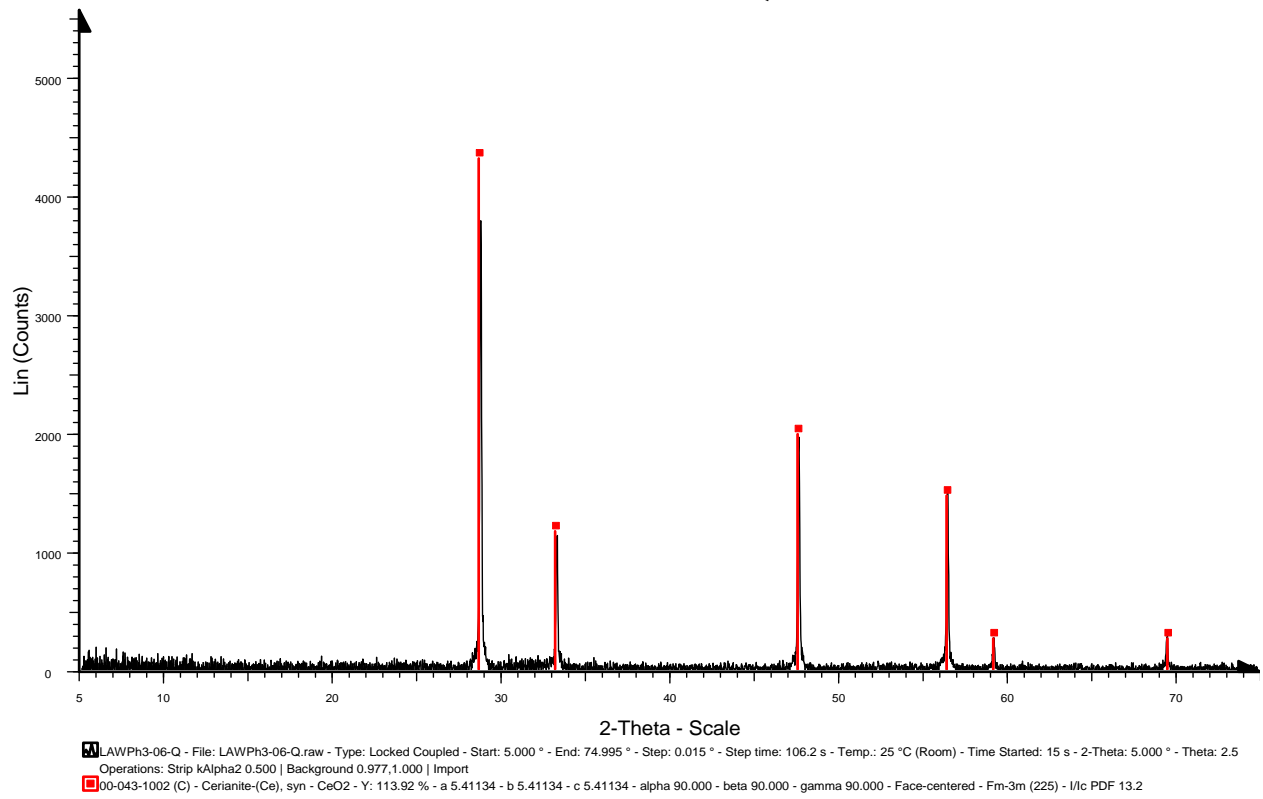


Figure G.6(a). XRD spectrum for LAWPh3-06-Q.

LAWPh3-06-CF_950_24hr-XRD

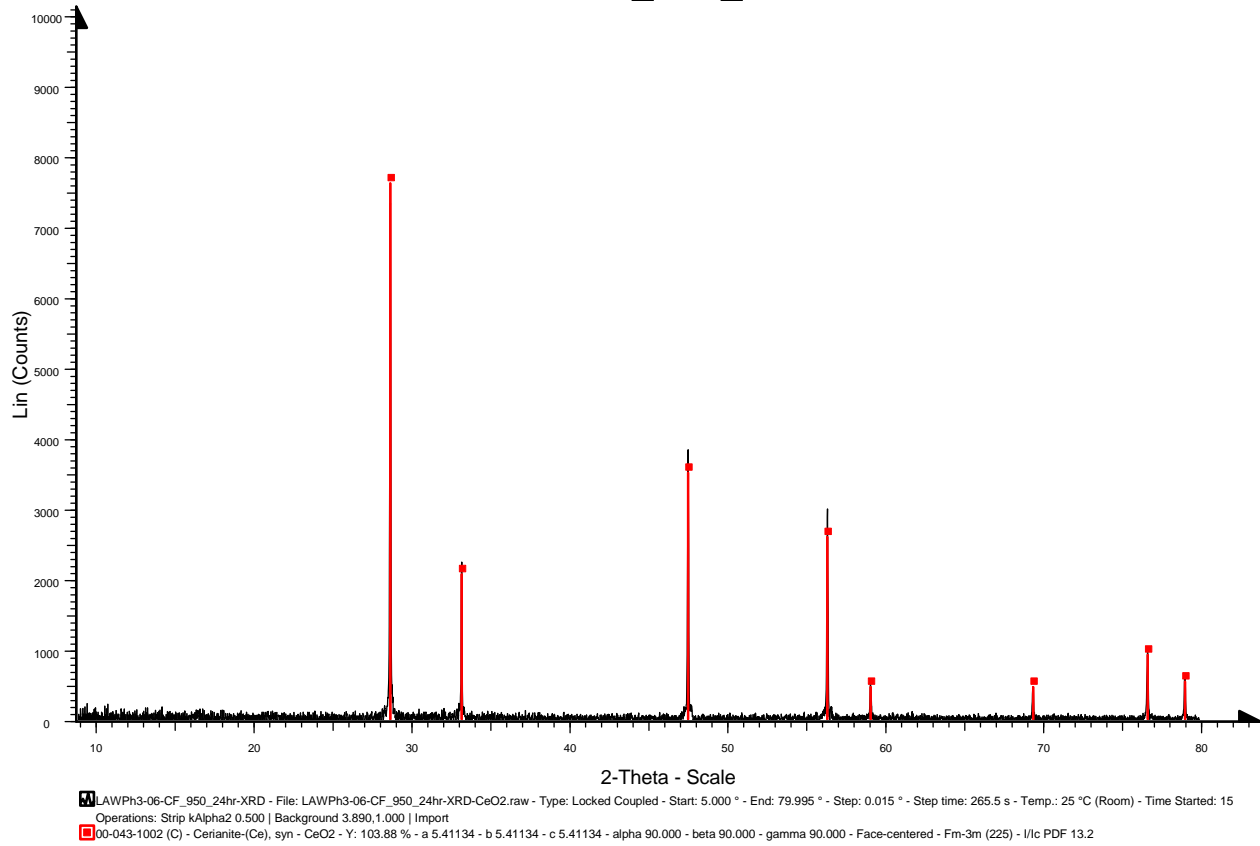


Figure G.6(b). XRD spectrum for LAWPh3-06-CF.

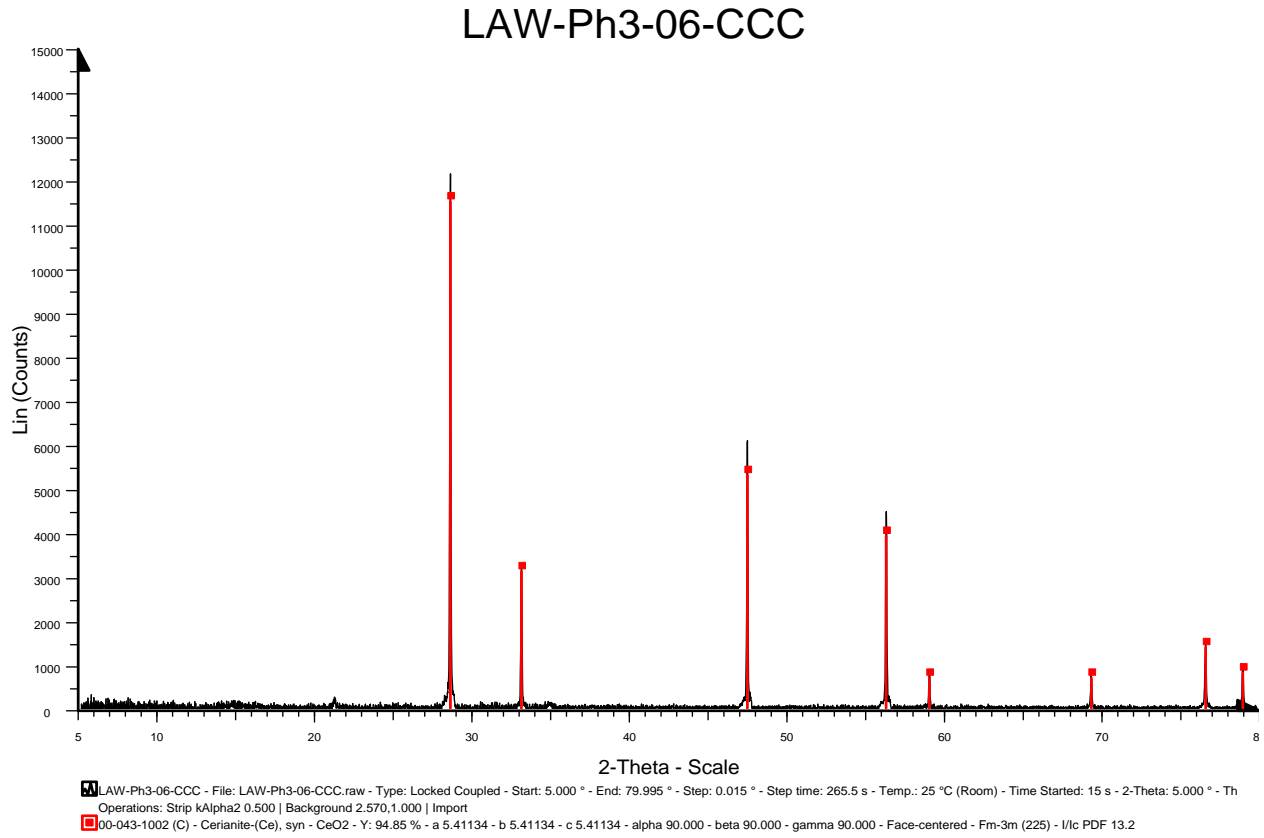


Figure G.6(c). XRD spectrum for LAWPh3-06-CCC.

LAWPh3-07-Q

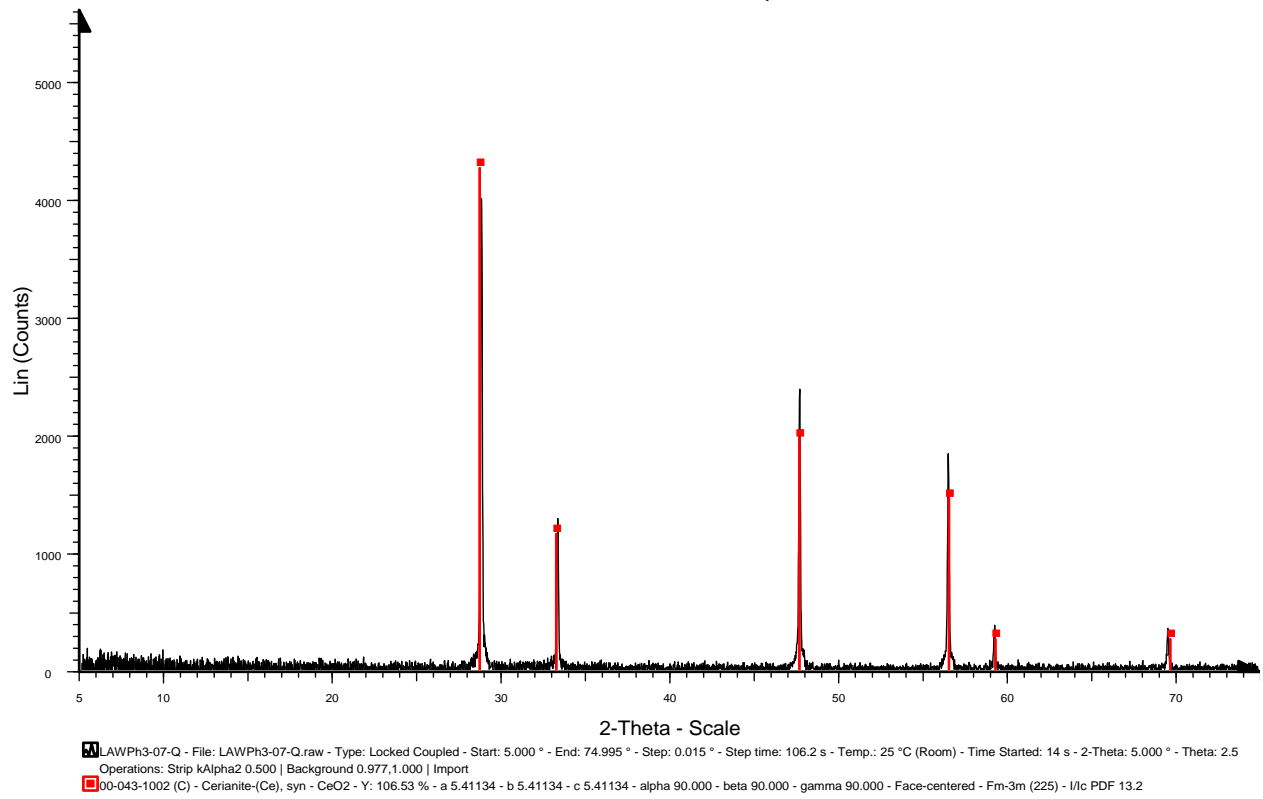


Figure G.7(a). XRD spectrum for LAWPh3-07-Q.

LAWPh3-07-CF_950_24hr-XRD

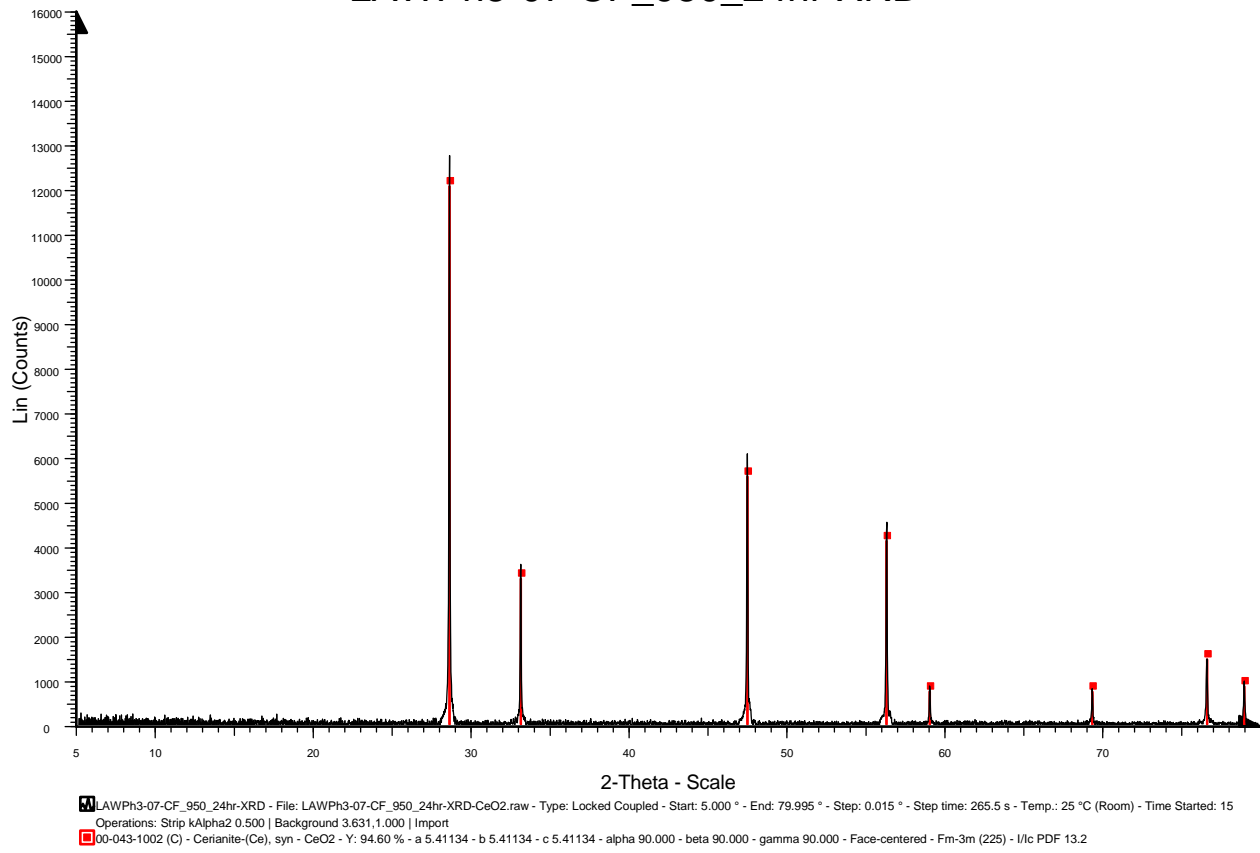


Figure G.7(b). XRD spectrum for LAWPh3-07-CF.

LAW-Ph3-07-CCC

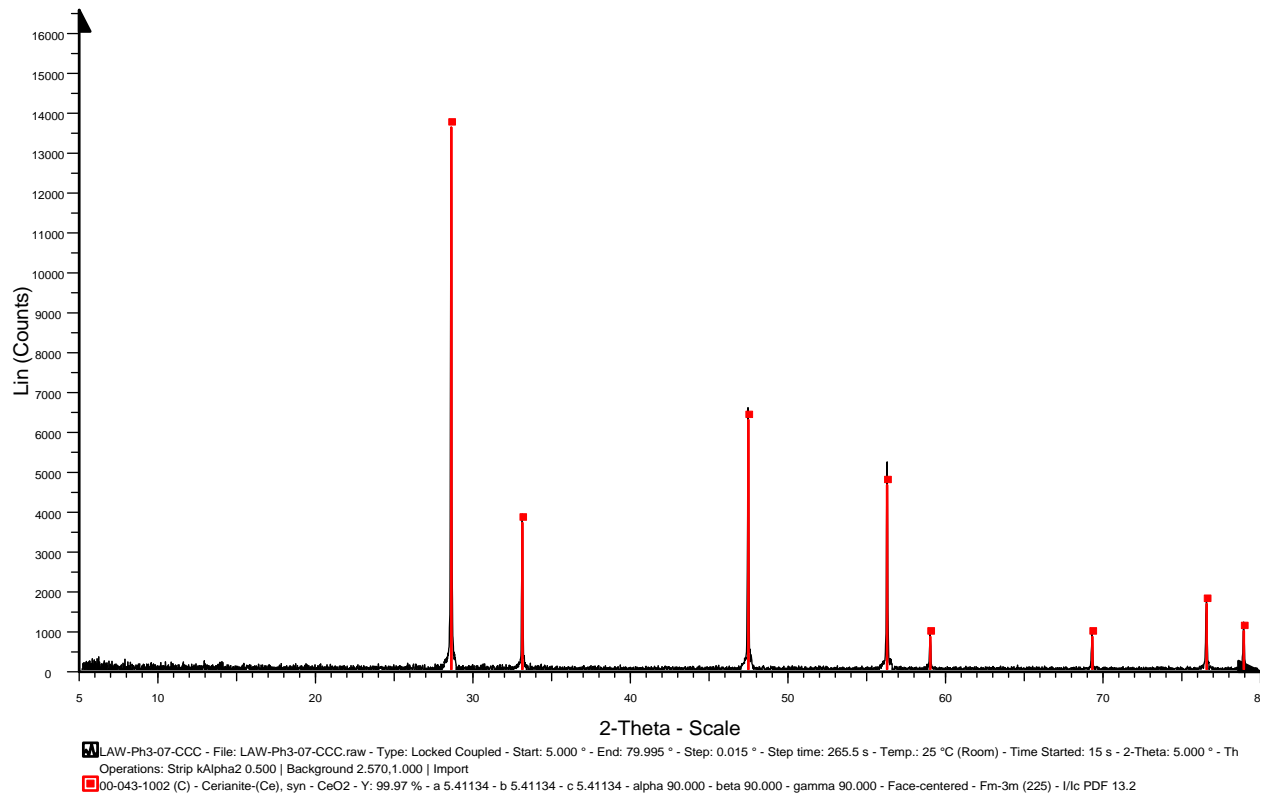


Figure G.7(c). XRD spectrum for LAWPh3-07-CCC.

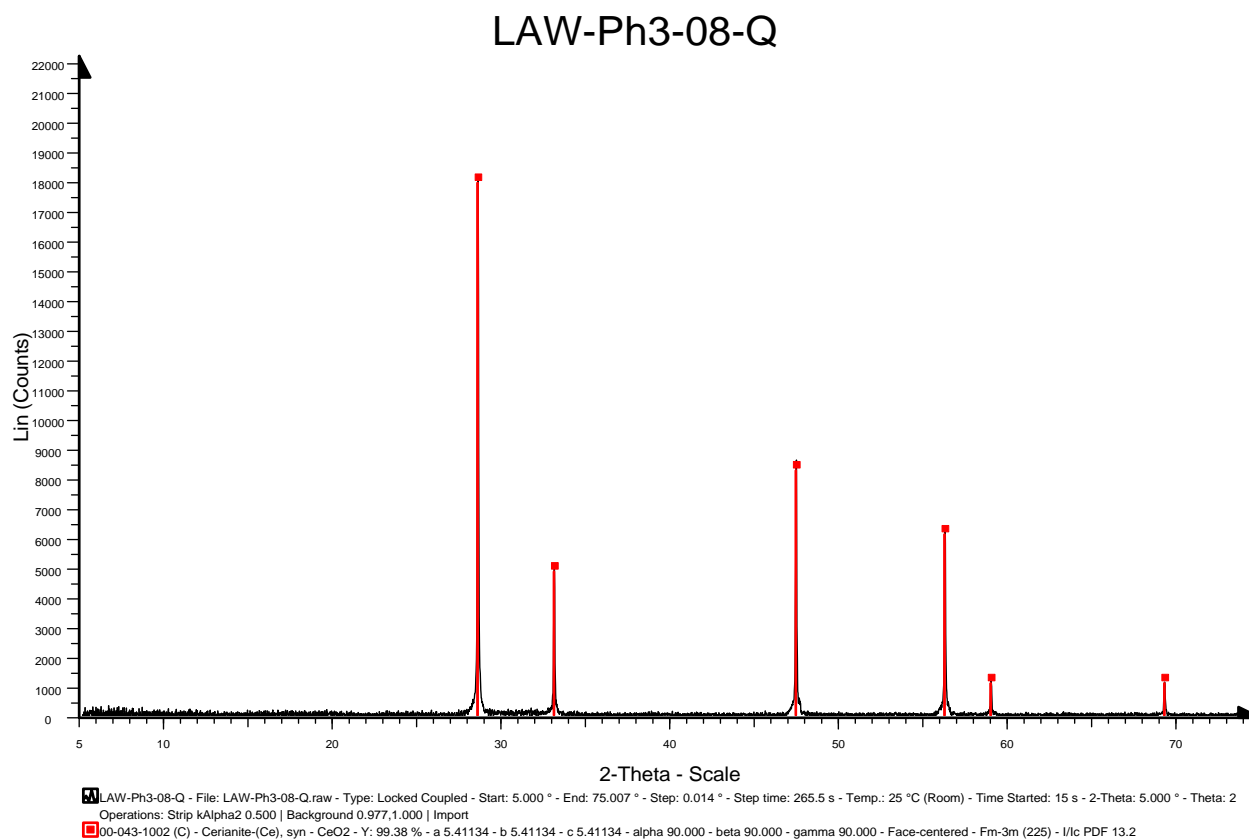


Figure G.8(a). XRD spectrum for LAWPh3-08-Q.

LAWPh3-08-CF_950_24hr-XRD

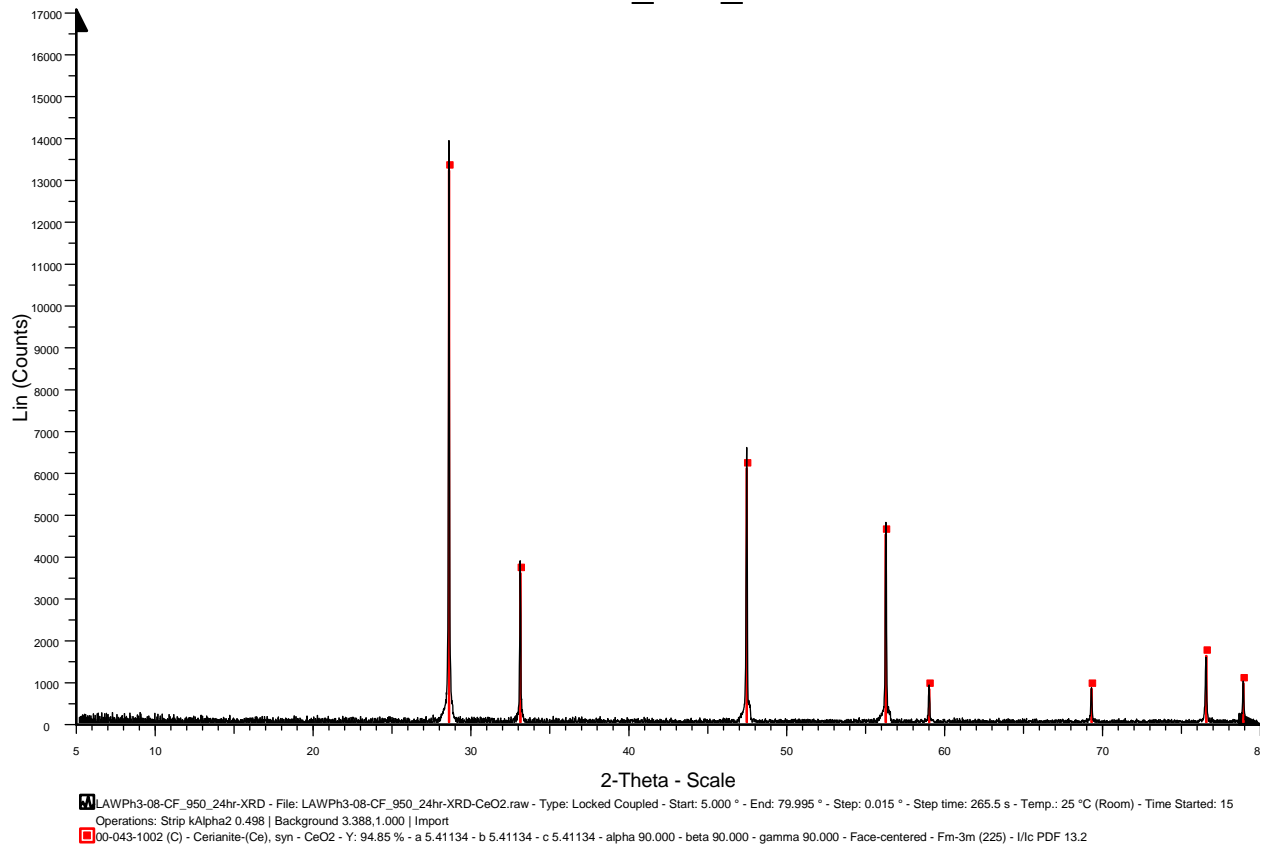


Figure G.8(b). XRD spectrum for LAWPh3-08-CF.

LAW-Ph3-08-CCC

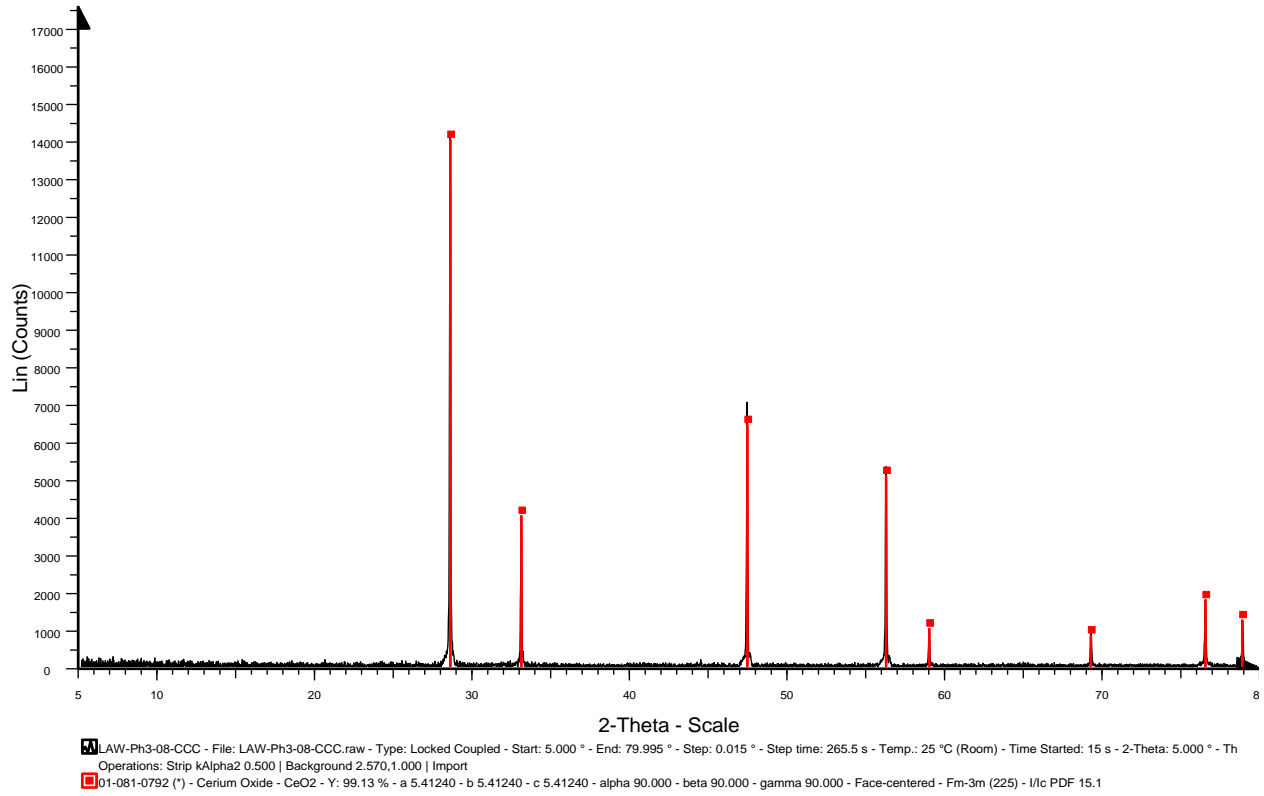


Figure G.8(c). XRD spectrum for LAWPh3-08-CCC.

LAW-Ph3-09-Q

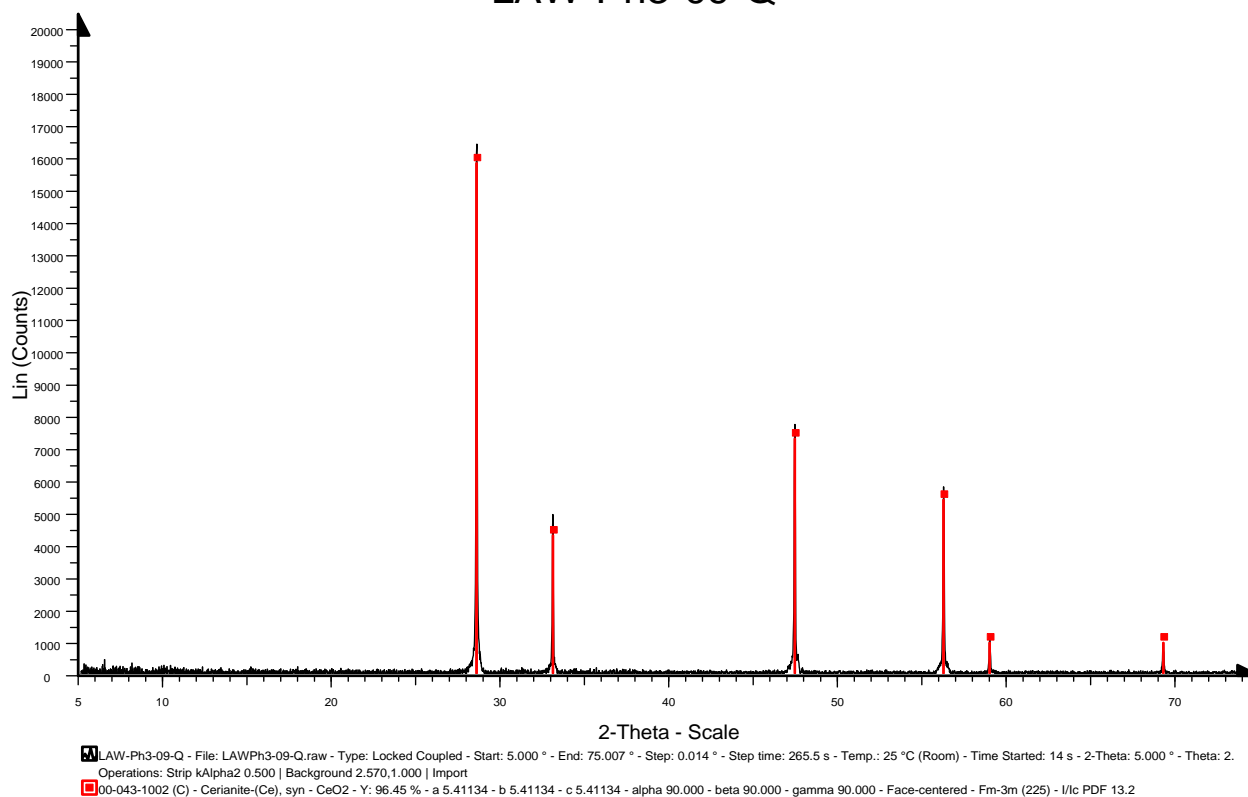


Figure G.9(a). XRD spectrum for LAWPh3-09-Q.

LAWPh3-09-CF_950_24hr-XRD

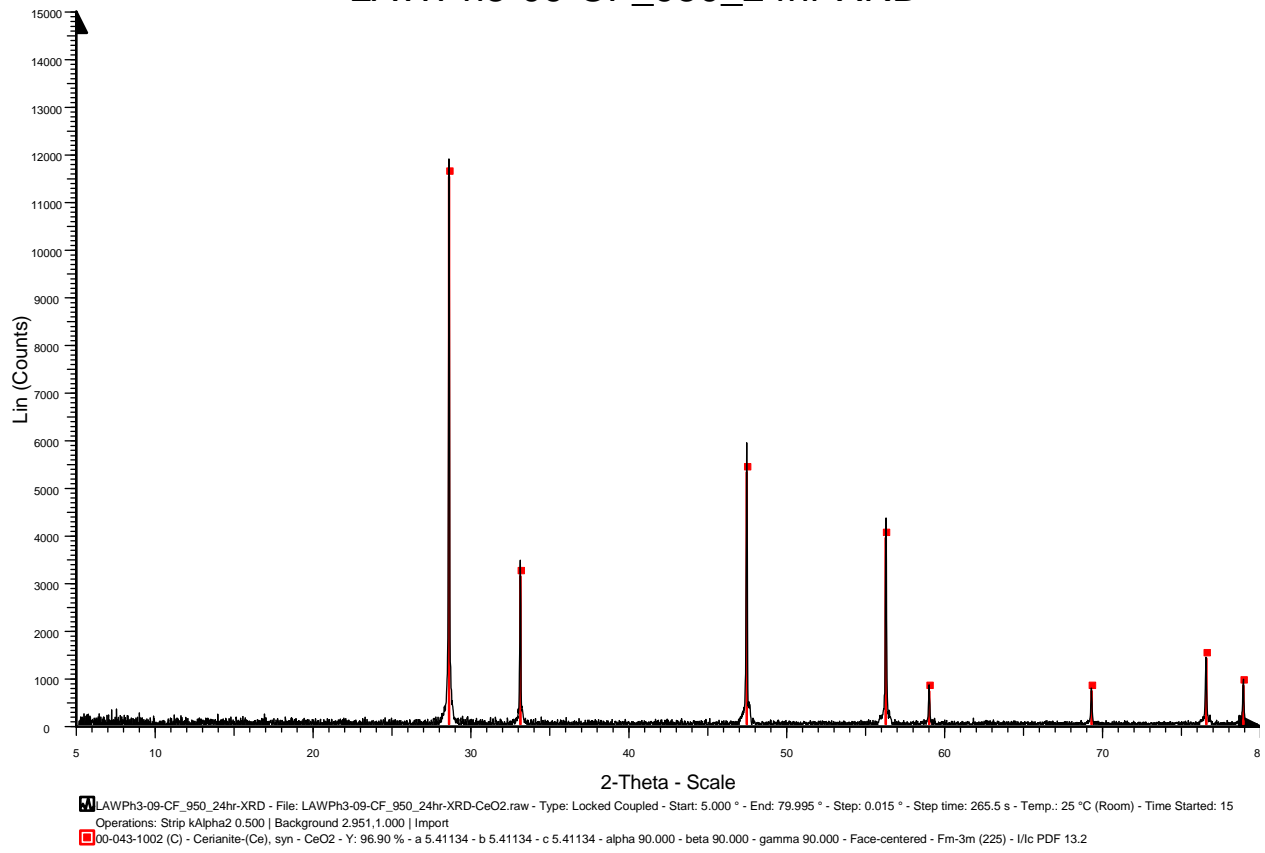
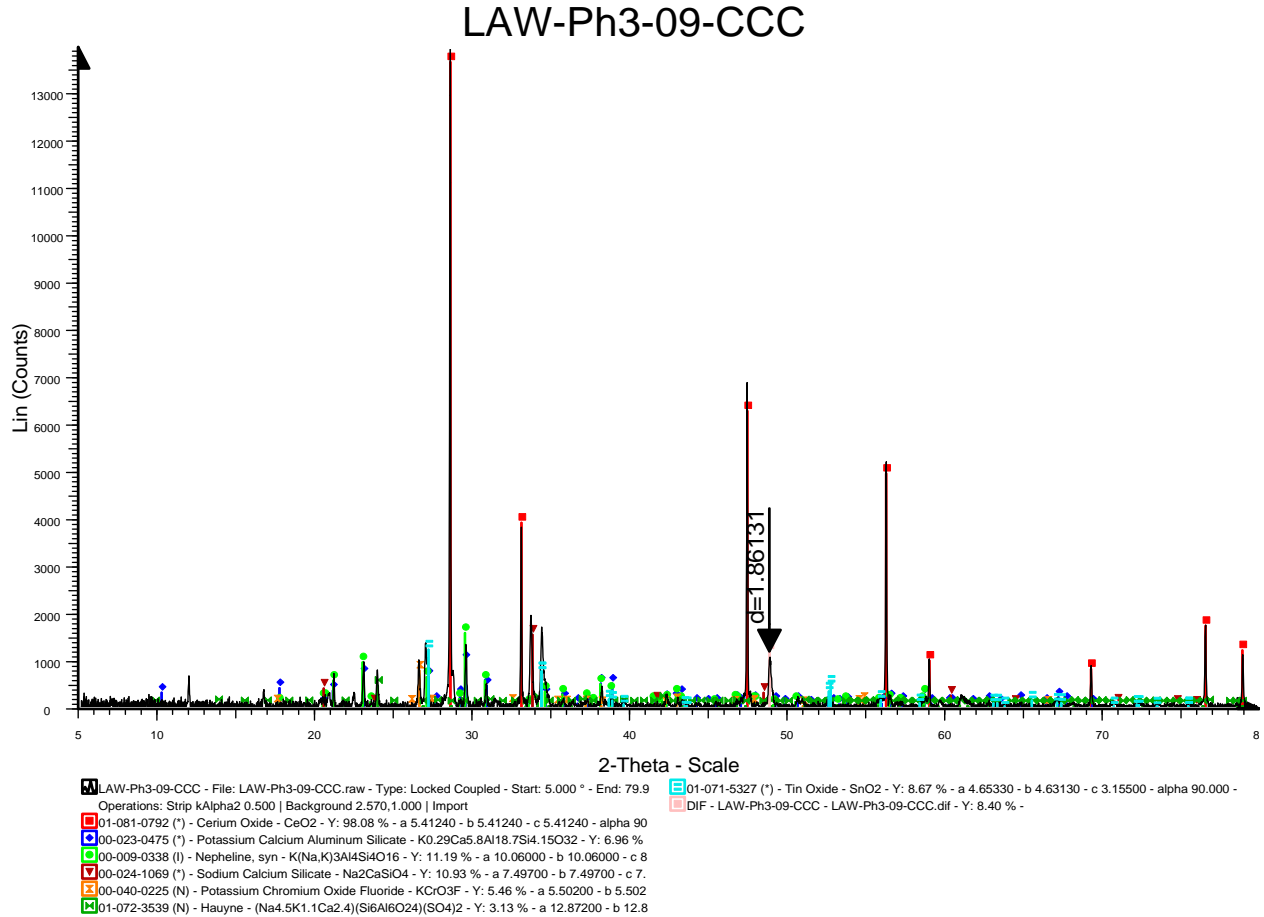


Figure G.9(b). XRD spectrum for LAWPh3-09-CF.



Phase Name	Wt% of Spiked	Wt% in Spiked Sample	Wt% in Original Sample
CeO ₂	5.019	5.000	0
Hauyne	0	1.168	1.229
Tin oxide	0	1.116	1.175
Potassium chromium oxide fluoride	0	1.167	1.229
Nepheline	0	6.201	6.527
Sodium calcium silicate	0	5.976	6.29
Sodium phosphate	0	8.353	8.793

Figure G.9(c). XRD spectrum for LAWPh3-09-CCC.

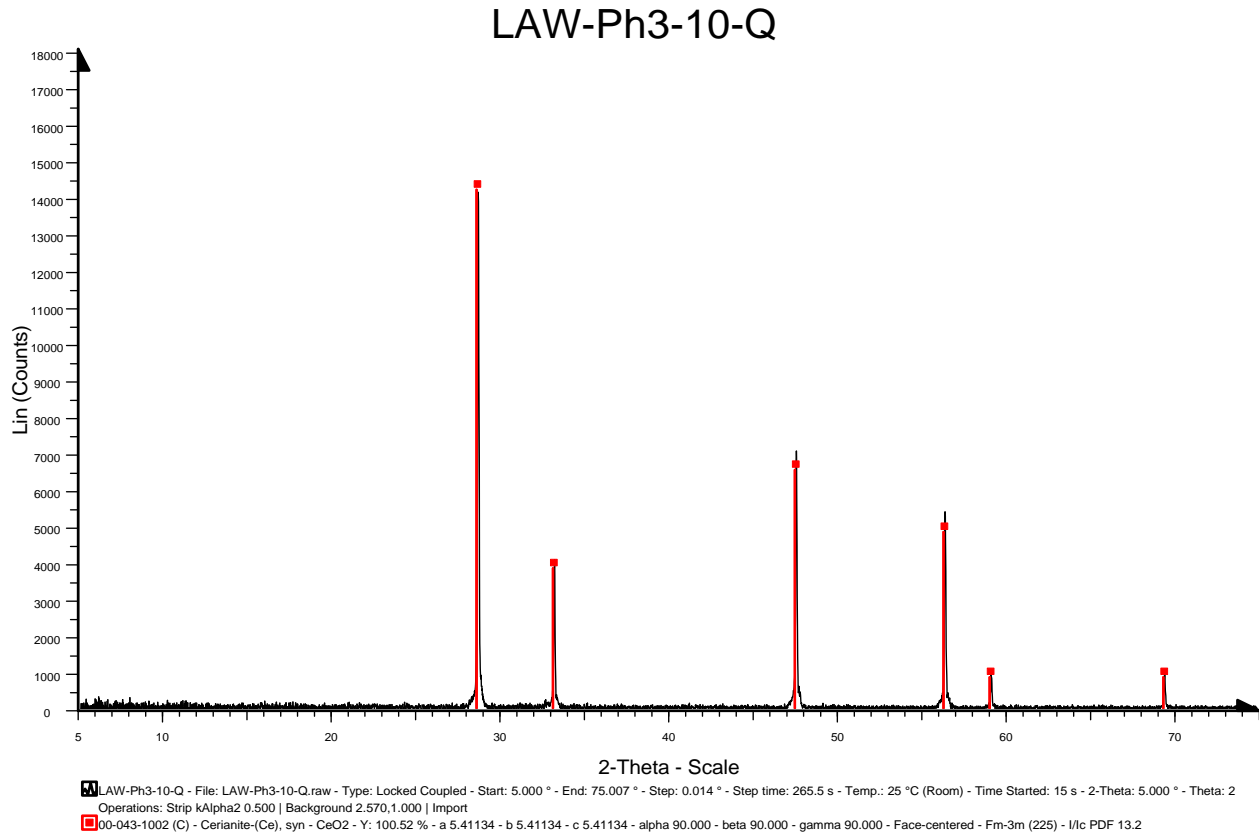
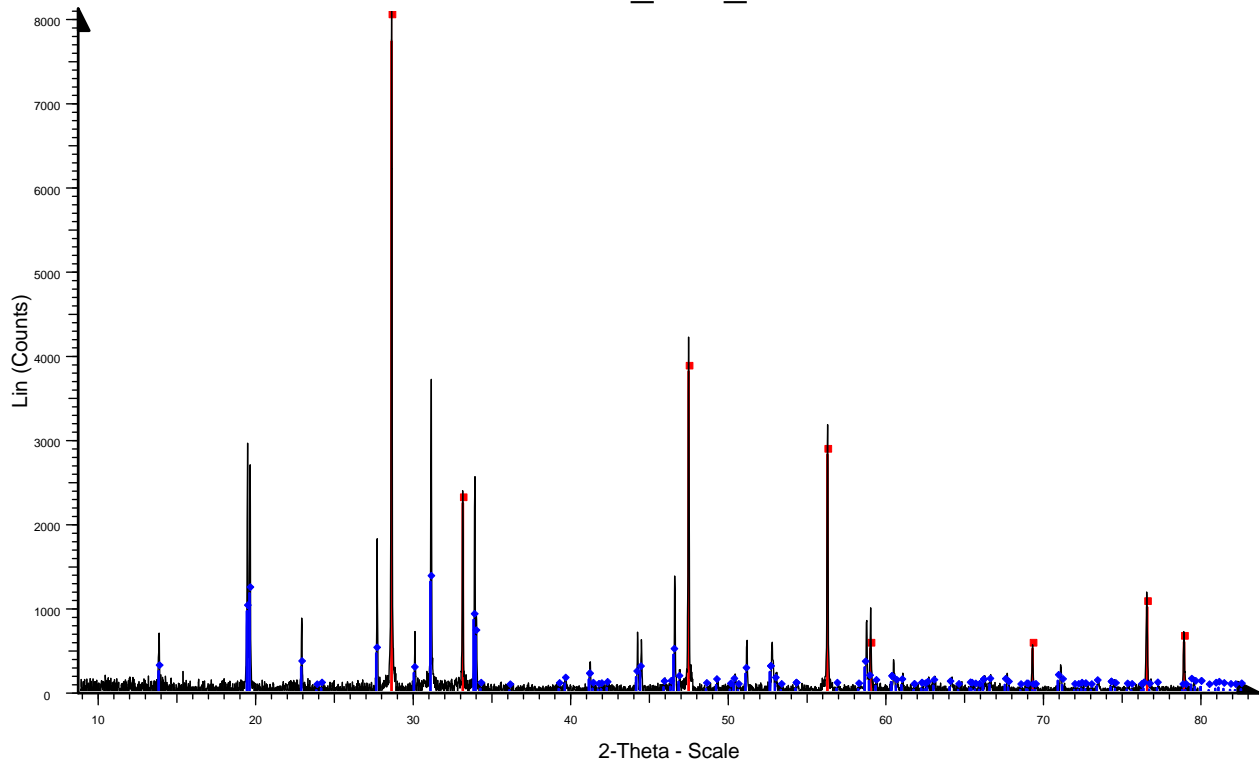


Figure G.10(a). XRD spectrum for LAWPh3-10-Q.

LAWPh3-10-CF_950_24hr-XRD



■ LAWPh3-10-CF_950_24hr-XRD - File: LAWPh3-10-CF_950_24hr-XRD-CeO2.raw - Type: Locked Coupled - Start: 5.000 ° - End: 79.995 ° - Step: 0.015 ° - Step time: 265.5 s - Temp.: 25 °C (Room) - Time S
 Operations: Strip kAlpha2 0.492 | Background 1.820,1.000 | Import
■ 00-043-1002 (C) - Cerianite-(Ce), syn - CeO2 - Y: 102.05 % - a 5.41134 - b 5.41134 - c 5.41134 - alpha 90.000 - beta 90.000 - gamma 90.000 - Face-centered - Fm-3m (225) - I/Ic PDF 13.2
■ 01-077-0087 (*) - Sodium Zirconium Silicate - Na4Zr2Si3O12 - Y: 16.00 % - a 9.18600 - b 9.18600 - c 22.18600 - alpha 90.000 - beta 90.000 - gamma 120.000 - Primitive - R-3c (167) - I/Ic PDF 2.3

Phase Name	Wt% of Spiked	Wt% in Spiked Sample	Wt% in Original Sample
CeO ₂	4.998	4.998	0
Nasicon	0	12.75	13.421

Figure G.10(b). XRD spectrum for LAWPh3-10-CF.

LAWPh3-10-CCC

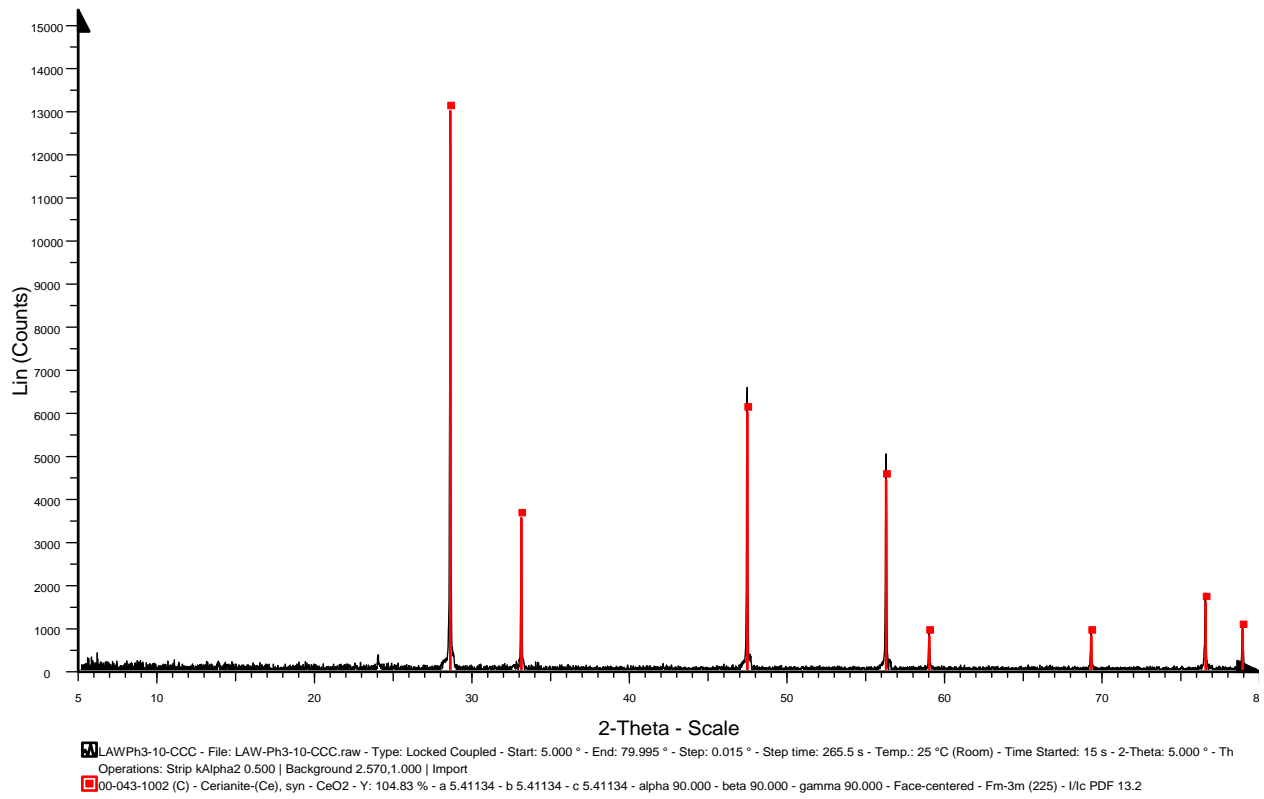


Figure G.10(c). XRD spectrum for LAWPh3-10-CCC.

LAW-Ph3-11-Q

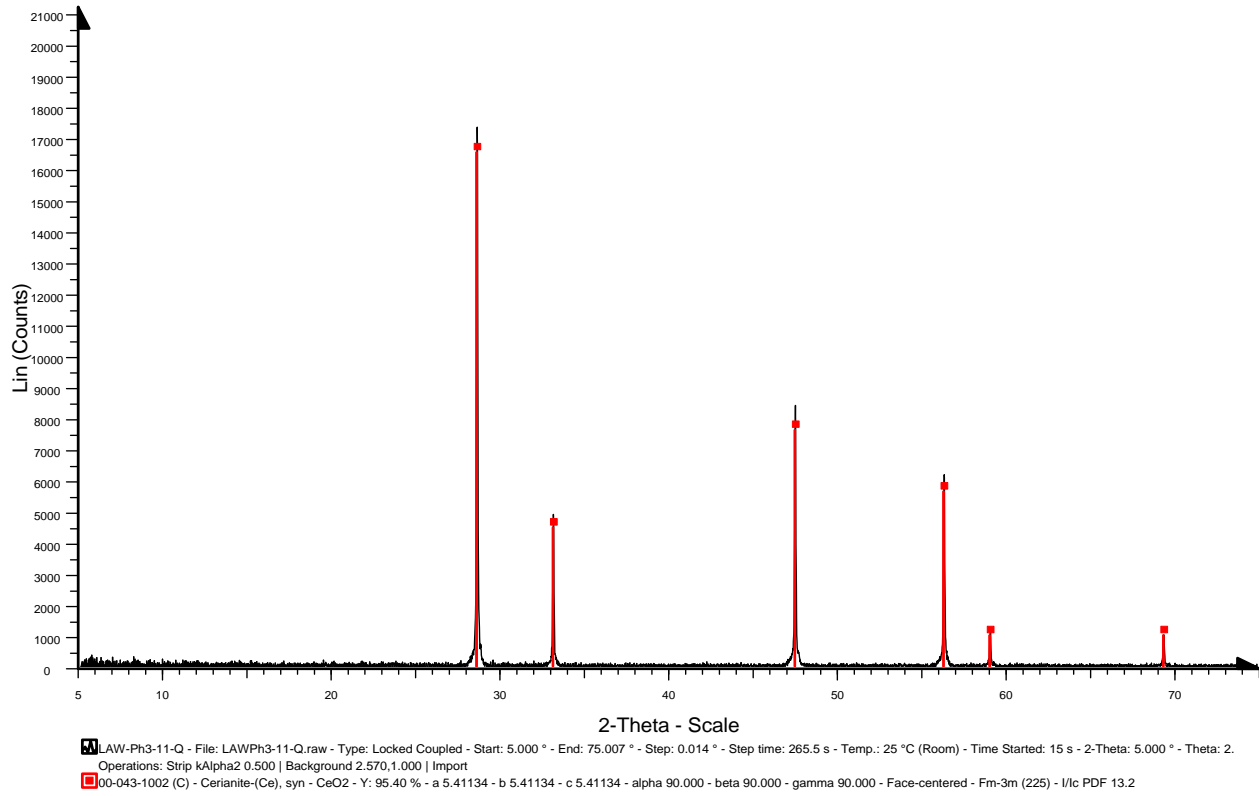


Figure G.11(a). XRD spectrum for LAWPh3-11-Q.

LAWPh3-11-CF_950_24hr-XRD

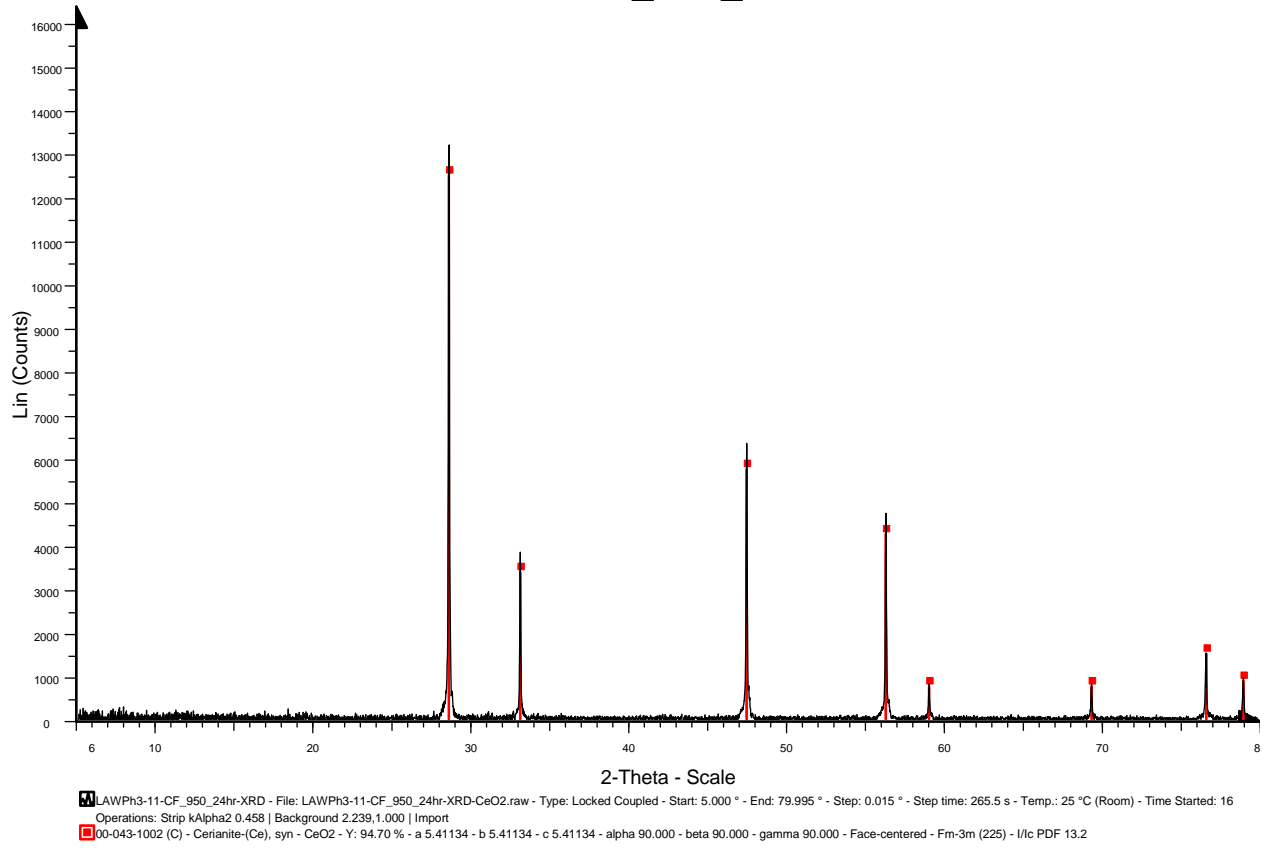


Figure G.11(b). XRD spectrum for LAWPh3-11-CF.

LAWPh3-11-CCC

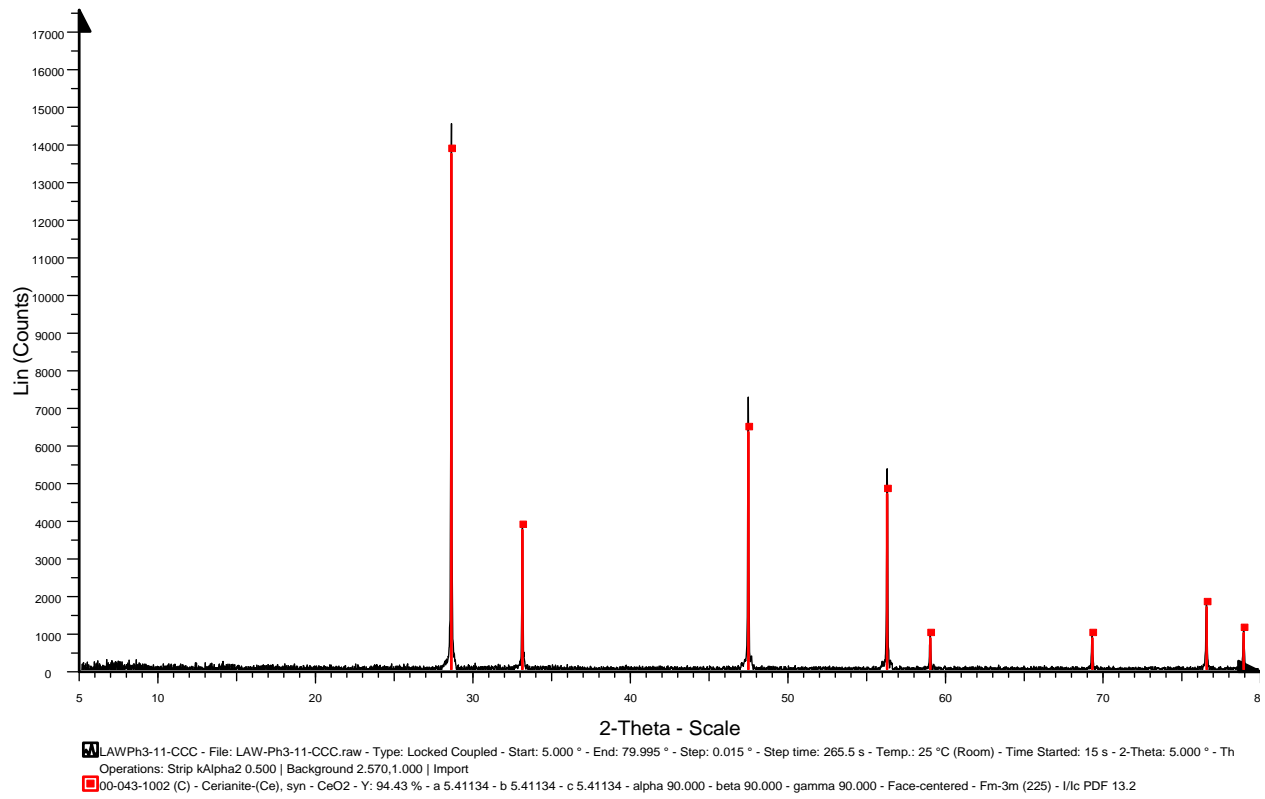


Figure G.11(c). XRD spectrum for LAWPh3-11-CCC.

LAW-Ph3-12-Q

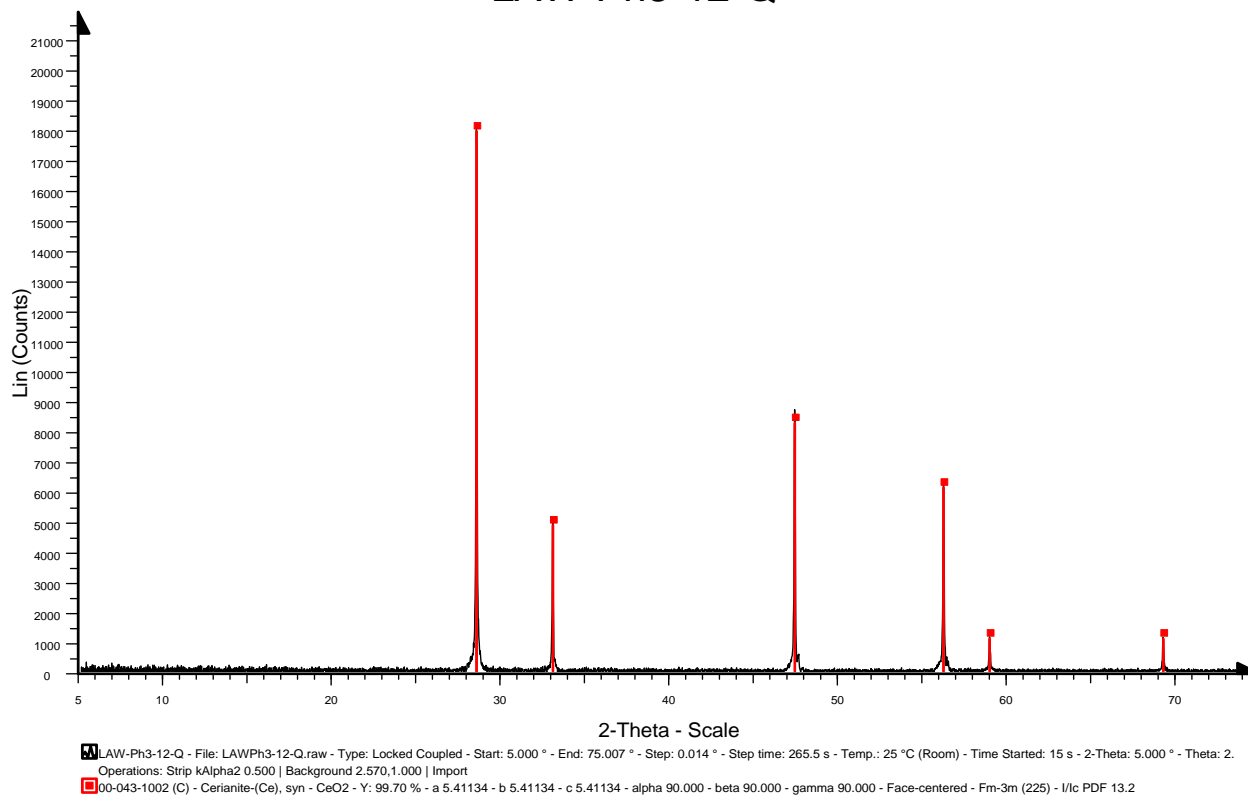


Figure G.12(a). XRD spectrum for LAWPh3-12-Q.

LAWPh3-12-CF_950_24hr-XRD

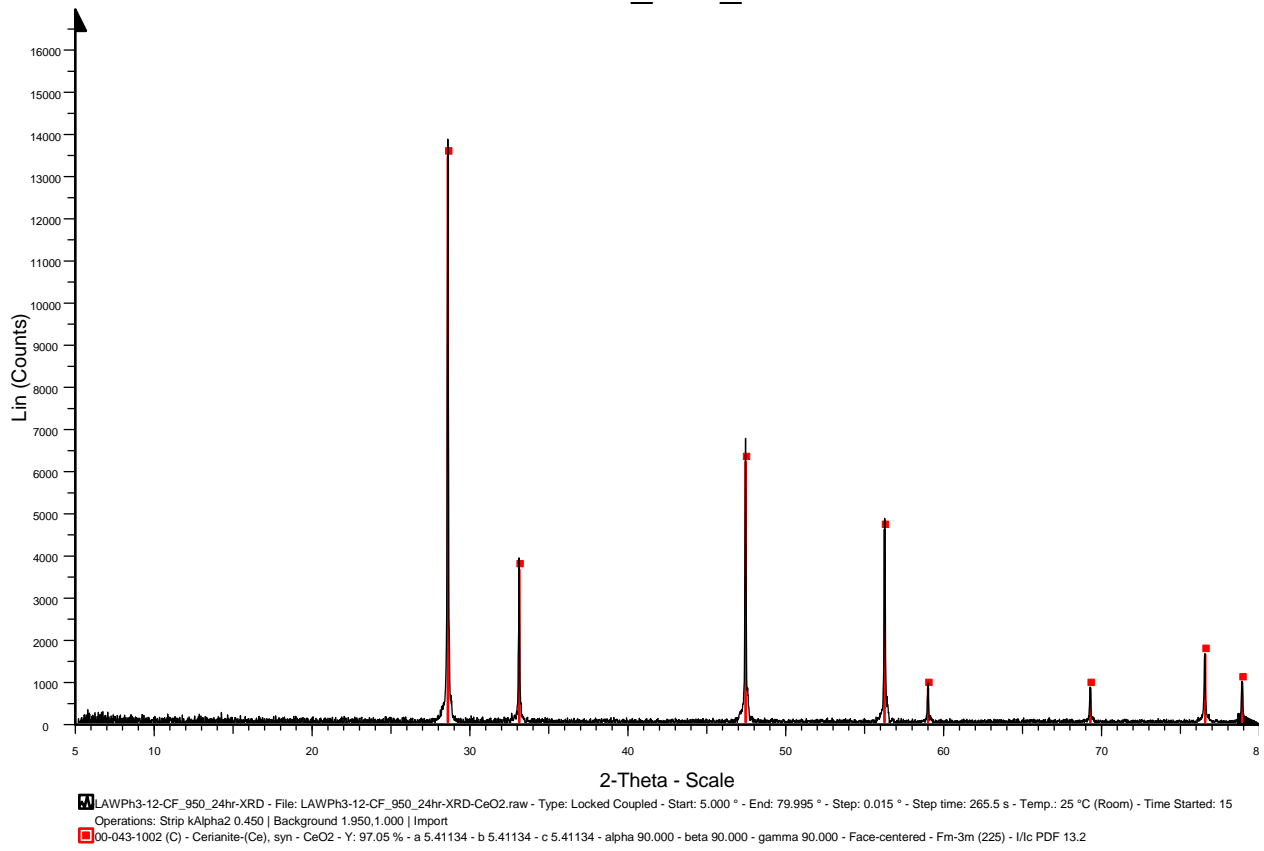


Figure G.12(b). XRD spectrum for LAWPh3-12-CF.

LAWPh3-12-CCC

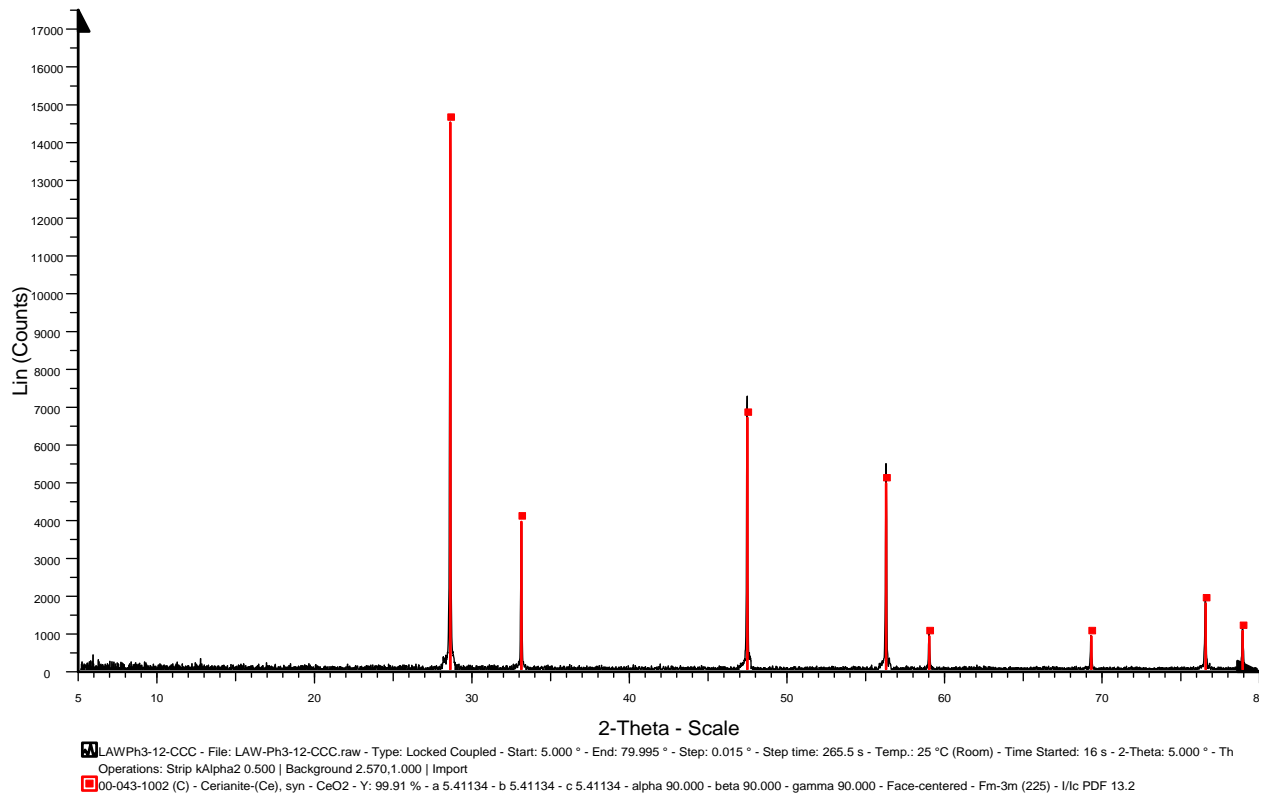


Figure G.12(c). XRD spectrum for LAWPh3-12-CCC.

LAW-Ph3-13-Q

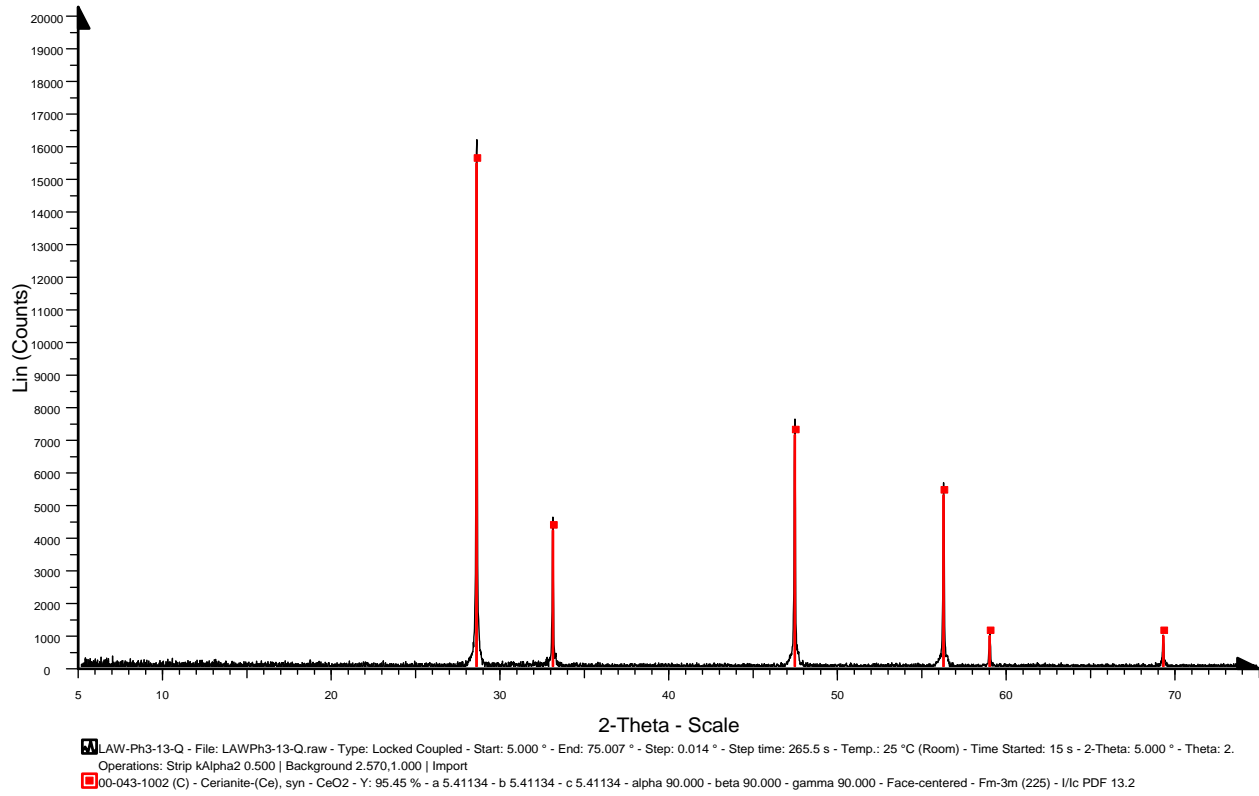


Figure G.13(a). XRD spectrum for LAWPh3-13-Q.

LAWPh3-13-CF_950_24hr-XRD

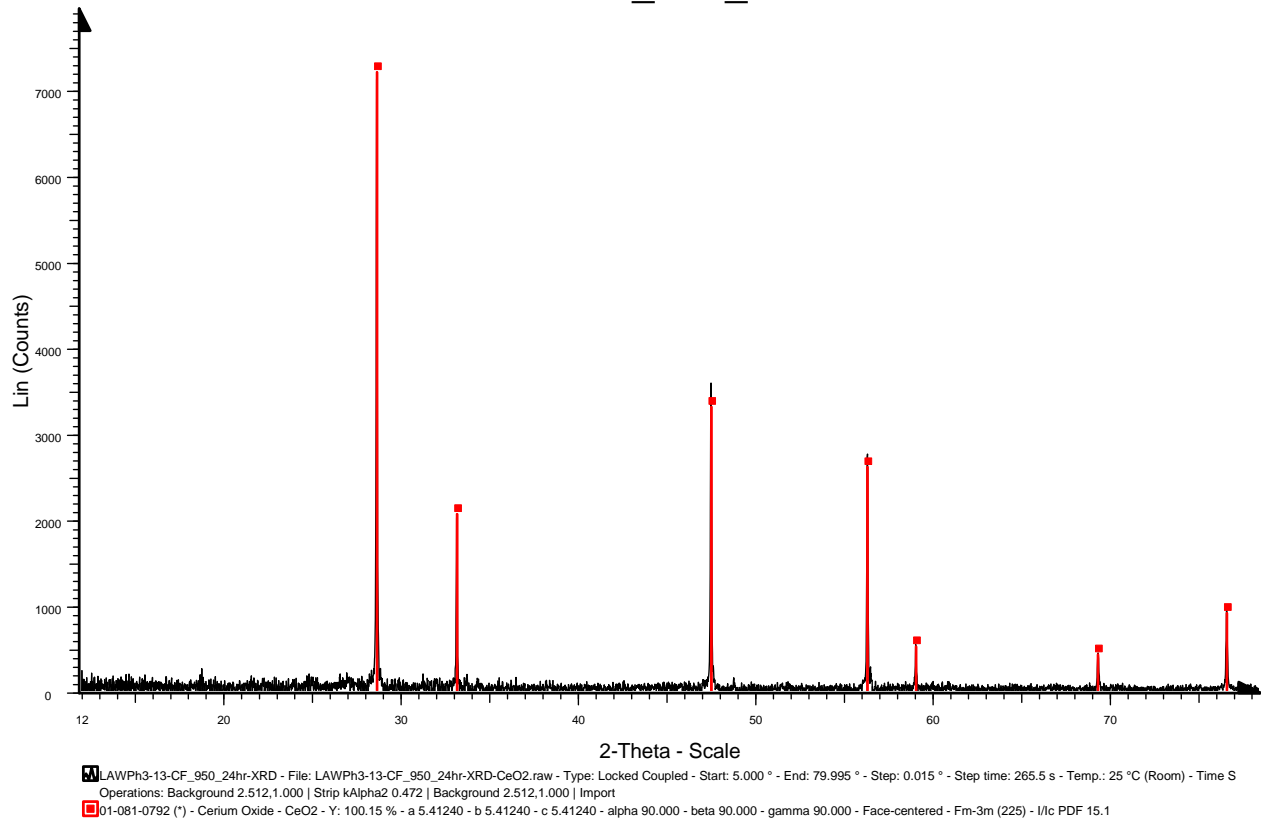
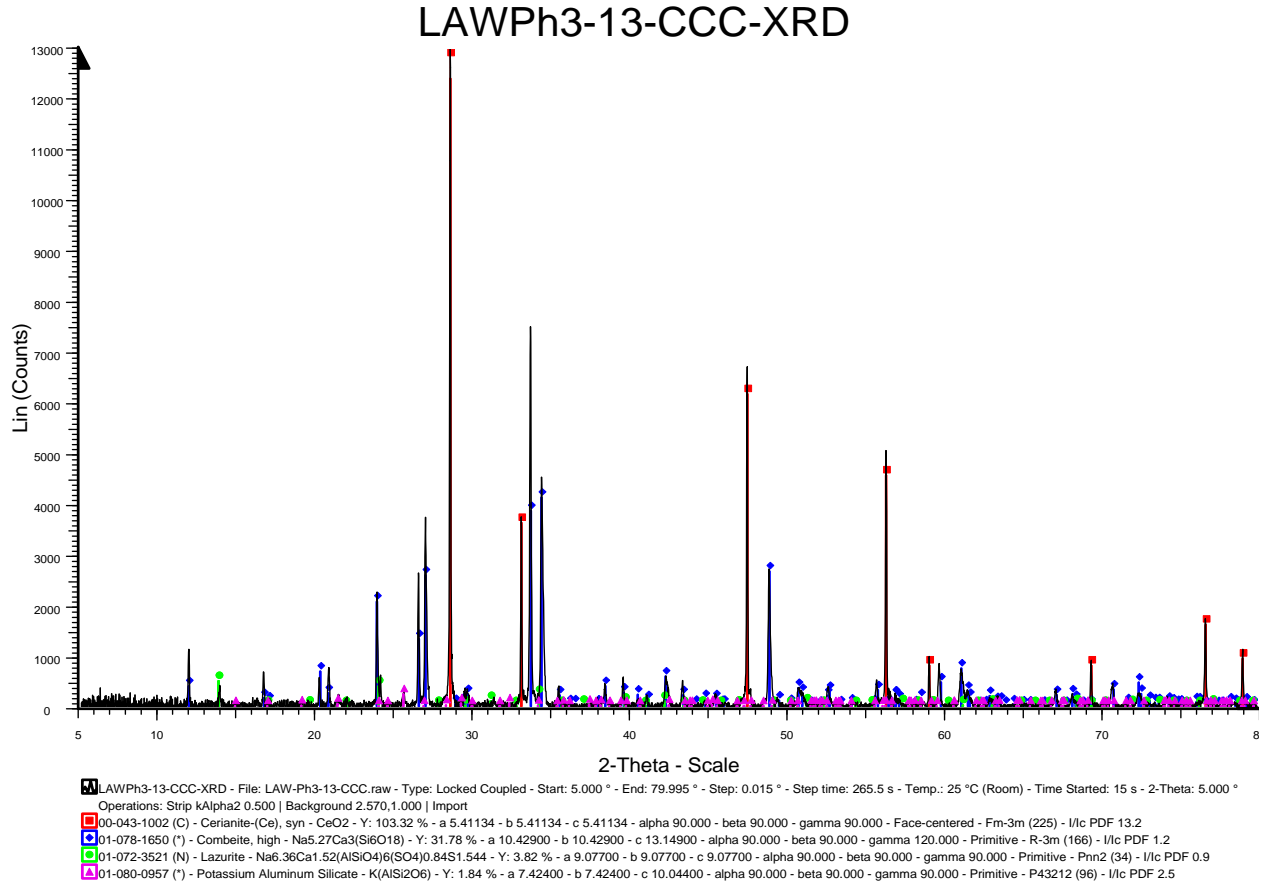


Figure G.13(b). XRD spectrum for LAWPh3-13-CF.



Phase Name	Wt% of Spiked	Wt% in Spiked Sample	Wt% in Original Sample
CeO ₂	5.007	5.007	0
Combeite	0	43.104	45.376
Potassium aluminum silicate	0	1.016	1.07

Figure G.13(c). XRD spectrum for LAWPh3-13-CCC.

LAW-Ph3-14-Q

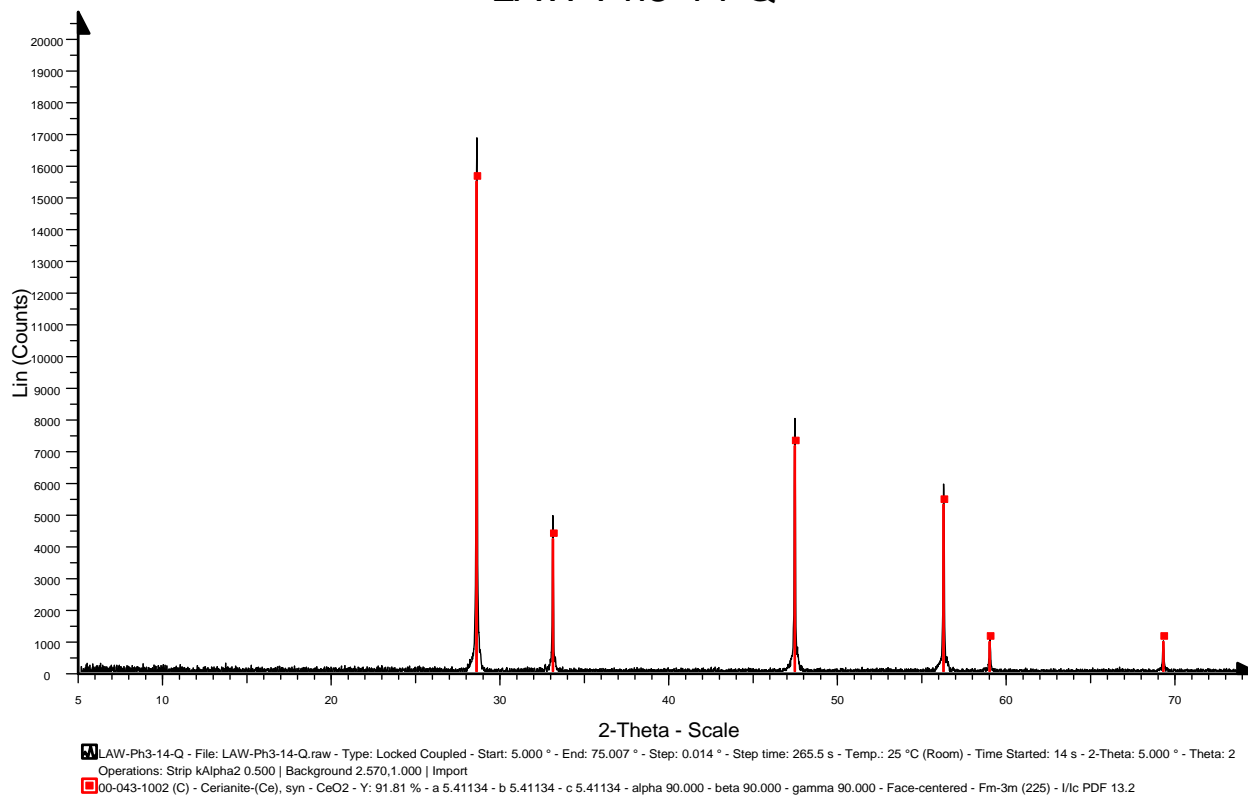


Figure G.14(a). XRD spectrum for LAWPh3-14-Q.

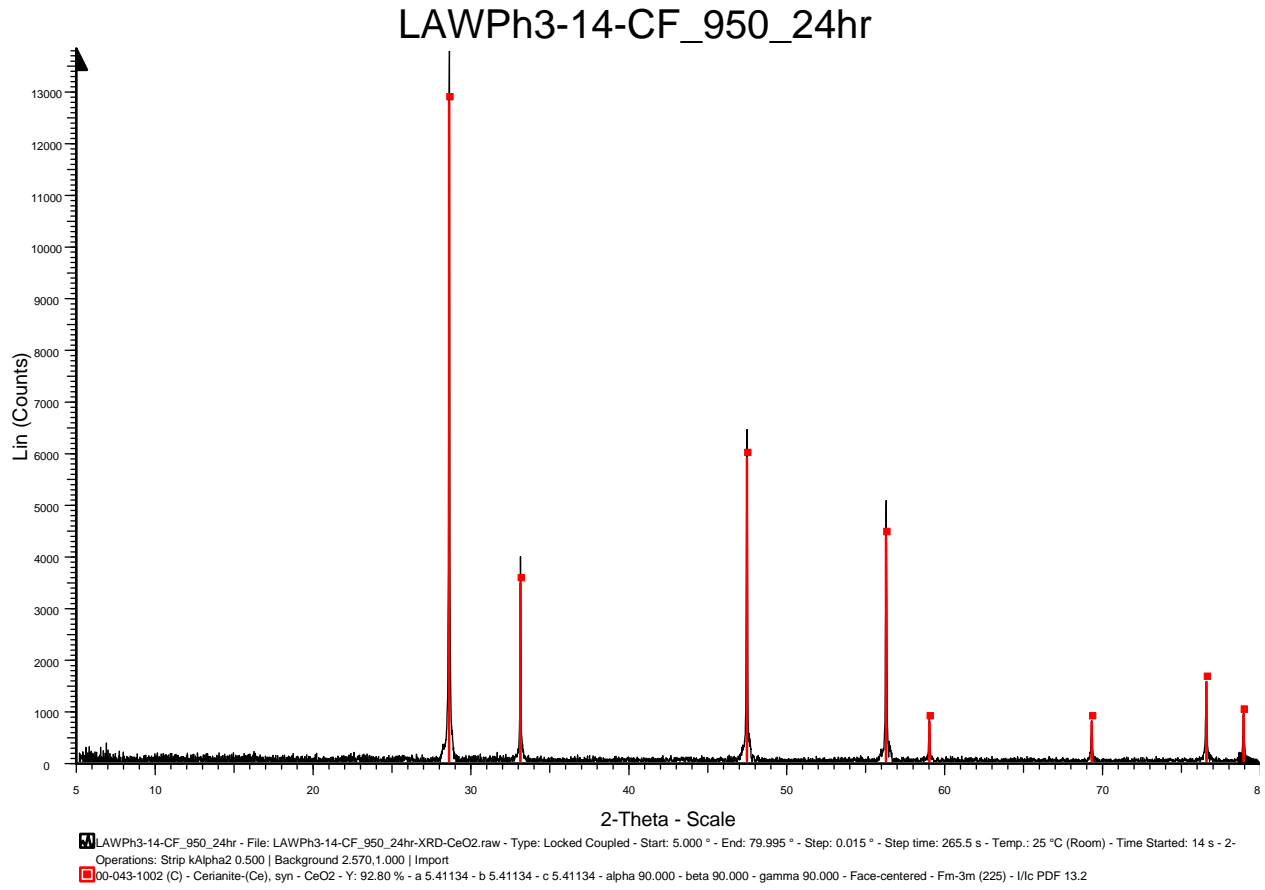


Figure G.14(b). XRD spectrum for LAWPh3-14-CF.

LAWPh3-14-CCC-XRD

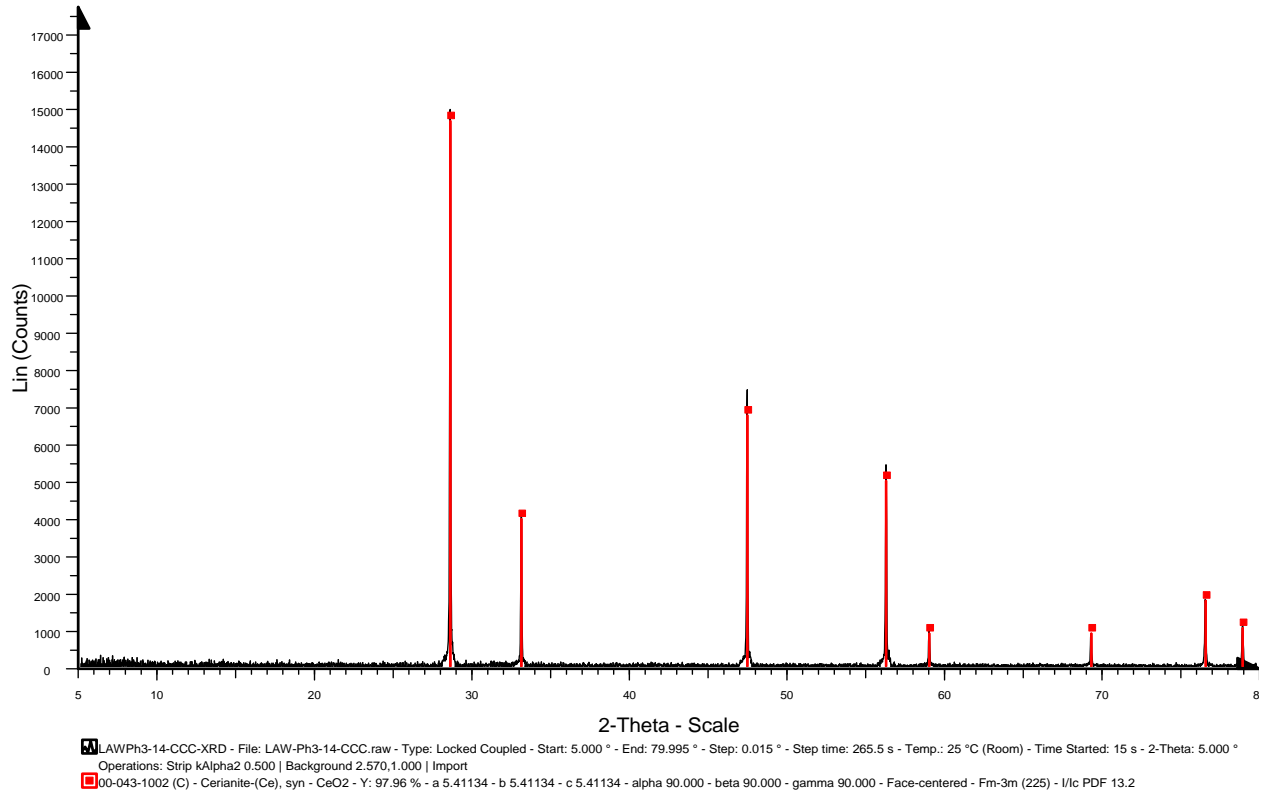


Figure G.14(c). XRD spectrum for LAWPh3-14-CCC.

LAWPh3-15-Q

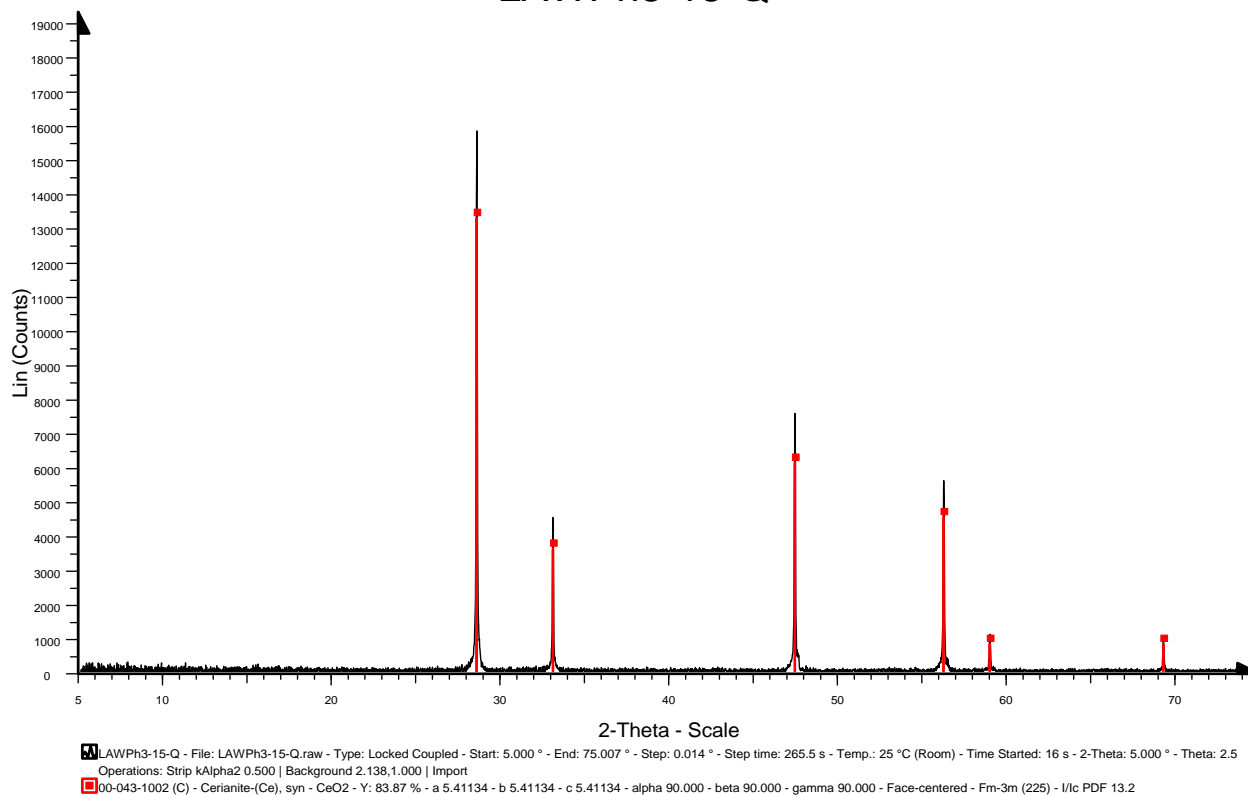


Figure G.15(a). XRD spectrum for LAWPh3-15-Q.

LAWPh3-15-CF_950_24hr-XRD

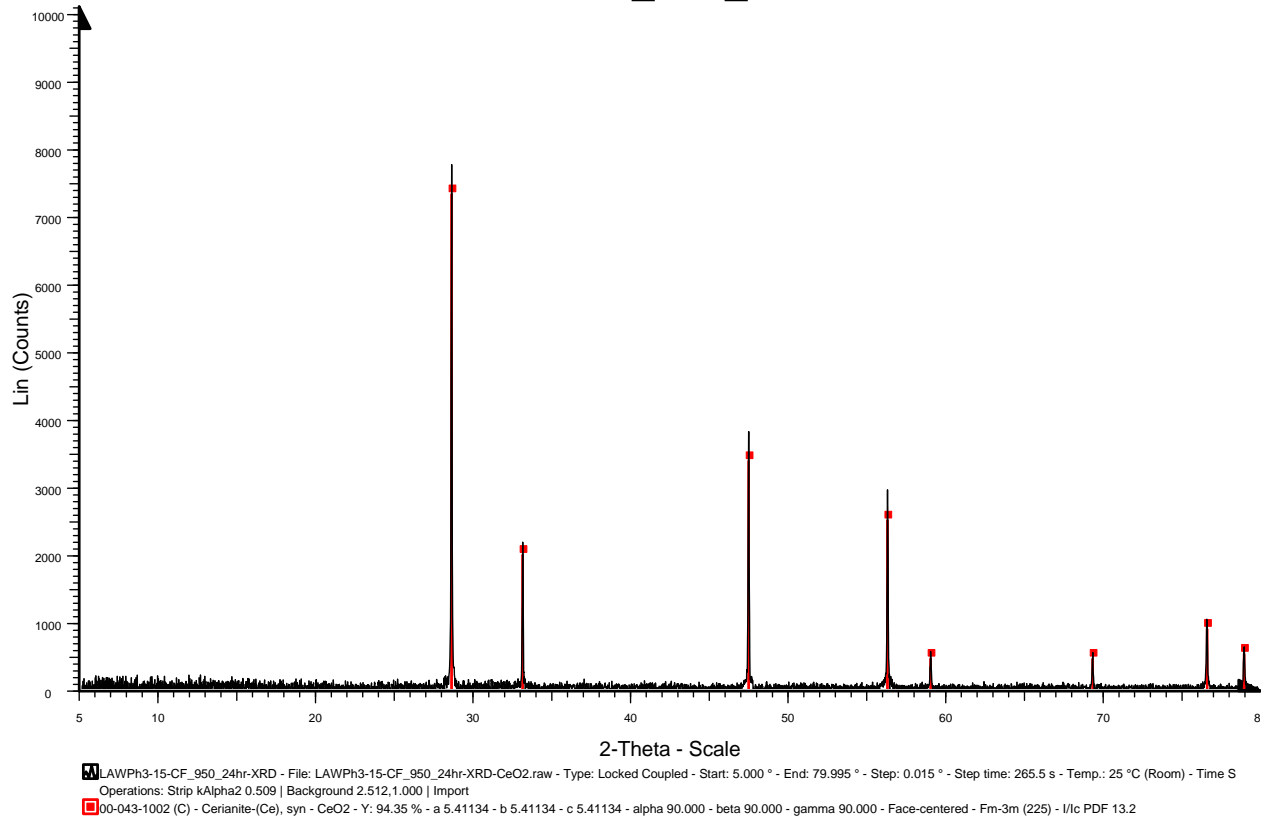


Figure G.15(b). XRD spectrum for LAWPh3-15-CF.

LAWPh3-15-CCC-XRD

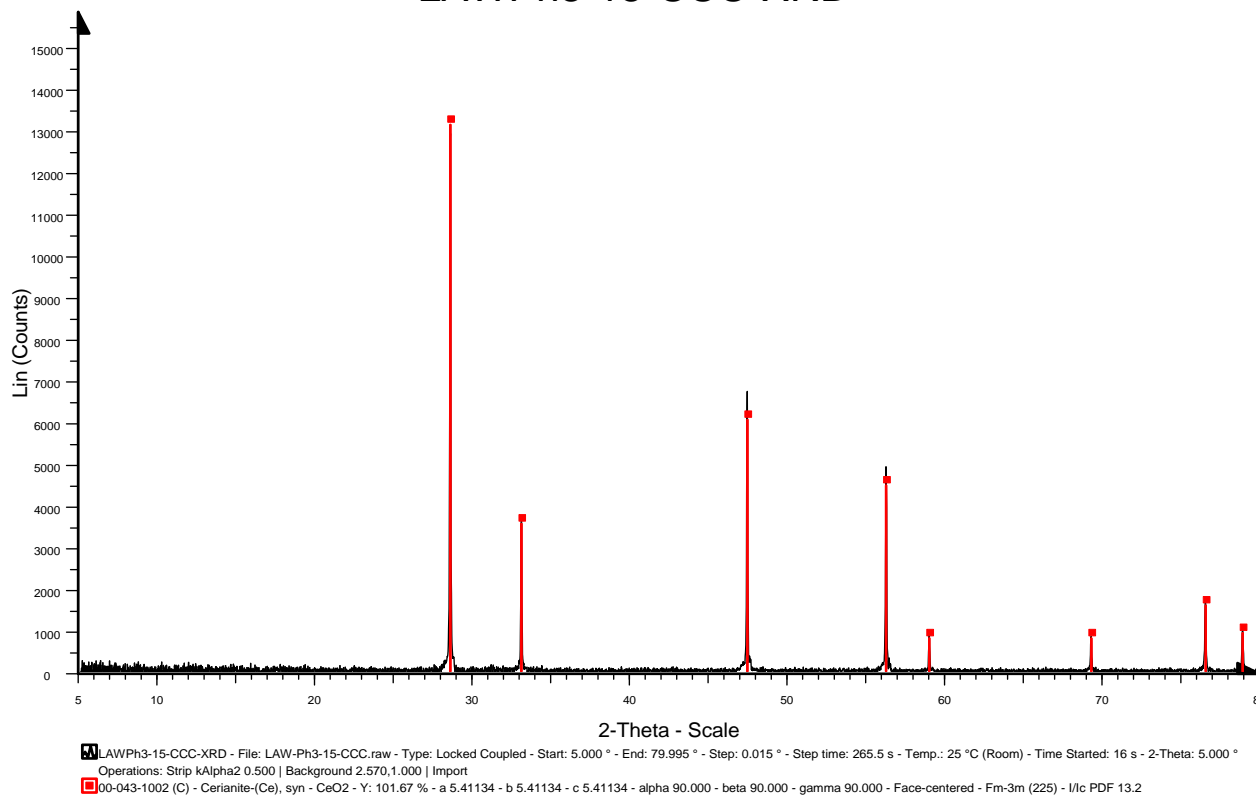


Figure G.15(c). XRD spectrum for LAWPh3-15-CCC.

LAWPh3-16-Q

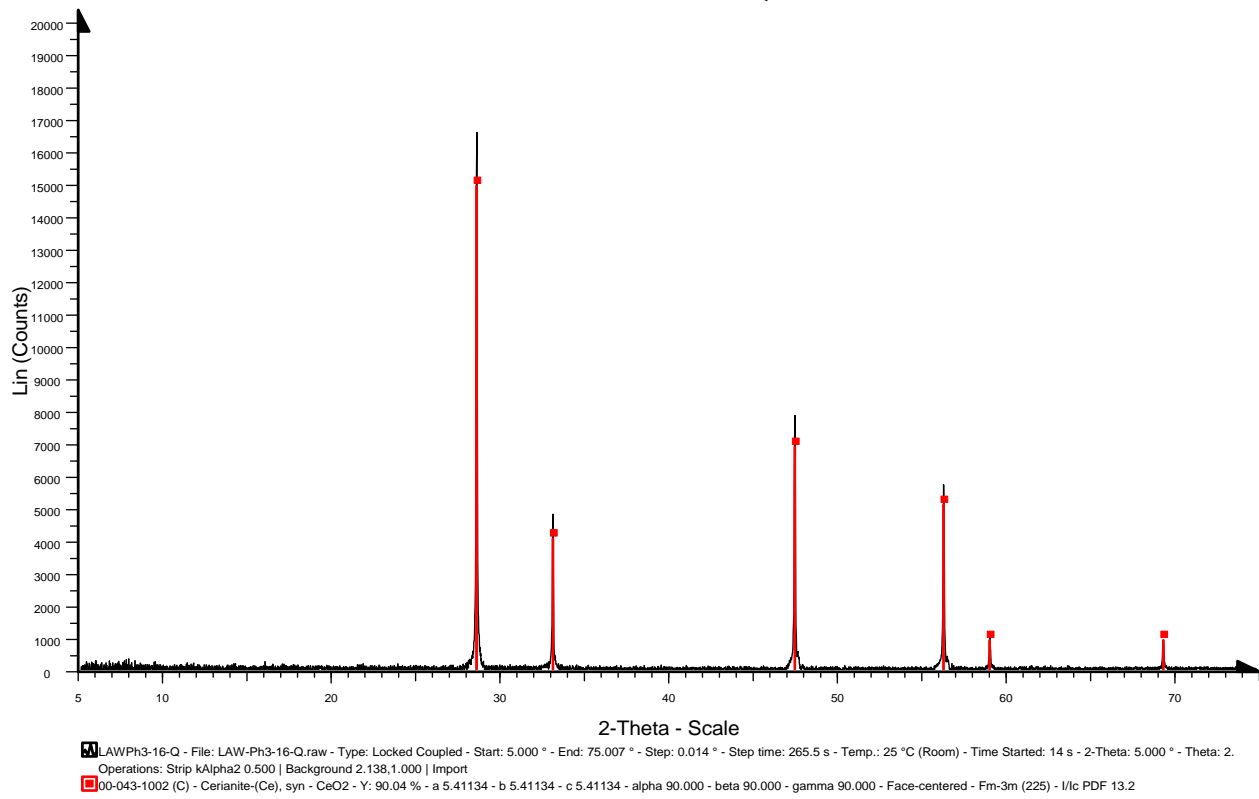


Figure G.16(a). XRD spectrum for LAWPh3-16-Q.

LAWPh3-16-CF_950_24hr-XRD

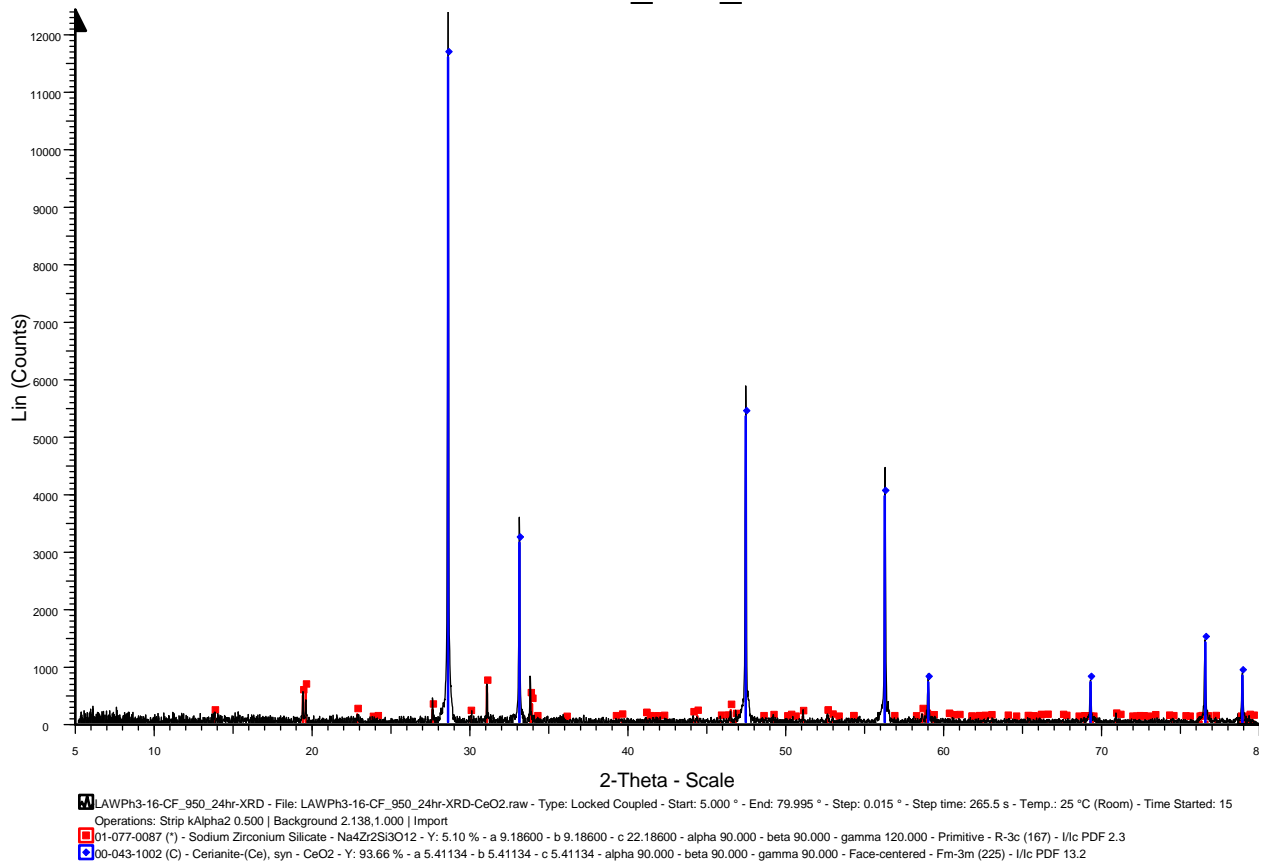


Figure G.16(b). XRD spectrum for LAWPh3-16-CF.

LAWPh3-16-CCC-XRD

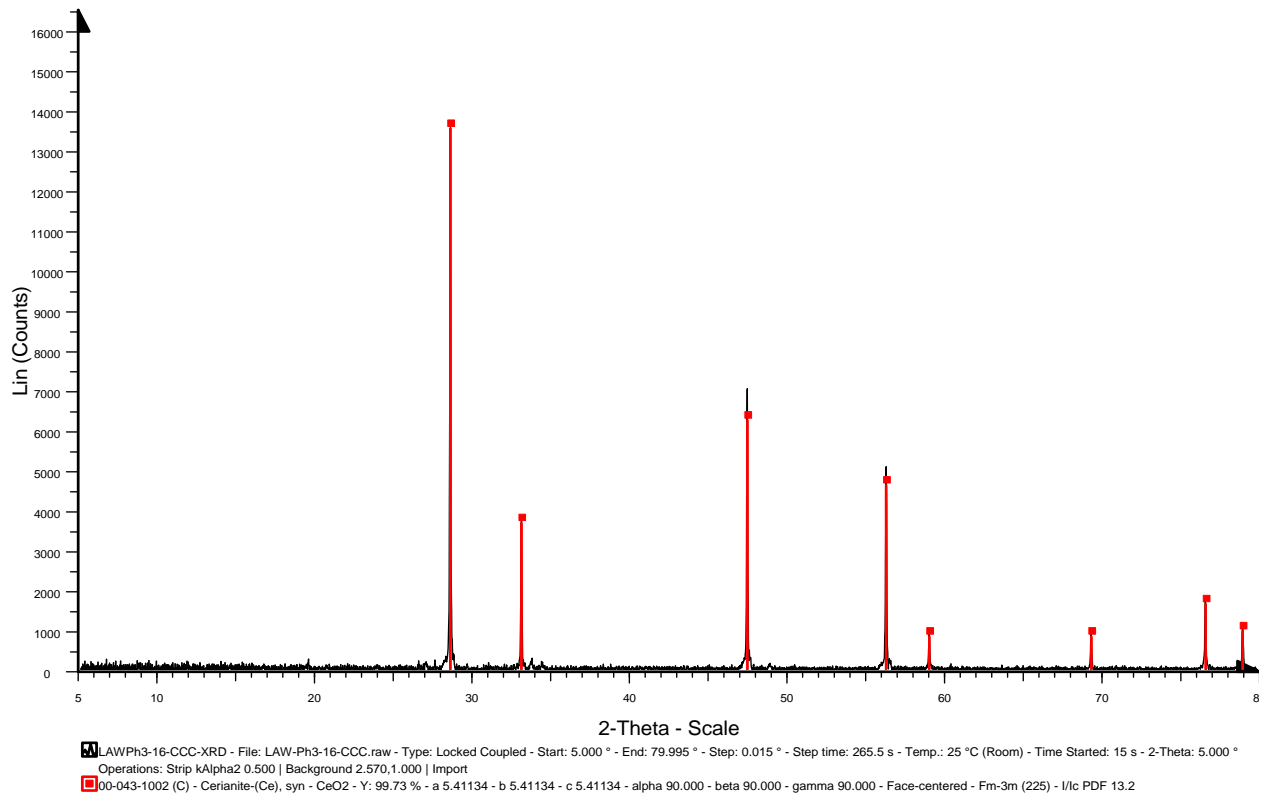


Figure G.16(c). XRD spectrum for LAWPh3-16-CCC.

LAWPh3-17-Q

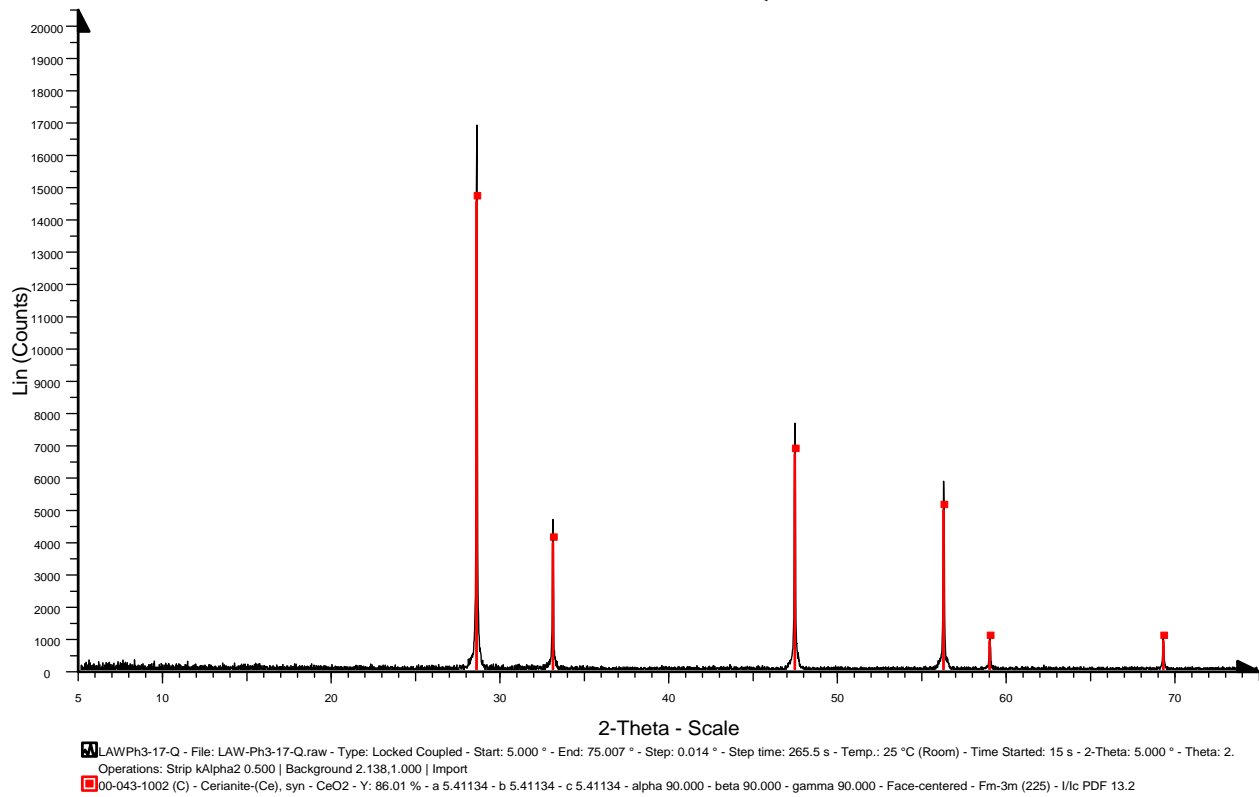
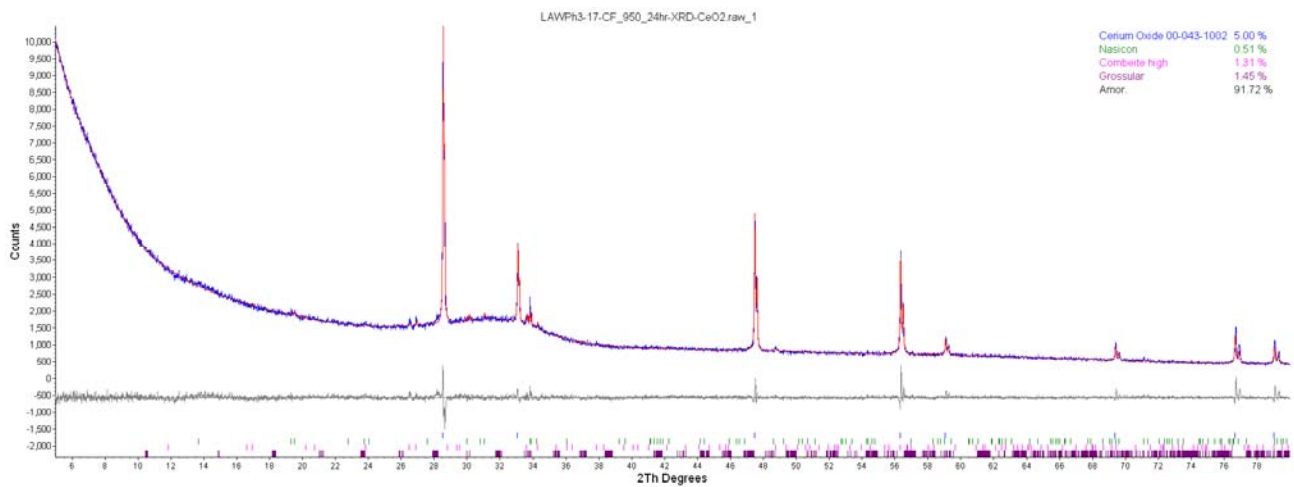
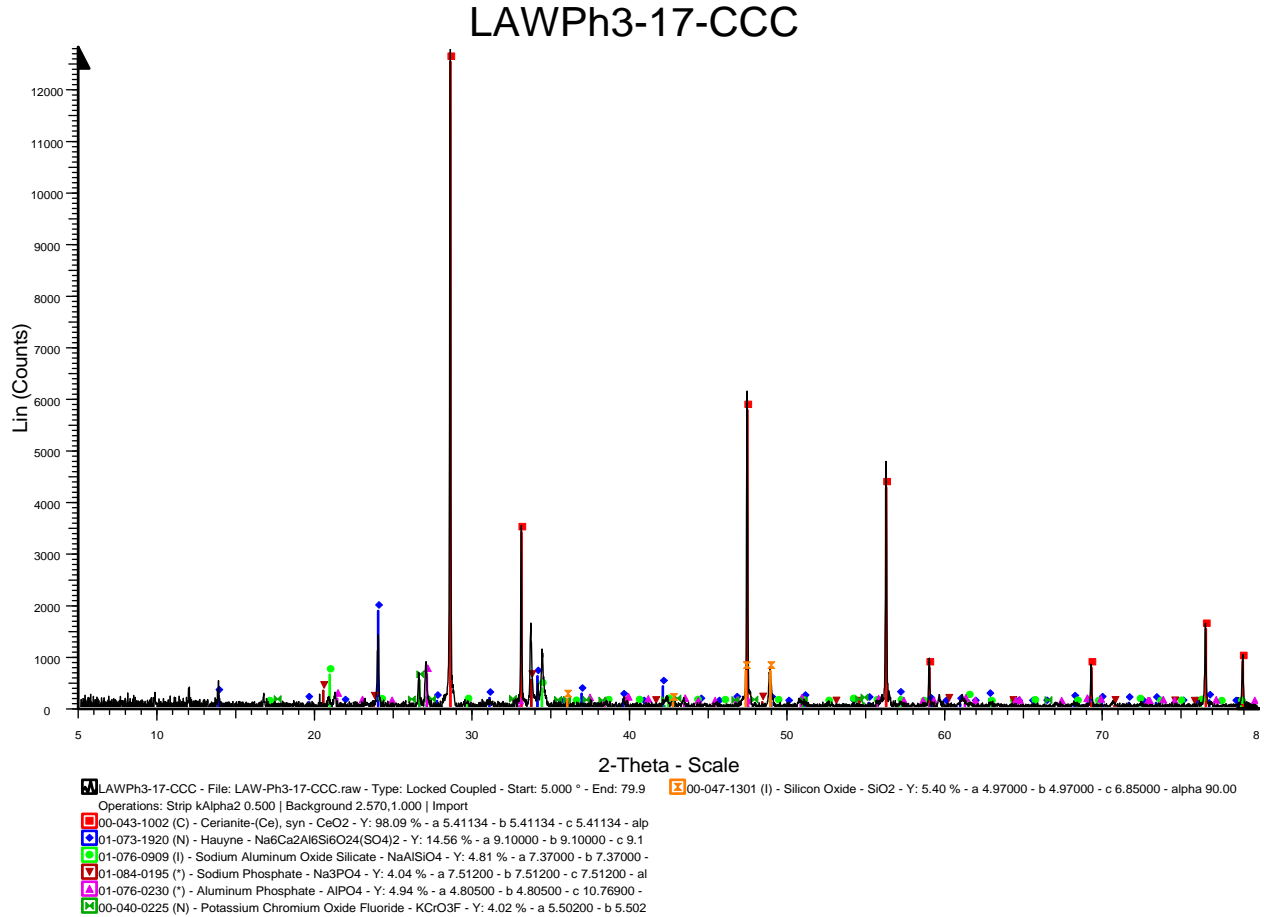


Figure G.17(a). XRD spectrum for LAWPh3-17-Q.



Phase Name	Wt% of Spiked	Wt% in Spiked Sample	Wt% in Original Sample
CeO ₂	4.998	4.998	0
Nasicon	0	0.514	0.541
Combeite high	0	1.309	1.377
Grossular	0	1.455	1.531

Figure G.17(b). XRD spectrum for LAWPh3-17-CF.



Phase Name	Wt% of Spiked	Wt% in Spiked Sample	Wt% in Original Sample
CeO ₂	5.076	5.076	0
Hauyne	0	3.209	3.38
Aluminum phosphate	0	0.759	0.799
Potassium chromium oxide fluoride	0	0.452	0.476

Figure G.17(c). XRD spectrum for LAWPh3-17-CCC.

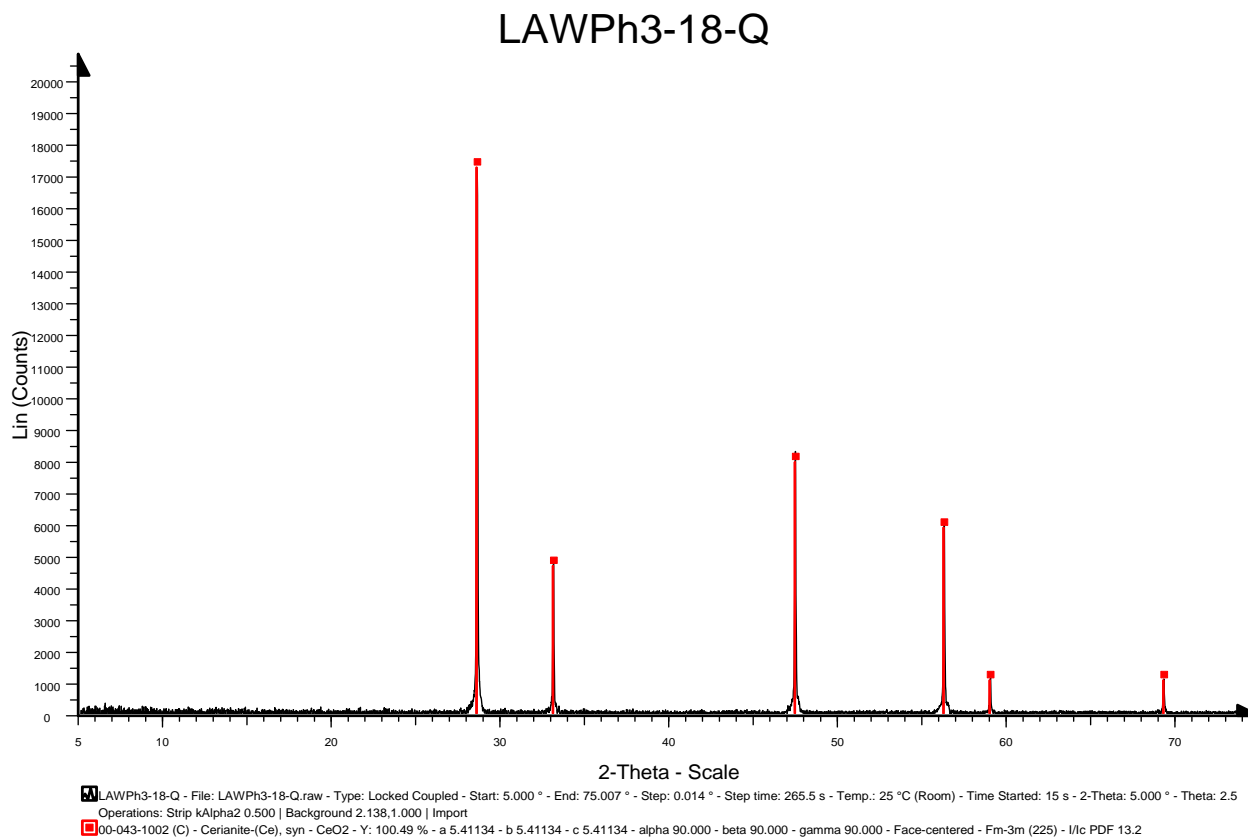


Figure G.18(a). XRD spectrum for LAWPh3-18-Q.

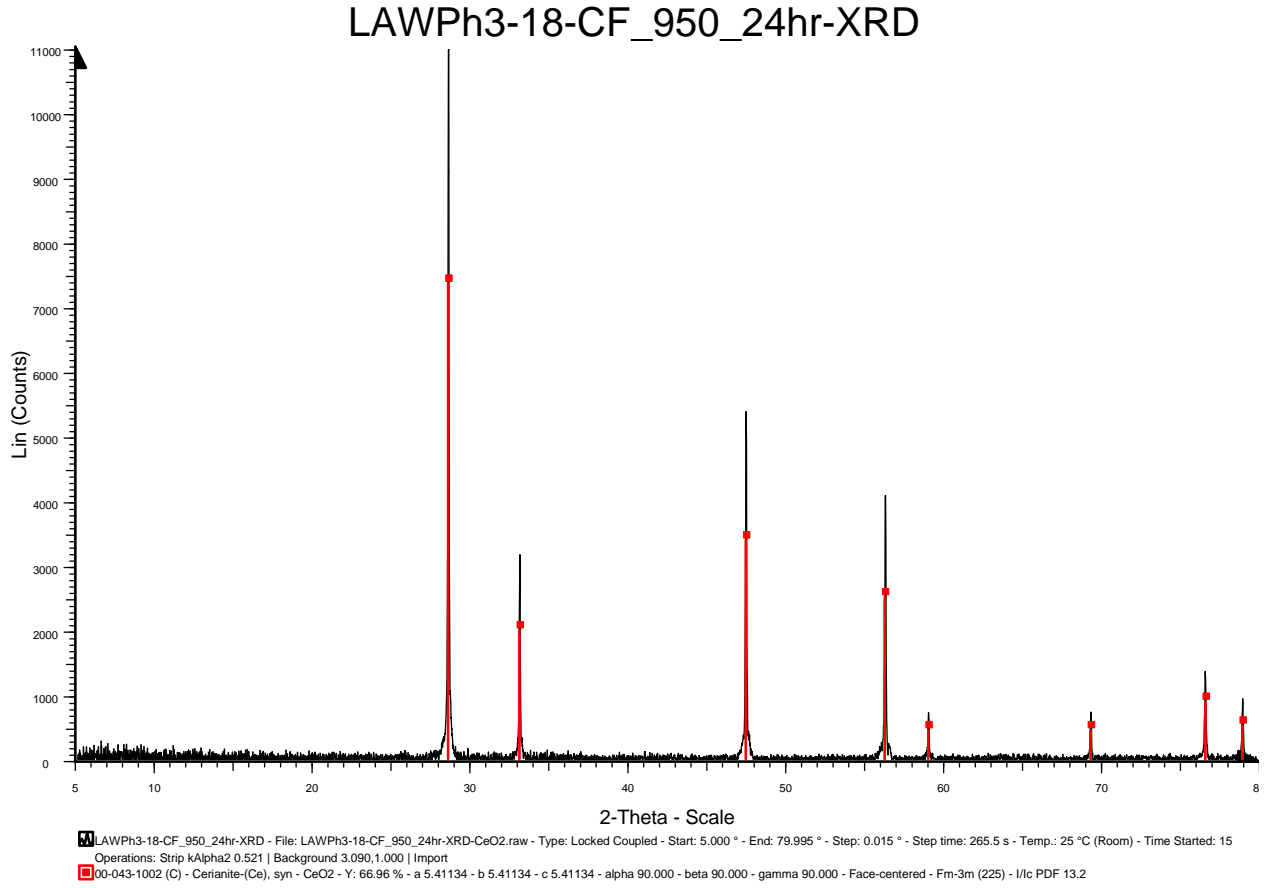


Figure G.18(b). XRD spectrum for LAWPh3-18-CF.

LAWPh3-18-CCC

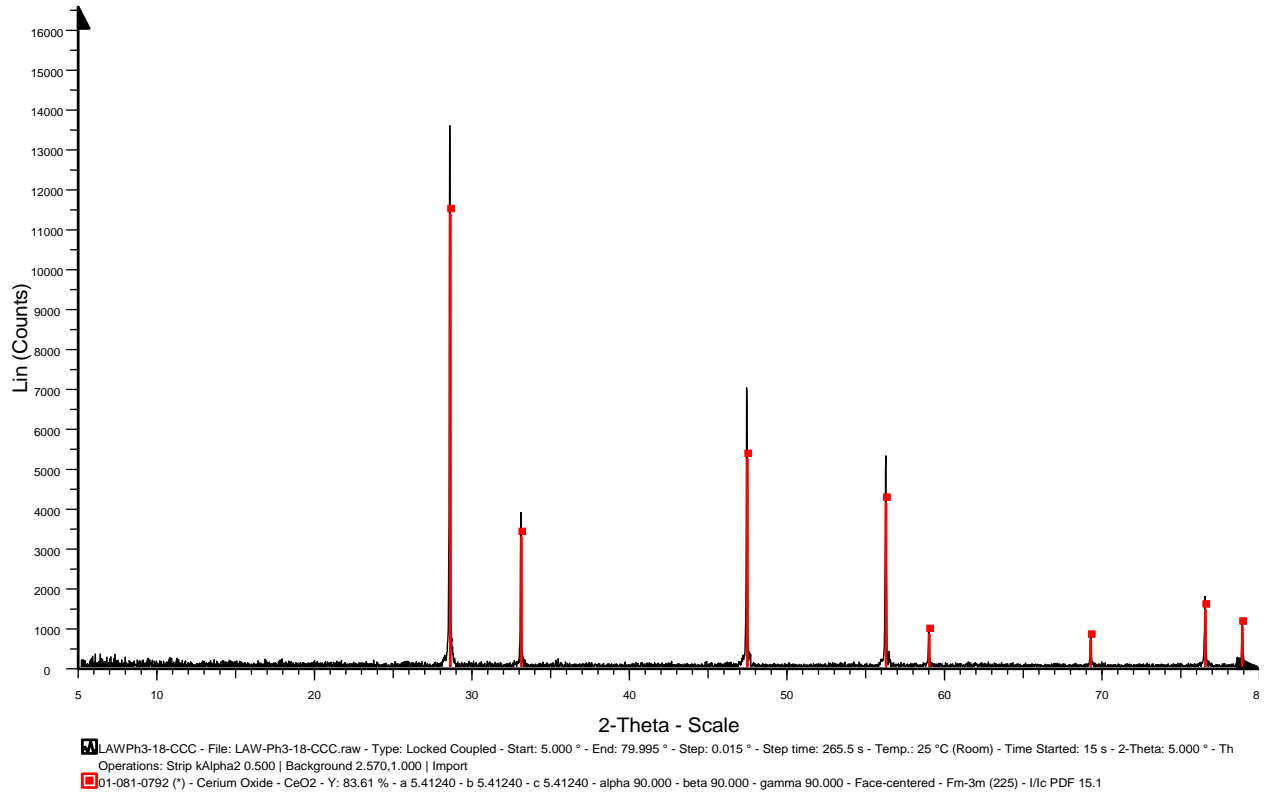


Figure G.18(c). XRD spectrum for LAWPh3-18-CCC.

LAW Ph3-19_mod-Q

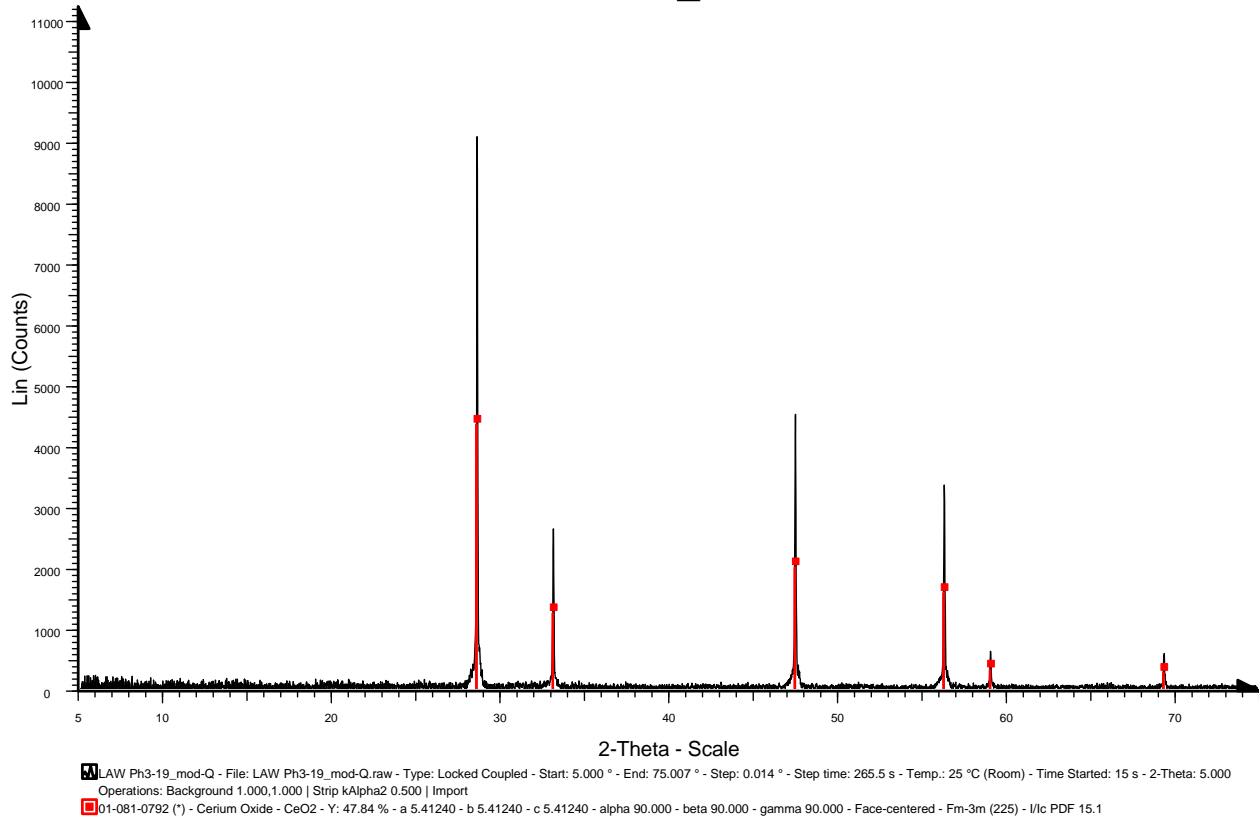


Figure G.19(a). XRD spectrum for LAWPh3-19_mod-Q.

LAW Ph3-19_mod-CF

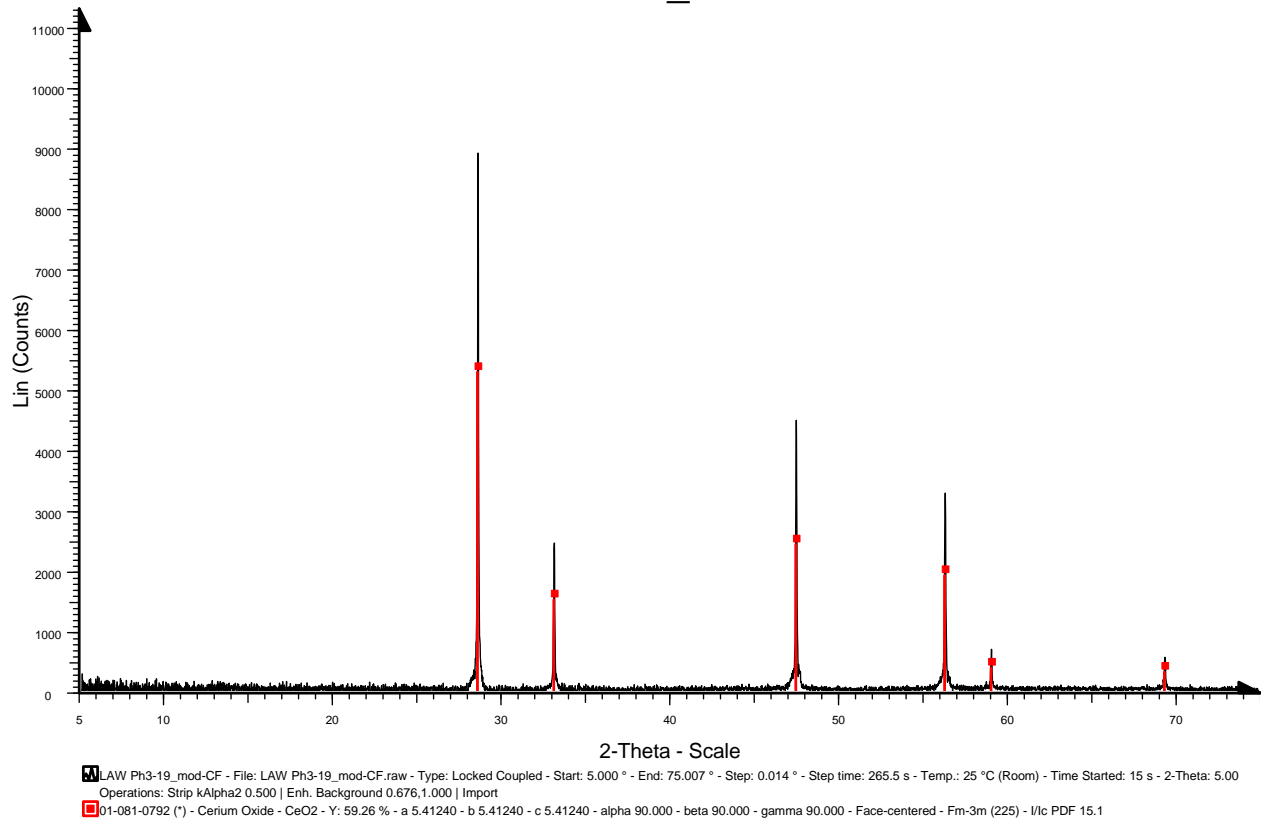
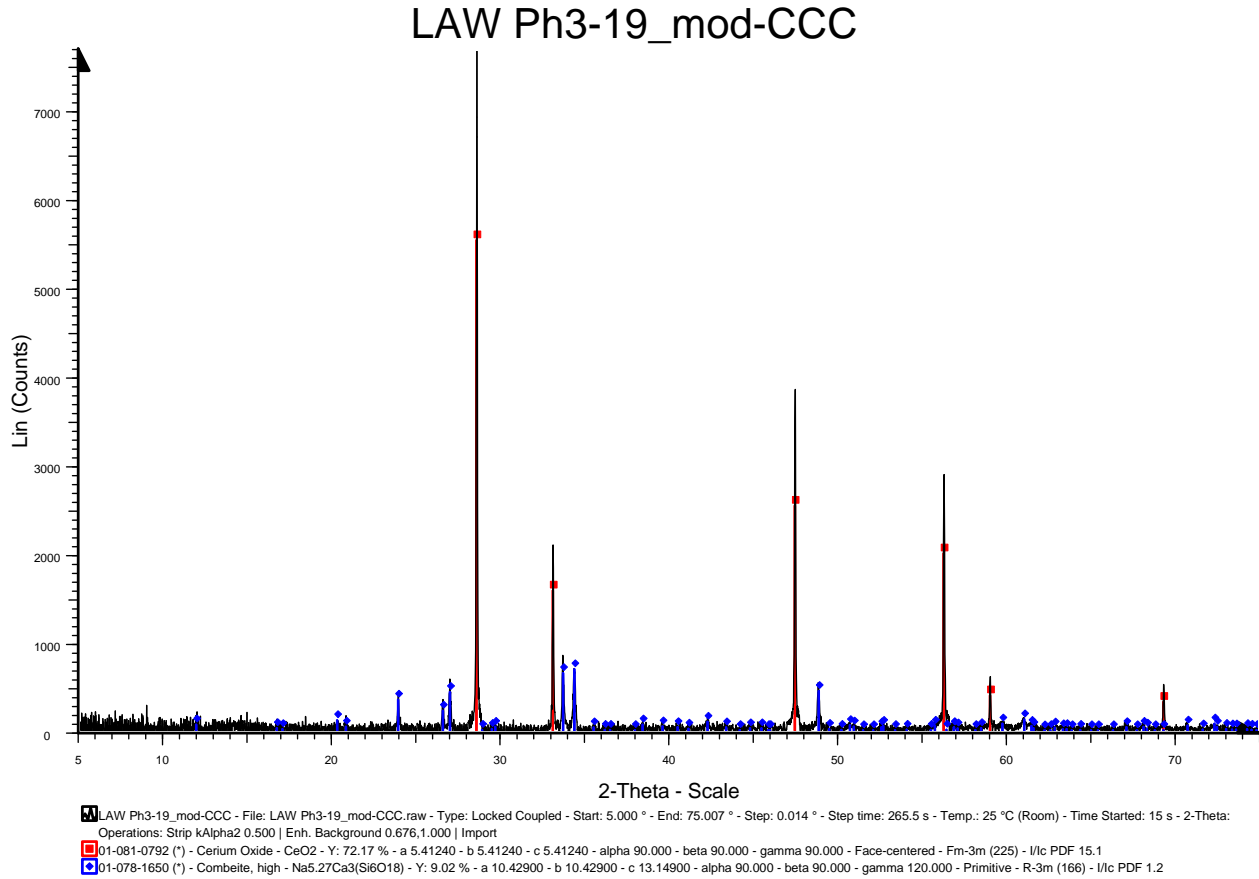


Figure G.19(b). XRD spectrum for LAWPh3-19_mod-CF.



Phase Name	Wt% of Spiked	Wt% in Spiked Sample	Wt% in Original Sample
CeO ₂	4.995	4.995	0
Combeite	0	11.246	11.838

Figure G.19(c). XRD spectrum for LAWPh3-19_mod-CCC

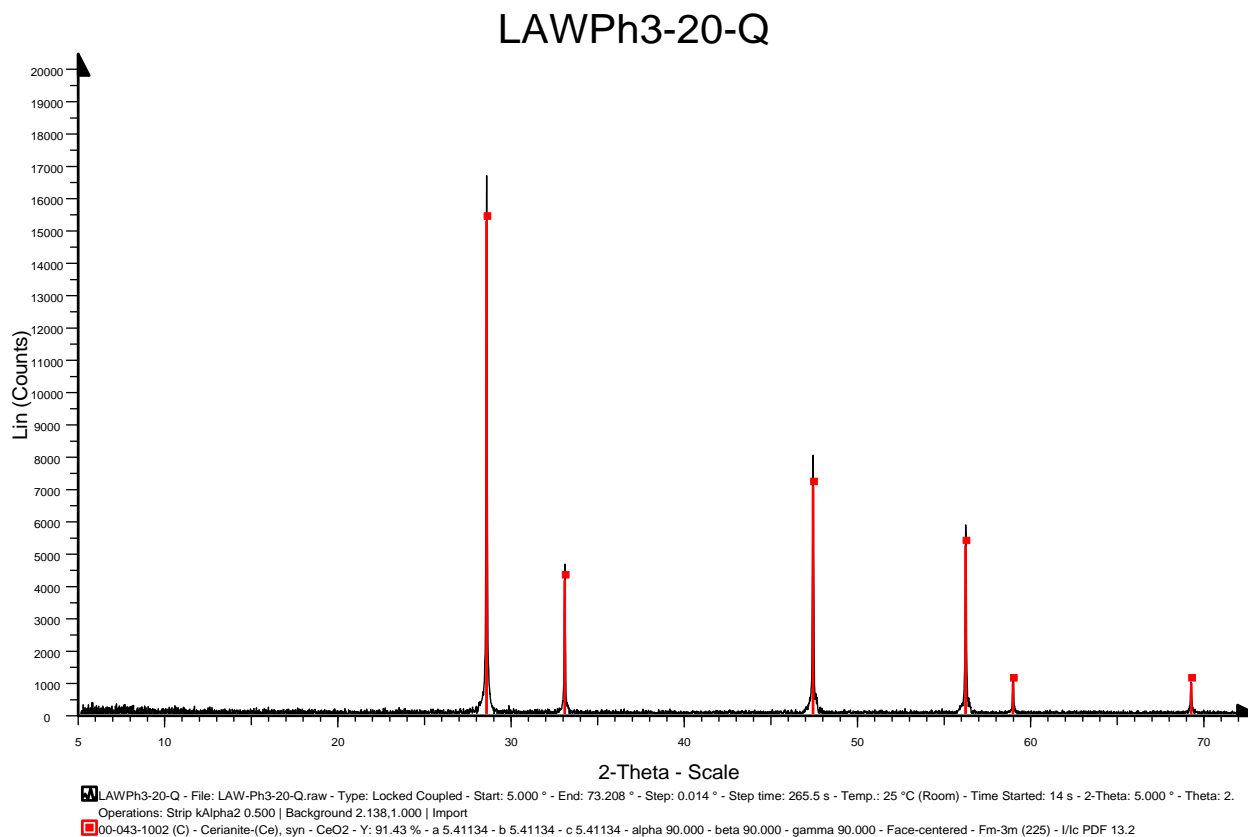


Figure G.20(a). XRD spectrum for LAWPh3-20-Q.

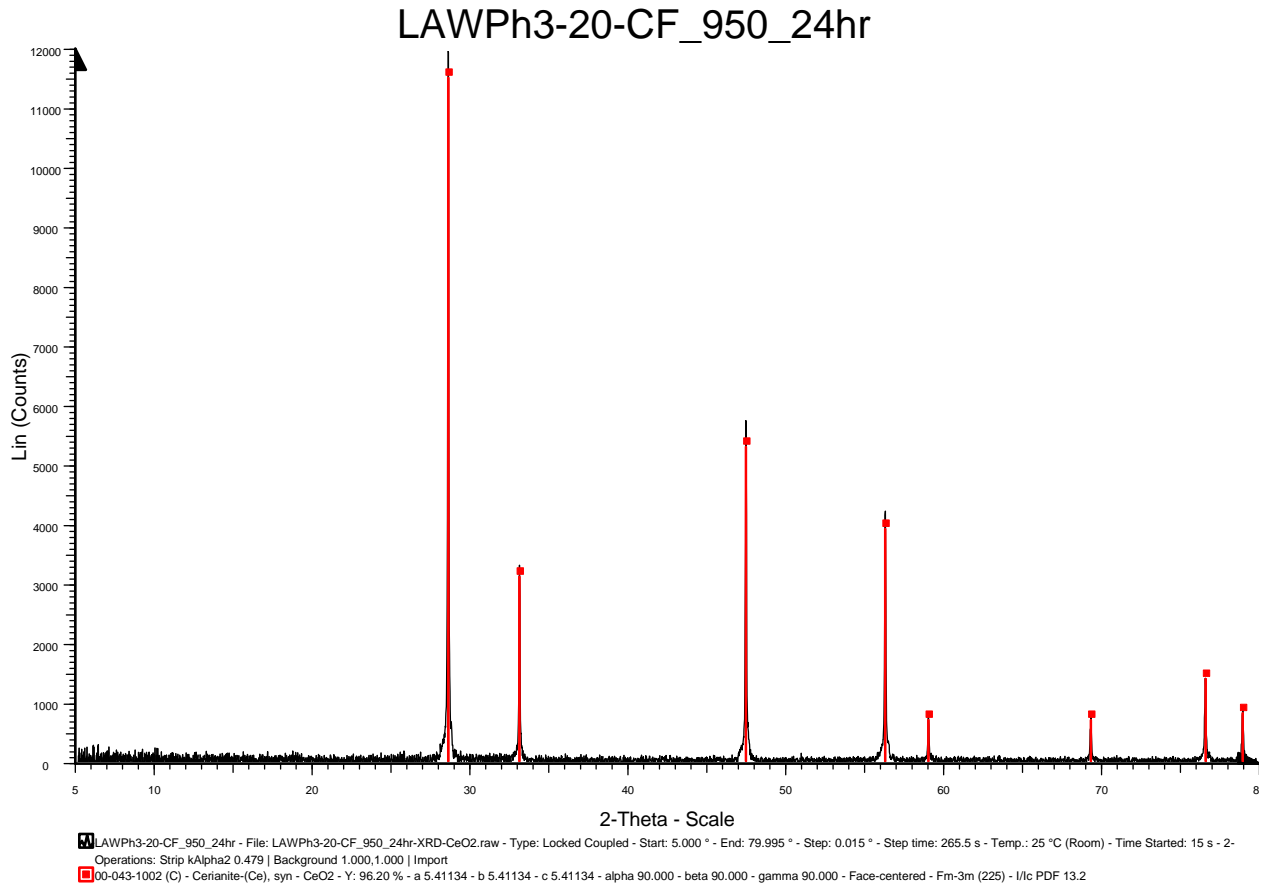


Figure G.20(b). XRD spectrum for LAWPh3-20-CF.

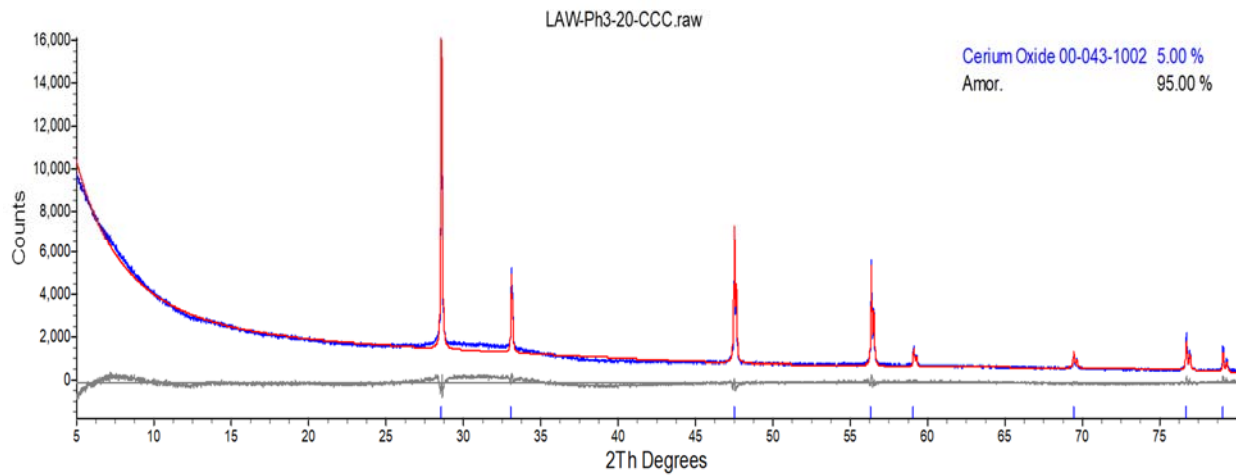


Figure G.20(c). XRD spectrum for LAWPh3-20-CCC.

Appendix H – Sulfate Solubility Compositional Analysis

This appendix presents and compares the compositional analyses of the measured baseline values and sulfur-saturated Phase 3 low-activity waste (LAW) glasses and sulfur-wash solutions using inductively coupled plasma atomic emission spectroscopy and ion chromatography. The comparisons in the tables are shown as percent differences (%Diff). The %Diff results show how much SO₃ was retained in the glass.

Table H.1. Measured baseline and sulfur-saturated values, as well as the percent difference value between measured baseline and saturated concentrations, for the 20 glasses of interest.

Components, mass%	LAWPh3- 01-1	LAWPh3- 02	LAWPh3- 03	LAWPh3- 04	LAWPh3 -05_mod6	LAWPh3- 06	LAWPh3- 07	LAWPh3- 08	LAWPh3- 09	LAWPh3- 10
Al ₂ O ₃	6.264	6.268	6.193	5.82	5.84	8.446	9.273	6.391	7.553	7.832
B ₂ O ₃	13.524	12.864	6.697	12.469	10.2	6.689	7.688	6.585	8.758	6.464
CaO	4.817	4.834	4.383	9.756	2.3	10.456	9.403	6.573	9.836	5.992
Cl	0.054	0.05	0.095	0.072	0.136	0.05	0.119	0.116	0.062	0.05
Cr ₂ O ₃	0.277	0.261	0.16	0.281	0.213	0.241	0.152	0.215	0.146	0.146
F	0.151	0.163	0.555	0.283	0.381	0.155	0.427	0.446	0.277	0.141
Fe ₂ O ₃	0.539	0.143	1.396	0.382	1.08	0.265	0.531	0.143	0.845	0.767
K ₂ O	0.554	2.328	3.882	0.749	2.23	1.777	0.629	1.187	4.041	1.867
MgO	1.179	1.036	1.139	0.459	1.11	1.126	0.166	0.218	0.27	0.365
Na ₂ O	23.961	21.905	20.928	20.759	20.5	19.95	23.422	20.827	21.063	23.085
P ₂ O ₅	0.393	0.229	1.128	0.598	1.17	0.296	0.274	1.261	0.691	0.259
SiO ₂	36.368	34.068	40.861	35.405	37.6	35.512	35.138	44.711	36.529	35.833
SnO ₂	3.142	1.562	1.644	0.363	2.18	3.415	0.696	0.558	0.231	1.663
SO ₃	1.714	1.95	1.29	2.416	1.58	1.592	1.905	1.317	1.641	1.557
V ₂ O ₅	0.269	2.642	0.237	2.629	2.87	2.12	2.87	0.179	0.591	3.276
ZnO	2.11	3.044	3.059	2.262	2.16	2.891	3.187	3.38	2.387	3.115
ZrO ₂	4.961	4.191	4.65	2.965	3.19	2.57	2.188	5.535	4.448	5.4
SUM	100.276	97.538	98.296	97.668	94.7	97.551	98.064	99.638	99.367	97.812

Components, mass%	LAWPh3- 11	LAWPh3- 12	LAWPh3- 13	LAWPh3- 14	LAWPh3 -15	LAWPh3- 16	LAWPh3- 17	LAWPh3- 18	LAWPh3- 19_mod	LAWPh3- 20
Al ₂ O ₃	8.696	10.577	6.665	6.169	6.76	5.687	5.631	7.997	6.25	5.716
B ₂ O ₃	9.418	13.355	6.102	8.114	9.249	6.891	6.142	6.158	8.09	9.12
CaO	3.977	2.987	9.084	5.558	9.091	7.899	9.973	3.893	8	5.037
Cl	0.086	0.078	0.05	0.13	0.05	0.058	0.068	0.059	0.0404	0.053
Cr ₂ O ₃	0.247	0.253	0.205	0.16	0.171	0.195	0.176	0.179	0.174	0.231
F	0.324	0.284	0.26	0.5	0.192	0.186	0.253	0.307	0.0512	0.159
Fe ₂ O ₃	0.143	1.04	0.143	0.143	1.198	0.34	1.323	0.409	1.33	1.073
K ₂ O	1.071	0.215	2.352	0.189	3.102	3.186	0.271	2.259	2.3	0.129
MgO	0.798	1.184	1.22	0.166	0.166	0.791	1.271	1.243	0.257	0.166
Na ₂ O	24.466	20.726	21.939	24.163	21.197	23.085	24.77	22.107	19.2	21.77
P ₂ O ₅	0.705	0.731	0.47	0.401	0.294	0.543	0.533	0.816	0.243	0.365
SiO ₂	35.94	35.192	39.898	39.31	35.138	36.956	37.384	41.021	39.1	38.614
SnO ₂	0.755	0.903	0.277	2.196	1.663	0.127	0.773	3.39	1.21	2.761
SO ₃	1.559	1.353	1.628	2.01	1.749	1.95	2.076	1.143	1.96	1.727
V ₂ O ₅	2.977	3.712	0.718	1.991	1.446	3.396	2.133	0.384	2.61	3.298
ZnO	2.3	2.854	3.42	2.496	2.848	3.495	2.256	3.579	2.06	3.246
ZrO ₂	5.434	2.871	2.766	2.644	3.894	4.934	3.022	4.015	2.39	2.968
SUM	98.896	98.313	97.197	96.339	98.208	99.716	98.055	98.959	95.3	96.433

Pacific Northwest National Laboratory

902 Battelle Boulevard
P.O. Box 999
Richland, WA 99354
1-888-375-PNNL (7665)

www.pnnl.gov